CRANFIELD UNIVERSITY

ATHANASIOS P. DEDOUSIS

AN INVESTIGATION INTO THE DESIGN OF PRECISION WEEDING MECHANISMS FOR INTER AND INTRA-ROW WEED CONTROL

SCHOOL OF APPLIED SCIENCES

PhD THESIS

CRANFIELD UNIVERSITY

SCHOOL OF APPLIED SCIENCES

PhD THESIS

ACADEMIC YEAR 2004 – 2007

ATHANASIOS P. DEDOUSIS

AN INVESTIGATION INTO THE DESIGN OF PRECISION WEEDING MECHANISMS FOR INTER AND INTRA-ROW WEED CONTROL

SUPERVISORS: R. J. GODWIN

J. L. BRIGHTON

OCTOBER 2007

THIS THESIS IS SUBMITTED IN FULFILMENT OF THE REQUIREMENTS FOR THE DEGREE OF DOCTOR OF PHILOSOPHY

Abstract

There is an increasing interest in the use of mechanical intra-row weeders because of concern over environmental degradation and a growing demand for organically produced food. The aim of this study was to investigate the factors that influence the design of precision weeding mechanisms for inter-and intra-row weed control. The purpose is to increase the understanding of the dynamics of the soil-machine interactions and to develop a system for either organic farming or to reduce the environmental loading of agrochemicals in conventional agriculture.

Both the graphical computer simulation studies and the use of a mathematical model (O'Dogherty *et al.,* 2007) for the kinematics of discs were used as tools to aid the disc design to determine the optimum geometric characteristics for a rotating disc that will be able to treat the intra-row area between the crop plants undisturbed circle. The model has wide applicability for the interactive design of discs for a range of crops.

A force prediction model for shallow asymmetric static and rotating discs (about a vertical axis) developed to predict the forces on rotating discs. The model takes into account the geometric parameters of the discs, the speed of operation, the working depth and the physical properties of the soil based upon those required for the general soil mechanics equation which obeys the Mohr-Coulomb failure criterion. A comparison of all experimental work encompassing the laboratory experiments with non-rotating and rotating discs, incorporating the deflection effect of the shaft when working at 0^o inclination angle showed that the model is able to predict the draught force with good accuracy. The predicted forces were 3.5% more than the measured forces overall for a linear regression line (with a coefficient of determination of 0.7) and 61% of the data were within bounds of $\pm$ 25% a line of equal magnitude.

The effect of working depth, inclination angle and disc geometry on draught and penetration force requirements for flat and convex discs were assessed under controlled laboratory conditions. Because of its simplicity a flat disc was an obvious one to study as it is a circular blade with incorporating a cut-out sector, whilst the

convex disc has the advantage of underside clearance. The effect of the concavity on soil failure proved to be of interest by providing smaller aggregates. Four inclination angles (0^o - 15^o) were examined at 0.5 m s^{-1} (1.8 km h^{-1}) driving speed and 1 rev s^{-1} rotational speed at 10 mm deep. Four depths (10 mm - 25 mm) were examined at 0.5 m s^{-1} driving speed and 1 rev s^{-1} rotational speed at 10 mm deep and 0^o inclination angle were tested under controlled conditions. Inclination angle and disc geometry had a significant effect on disc forces and soil failure. A small increase in inclination angle to the direction of travel reduces the magnitude of draught and vertical force by 70% and 80% respectively on average for both flat and convex disc geometries. The convex disc requires 15% less draught force than an equivalent flat disc. This allowed the optimum working parameters for a disc to be selected to eliminate the weeds with the minimum force requirements.

The results of a field experiment after 16; 23; and 33 days transplanting with a working speed of 0.5 m s^{-1} (1.8 km h^{-1}) showed that the proposed novel mechanical weed control system can achieve a weed reduction within the crop row up to 87%.

The disc-hoe has a lower cost for an area of 125 ha of £81 ha^{-1},in comparison to £139 ha^{-1} for the inter-row and hand weeding combination and £690 ha^{-1} for a six man gang manual intra-row weeding, for two passes. It is also less expensive than the cost of the 24 m tractor mounted sprayer of £100 ha^{-1}

The use of the rotating disc-hoe for mechanical weed control would have the benefits of lower mechanical weeding cost, increased potential for organic production and reduction in the number of weeding operations through better targeting to minimise problems caused by frequent soil disturbance and reduced herbicide use having the benefits of environmental advantage.

To my family,

Panagiotis, Lambrini and Nely

Publications

The following papers were produced from this work and are incorporated in this Thesis.

1. Dedousis A.P. & Godwin R.J. (2005a) Precision mechanical weed control. *In*: *Proceedings of the 13th European Weed Research Society Symposium,* Bari, Italy.

2. Dedousis A.P., Godwin R.J., O'Dogherty M.J., Tillett N.D. & Brighton J.L. (2005) An investigation into the design and performance of a novel mechanical system for inter and intra-row weed control. *In*: Proceedings *Brighton Crop Protection Conference,* Glasgow, Scotland, Vol. 2.

3. Dedousis A. P., Godwin R. J., O'Dogherty M. J., Tillett N. D. & Brighton J. L. (2006) Effect of implement geometry and inclination angle on soil failure and forces acting on a shallow rotating disc for inter and intra-row hoeing. *In*: Advances in GeoEcology, *Soil management for sustainability*. Vol. 38, 15-20.

4. Dedousis A.P., O'Dogherty M J., Godwin R J, Tillett N.D. & Brighton J.L. (2006) A novel approach to precision mechanical weed control with a rotating disc for inter and intra-row weed hoeing. *In*: Proceedings of the *17th Triennial Conference of the International Soil Tillage Research Organisation,* Kiel, Germany.

5. Dedousis A. P., Godwin R.J., O'Dogherty M.J., Brighton J.L. & Tillett N.D. (2005) The design and performance of a novel mechanical system for inter and intra-row weed control. *In*: *Workshop in "Spatial and dynamic weed measurements and innovative weeding technologies" of the European Weed Research Society* Bygholm, Denmark.

6. Dedousis A. P., Godwin R.J., O'Dogherty M.J. & Tillett N.D., Grundy A. C. (2007) Inter and intra-row mechanical weed control with rotating discs. *In:* Proceedings of the *6th European Conference in Precision Agriculture,* Skiathos, Greece.

7. Dedousis A. P., Godwin R.J., O'Dogherty M.J. & Tillett N.D., Grundy A. C. (2007) A novel system for within the row mechanical weed control. In: Proceedings of the 7th Workshop of the EWRS Working Group: Physical and Cultural Weed Control, Salem, Germany.

8. Dedousis A. P., Godwin R. J. (2007) Design construction and evaluation of a novel machine for intra-row mechanical weed control. *In:* Proceedings of the 5th National Hellenic Agricultural Engineering Society Conference, Larisa, Greece.

9. Dedousis A. P., Godwin R.J., O'Dogherty M.J. & Tillett N.D. (2007). The design and performance of a novel system for inter- and intra-row hoeing. *Biosystems Engineering* (to be submitted)

10. Dedousis A. P., Godwin R. J. (2007). Mechanical weed control with rotating discs. *Precision Agriculture* (invited paper, to be submitted).

11. O'Dogherty M. J., Godwin R. J., Dedousis A. P., Brighton J. L. and Tillett N. D. (2007) A mathematical model of the kinematics of a rotating disc for inter and intra-row hoeing. *Biosystems Engineering*, 96 (2), 169-179.

12. O'Dogherty M. J., Godwin R. J., Dedousis A. P., Brighton J. L. and Tillett N. D. (2007) A mathematical model to examine the kinematics of a rotating disc with a cut-out sector for use as an inter- and intra-row hoeing device. *In:* Proceedings of the *6th European Conference in Precision Agriculture*, Skiathos, Greece.

13. Tillett N. D., Hague T., Grundy A., Dedousis A. P. (2007 a) A vision guided system using rotating discs for within-row mechanical weed control. *In:* Proceedings of the *6th European Conference in Precision Agriculture*, Skiathos, Greece.

14. Tillett N. D., Hague T., Grundy A., Dedousis A. P. (2007 b) Mechanical within-row weed control for transplanted crops using computer vision. *Biosystems Engineering* (in press).

Acknowledgements

First I would like to thank my supervisor Professor R. J. Godwin for his continuous encouragement, advice and guidance during the period of this study. I am also grateful to Professor M. J. O'Dogherty for his help and enthusiasm he put in this project. Also I would like to thank Dr. J. L. Brighton, Dr. K. Blackburn, and Dr. T. Richards for their personal involvement and support in different stages of the project.

The author is grateful for the collaboration and personal involvement of Dr. N. Tillett and Dr. T. Hague as well to Garford Farm Machinery.

Many thanks go to all the technical staff of Cranfield University at Silsoe and especially to Phil Trolley, Simon Stranks, Roger Swatland and Margaret Boom.

The author is grateful to the Greek State Scholarship's Foundation for the generous scholarship awarded that made this research possible.

The last but not least "thank you" goes to my family for their never ending support.

Table of Contents

List of Figures

List of Tables

Nomenclature

a	distance of line of motion of disc centre from crop row, m
c	radius of no-till circle about plant centre, m
d	distance between plant centres along crop row, m
e	length of straight bevel cut parallel to diameter of opposite semicircle, m
h	length of angled bevel cut to disc circumference, m
l	length of perpendicular from plant centre to edge of cut-out sector, m
m	length from plant centre to end point of edge of cut-out sector, m
p	distance travelled by disc centre from an origin opposite a plant location, m
q	distance from centre of disc to a point on a bevel edge, m
R	rotational speed of disc, r s^{-1}
r	radius of disc, m
s	distance along cut-out edge of sector to end point of a bevel, m
t	time for disc to travel between plant centres, s
t^1	time for disc to travel a distance p, s
v	forward speed of disc centre parallel to crop row, m/s
y_B, y_C	coordinates for points B and C
α	cut-out angle of disc sector, rad
β	angle of rotation of disc in a time t^1, rad
δ	angle made by the angled bevel with the cut-out sector edge, rad
γ	angle made by the radius to the circumferential point of a bevel with the cut-out sector edge, rad
λ	angle made by a line from disc centre to a point on a bevel with the cut-out sector edge, rad
θ	angle of cut-out sector edge to line of motion of disc centre for initial position of disc centre at the origin opposite a plant centre, rad
ϕ	angle of cut-out sector edge to line of motion of disc centre, where $\phi = \theta + \frac{2\pi p}{d}$, rad
ω	angular velocity of disc (=2πR), rad/s

Chapter 1

Introduction

1. Introduction

1.1 Background

Today the agricultural sector requires non-chemical weed control that ensures food safety. Consumers demand high quality food products and pay special attention to food safety. Through the technical development of mechanisms for physical weed control, such as precise inter-and intra-row weeders, it might be possible to control weeds in a way that meets consumer and environmental demands. These mechanisms contribute significantly to safe food production (Pullen & Cowell, 1997; Fogelberg & Kritz, 1999; Kurstjens & Perdok, 2000; Blasco *et al.*, 2002; Dedousis 2003; Dedousis *et al*., 2005 and 2006 a and b).

Over the last six decades, weed management in agriculture of developed countries has been characterised by intensive use of herbicides. High production agriculture has utilised agro-chemical inputs such as fertiliser and sprays to increase and protect crop production. Recent food scares in Europe have highlighted public concern about food safety as that supermarkets are now willing to pay a premium for food products that have a record of all the treatments carried out on them (Blackmore and Griepentrog, 2002).

In developing countries, national and international organisations have generally promoted herbicides as a requirement for modernisation and increases in agricultural production. Increasing governmental restrictions together with increasing consumer-demands require foolproof registration methods throughout the food production chain. Dekker *et al*., (2002) reviewed that after the golden era of increasing agricultural production it is now time to focus on food safety. Several recent trends are forcing agriculturists in both developed and developing countries to reappraise their dependence on herbicides.

Economic, environmental, and biological developments are leading farmers and researchers to seek effective weed management strategies that minimize their reliance on herbicides. Awareness of the public, interest in organic food production and some problems with herbicide use, has led to a range of techniques and machines being developed for non-chemical weed control using physical methods.

1.2 Weed control methods

A weed can be thought of as any plant growing in the wrong place at the wrong time and doing more harm than good (Parish, 1990). Weeds compete with the crop for water, light, nutrients and space. Therefore, weeds reduce crop yields and also affect the efficient use of machinery (Parish, 1990). According to Parish (1990) a characteristic example of reduced efficient use of machinery is in harvesting and crop storage. The most frequent occasion that weeds reduce agricultural equipment efficiency is during the harvesting operations. The machinery (i.e. combine harvester) in addition to the utilized plants also harvests weeds (weeds are located between and within the rows), which reduce the efficiency of the equipment. Various methods are used for weed control. Among them, mechanical cultivation is commonly used in many vegetable crops to remove weeds, aerate soil, and improve irrigation efficiency.

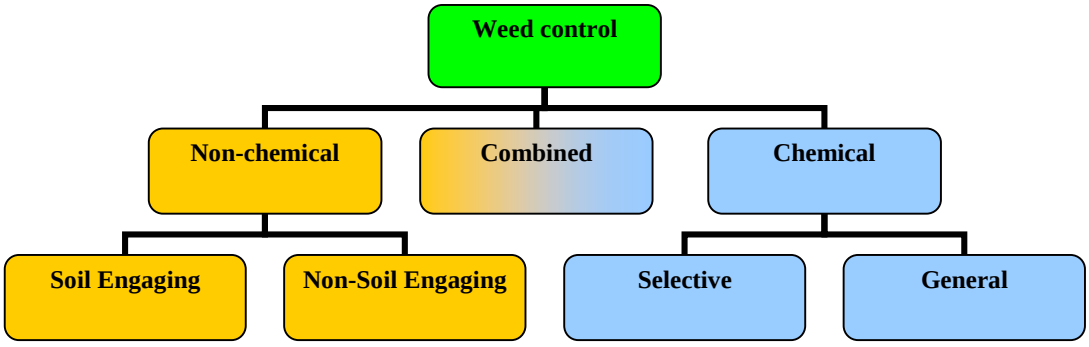

Figure 1-1 Weed control methods (*After Home, 2003*)

The most widely used method for weed control is spraying of herbicides; however, many consumers now require products that are not treated with chemicals. The biggest disadvantage of herbicide use is the environmental impact and soil and water

pollution. Apart from the above negative properties chemical weed control has beneficial effects. The virtue of chemical weed control is the immediate elimination of weeds without replication although this depends on the weed and how tolerant it is. Furthermore, chemical weed control demands less energy input, compared with flaming applications, or other alternatives in weed control (Ascard, 1995).

Thermal and mechanical techniques are used nowadays without any precise application for non-chemical weed control. In addition, many techniques have been developed for non-chemical weed control, to reduce chemical costs in conventional agriculture, in response to environmental pressures and to provide for the needs of organic food production (Parish, 1990).

Electricity is one of the power sources that has been used by researchers around the world, and is used both as a heat energy source and for electrical shock treatment. Infrared application is a technique that is used in small-scale horticulture organic crop production in The Netherlands. The infrared weeders use propane combustion to provide heat. Ascard, (1998) made a comparison of flaming and infrared radiation techniques for thermal weed control, with very positive results for the use of infrared. Both thermal weeders used propane combustion to provide heat from either a covered flamer or an infrared radiator. The flamer showed better performance than the infrared radiator on plants at the four-leaf stage, but the opposite was true on plants at the cotyledon stage. Both thermal weeders required an effective application of propane of about 60 kg/ha to obtain 95% reduction of plants at the zero- to two-leaf stage (Ascard, 1998).

Although all these techniques are not widely used because of problems such as the short time effect of the method, more replications being needed to completely damage weeds and low selectivity does not enable elimination weeds individually. Replication and the equipment-labour cost is high. According to Ascard (1994) flame weeding is often associated with problems such as high-energy consumption, low driving speed, and irregular weed control.

1.3 Mechanical weed control

Mechanical methods control weeds by physical damage, such as cutting leaves and roots, bruising stems and leaves, covering plants by soil or by uprooting them (Kurstjens, 2002).

The majority of the work that has been done in the last decades concerns weed control between the crop rows with implements such as hoes, row cultivators, rotary tillers, brushes and rolling cultivators (Pullen & Cowell, 1997; Fogelberg & Kritz, 1999; Peruzzi *et al.*, 2005). According to Kurstjens (2002) some of the aforementioned implements can also control weeds between the crop (intra-row) by throwing soil into the row.

In general, inter-row weeding is effective and assessments are quite straightforward. According to Kurstjens (2002) the main challenge to both practical farmers and researchers is the selective control of the intra-row weeds.

During the last decade several studies have been initiated in controlling the weeds within the crop, especially for high value crops such as vegetables (Fogelberg & Kritz, 1999) with implements such as brush weeders, finger weeders, torsion weeders which are widely used for intra-row weed control. Also a number of investigations have been made to develop novel systems to achieve sufficient within the row weed control (Kouwenhoven, 1997; Bontsema *et al.*, 1998; Home, 2003; Griepentrog *et al.*, 2006; Dedousis *et al.*, 2007). The common principle of these systems is to actively guide or activate a tool to treat the intra-row area based on information about where individual crop plants are located (Griepentrog *et al.*, 2006). Information concerning individual crop plant locations can be derived from real-time sensors (Tillett *et al.*, 2002; Aastrand & Baerveldt, 2005; Tillett & Hague, 2006; Tillett *et al.*, 2007) or off-line from GPS data and from the seed drop position logged during seeding operations (Griepentrog *et al.*, 2005).

1.4 Necessity for this research

The review by Home (2003) concluded that "there are currently no commercial techniques available to viably control intra-row weeds and there had been no significant advances in inter-row cultivation apart from the introduction of guidance systems to improve their overall lateral positioning accuracy". However (Ascard, 2007) suggests that a number of machines have been recently developed and evaluated in research but the constraints and limitations of cost, low capacity, low selectivity and time to perform all the necessary adjustments made them unattractive. This reveals that there is a need for the development of mechanical weed control systems in the intra-row area, that can overcome the aforementioned limitations.

1.5 Aim

The aim of this project is to investigate the factors that influence the design of precision weeding mechanisms for inter-and intra-row weed control. The purpose is to increase the understanding of the dynamics of the soil-machine interactions and to develop a system for either organic farming or to reduce the environmental loading of agrochemicals in conventional agriculture.

1.6 Objectives

i. To quantify the dynamics of the soil-disc interactions and to develop mathematical prediction models for the disc kinematics and for the force and torque requirements.
ii. To determine the effect of disc geometry, working speed, disc rotational speed, and soil conditions to perform effective weed control without damaging the nearby plants. This would allow the determination of improved cutting and burial weed control techniques.
iii. To develop a prototype experimental system to evaluate different disc geometries.
iv. To evaluate the effectiveness of a prototype rotary disc hoe in high value crops (i.e. field vegetables).

v. To evaluate the cost of the rotating disc hoe in relation to existing alternatives.

1.7 Outline methodology

i. To conduct a graphical computer simulation of the disc kinematics to determine the optimum geometric characteristics for a rotating disc that will be able to treat the intra-row area between the crop plants the undisturbed zone.
ii. To develop a mathematical model of the kinematics of a rotating disc for inter- and intra-row hoeing, for any given plant spacing and undisturbed zone surrounding the plants. The model will enable optimisation of the effects of the distance of the disc centre from the crop row, the disc radius, the plant spacing within the crop row and the undisturbed zone of the plant.
iii. To conduct laboratory soil bin investigations to quantify the soil dynamics of working discs for various disc geometries, working speeds, rotational speeds, depths and inclination angles.
iv. To develop a mathematical prediction model for both the force requirements and torque.
v. To evaluate the effectiveness of a prototype rotating disc hoe system in field vegetables using a traditional plant spacing for cabbage.
vi. To evaluate the cost of the rotating disc hoe in comparison with current commercial alternatives for weed control in both conventional and organic farming.

The structure of the research program is shown in Figure 1-2.

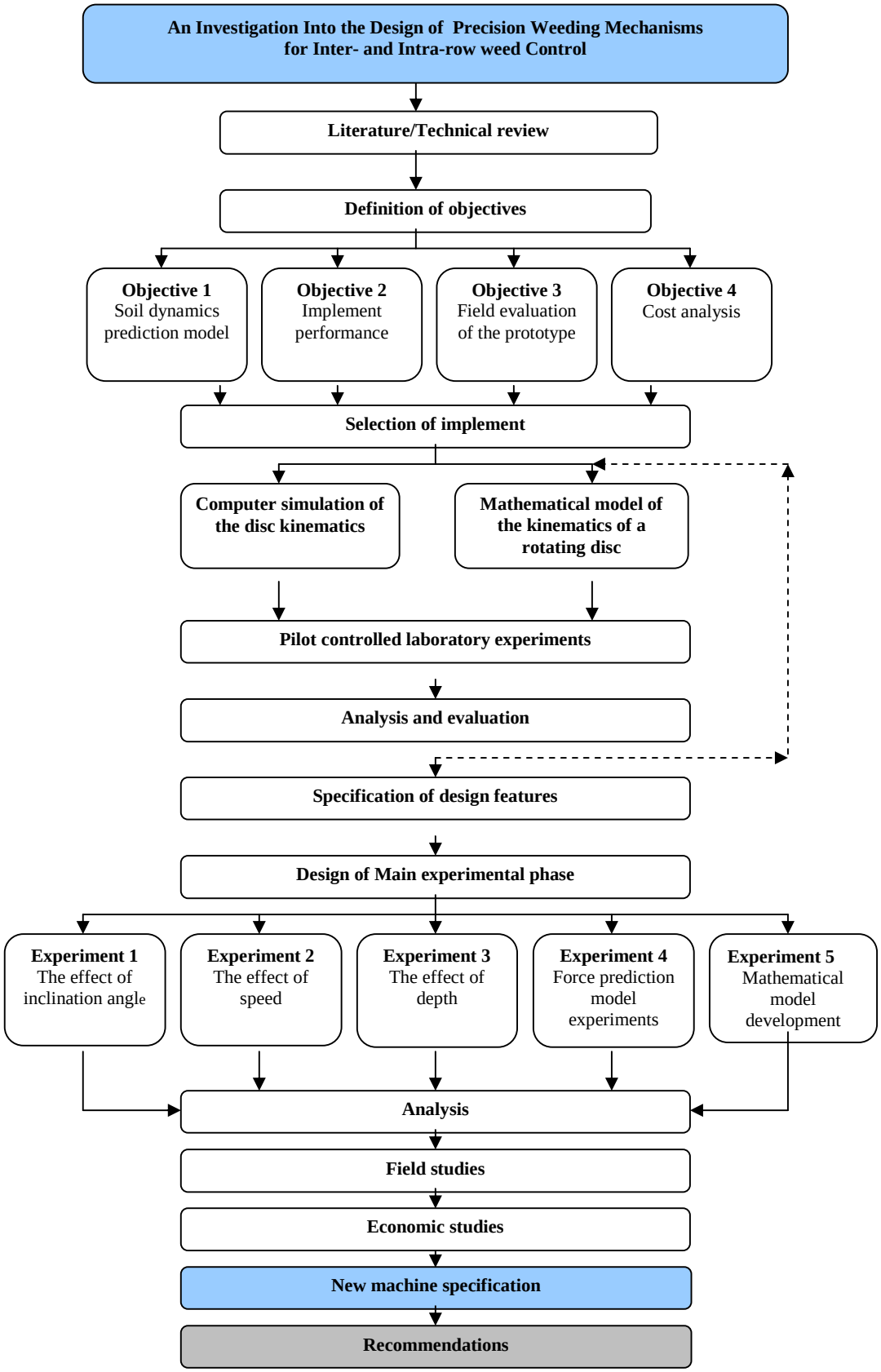

Figure 1-2 Structure of research program

Chapter 2

Literature Review

2. Literature review

The aim of this Chapter is to investigate the existing weeding mechanisms that are used for physical weed control with the utilization of soil engaging implements for inter and intra-row weed control. In the light of this review an attempt has been made to highlight the advantages and disadvantages of each mechanical weed control system.

2.1 Necessity for weed control

A weed can be thought as any plant growing in the wrong place at the wrong time and doing more harm than good (Parish, 1990). Weeds compete with the crop for water, light, nutrients and space. Therefore, weeds reduce crop yields and also affect the efficient use of machinery (Parish, 1990), especially that required for harvesting and can spoil the quality of the product. Even though many strategies for weed control can be contrived, weeding usually forms the most serious bottleneck in the farming operations (Hoogmoed, 2002).

Today consumers demand natural quality products, without any or with limited chemical treatment (Blasco *et al.*, 2002). This is why researchers are studying in more detail alternative techniques to eliminate weeds such as thermal techniques and precision weeding with the use of robotic technology. Likewise there has been an interest in mechanical intra-row weed control methods during recent years due to the public debate about environmental degradation and the growing request for organically grown food (Fogelberg & Kritz, 1999; Pullen & Cowell, 1997).

Because of weeds ability to grow wherever they find desirable environmental conditions it is necessary to classify them in relation to their position in the field. The weeds that are between the crop rows are called inter-row weeds and the ones that are located within the crop row are called intra-row weeds (Figure 2-1).The inter-row

weeds are easier to control because of the easy access of simple cultivation implements between the crop rows as it can be seen in Figure 2-1. Furthermore most of the research carried out in mechanical weed control and technical developments that have been achieved concerns the elimination of the inter-row weeds.

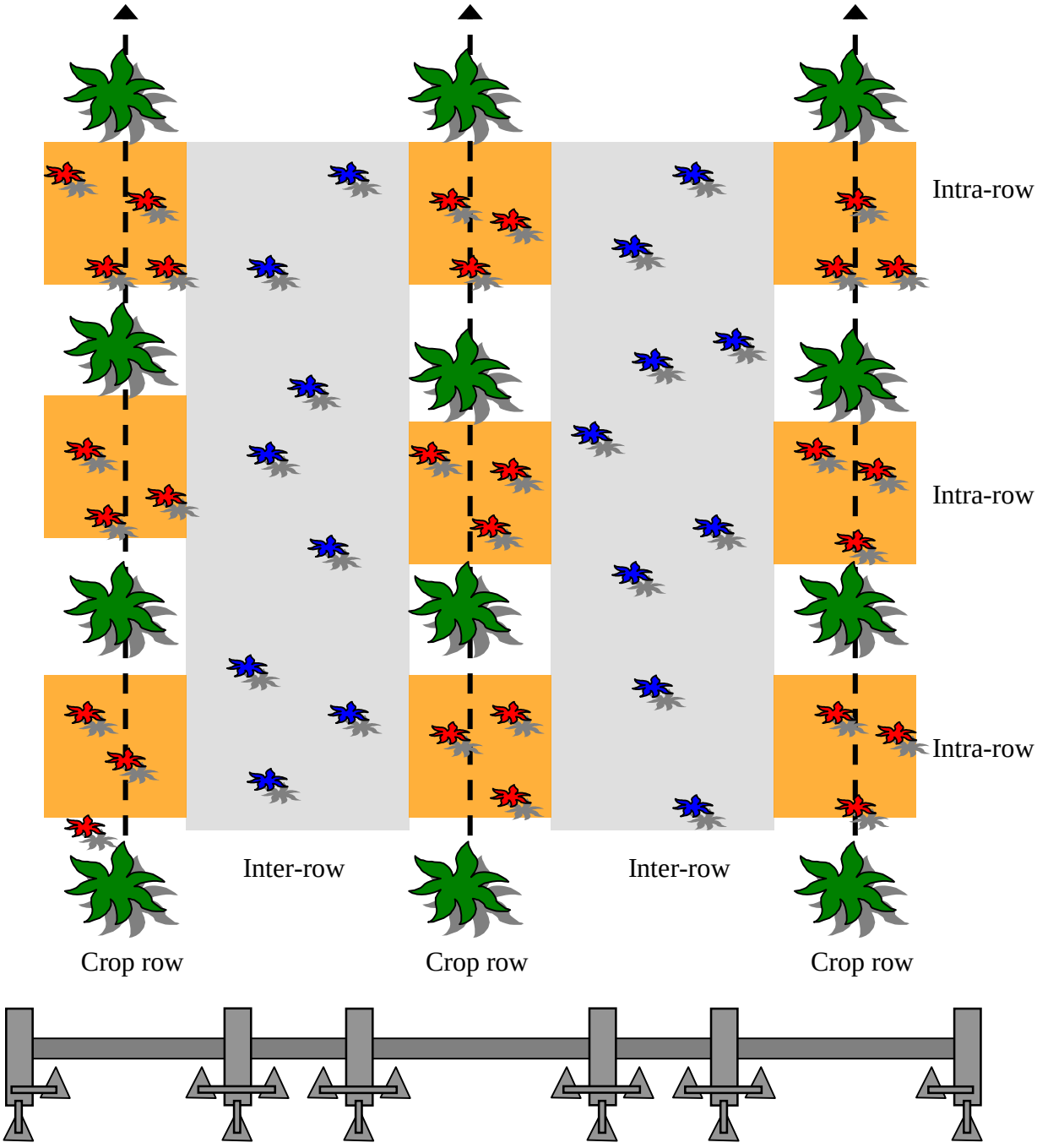

Figure 2-1 Inter and intra-row weeds (weeds are in the shaded areas)

On the other hand intra-row weeds are more difficult to control as they are located very close to the plant in various positions and there is a danger of damaging the utilized plants when approaching very close to kill the weeds. So a better understanding of soil failure and soil movement around the soil-engaging tools influence the uprooting and covering performance could help to improve selectivity beyond the limits imposed by the actual design of implements (Kurstjens, 2002). This will enable the design of specialized and efficient equipment for mechanical weed control purposes. Intra-row weed control is a significant challenge for both researchers and farmers, especially those weeds that are located in sensible areas peripheral to the utilized crop as it can be seen in Figure 2-1, and special equipment is needed and the soil-engaging processes are more complicated.

There are currently no commercial techniques available to viably control intra-row weeds and there had been no significant advances in inter-row cultivation apart from the introduction of guidance systems to improve their overall lateral positioning accuracy (Home, 2003). Such knowledge could support farmers in optimizing their mechanical weeding operations and take maximum advantage of versatile, simple and cheap non-chemical weed solutions, before introducing more complex high-tech machines like weeding robots (Kurstjens, 2002).

2.2 Types of weeds

It is estimated that world-wide there are about 1200 weed species (Hoogmoed, 2002). Adding to this number the crops that sometimes act as weeds, it is clear that there is a need to adopt a classification of weed plants with respect to their control, to be based on the way the plants develop and propagate.

Table 2-1 Type of weeds

Type of weeds	Multiplication by
Annual weeds	Seeds
Perennial weeds: roots	Roots, root-like plant parts and seeds
Perennial weeds: bulbs	Bulbs, bulb-like plant parts and seeds

2.3 Weed control techniques

The weeding methods can be distinguished in three major divisions according to the measure in chemical, biological, and physical. Chemical weed control is a very common measure applied to eradicate weeds, by using chemical substances (herbicides). Biological control involves the action of parasites, predators or pathogens on the population of weeds. This means a control by letting insects or disease attack the weed plants. Physical control of weeds uses methods that do not utilize chemicals, insects or pests. It is exemplified by the control through tillage, although other methods such as mowing, burning, mulching, flooding and competition can be mentioned. This review examines only physical weed control techniques using only soil engaging implements.

In this section weed control techniques are described that do not utilize chemicals, insects or pests. There are two categories of non-chemical weed control and these are (a) with soil engaging implements that are exemplified by control through tillage or other methods such as mowing and (b) the non-soil engaging techniques that use other devices to control weeds in a physical way such as burning the weeds, without the use of chemicals.

2.3.1 Soil engaging

This section reviews the relative merits and ability of soil engaging weeding mechanisms to operate in crops planted at different row widths.

2.3.2 Harrows

Commercial harrows exist in two forms, the spring tine harrow and the chain harrow. The action of the harrow is simple as it acts uniformly over the entire area controlling both the inter-row and intra-row weeds. Its relative simplicity has made it one of the most commonly used weed control tools.

Spring-tine harrow weeders, consisting of multiple gangs of tines mounted onto a tool bar, are pulled across the field by the tractor. The spring tine harrow (Figure 2-2) is used broadcast, both over and between the crop rows. Spring-tine harrows operate through growing crops, and work on the principle that more damage is done to the weeds than to the crop (Pullen, 1995). They are most efficient when weeds are in the white thread or cotyledon development stage (Bellinder, 1997). The weeding effect can be changed by adjusting the pressure on the tines (Pullen, 1995), by changing the diameter of the tines it is possible to either increase or decrease the aggressiveness in the soil; the tines may be either rigidly fixed or spring loaded (Home, 2003).

The chain harrow illustrated in Figure 2-3 consists of a chain mesh supported from the steel frame of the implement with much smaller tines or spiked teeth. It is often considered to be more aggressive to the crop and weed. In both forms of harrow the tines engage in the soil and destroy the weeds by loosening and uprooting them for desiccation and burial (Home, 2003).

Figure 2-2 Spring-tine harrow weeder

Figure 2-3 Flexible chain harrow weeder

Kouwenhoven (1997) reported that the spring-tine harrow weeders have a working width of 6 to 24 m and a working speed of about 6 km/h to 8 km/h, thus providing a large area capacity at relatively low capital cost. In order to achieve a high degree of weed control with this type of implement, selectivity decreases. According to Rasmussen (1990) and Kouwenhoven (1997) the weed/crop selectivity can be influenced by the timing of operation, the forward speed, the angle of the tines, the composition of the weed flora, the difference in the growth stage and plant height between the crop and weeds.

Kurstjens *et al.,* (2000) studied the selective uprooting by weed harrowing on sandy soils and found that harrowing uprooted 51% of the emerging plants and 21% of the plants in the seedling stage; 70% of all uprooted plants were completely covered by soil. This study indicated that uprooting was supported by the higher level of soil moisture content and increased working speed.

According to Bellinder (1997) the advantages of harrow weeders are:

- They are available in large widths.
- When used at pre-emergence they can operate at high speeds.
- Flex-tine implements are useful for a number of row crops and row spacings with little or no equipment modifications.
- Tines that pass over the crop row can be lifted, allowing for aggressive between row harrowing when the crop is sensitive to cultivation damage.
- Pre-emergence harrowing breaks crusted soils and may increase crop emergence rates.

Bellinder (1997) also listed the disadvantages of the harrow weeders as follows:

- Cultivation timing is critical; weeds with four or more leaves and emerged grasses at any stage are rarely controlled.
- Early season flex-tine harrowing should be integrated with a more aggressive cultivator or with post emergence herbicides for control of escaped or newly germinated weeds.
- Research had shown that in some crops (broccoli, snap beans, sweet corn) spring-tine harrows can reduce the yield if they are used before the crop establishes its roots.

2.3.3 Hoes

Broadly hoes exist in two forms, the sweep and the ducksfoot. Hoes operate between the row crops, and thus are less dependent on the growth stage of the weed population than harrows. Hoes consist of a toolbar that is mounted on the tractor and is attached the weeding mechanism (soil engaging blade attached to the leg) as can be seen below in Figure 2-4.

Figure 2-4 Tractor mounted hoe for inter row cultivation

Each row is covered by one or more hoes depending on the spacing. The unit normally has its own depth wheel and is attached to the main tool frame by a spring loaded parallel linkage, thus ensuring operation at a precise working depth.

There are several machines on the market but they are all similar in design. The blade configured is either an “L” or “A” shape (Figure 2-5 (a)) and controls the weeds by cutting their roots just below the surface. According to Pullen (1995) the operating depth is normally about 25 mm. The ducksfoot blade shown in Figure 2-5 (b) differs from a sweep in that it has a raised profile where the tool is attached and controls the weeds by subsurface cutting, burial and mixing. The ducksfoot blade is normally attached to a spring tine.

(a) (b)

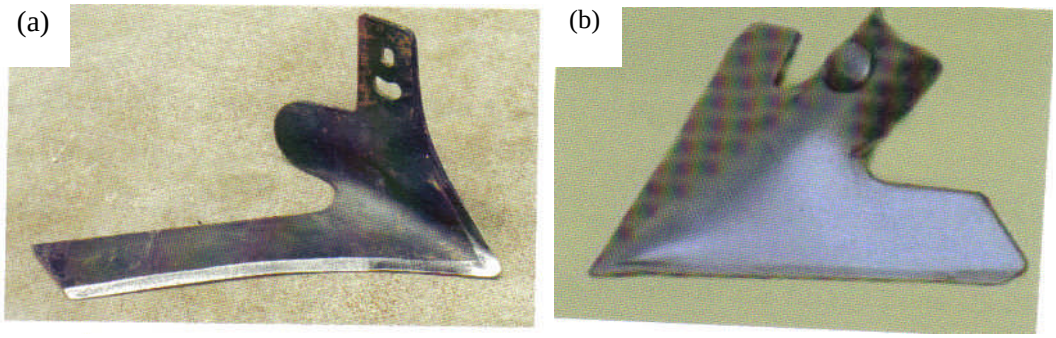

Figure 2-5 (a) sweep “L” shape (b) ducksfoot

During the last decade a lot of research has been conducted in the EU concerning the inter-row and intra-row control of weeds by the use of hoes. Cowell (1992) studied the accuracy of control of tractor mounted hoes, so as to minimize the damage to the utilized crop. In addition, promising results have arisen from research on weed control by precision guided implements (Pullen, 1995; Zuydam *et al*., 1995; Melander & Hartvig, 1997; Home *et al.*, 2001; Wiltshire *et al.*, 2003; Tillett & Hague, 2004) and two mechanisms are commercially available in the market by Eco-Dan (Denmark) and Garford, "Robocrop" (United Kingdom).

Furthermore, there are hoe-ridgers (Figure 2-6) in which the primary target is to control the intra-row weeds by burial whilst also controlling the inter-row weeds through burial and subsurface cutting. The hoe-ridger forces the soil to move outward from the row and placement of soil is between the crops due to its high rake angle (Home, 2003).

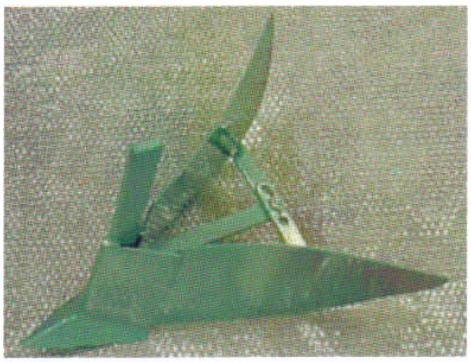

Figure 2-6 Hoe ridger

Terpstra and Kouwenhoven (1981) in their study of the use of a hoe ridger for inter-row and intra-row weed control found that 57% of the inter-row weeds were killed by covering with soil and 33% by uprooting and drying at the soil surface. Also alongside the hoe path, in a band of width 150 to 200 mm, 45% of the weeds were killed by being covered with soil loosened in the path of the hoe with a soil cover of 15 mm to 20 mm in a band of width 50 to 100 mm. Furthermore in the same study Terpstra and Kouwenhoven (1981) investigated the influence of the working depth and found that when increasing it from 25 mm to 40 mm there is an increase of 10% in the number of the weeds killed.

The advantages of the hoes used in this study were:

- Hoes are available in large widths.
- They can operate at high speeds.
- They are more effective with larger weeds than harrows because of the weeding action, subsurface cutting and/or burial instead of uprooting only.

The disadvantage was:

- Risk of crop burial due to extreme lateral translocation of soil.

2.3.4 Rotary hoe

The rotary hoe (Figure 2-7) is simple in design and reliable to use, which makes it attractive for use in developing countries. It is a non-powered rotary weeder with "star" or "spider" rotors placed between rows. The rotors are set at a small angular offset to the direction of travel such that there is a scuffing action that moves soil away from, or towards the row. Mattson *et al.*, (1990) in their study reported that such machines worked best on light, stone free soils where penetration was easy. Weed control was achieved partly by dragging entire plants on to the soil surface and partly by burial. The small weeds were the easiest to control. Also Rasmussen (2002) in his study recommended a speed of 10 to 20 km/h, which indicates a very high field capacity for the tool.

Figure 2-7 Rotary hoe

The advantages of the rotary hoe are:

- High capacity owing to the high operating speed (up to 14 km/h)
- Low draught requirement
- Ease of use and maintenance
- Easy to adapt to other conditions or to increase its width
- Can be combined with other implements
- Can be used over a wide range of soil moisture content provided that the soil can take traffic
- Work very well in dry soils

The disadvantages of the rotary hoe are:

- The possibility that a compacted layer may be formed at a shallow depth
- Not effective for larger weeds
- There is a risk of choking

2.3.5 Split hoe

The split hoe (Figure 2-8) is also another non-powered rotary weeder. It consists of a number of spring tines radially mounted on steel discs that are mounted on a common horizontal shaft that is free to rotate. Forward tractor movement results in the tines rotating and engaging the soil. Weed kill from the split hoe is attributed to uprooting with some burial and stripping, although this has not been quantified (Home, 2003).

Figure 2-8 Split hoe

Tei *et al*., (2002) found that the split hoe can give optimum results when operating at a depth of 50 mm and at a forward speed of 3 km/h. A study by Meyer *et al.*, (2002) shows that the split hoe achieves a better result than the standard spring-tine harrow. It was reported that it worked well in wet/crusted soils with large weeds and also gave high efficacy on lighter well-structured soils, controlling weeds up to 600 mm high.

2.3.6 Basket/cage weeder

The split hoe is another non-powered rotary weeder. As it can be seen in Figure 2-9 there are two horizontal axes upon which the baskets are mounted. The two axes are connected via a chain and sprocket arrangement providing a difference in rotating speed between them. As they are dragged across the ground, the baskets have a "scuffing" action on the soil. The bars that scrub the soil are either parallel to the rotary axis, or are skewed for different levels of aggressiveness.

Figure 2-9 Basket/cage weeder

The hoe works only for small weeds in friable soil in the top 25 mm without moving soil into the crop row and cannot deal with long stemmed residue (Bowman, 1997). The weeder is often used in conjunction with a sweep or ducksfoot to loosen the soil, and provide a tilth in which it works well (Home, 2003).

2.3.7 Finger weeder

The finger weeder (Figure 2-10) is a machine designed specifically for intra row weed control. Normally it would be used with an inter-row cultivation blade. Steel cone wheels rotated by ground-driven spike tines, push 'fingers' just below the soil surface, reaching into the row. A difference in rolling radius between the spiked tines and rubber fingers results in a scuffing action within the row.

Figure 2-10 Finger weeder

The finger weeder has changed weed control strategy in many organic vegetable farms, where hand weeding or hand hoeing of planted vegetables has been nearly completely replaced by machine work (Leinonen *et al.,* 2004). According to Bellinder (1997) the finger weeder is most effective on small-acreage, high value crops. Kouwenhoven (1998) in his study recommended finger weeding as a low-tech solution. Also finger weeders work best at high speeds (>10 km/h) (Kouwenhoven, 1998). In loose soil, finger weeders were not able to significantly move soil and weeds from the row, because of lacking slip of the rubber fingers. There is requirement to study the weeding effect of these machines in more soils (Sogaard, 1998; Peruzzi *et al*., 1998; Bleeker and Weide, 1998; Kurstjens and Bleeker, 2000; Bleeker *et al*., 2002). Bellinder (1997) in his study listed the advantages and disadvantages of finger weeders as given below.

The advantages of finger weeders are:

- They offer excellent in-row weed control.
- They are lightweight and can be semi-mounted on a small tractor.

The disadvantages of finger weeders are:

- They must be used when weeds are small; therefore timing is critical.
- Between row control is poor and they should be used in combination with an inter-row cultivator.
- Slow and precise cultivation is necessary to minimize crop damage.

2.3.8 Torsion Weeder

The torsion weeder (Figure 2-11) is mounted on an existing inter-row cultivator for improved intra-row weed control. It is a simple tool that has spring-loaded steel rods on each side of the crop row that undercut small weeds. The width of the uncultivated strip is easily adjusted for each crop and development stage (Bellinder, 1997). The tines control the intra-row weeds and a secondary hoe is required to control the inter-row weeds. The weeder is relatively inexpensive and simple in design. The aggressiveness of the implement can be adjusted by changing the diameter of the tine.

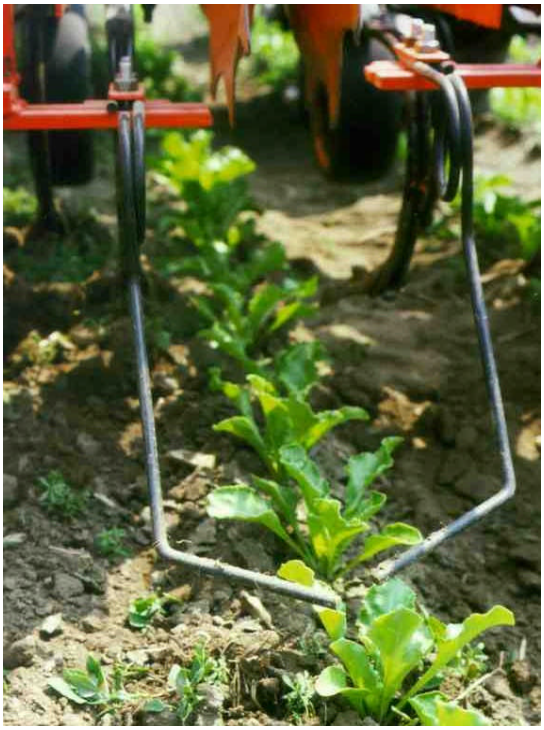

Figure 2-11 Torsion weeder

The weeding actions are up-rooting and soil covering (Home, 2003). Kurstjens (2000) in his study found that torsion weeders at the 8-10 leaf stage uprooted 86% of the small weeds and 34% of the large weeds, whit 5% crop loss.

The advantages of torsion weeders according to Bellinder (1997) are:

- They offer excellent in-row weed control.
- The simple design minimizes potential cultivator repairs.
- They are an economical addition to an existing cultivator.

The disadvantage is:

- Careful, and accurate cultivation is important.

2.3.9 Brush weeder

Brush weeders can be divided into two types; those with a horizontal axis (Figure 2-12) and those with a vertical axis (Figure 2-13). The first type is only suitable for inter-row weed control, whereas the second can be used both inter-row and intra-row. The horizontal brush weeder is typically powered by the tractor mechanical power take off (PTO), and the vertical brush weeder is normally driven by hydraulic motors. It consists of flexible polypropylene brush discs assembled into units of the desired width and spacing for the crop. Both types work in the soil to a depth of 20 to 30 mm and are designed to uproot small weeds (Kouwenhoven, 1997). The effect of the brushing action is to lift the weeds out of soil, strip leaves, break stems and expose roots as leaving them vulnerable to desiccation (Parish, 1990).

Figure 2-12 Horizontal brush weeder

Figure 2-13 Vertical brush weeder

To obtain a satisfactory effect in mature weeds, a further increase in the normal speed of rotation of the brush is necessary (Pullen & Cowell, 1997). In the same study the maximum diameter of the brushes for inter-row work was found to be limited by the row spacing. When they are only used for intra-row weed control, the diameter must be smaller (0.3 to 0.4 m). Brush weeding in dry conditions results in dust becoming a major problem (Pullen & Cowell, 1997).

The weed control effect is very good with small seed-propagated plants (Mattsson *et al.*, 1989). Fogelberg and Kritz (1999) in their study found that brush rotation direction has a crucial influence on the in-row soil ridge. Furthermore, in the same study, an increase in working depth and soil moisture increases the ridge height when the brushes are operating in a ridging mode.

Brush weeders have an advantage over mechanical hoes as they can operate in soil conditions with increased soil moisture levels (Parish, 1990).

Although brush weeders are used for intra-row weed control there is a risk that the crop will be damaged (Bontsema *et al.*, 2000). Also Fogelberg (2007) mentioned that the system was taken off the market due to the requirement of many settings prior the treatment.

2.3.10 Powered rotary weeder

The powered rotary cultivator operates between the crop rows and controls the inter-row weeds (Figure 2-14). A frame supports the main shaft which is mounted across the direction of travel and supported by bearings, either in the centre or at both ends. The rigid soil-engaging tools (blades or knives), are mounted on separate flanges (at > 20 cm) each with up to 6 tools arranged in “working sets”. The blades are set to the left and right in equal numbers of pairs (2 to 6), except for the sets at the sides. The complete unit made up of shaft and tools is called the rotor. The blades are arranged in a spiral pattern to provide smooth operation: only one blade should engage the soil at

a time. The rotor is driven by chain transmission or gear-wheels from the centre or at one of the sides. There is usually a gearbox and overload safety device between the tractor drive system (PTO shaft and drive shaft with universal joints) and the drive system of the rotor. The rotor usually rotates in the same direction as the tractor wheels. On both types a hood is used for additional crumbling of the soil aggregates and for guiding the flow of soil material produced by the rotor protection against flying stones. One or more trailing screens extending over the entire working width may be used to level the soil surface. Rotary cultivator working depth can be adjusted by gauge wheels or skids or by using a packer. Because of their short length rotary tillers are very suitable for attaching tools to the rear (rollers to compact or crumble the soil) and for mounting sowing equipment (direct drilling).

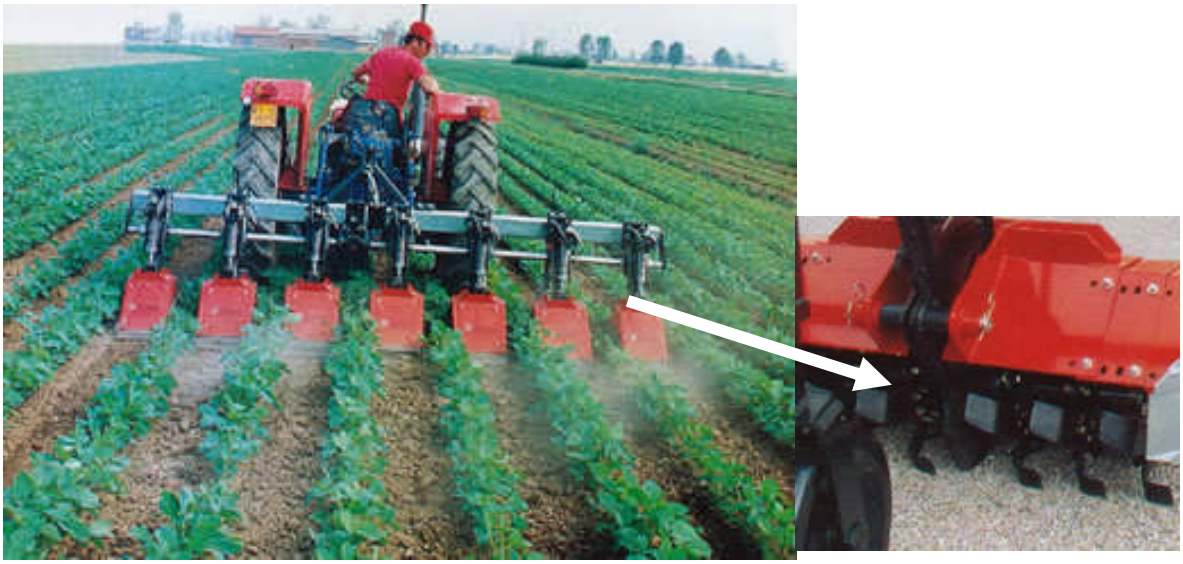

Figure 2-14 Powered rotary inter-row weeder

Mattsson *et al.,* (1989) found that powered rotary cultivators worked well on light, stone-free soils but could damage soil structure in some conditions. Weed control was achieved partly by dragging entire plants on to the soil surface and partly by burial (Mattson *et al.*,1989).

The advantages of powered rotary cultivators are:

- The desired crumbling and mixing can be achieved at a wide range of soil conditions by adjusting the speed of revolution and forward speed.
- They are suitable for working in organic material, mulching, grassland clearing (accelerating decomposition);
- They produce hardly any tillage or compaction pans;
- The power transmission is very efficient (about 80%) because of the PTO drive.
- They cause little slippage of the tractor driving wheels and so uphill working is possible.
- Their short length removes less load from the front axle of the tractor.
- They can be combined with mounted sowing machines.

The disadvantages of powered rotary cultivators are:

- The power required per volume of manipulated soil is high compared with a (chisel) plough because of the operating intensity.
- When the tillage intensity is too high (high rotational speed, low forward speed), the operation may cause surface slaking, crusting and soil erosion.
- Accelerated decomposition of organic matter can be expected.
- The drive shaft must match the tractor PTO shaft (profile, length) and adaptors are sometimes necessary.

Table 2-2 gives a summary of the equipment available for physical weed control.

Table 2-2 Commercial equipment (*After Home, 2003*)

Device	Average Speed (km/h)	Depth (mm)	Weed control	Mode of action	Weed size (mm)
Harrow	7	20-30	Inter/Intra-row	Uprooting/burial	<50
Brush weeder	<3.5	15-45	Inter/Intra-row	Uprooting/burial	<25
Split hoe	3	50	Iner-row	Uprooting/burial	<50
Finger weeder	10	12-19	Iner-row	Uprooting	<25
Torsion weeder	<10	25	Iner-row	Uprooting/burial	<25
Hoe ridger	7	25-40	Inter/Intra-row	Burial/cutting/uprooting	Large
Subsurface tiller	8	100	Iner-row	Cutting	Large
Powered rotary	6	120	Iner-row	Cutting/burial/uprooting	<150
Rotary cultivator	10	20-50	Iner-row	Cutting/mixing	<25
Basket weeder	8	25	Iner-row	Scrubbing, uprooting	<20
Sweep	6	20-40	Iner-row	Cutting/burial/uprooting	Large
Ducksfoot	6	20-40	Iner-row	Cutting/burial/uprooting	Large

2.4 Novel intra-row mechanical weed control systems

2.4.1 Rotating disc tine

An intra-row weed control system developed by Wageningen University (NL) that consists of a vertical rotating disc of 300 mm diameter that has attached with springs two or more knives and moves above the crop row (Lempens *et al*., 1996).

The rotating disc tine rotates at a constant speed of 850 rev/min and the knives are folded out due to the centrifugal force magnitude being larger than the spring force (Figure 2-15). When a plant is detected the disc decelerates to 700 rev/min and due to the inertia forces the knives are folded in, allowing the disc to avoid the plant without contact (Bontsema *et al*., 1998; Cavalieri *et al*., 2001, Home, 2003).

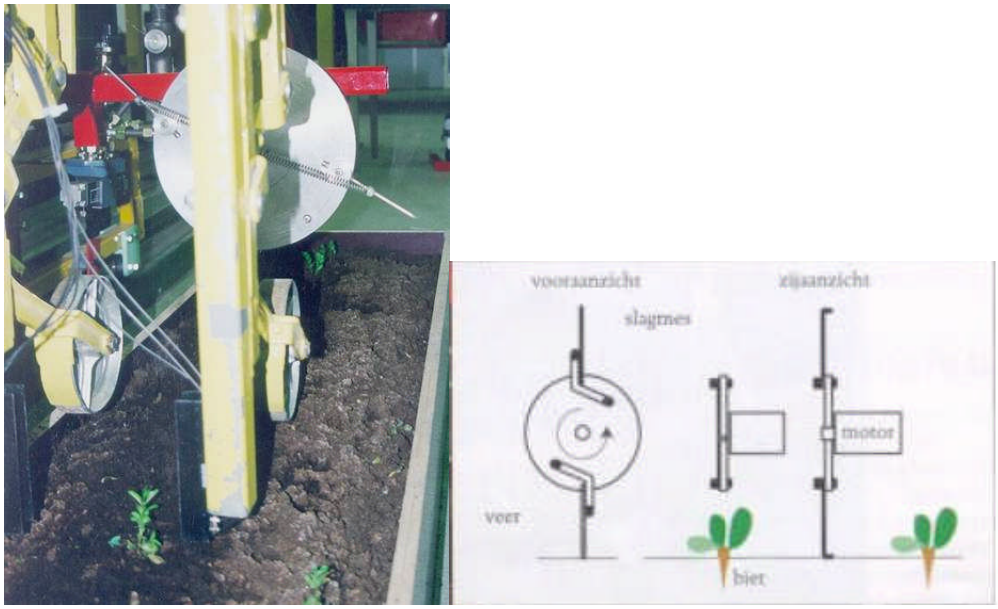

Figure 2-15 Rotating disc tine (Cavalieri *et al.*, 2001)

The detection system is placed in front of the disc and consists of three infrared transmitters and three infrared receivers that move at a constant height along the crop row (Bontsema *et al*., 1998). The signal is then sent to a digital signal processor (DSP) consisting of a single chip microprocessor (Bontsema *et al*., 1998).

The rotating disc tine did not reach the market due to several limitations. The weeding action is performed by cutting the weed above the soil surface, and studies of Jones *et al.*, (1995 & 1996) indicate that weed kill efficacy is reduced if there is only one mode of action, of the three possibilities i.e. cut, cover and uproot. Also the detection system cannot discriminate between plants and weeds, thus making the system appropriate only for transplanted plants.

2.4.2 Cycloid hoe

Osnabrueck University (DE) in collaboration with Amazone Werke developed a mechanical weed control system for inter and intra-row weed control, principally for maize (Cavalieri *et al.*, 2001)

The inter-row weeds are treated by the widely used commercially available 'goose foot' hoe blades. Each rotor consists of eight tines (Figure 2-16) that are placed in a circle around an axis, with a rotational diameter of 0.234 m (Griepentrog *et al*., 2006). The rotor rotates as do the tines in a circular motion. The combination of the circular movement of the tines and the linear movement of the implement leads to a cyclic path (Cavalieri *et al.*, 2001). Figure 2-17 shows the working principle of the cycloid hoe. Every individual tine in the rotor can be folded in and out by an electromagnetic circuit in order to avoid the crop. The cyclic movement of the hoe can be changed by adjusting the translation and rotation speed, as well the shape of the tines (Bakker, 2003). Cavalieri *et al*., (2001) reports that the cycloid hoe can operate at a speed up to 8.5 km/h.

Figure 2-16 The cycloid hoe (Griepentrog, 2007)

However Griepentrog *et al.*, (2007) tested the system at speeds up to 1.44 km/h and reported excessive crop damage and very low weed control efficacy. The cycloid hoe is still under development, Griepentrog *et al.*, (2007). There are some constraints that make the cycloid hoe an unattractive system for mechanical weed control. The design complexity, with many working parts which increase the maintenance and capital cost. Cavalieri *et al.*, (2001) forecast a capital cost of a six row machine of £21,051 with an additional cost of £29,599 for RTK GPS.

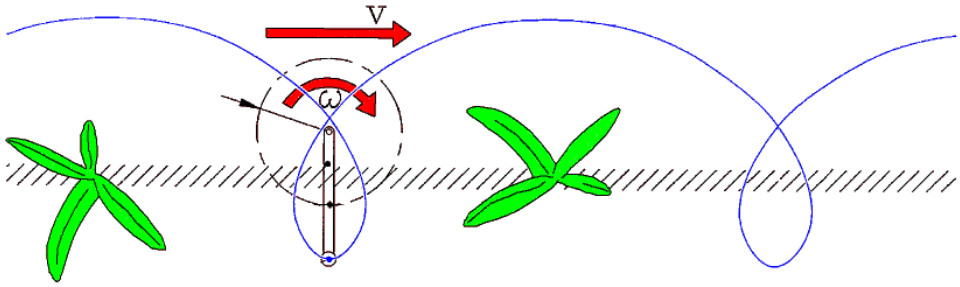

Figure 2-17 Working principle of the cycloid hoe (Gripentrog *et al.*, 2007)

These limitations together with an undisturbed circle around the plant of 18 mm, make the system difficult for adoption by organic farmers, due to crop damage if not adjusted properly. Also because of its mechanical design the system is difficult for use in crops over the two true leaf stage (two cotyledons) due to potential foliage damage. The soil type is another crucial factor for the system as is will be very difficult not to damage the crop as clods of soil will destroy the crop.

2.4.3 Radis moving tine

An intra-row weed control system which consists of blades mounted on a pivoting arm (Figure 2-18) developed by Radis Mechanisation (FR). Light sensors similar to the ones used by the rotating disc tine (Section 2.4.1) sense the plants. When no plant is detected the pivoting arm is moved in the intra-row area by an air pressure cylinder, thus cultivating and removing the intra-row weeds. Bakker (2003) report that at a

driving speed of 5 km/h weeds are removed up to 20 mm from the plant. However Bleeker (2005 and 2007) report a maximum speed of 3 km/h due to the mechanical transition of the intra-row hoe. The system is designed for wide spaced vegetables and the minimum intra-row spacing that the system can work is 220 mm (Bakker, 2003). The limitation of this system is the plant detection as mentioned earlier (Section 2.4.1). In transplanted crops in which the plant is way ahead of the weeds growing stage will not present a problem. For that reason (Bleeker & Van der Weide, 2007) intend to evaluate the system with a vision guidance system instead of light sensors.

Figure 2-18 The Radis intra-row weeder (Bleeker, 2007)

Another important factor that makes that system unattractive to organic farmers is the working speed of 3 km/h. However there are several implements sold in the European market purchased principally by Research Institutes and Universities, in order to further develop this weed control system.

2.4.4 Rotating wheel

Halmstad University (SE) have developed an intra-row weed control system that utilises a wheel that is rotating perpendicular to the crop-row (Figure 2-19). When the crop is detected by a computer vision guidance (Aastrand & Baerveldt, 2005), the rotating wheel is lifted up by a pneumatic cylinder and lowered down when it has passed the plant. Aastrand and Baerveldt (2002) evaluated the system in greenhouse experiments with sugar beet plants at an intra-row plant spacing of 170 mm and reported that "the robot was able to recognize all the plants and the weeding tool worked well". No information is given for working speed and weed control efficacy.

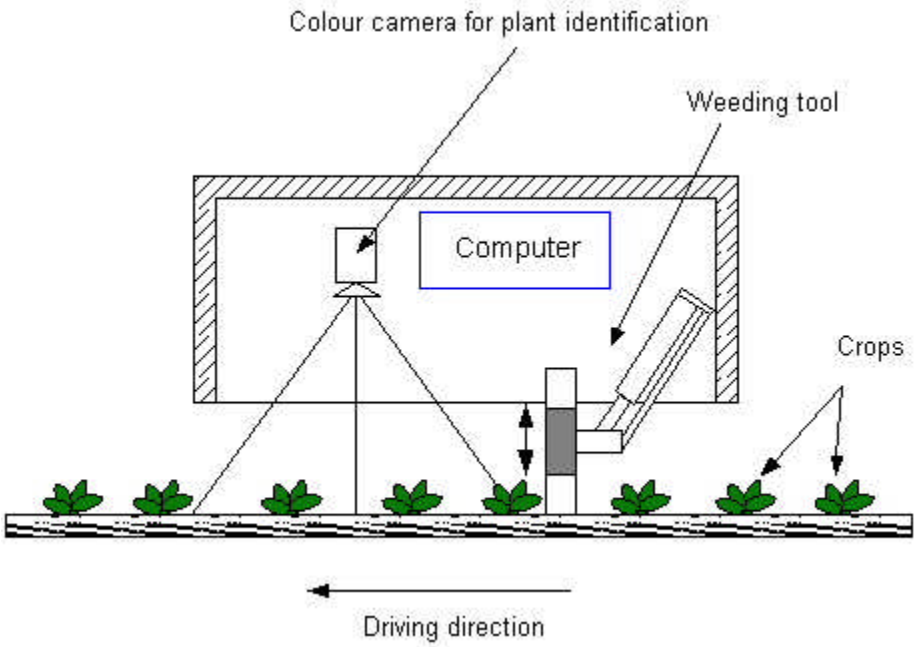

Figure 2-19 Description of the weeder with the weeding tool at the rear (Aastrand & Baerveldt 2002)

2.4.5 The rolling harrow

Pisa University (IT) developed an intra-row weed control system that consists of spiked discs placed at the front and gauge rolls similar to the ones used by the basket weeders mounted at the rear (Figure 2-20). The front and rear mechanisns are connected via a chain drive with a ratio equal to two (Peruzzi *et al*., 2005 a).

The spiked discs cultivate the top 30 to 40 mm of the soil followed by the gauge rolls that work shallower at a higher peripheral speed tilling and crumble the soil at the top 10 to 20 mm layer (Peruzzi, 2005 b). Intra-row weed control is achieved by placing flexible tines (Figure 2-21) at the rear of the machine acting as both vibrating tines and torsion weeders. The rolling harrow is controlled manually for lateral steering via a steering wheel as it can be seen in Figure 2-19 (Peruzzi, 2006).

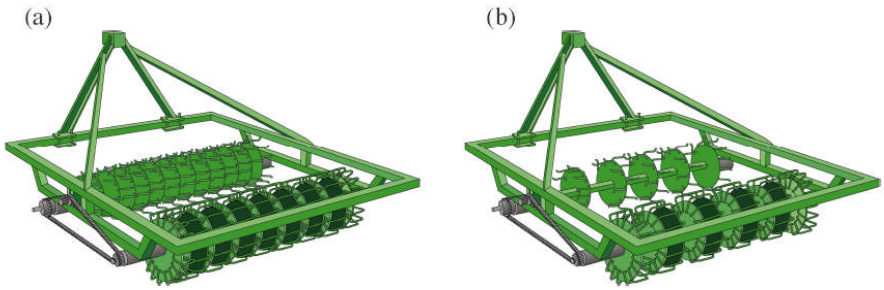

Figure 2-20 The rolling harrow arrangements (a) for non-selective and (b) selective treatment (Peruzzi *et al.*, 2005)

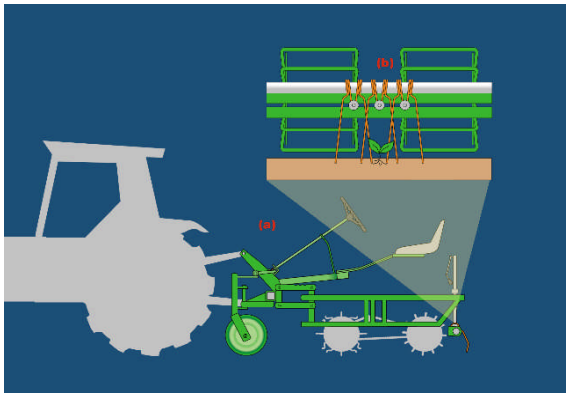

Figure 2-21 (a) The rolling harrow with (b) the elastic tines attached for intra-row weed control (Peruzzi 2006)

2.4.6 Intra-row cultivator

A novel intra-row system developed at Cranfield University at Silsoe and Silsoe Research Institute (UK) by Home (2003) that consists of an inter-row "ducks foot" blade that has attached to it reciprocating blades to treat the intra-row weeds (Figure 2-22). The plants are detected using computer vision and can discriminate between plants and weeds (Figure 2-23). When the plant is detected that blades are folded in and when there are no plants the motor activates the cam and the blades are folded out (Figure 2-22 b). Home (2003) undertook several field investigations of the proposed system with various intra-row plant spacing and working speeds. He found out that at a spacing of 300 mm the reciprocating intra-row blades avoid entering the root zone up to speeds of 4 km/h, but at 8 km/h 17% of the crop root zone was entered. At 250 mm intra-row plant spacing excessive damage was occurred with 70% of the crop zone being touched by the intra-row blades, and this was also made worse by increasing the working speed (Home, 2003). The rotating disc hoe presented in this thesis is a continuation of Home's (2003) intra-row weed control system.

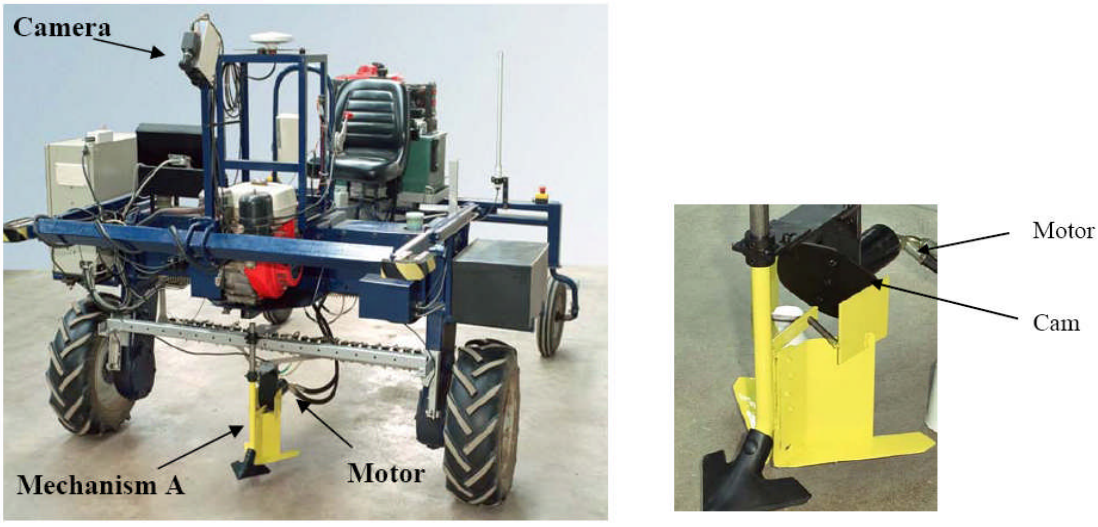

(a) (b)

Figure 2-22 (a) Autonomous vehicle with intra-row mechanism (b) Intra-row blade (Home, 2003)

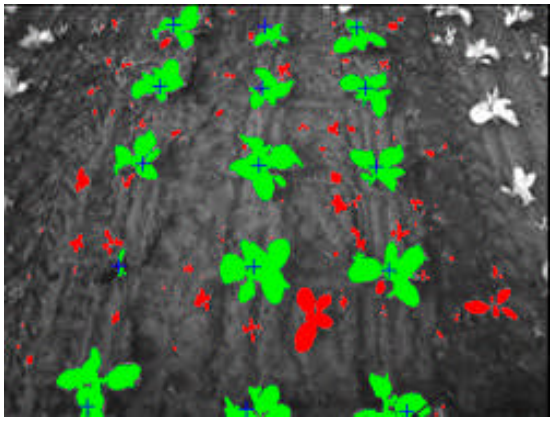

Figure 2-23 The vision guidance system (green is for plants and red for weeds)

2.4.7 Rotary hoe

University of Bonn (DE) developed an intra-row weed control system which consists of a rotary hoe rotating around the horizontal axis above the crop row (Figure 2-24). The hoeing tool consists of an arm holder and three or more integrated arms rotating around the horizontal axis above the crop row (Gobor & Lammers, 2006). The weeding tool is attached via a shaft to the motor and the working height of the whole assembly is adjustable (Gobor & Lammers, 2007). The system, to date, has only been tested in a virtual environment.

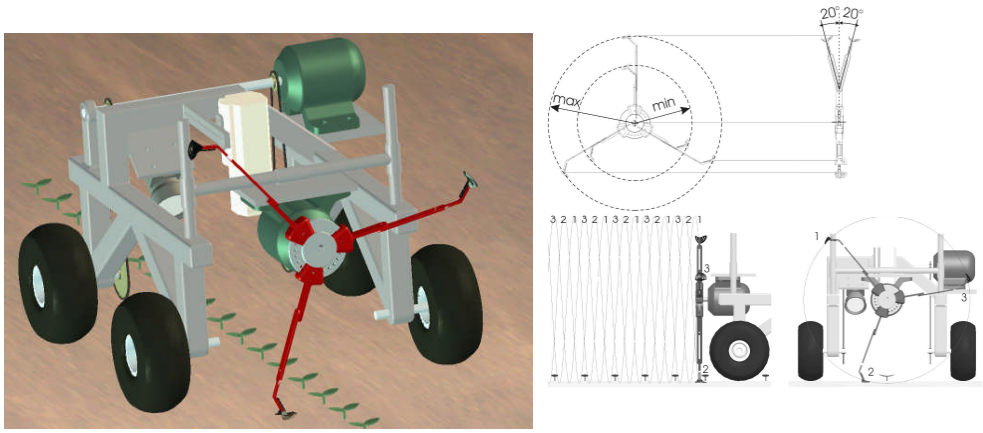

Figure 2-24 The rotary hoe (Gobor & Lammers, 2007)

2.5 Summary

There has been much research on physical weed control in row crops over the last decades (Ascard, 1990; Bond and Grundy, 2001, Home, 2003, Gabor, 2007, Dedousis *et al.*, 2007). Precision guided implements (Kouwenhoven *et al.*, 1991; Van Zuydam *et al.*, 1995; Pullen, 1995; Tillett *et al.*, 2002) and robotic systems (Tillett *et al.*, 1998; Lee *et al.*, 1999; Slaughter *et al.*, 2000 Blasco *et al.*, 2002) receive much current attention due to the excessive damage to soils by compaction and the requirements for less energy expenditure. Other approaches such as band streaming soil have been tried to reduce weed emergence (Hansson & Svensson, 2007). There are still problems with weeds that grow in the row (intra-row) especially in organically grown crops when physical weed control is insufficient (Ascard, 1990; Melander & Rasmussen, 2001). New labour-saving methods for controlling the intra-row weeds are required as weeding is still the most serious bottleneck in farming operations (Rasmussen, 2003).

However, according to the review conducted by Home (2003) there are currently no commercial techniques to viably control intra-row weeds and there had been no significant advances in inter-row cultivation apart from the introduction of guidance systems to improve their overall lateral performing accuracy. In addition, the translocation of soil close to the crop has not yet been fully studied. Such knowledge could support farmers in optimizing their mechanical weeding operations and take maximum advantage of versatile, simple and cheap non-chemical weed control solutions (Kurstjens, 2002).

There is a large demand to improve physical weed control (Ascard, 2007) and a clear need for an improved technology. Both preventive methods and mechanical control should be further optimized.

Chapter 3

Design of Rotating Discs

3. Design of disc

The reason for designing a rotating disc that can work in the intra-row area is to overcome the limitations of the current intra-row weed control systems as mentioned earlier (Section 2.5). It eliminates weeds by cutting them (which is more effective) and also by covering them with soil. The disc can work at a constant distance from the plant centre without any reciprocation motion in the system that may cause problems in the operation as with the system proposed by Home (2003) with reciprocating blades which moved in and out of the row. This makes the rotating disc system simple as the only lateral movement results from the lateral steerage of the hoe to follow the plant row.

The purpose of this research was to investigate and design a precision weeding mechanism for inter-row and intra-row non-chemical weed control, overcoming the limitations mentioned in the literature and technical review (Chapter 2). The limitations identified provided us with the following criteria in order to design a feasible intra-row mechanical weed control system for high value crops. These are:

- Simple design of the weeding tool
- Acceptable capital cost targeting the organic vegetable market
- Minimum intra-row area of 150 mm
- Versatile design in order to cope with various inter- and intra-row spacing
- Combination of weeding actions for efficient weed kill by both cutting and soil covering
- Treat weeds close to the crops with an undisturbed zone (50 mm)
- Target a forward speed of 1 m/s (3.6 km/h)
- Adaptability to existing drilling/transplanter establishment

The selection of the disc geometry was a compromise between the required maximum cultivated area and the adequate tolerance to lateral and angular misalignment, which if insufficient, might led to crop damage. The tolerance required depended on the

dynamic performance of the whole system and the growth habit of the crop plants (Tillett *et al.*, 2007).

The aim of the graphical computer simulation of the disc kinematics study was to determine the optimum geometric characteristics for a rotating disc that will be able to treat the intra-row area between the crop plants undisturbed circle (Dedousis *et al.*, 2007).

3.1 Graphical computer simulation of the disc kinematics

A 300 mm inter- and intra-row plant spacing was taken and a 80 mm diameter of the undisturbed circle (non-till zone) surrounding the plant was specified (Figure 3-1). An initial cut-out angle was designed and then the disc was rotated by 36^{o} after moving forward by 30 mm (Dedousis *et al.*, 2007). This was repeated until the disc rotated 360^{o} in 300 mm (Figure 3-2). A number of disc combinations were investigated using Autodesk Inventor ®, Professional, version 9 (Dedousis *et al.*, 2005) to determine the optimum geometry and working distance of the disc from the crop row and the cut-out sector.

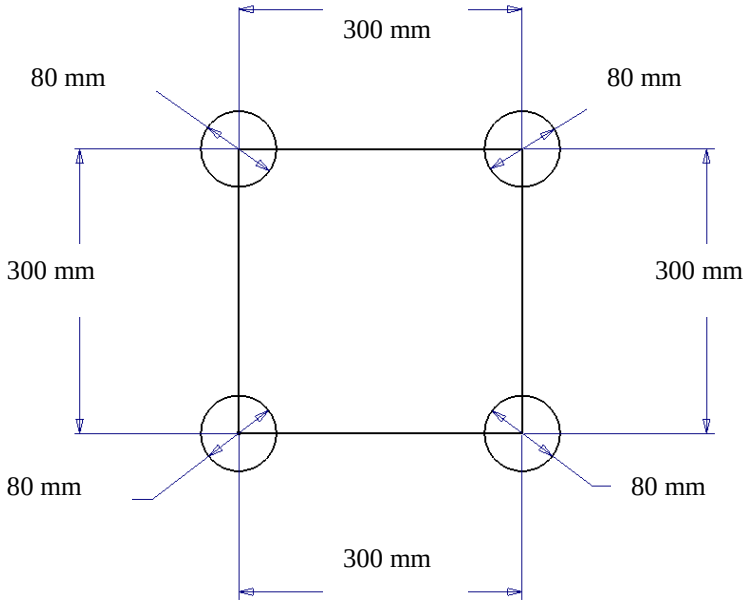

Figure 3-1 Template used during the graphical computer simulation of the disc kinematics showing inter, intra-row and crops undisturbed circle dimensions

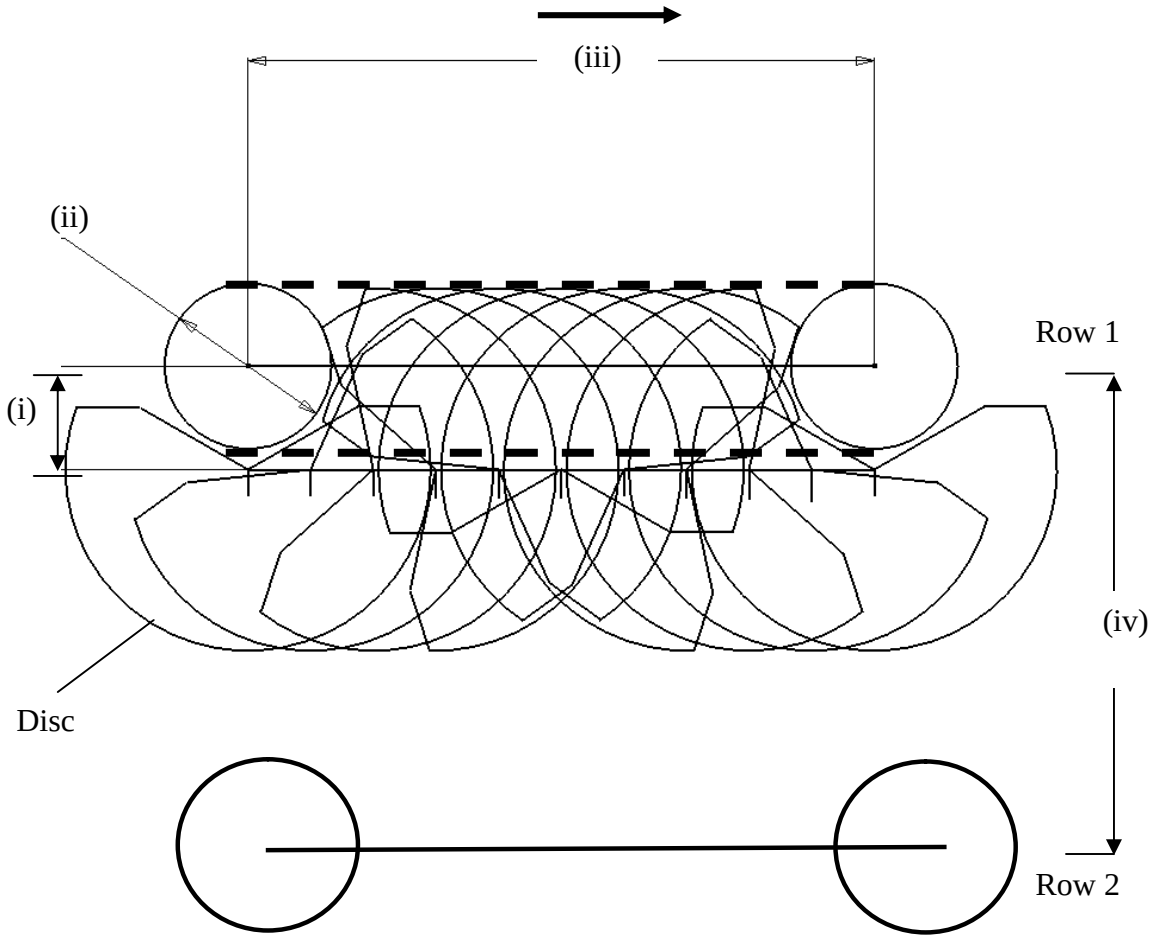

Figure 3-2 Graphical computer simulation of the disc kinematics (i) disc movement parallel to crop row, 50 mm (ii) crop undisturbed zone, 80 mm (iii) intra-row plant spacing, 300 mm (iv) inter-row plant spacing, 300 mm. The broken lines surround the intra-row treated area. The disc rotated by 36^{o} anti-clockwise every 30 mm of forward travel (Dedousis *et al.*, 2007).

Initially after considering a simple prototype (disc 0, Figure 3-4) one disc was chosen to be used in the soil bin laboratory experiments after the kinematic study as it did not penetrate the plants undisturbed zone. The geometry of the discs evaluated under the graphical simulation of the disc kinematics are given in Table 3-1. A diameter of 175 mm was found to be the most appropriate for the disc concerning the plant inter-row and

intra-row spacing of 300 mm. All the discs were simulated with a distance from the centre of the plant to the centre of the disc of 50 mm, 60 mm and 70 mm.

Table 3-1 Disc characteristics used in the pilot study

Characteristics	Disc 0	Disc 1	Disc 2	Disc 3
Diameter (mm)	175	175	175	175
Cut-out angle (deg)	130	120	120	130
Cut-out sectors (mm)	0	33.5	20	33.5
Thickness (mm)	3	3	3	3

Disc 1 was able to work only at a 50 mm distance from the centre of the plant. The kinematic study showed that while the disc was working 60 mm and 70 mm away from the centre of the plant a small penetration occurred (Figure 3-4 (b)). Discs 2 and 3 were able to work at all distances from the centre of the undisturbed zone (50 mm, 60 mm, 70 mm) without entering the plants undisturbed zone (Figure 3-4 (c) and (d) respectively). Also the cut-angle of no less than 130 degrees is essential and a disc with bigger cut-out sector is required.

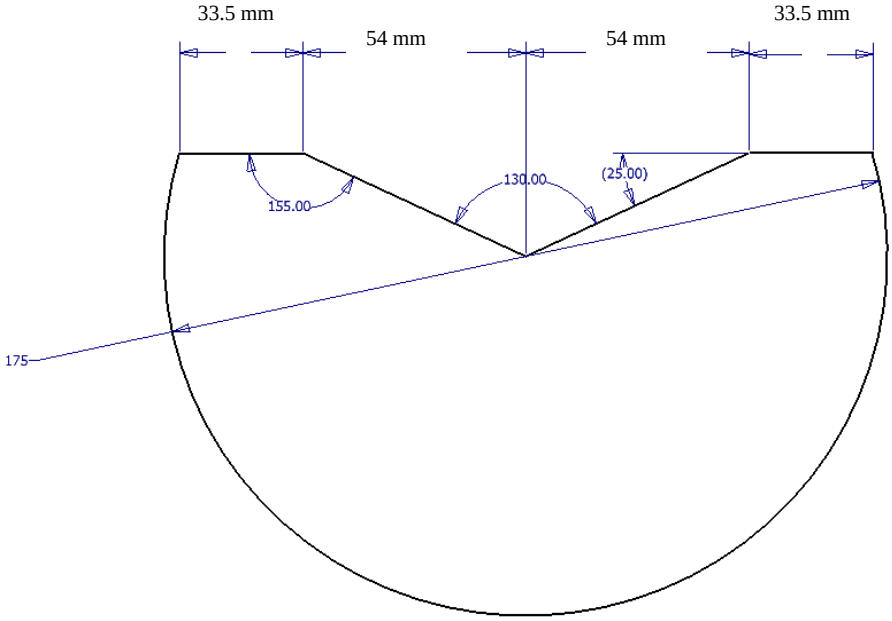

Figure 3-3 Disc 2D design used in graphical computer simulation (Dedousis *et al*., 2005)

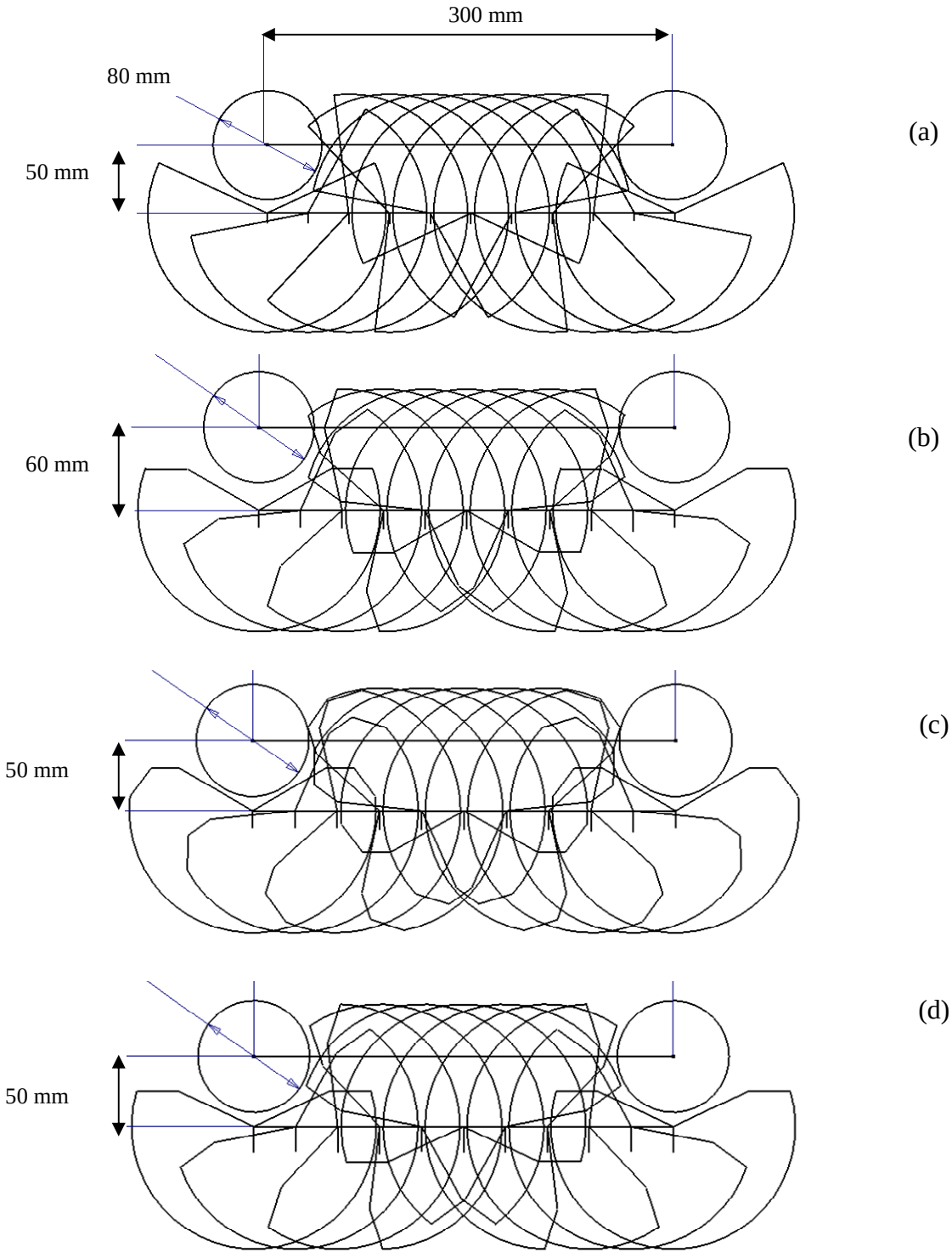

Figure 3-4 Computer study of disc kinematics results (a) Disc 0 used as the simple conceptual prototype (b) Disc 1, 60 mm from the centre of the plant to the centre of the disc (c) Disc 2, 50 mm from the centre of the plant to the centre of the disc (d) Disc 3, 50 mm from the centre of the plant to the centre of the disc

3.2 Mathematical model of the disc kinematics

A mathematical model for the kinematics of rotating discs was developed by O'Dogherty *et al.*, (2007 a and b) for use as an engineering tool to aid disc design. The results from the graphical computer simulation were confirmed by the mathematical model of the kinematics of rotating discs, with agreement between the graphical and mathematical simulation. The analysis on disc geometry in this thesis is based on the model of the kinematics of the rotating disc discussed in Section 3.1 that was described by O'Dogherty *et al.*, (2007 a and b) and is given in Appendix I. The model is based on an interactive spreadsheet (Figure 3-5) and allows fast computation by entering data such as disc radius, distance of line of motion of disc centre from the crop row and distance between plants centre, from which is possible to calculate the distance of any part of the disc along the crop row. The mechanism described in this thesis (Dedousis *et al.*, 2005, 2006) consists of a rotating disc which acts in a horizontal plane and has a cut-out sector and bevels cut back at its circumference, as shown in Figure 3-6. The results from the graphical computer simulation study were confirmed by the mathematical model of the disc kinematics. Figure 3-7 shows a comparison between the graphical and the predicted trajectory of two different discs.

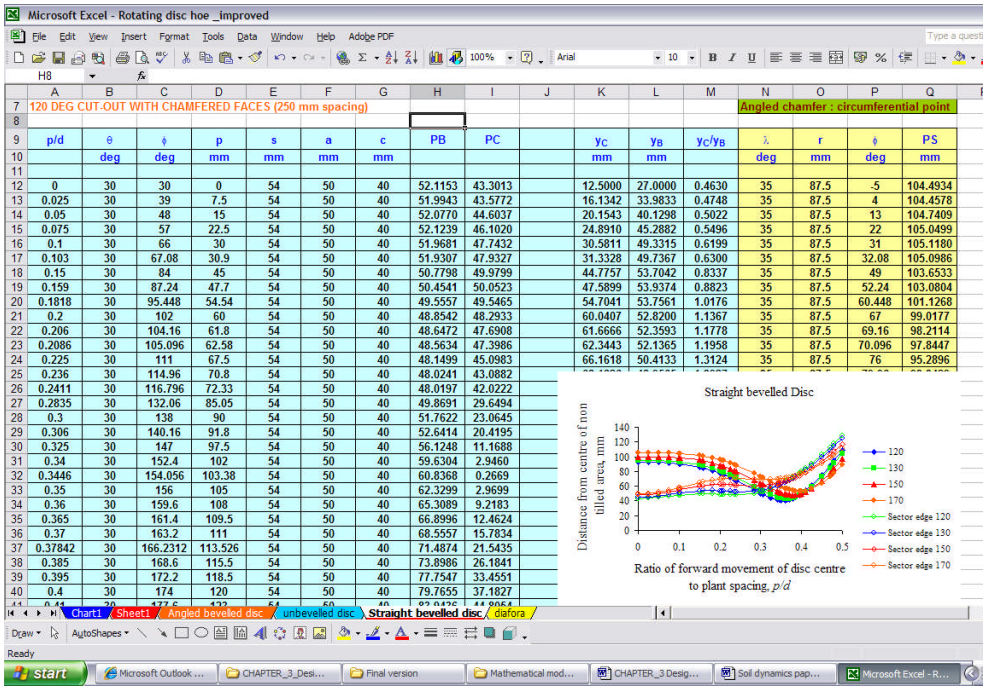

Figure 3-5 Screen image of the disc kinematics model

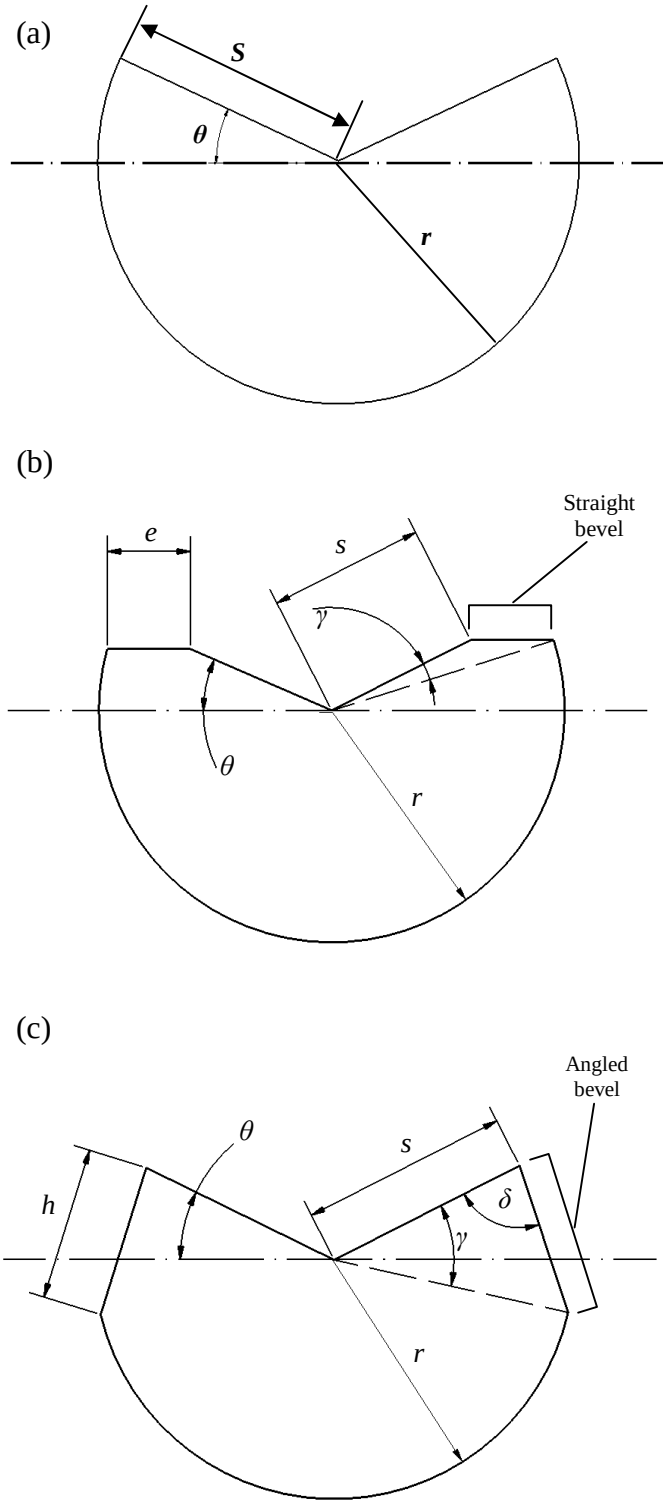

Figure 3-6 Examples of discs: (a) Unbevelled; (b) straight bevel; (c) angled bevel

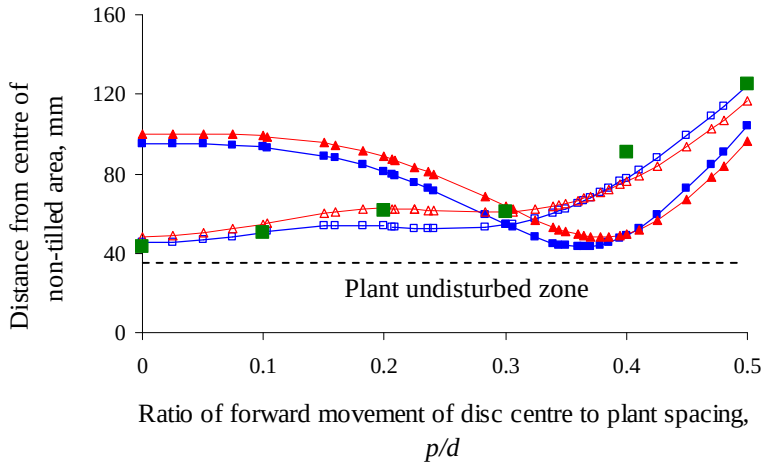

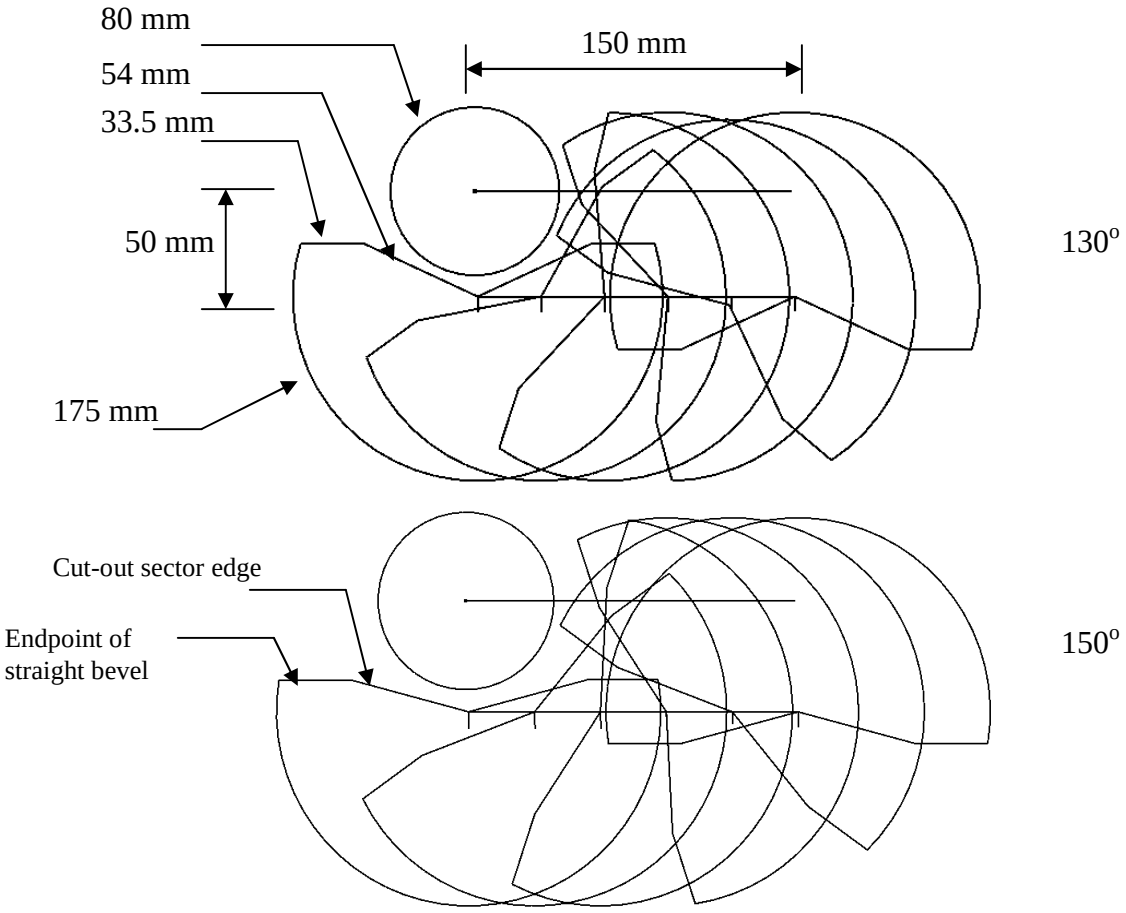

Figure 3-7 Predicted trajectories of two disc geometries for the cut-out sector edge, (□) 130° and (▵) 150° and endpoint of straight bevel (■)130° and (▲) 150° and the graphical simulation of the same disc geometries with the measured distance of the 150° cut-out sector edge from the centre of the non-tilled area (■) for the graphical computer simulation of the disc kinematics

3.3 Mathematical model results

To determine the transition between the criteria used for the distances *l* and *m*, it is necessary to determine the value of *p/d* for which y_B is equal to y_C. It is not possible to solve Eqn (19) (Appendix I) analytically but the relevant value of *p/d* can be found from a tabulation of the values for y_B and y_C using an interpolation procedure until y_B is equal to y_C .

The criterion used in the analysis was the distance from a plant centre of the nearest approach of any point on the disc during its motion parallel to the row. The distance must be greater than or equal to the radius of the no-till circle.

3.3.1 Simple disc geometry

The simplest disc design is that of a disc with a cut-out sector with an included angle α and no bevelled edges (Figure 3-6 (a)). In order to simulate the disc's performance it is necessary to take a particular example of disc and crop parameters. The following values were chosen as representative of a crop situation to provide adequate intra-row weed removal: plant spacing 300 mm; non-tilled area radius 40 mm; distance of disc centre from plant row 50 mm; and disc radius 87.5 mm. A series of simulations was carried out in order to investigate and find the most appropriate cut-out sector. For the simple disc geometry four cut-out sector angles were investigated, 120^o; 130^o; 150^o; and 170^o (Figure 3-8). For the 120^o cut-out sector disc the minimum distance of the sector edge from the centre of the non-tilled area was 24.3 mm, so that the end point of the sector will intrude into the non-tilled area, by 15.7 mm. For the 130^o; 150^o, cut-out sector discs the minimum distance of the sector edge from the centre of the non-tilled area was 28.4 mm and 36.7 mm, thus the end point of the sector will intrude 11.6 mm and 3.3 mm for the 130 and 150 cut-out sector disc. The 170^o cut-out sector disc did not enter the non-tilled area and had a 5.3 mm clearance. The results for the simple disc design showed that it is necessary to use an angle of 160^o or greater to avoid entering the non-tilled area.

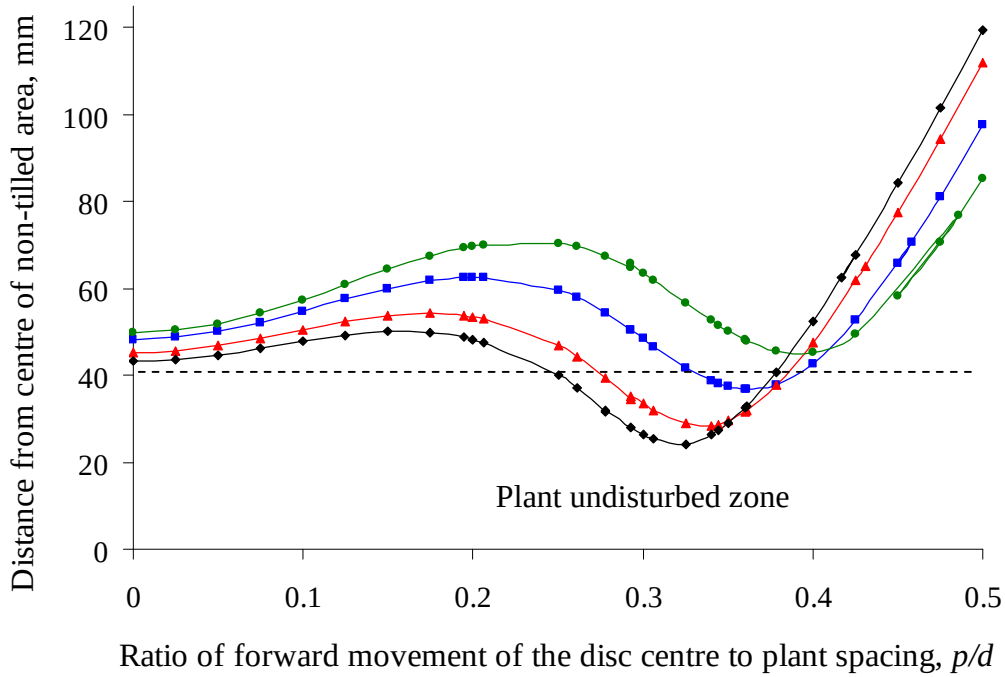

Figure 3-8 Effect of *p/d* distance from the centre of the plants undisturbed circle for unbevelled disc with cut-out sector angles of 120° (◆), 130° (▲), 150° (■), and 170° (●) (disc radius, 87.5 mm; plant spacing 300 mm; disc centre 50 mm from crop row)

3.3.2 Bevelled disc geometry

The results from the simple disc design geometry showed that modification of the disc is needed in order to avoid any part of the disc entering the non-tilled zone in case of lateral or angular misalignment. Figure 3-6 (b) shows a disc of the same radius, 87.5 mm and cut-out sector angle 130° with a straight bevel from a point on the cut-out sector parallel to the disc diameter of the uncut semicircle of the disc. It was found necessary to investigate the angled bevel as shown in Figure 3-6 (c) from a point on the cut-out sector to a point at the circumference of the disc.

3.3.3 Straight bevel

The same values were used as given in Section 3.3.1 as representative of a crop situation to provide adequate intra-row weed control. A series of simulations was carried out with cut-out sectors of 120^o; 130^o; 150^o; and 170^o with a cut-out sector edge of 54 mm and a straight bevel of 33.5 mm parallel to the disc diameter of the uncut semicircle of the disc (Figure 3-9). For the 120^o cut-out sector disc the minimum length of the sector edge is 48 mm and for the straight bevel is 40.7 mm. Hence, both the sector edge and the straight bevel do not penetrate into the non-tilled area, but lie outside it with 8 mm and 0.7 mm clearance for the sector edge and the straight bevel. For the 130^o cut-out sector disc the minimum distance of the sector edge is 52.3 mm and for the straight bevel it is 43.2 mm. Hence, both the sector edge and the straight bevel lie outside the non-tilled area with 12.3 mm and 3.2 mm clearance for the sector edge and the straight bevel. For the 150^o cut-out sector angle disc the minimum distance of the sector edge is 60.5 mm and for the straight bevel it is 47.9 mm. Hence, both the sector edge and the straight bevel lie outside the non-tilled area with 20.5 mm and 7.9 mm clearance for the sector edge and the straight bevel. For the 170^o cut-out sector angle disc the minimum distance of the sector edge is 68.9 mm and for the straight bevel is 53 mm. Hence, both the sector edge and the straight bevel lie outside the non-tilled area with 28.9 mm and 13 mm clearance for the sector edge and the straight bevel.

3.3.4 Angled bevel

A series of simulations was carried out with cut-out sectors of 120^o; 130^o; 150^o; and 170^o with a cut-out sector edge of 70 mm and an angled bevel of 35 mm cutback from a point on the cut-out sector edge to a point at the circumference of the disc (Figure 3-10). The values given in Section 3.3.1 were used as representative of a crop situation to provide adequate intra-row weed control. For the 120^o cut-out sector disc the minimum distance of the sector edge is 38.1 mm and for the angled bevel it is 53.4 mm. Hence, the sector edge will intrude into the non-tilled area by 1.9 mm but the angled bevel lies outside it with 13.4 mm clearance. For the 130^o cut-out sector disc

the minimum distance of the sector edge is 42.2 mm and for the angled bevel is 57.7 mm. Hence, both the sector edge and the angled bevel lie outside the non-tilled area with 2.2 mm and 17.7 mm clearance for the sector edge and the angled bevel. For the 150^o cut-out sector disc the minimum distance of the sector edge is 50.7 mm and for the angled bevel is 66 mm. Hence, both the sector edge and the angled bevel lie outside the non-tilled area with 10.7 mm and 26 mm clearance for the sector edge and angled bevel. For the 170^o cut-out sector disc the minimum distance of the sector edge is 58.8 mm and for the angled bevel is 74.4 mm. Hence, both the sector edge and the angled bevel lie outside the non-tilled area with 18.8 mm and 34.4 mm clearance for the sector edge and the angled bevel.

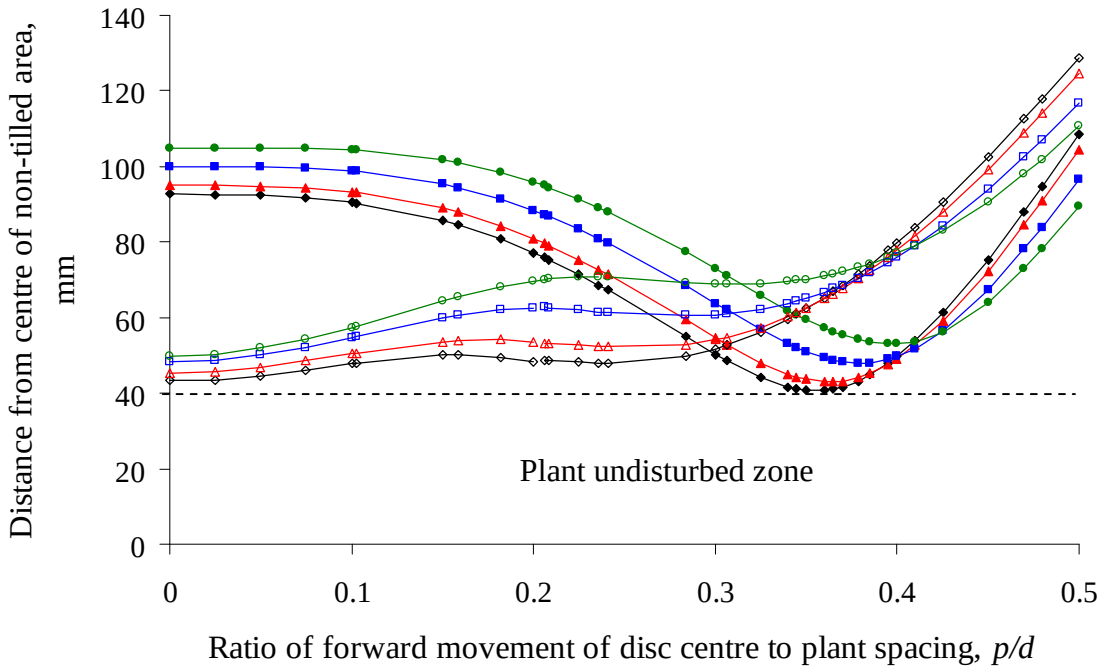

Figure 3-9 Effect of *p/d* distance from the centre of the plants undisturbed circle for a straight bevelled disc with cut-out sector angles of 120^o (◆), 130^o (▲), 150^o (■), and 170^o (●), distance of cut-out sector edge for 120^o (◊),130^o (△), 150^o (□), and 170^o (○) (disc radius, 87.5 mm; plant spacing 300 mm; disc centre 50 mm from crop row)

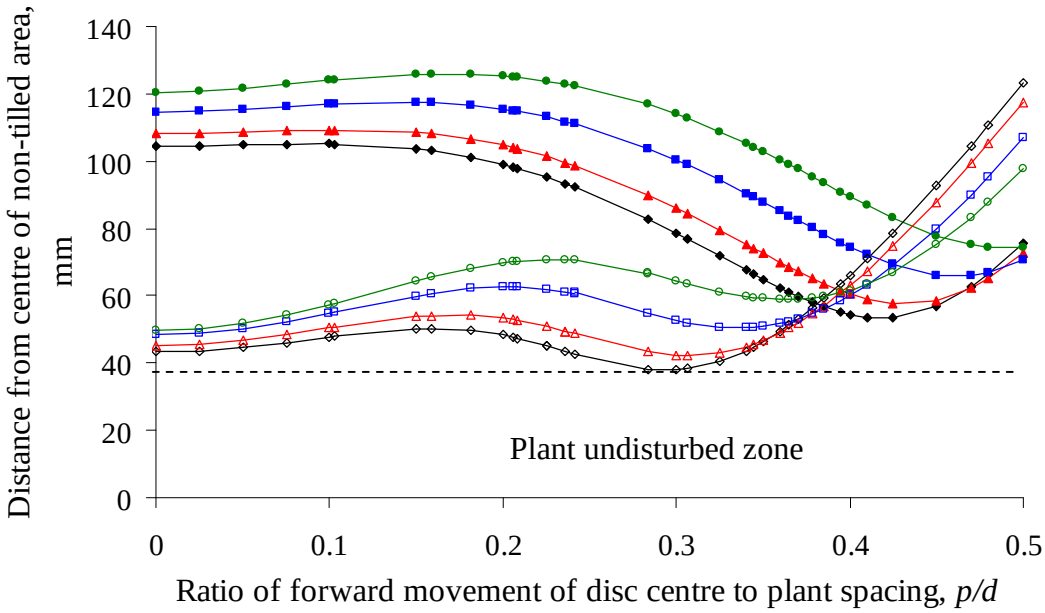

Figure 3-10 Effect of *p/d* distance from the centre of the plants undisturbed circle for a angled bevelled disc with cut-out sector angles of 120° (◆), 130° (▲), 150° (■), and 170° (●), distance of cut-out sector edge for 120° (◊),130° (△), 150° (□), and 170° (○) (disc radius, 87.5 mm; plant spacing 300 mm; disc centre 50 mm from crop row)

The analysis of the disc geometry using the mathematical model of the disc kinematics developed by O'Dogherty *et al.*, (2007 a and b) allowed rapid calculations for different disc geometries. An intra-row plant spacing of 300 mm showed that for an unbevelled disc a cut-out sector equal to or greater than 160° is required in order to avoid entering the crops no-till zone (Figure 3-11). For a disc with a straight and angled bevel the cut-out sector must be equal to or greater than 120° and 125° respectively in order for the disc to weed in the intra-row area without entering the crop no-till zone (Figure 3-11).

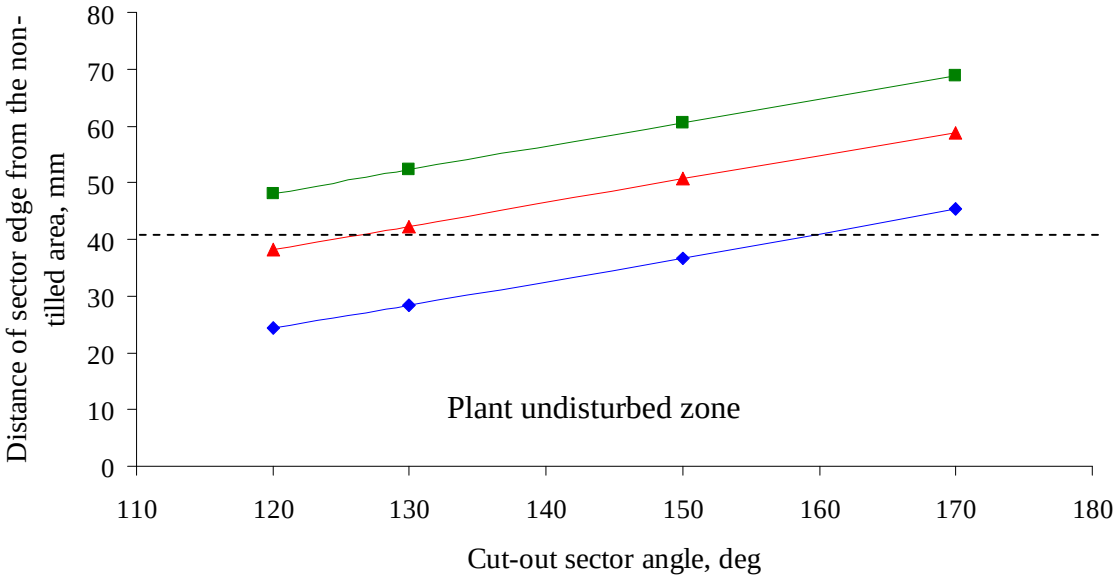

Figure 3-11 Effect of cut-out sector angle on distance from centre of the undisturbed zone of the crop for unbevelled (◆), angled bevelled (▲), and straight bevelled (■) disc (disc radius, 87.5 mm; plant spacing 300 mm; disc centre 50 mm from crop row)

Figure 3-12 shows the two different types of bevels and their distance from the undisturbed zone of the plant. As it can be seen the angled bevel provides more clearance with cut-out sector angles from 120^{o} to 170^{o} compared with a disc having a straight bevel for the same cut-out sector angles. The distance of the angled bevel from the undisturbed crop zone is 53.4 mm, 57.7 mm, 66 mm and 74.4 mm for cut-out sectors of 120^{o}, 130^{o}, 150^{o} and 170^{o}, respectively. For a disc with a straight bevel with the same cut-out sector angles, the equivalent distances were 40.7 mm, 43.2 mm, 47.9 mm and 53 mm, respectively.

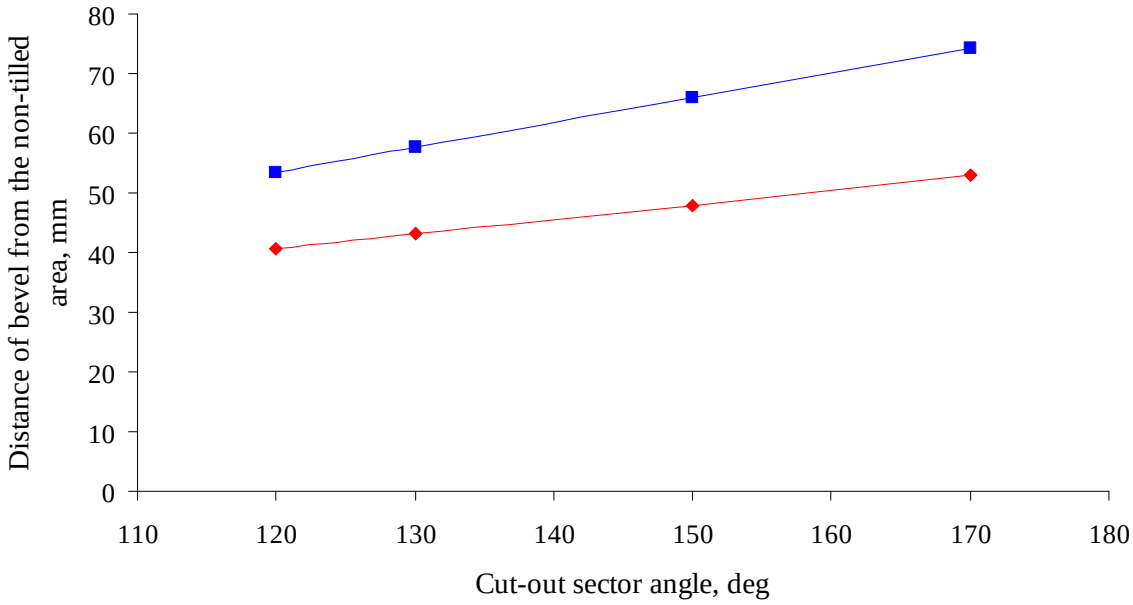

Figure 3-12 Effect of cut-out sector angle on distance from centre of the undisturbed zone of the crop for a straight (◆), and angled bevelled (■) (disc radius, 87.5 mm; plant spacing 300 mm; disc centre 50 mm from crop row)

The angled bevel is the most appropriate disc configuration and allows less of the disc to be cut away in the form of a cut-out sector. An angle of 130^{o} for the cut-out sector, with an angled bevel having an angle γ equal to 25^{o} at an edge radius of 70 mm is a disc design which provides clearance from the undisturbed zone for both the sector edge and the end of the bevel edge. The disc configuration is shown in Figure 3-13 with a radius of 87.5 mm as suitable for operating at 50 mm from the crop row at constant intra-row plant spacing of 300 mm (O'Dogherty *et al.*, 2007a).

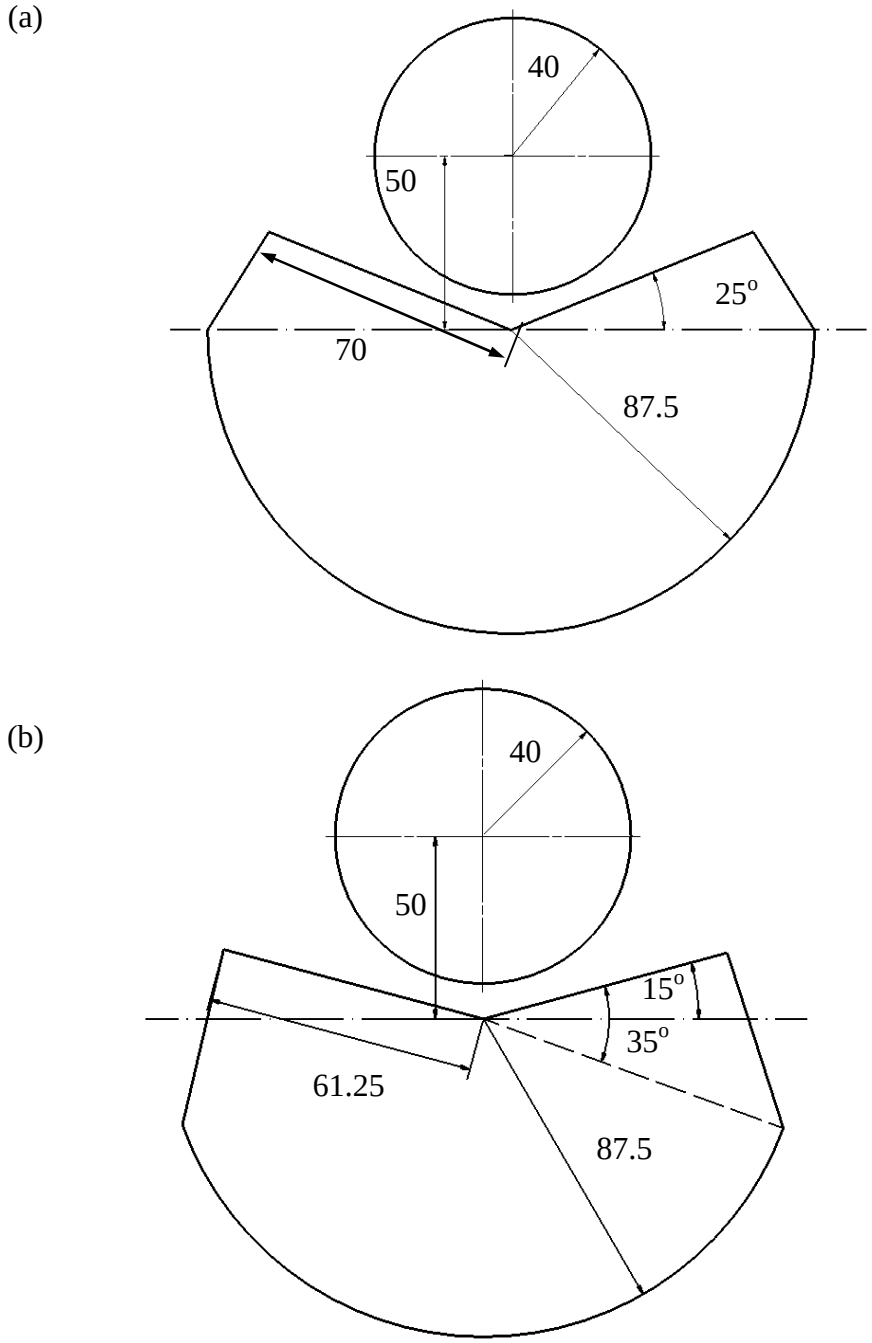

Figure 3-13 Disc designs to provide clearance from no-till circle: (a) for 300 mm plant spacing ; (b) for 250 mm plant spacing, all dimensions in mm (diameter of no-till circle, 40 mm; disc centre 50 mm from crop row) (O'Dogherty *et al.*, 2007 a)

3.3.5 Distance of disc centre from crop row

If the distance from the crop row of the path of the disc is changed it is necessary to change the disc radius in order to cover the same intra-row area to achieve the same area of weed control. To maintain the effect of the 87.5 mm disc radius at a distance for *a* of 50 mm, then the radius *r* must be equal to (37.5 + *a*) mm for any value of *a*. The edge radius of 70 mm for the 130° sector angle disc design also needs to be modified to 0.8*r* simultaneously in order to maintain proportionality.

Figure 3-14 shows the relationship of the minimum distance from the plant centre as the distance *a* from the crop row is varied over the range 40 mm to 70 mm for both the sector edge and the end point of the angled bevel edge with the sector edge providing the closest approach to the no-till circle. It is of interest that for a distance of 40 mm there is no intrusion into the no-till circle when the disc radius is reduced to 77.5 mm, and there is a greater clearance of 48.0 mm compared with 42.2 mm at 50 mm from the crop row. When the distance is increased to above 50 mm there is a small intrusion of 0.57 mm of the sector edge at 55 mm which increases to 7.9 mm at a distance of 70 mm, corresponding to a disc radius of 107.5 mm.

The figure shows that there is a linear decrease in the minimum distance of approach of the disc to the plant centre as the distance of the disc from the crop is increased. In practice, a distance of 55 mm or less is appropriate for the crop data considered.

3.3.6 Disc radius

The effect of disc radius was examined for the 130° sector angle disc with an angled bevel. Changes in radius were accommodated by taking the edge length equal to 0.8 times the radius to give the same proportion as for the 87.5 mm radius disc which had a 70 mm edge length at which the bevel was cut.

In Figure 3-15 the minimum distance from the plant centre is shown as a function of disc radius. There is a linear decrease in the minimum distance as radius increases for both the sector edge and the bevel end point with the sector edge giving the limiting condition. If the radius is taken beyond 90 mm, the edge of the sector will intrude into the no-till circle by 2.3 mm for a 95 mm radius because the minimum distance from the plant position falls below 40 mm. In practice, for the crop spacing (300 mm) and no-till circle (40 mm radius) taken, the appropriate radius is of the order of 87.5 mm to 90 mm.

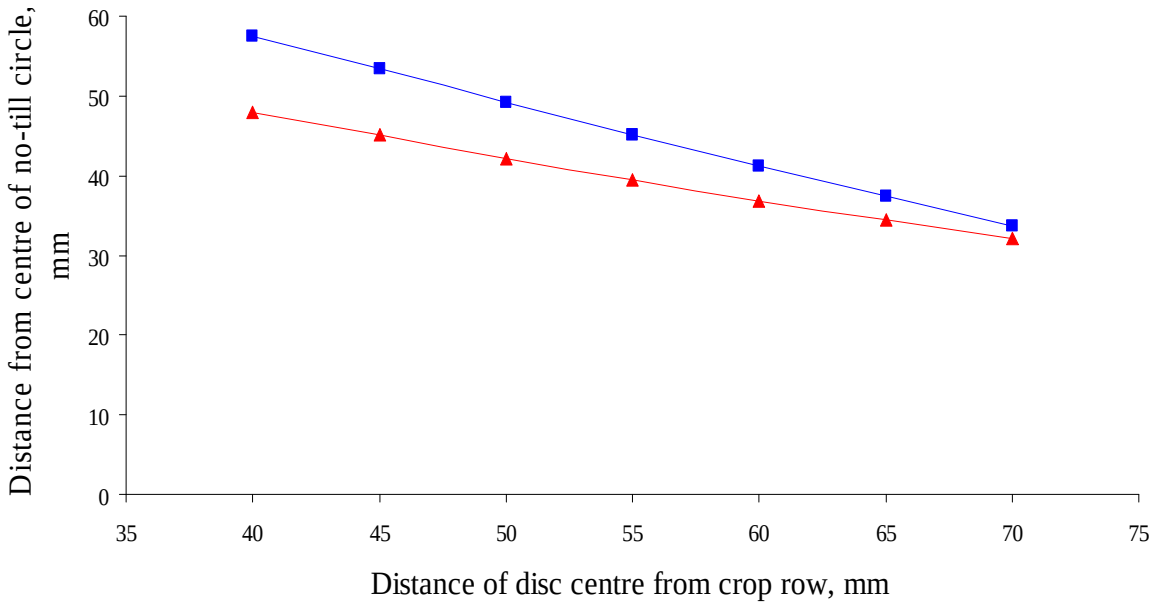

Figure 3-14 Effect of distance of disc centre from crop row (*a*) on distance from centre of no-till circle for sector edge (▲) and end point with bevel angle (γ) of 25° (■) (disc radius of (37.5+a) mm; cut-out angle, 130 deg; plant spacing, 300 mm; edge length, 0.8 times radius)

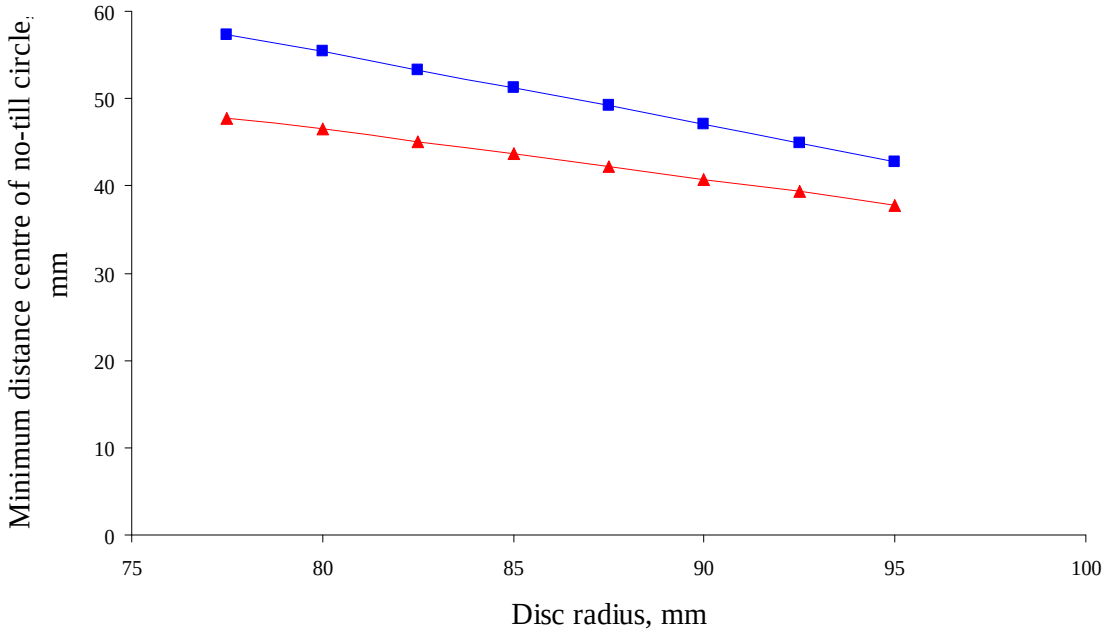

Figure 3-15 Effect of disc radius from crop row on distance from centre of no-till circle for sector edge (▲) and end point with bevel angle (γ) of 25° (■) (disc cut-out angle, 130 deg; plant spacing, 300 mm; disc centre 50 mm from crop row; edge length, 0.8 times radius)

3.3.7 Plant spacing

The effect of plant spacing was examined over a range from 200 mm to 350 mm for the disc with a 130° sector angle, 87.5 mm radius and an angled bevel at an edge radius of 70 mm. It was found that the minimum distance from the plant centre was linearly related to spacing and showed a rapid reduction as the spacing is reduced, to a value of approximately 10 mm at 200 mm spacing for both the sector edge and the bevel end point. This means that there is a need for a different disc design to operate at closer plant spacing, so as to avoid intrusion into the no-till area.

For particular crop situations, the model can be used interactively to design a suitable disc. If it is assumed that the plant spacing varies in a range from 250 mm to 350 mm it is necessary to make modifications to the disc design to accommodate spacing down

to 250 mm to avoid intrusion into the no-till circle. It was found to be necessary to employ a sector cut-out angle of 150° with a sector length of 61.25 mm (0.7 times the disc radius of 87.5 mm). The angled bevel needs to be cut back at an angle γ of 35° to the sector edge as shown in Figure 3-13 (b). As previously the disc centre is assumed to move at 50 mm from the crop row and the no-till circle has a radius of 40 mm. The disc shown in Figure 3-12 (b) will provide adequate clearance from the no-till circle for a plant spacing down to 250 mm. The distance of the sector edge and the end of the bevelled edge for this design are shown in Figure 3-16. The disc described will enable intra-row weeding for a crop with a nominal spacing of 300 mm and a range of spacing of ±50 mm.

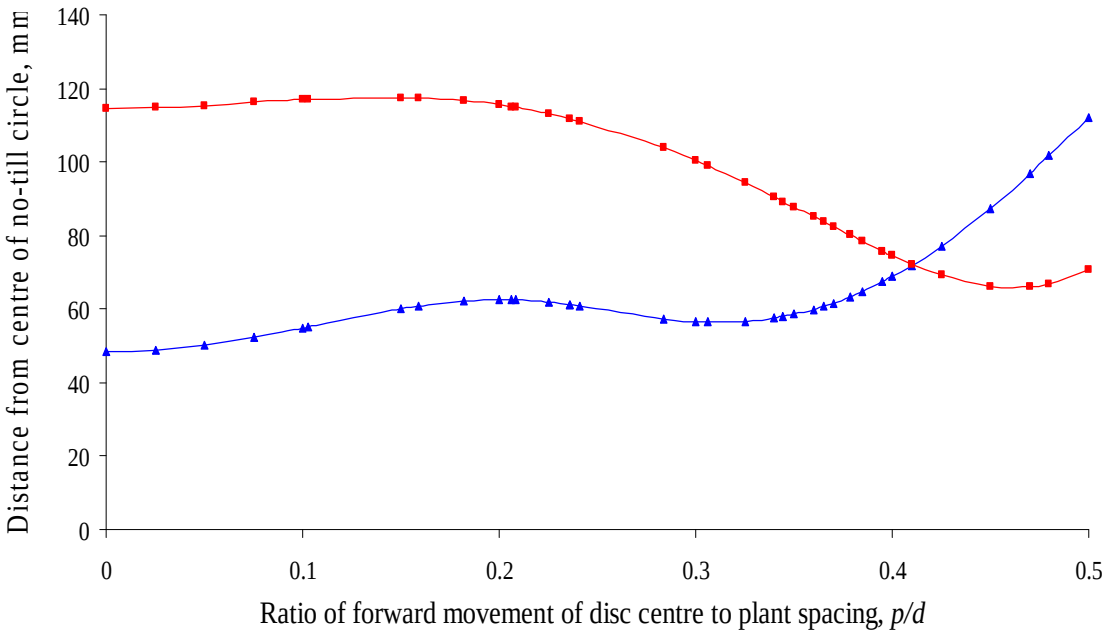

Figure 3-16 Effect of ratio p/d on distance from centre of no-till circle for cut-out sector edge (▲) and end point of angled chamfer (■) (disc radius, 87.5 mm; cut-out angle, 150 deg; plant spacing, 250 mm; disc centre, 50 mm from crop row; sector edge, 0.7 times disc radius; angled bevel at 35 deg to sector edge)

3.3.8 Disc cut-out sector

The effect of cut-out sector was examined over a range from 250 mm to 350 mm for a 87.5 mm disc radius working 50 mm parallel to the crop row. It was found that the minimum distance from the plant centre was linearly related to the disc cut-out sector. Figure 3-17 shows that for 250 mm intra-row plant spacing a cut sector angle equal or greater than 130^{o} is required in order to ovoid entering the plants no-till zone. For a intra-row plant spacing of 300 mm a cut-out sector angle equal or greater than 120^{o} is required and for 350 mm intra-row plant spacing a cut-out sector of 100^{o} provide us with adequate clearance without entering the plants no-till zone.

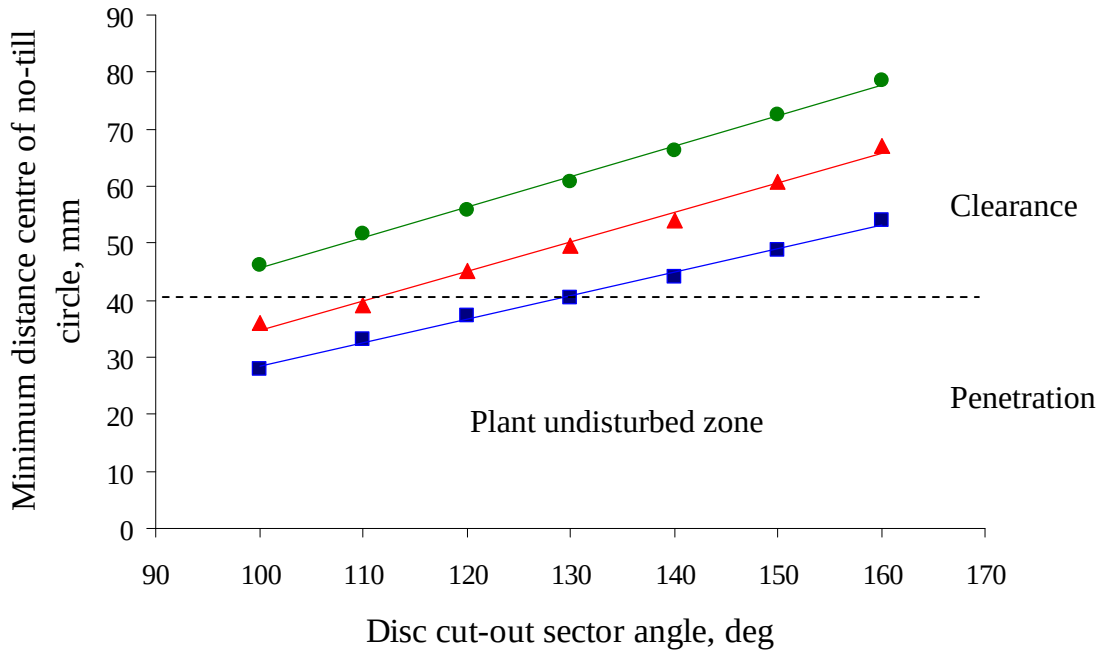

Figure 3-17 Effect of disc cut-out sector angle from crop row on distance from centre of no-till circle for 250 mm (■); 300 mm (▲); and 350 (●) (disc centre from crop row, 50 mm; edge length, 70 mm for 300 mm and 350 mm and 61.25 mm for 250 mm plant spacing)

3.3.9 Design considerations-limitations

The graphical computer simulation and mathematical model of the disc kinematics showed that the rotating disc hoe can work at intra-row spacing of 250 mm and greater. Figure 3-13 in Section 3.3.4 shows the proposed disc design for spacing of 250 mm and 300 mm. Figure 3-18 shows the treated area for the discs shown in Figure 3-13 for intra-row plant spacing from 200 mm to 500 mm, for three different distances of the centre of the disc from the centre of the plants undisturbed zone. As it can be seen increasing the intra-row plant spacing increases the treated intra-row area from 83% to 95%; 66% to 90% and 50% to 85% for distances of the disc centre from the plants undisturbed zone centre of 50 mm; 60 mm; and 70 mm respectively. In general the plants are not growing in a straight line due to the variation of the transplanter's and/or the driver's skills. As mentioned earlier, the tolerance required depended on the dynamic performance of the whole system and the growth habit of the crop plants. If the deviation of the systems lateral move is 20 mm, then the distance of the disc centre from the plants undisturbed zone will vary from 50 mm to 70 mm, so the overall treated area will vary from 66% to 90% from 200 mm to 500 mm. In commercial farming vegetables growing at a nominal intra-row spacing of 300 mm, where the treated area is 82%.

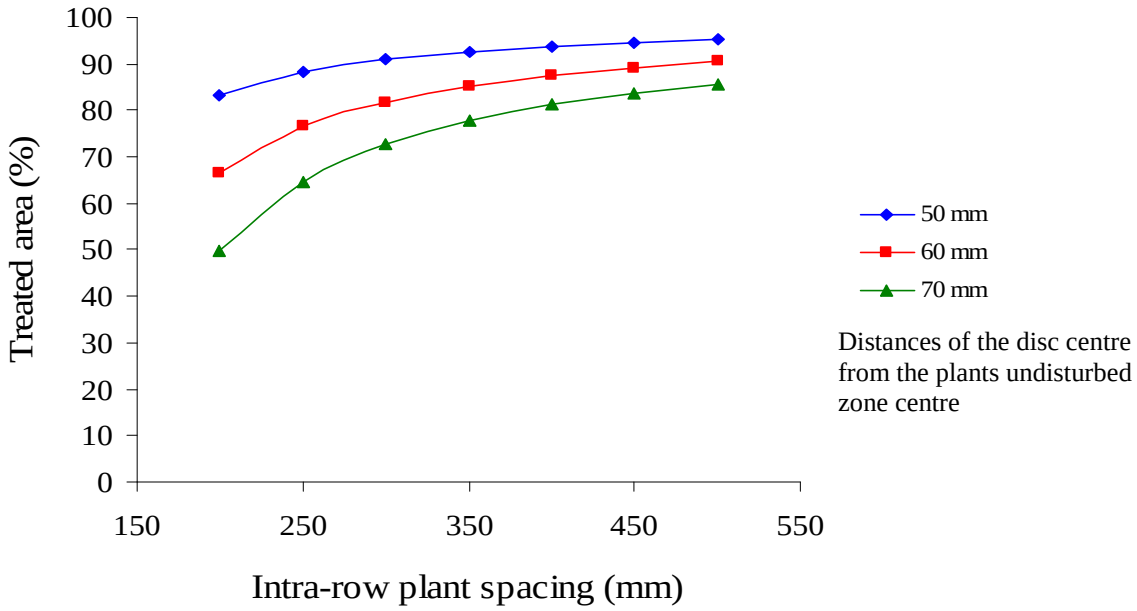

Figure 3-18 Treated area of the disc

The treated area and the crop damage will be affected by increasing speed and reducing the intra-row spacing down to 200 mm. It was found necessary to investigate alternative disc designs that will be able to treat the intra-row area at spacing down to 150 mm. Figures 3-19 and 3-20 show the proposed disc design for plant spacing of 150 mm and the graphical computer simulation on the kinematics respectively. This disc is based on the discs as mentioned earlier on Section 3.2 with one additional cut-out sector.

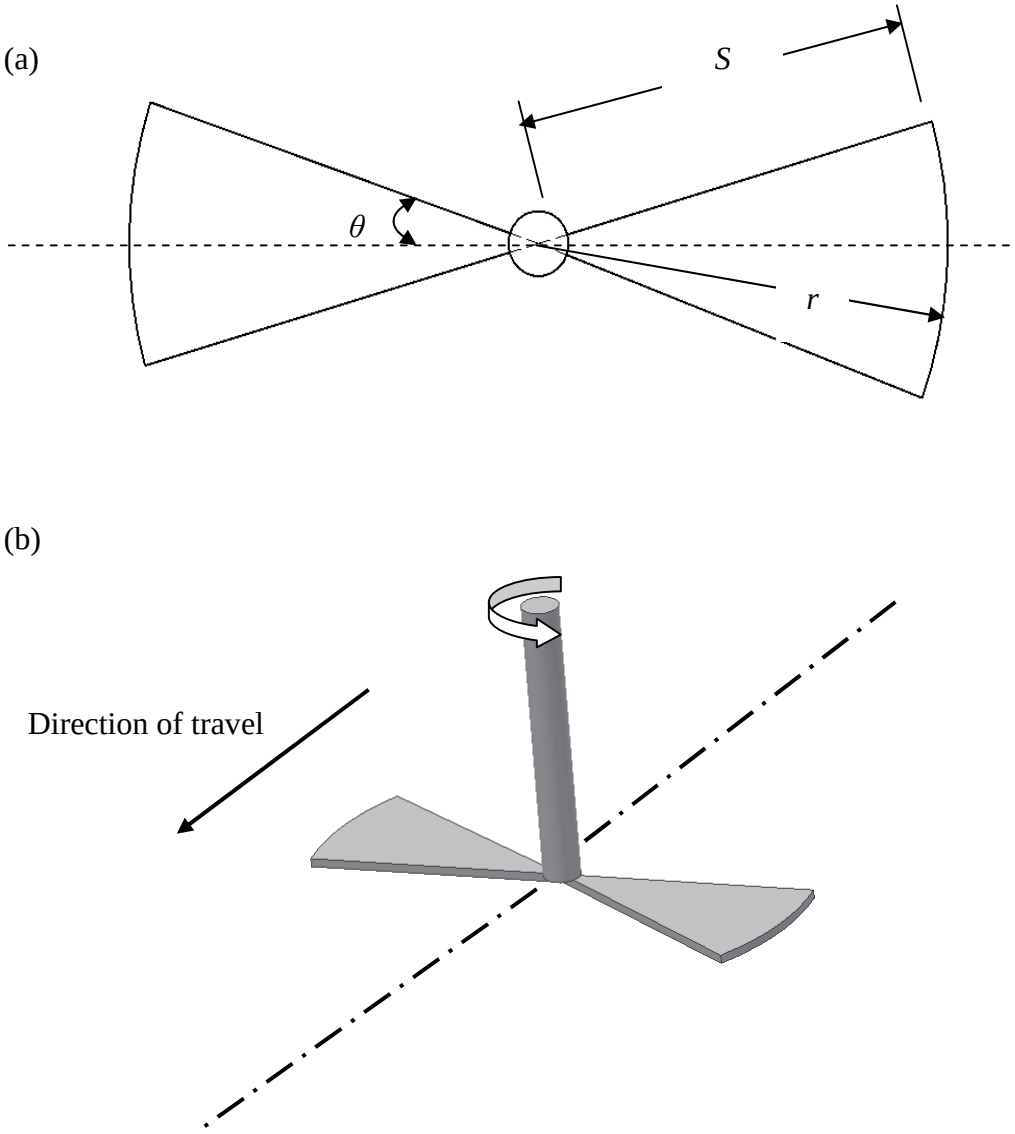

Figure 3-19 (a) Disc geometric characteristics (b) 3D design of double cut-out disc

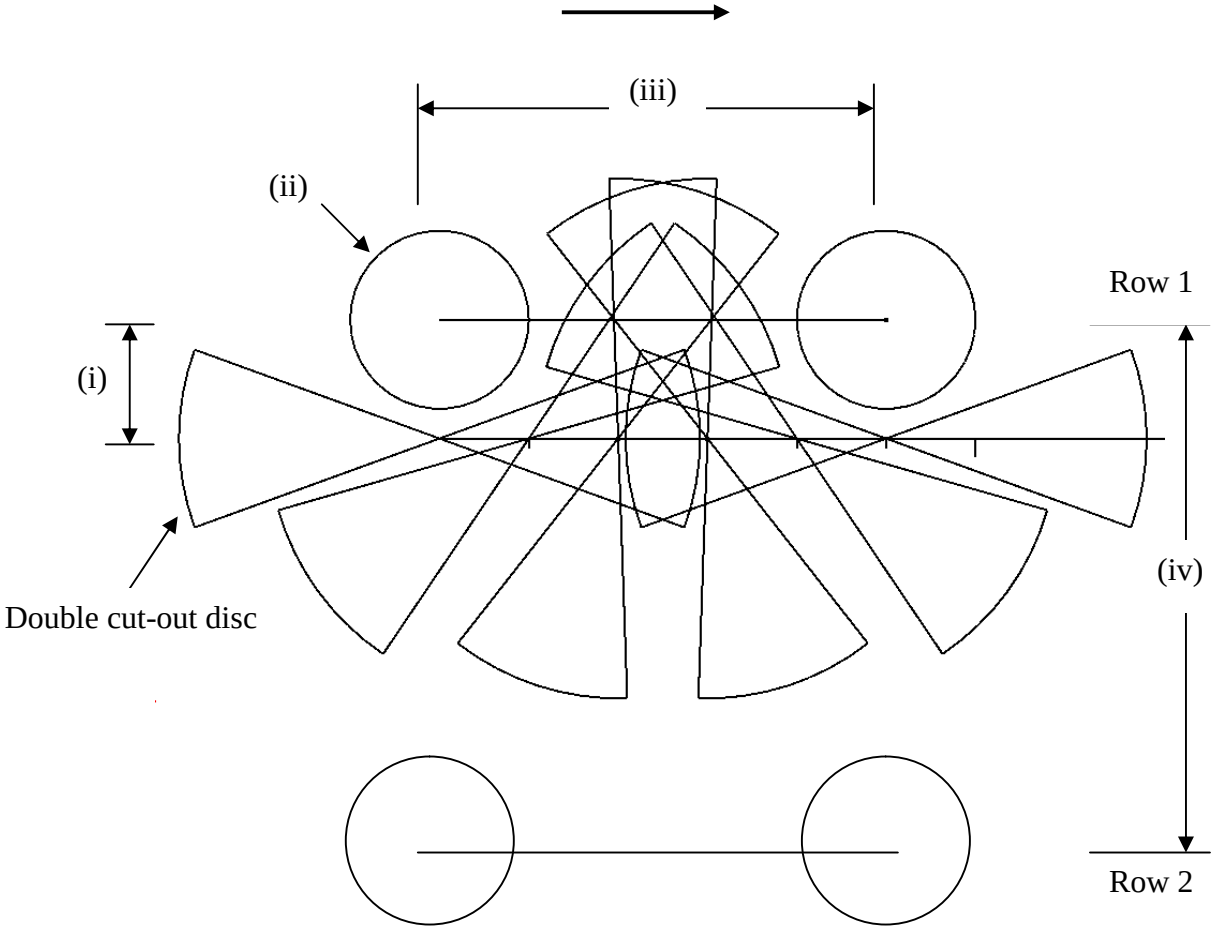

Figure 3-20 Graphical computer simulation of the double cut-out disc kinematics (i) disc movement parallel to crop row, 40 mm (ii) crop undisturbed zone, 60 mm (iii) intra-row plant spacing, 150 mm (iv) intra-row plant spacing, 200 mm

3.4 Conclusions

- The graphical computer kinematics analysis was important in gaining an understanding of the kinematics of various disc geometries as well as to identify and develop a mathematical model for rotating discs.
- A mathematical model developed by O'Dogherty *et al.*, (2007) to determine the geometry required for a horizontal rotating disc with a cut out sector to achieve intra-row weeding along a crop row. The mathematical model of the kinematics of rotating discs proved to be a valuable design tool and has wide applicability for the interactive design of discs for a range of crops.
- The model considers the kinematics of a disc as it moves along a line at a defined distance parallel to the row. The critical criterion is the minimum distance of any point on the edge of the cut-out section from the plant centre, which should be greater than the radius of the no-till circle. The effect of modifications in the form of bevels at the disc periphery can be investigated and an optimum design achieved for a given crop specification by the use of an interactive procedure using a spreadsheet.
- At a plant spacing of 300 mm and a no-till circle radius of 40 mm, with the disc centre moving at 50 mm parallel to the crop row, the optimum design of disc had a radius of 87.5 mm, a sector cut-out angle of 130° together with an angled bevel at 25^{o} to the cut-out edge at a distance of 70 mm along the sector edge to the end of the diameter of the uncut semicircle.
- The minimum distance of the disc cut-out edge from the plant centre decreased linearly with increasing distance of the disc centre from the row, while varying the disc radius to cover the same intra-row area. At a distance of 55 mm from the plant row or greater, there is intrusion of the sector edge into the no-till circle, but for distances less than 50 mm there was increasing clearance.
- Variation in the disc radius showed that the minimum distance from the plant centre decreased linearly as the radius was increased. For a radius greater than 90 mm, there was intrusion of the sector edge into the no-till circle.

- A reduction in plant spacing results in a linear reduction in the minimum distance from the plant centre to approximately 10 mm at a spacing of 200 mm. There is intrusion of the disc cut-out into the no-till circle at smaller plant spacing and modification of the disc design for 300 mm plant spacing is required.
- For a crop spacing of 250 mm and a no-till radius of 40 mm, with the disc centre at 50 mm from the crop row, a disc of 82.5 mm radius is required with a sector angle of 150°, a sector edge length of 61.25 mm and an angled bevel at 35° to the sector cut-out edge.
- The percentage of the intra-row area hoed increases from 83% to 95% when the plant spacing is increasing from 200 mm to 500 mm.
- The double cut-out disc (bowtie) can be used at plant spacing down to 150 mm.

Chapter 4

Soil Dynamics of Cut Out Rotating Discs

4. Controlled laboratory experiments into the soil dynamics of cut-out rotating discs

This Chapter details experiments in controlled laboratory soil conditions of cut-out rotating discs to investigate the soil forces and disturbance on different disc geometries and shapes. This would allow the optimum disc geometry for weed control with the minimum force requirements to be determined. For that reason an experiment was designed with three different disc geometries at a range of working depths and inclination angles.

4.1 Soil dynamics laboratory experimental apparatus

The experiments performed under controlled laboratory conditions at Cranfield University's, Silsoe soil dynamics laboratory (Figure 4-1). The indoor soil bin is 20 m long, 1.7 m wide and 1 m deep sunk (Hann & Giessibel, 1998) within the floor of a heated building.

The use of such soil tanks, or bins, for traction and tillage studies removes the inherent variability found in field conditions, allowing uniform soil conditions to be obtained following careful preparation. On the top of this tank run the rails that guide the main processor unit, which contains the hydraulically operating soil engaging implements, bucket and grabs, and rollers to enable a variety of soil preparations to be produced (Eatough, 2002). To the rear part of the soil bin processor an adjustable bracket is fitted enabling the experimental equipment to be attached. The whole unit is moved by cable driven system, which is operated by an electro-hydraulically controlled winch drum.

At the rear of the processor (Figure 4-2) the experimental equipment is attached via an octagonal ring transducer (EORT). The EORT is a machined aluminium block to

which strain gauge bridges are attached. During each run the strain gauge bridge output voltages are recorded in computer for further analysis. Details on EORT design and operation are reported by Godwin (1975) and O'Dogherty (1975 & 1996). The EORT provides information on the horizontal and vertical forces applied to the disc and in the plane of these two forces on moment as shown in Figure 4-3. The experiments on working depth and inclination angle performed under controlled laboratory experiments to ensure uniform soil conditions.

Figure 4-1 The soil bin and the processor

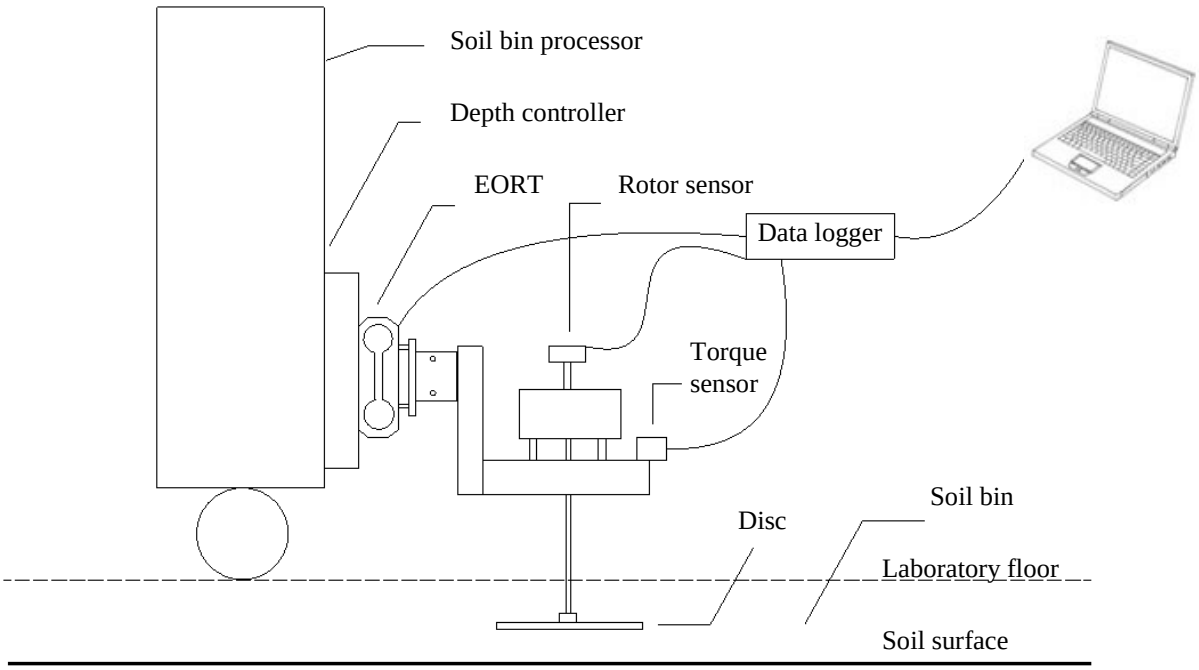

Figure 4-2 Experimental rig setup

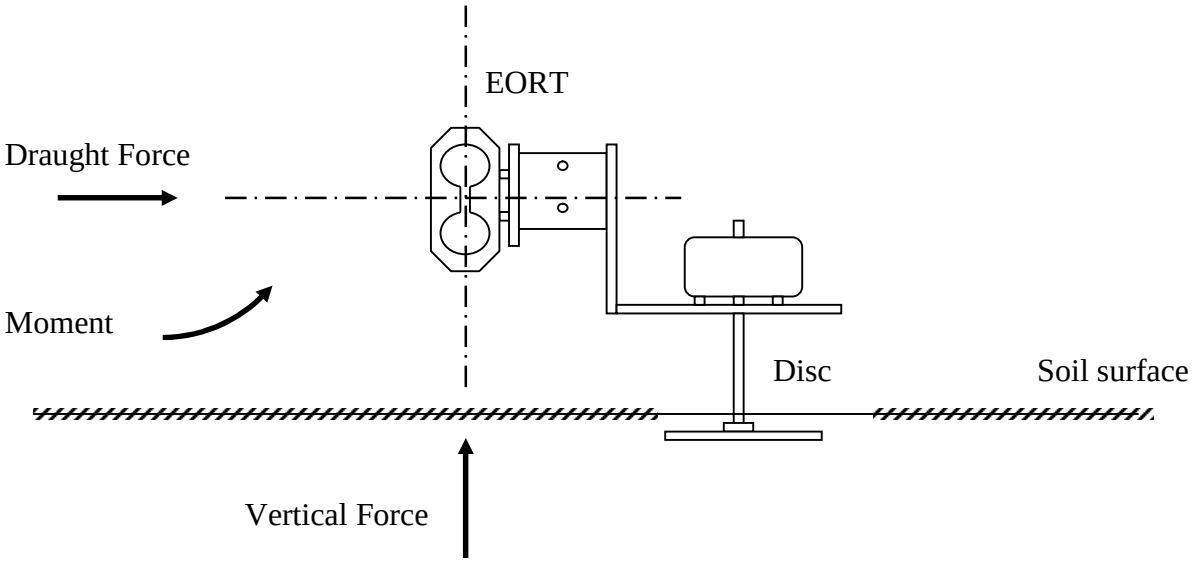

Figure 4-3 Experimental rig mounted on EORT

4.2 Rotating disc hoe test apparatus

To examine different disc geometries at different depths and inclination angles an experimental rig was designed and built in accordance with the requirements of the study and the soil laboratory. Figure 4-4 shows the experimental rig. Attached to a steel frame was a 190 W DC motor to which discs could be fitted via a mounting bracket at the bottom of a shaft from the motor. A rotary encoder was placed on the top of the shaft to monitor the rotary speed of the disc which could be adjusted from a gear box. A load cell was placed at 145 mm from the centre of the disc on a torque arm to measure the shaft torque. The experimental rig was equipped with speed controller in order to test the proposed disc geometries in different rotational speeds. The rig was attached to the rear of the soil bin processor on the EORT, as mentioned earlier. A data acquisition module was used to record the draught force, vertical force, moment, rotational speed and torque.

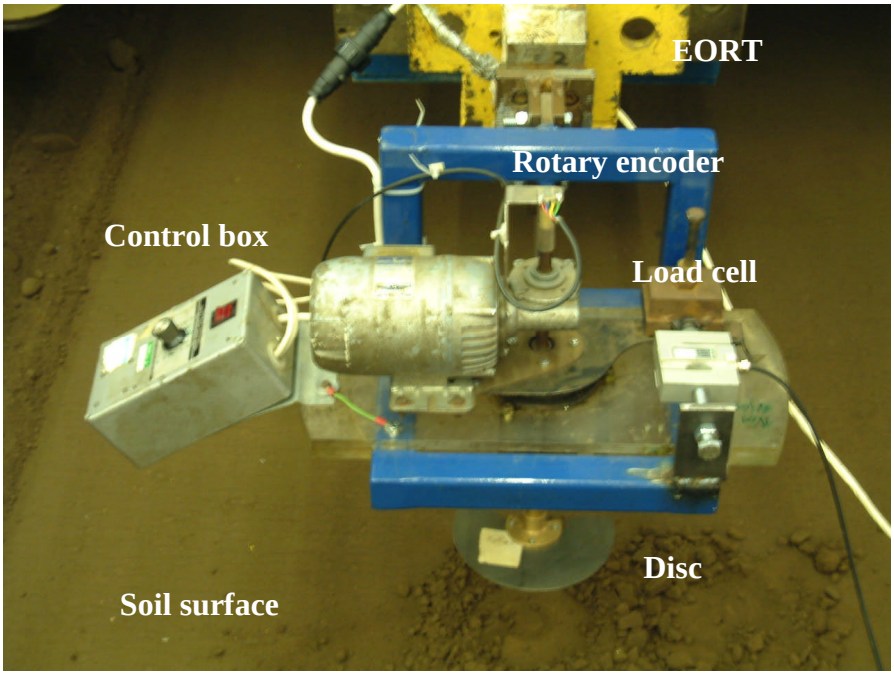

Figure 4-4 Rotating disc hoe test apparatus

4.3 Instrumentation software system

Data from all the transducers was recorded on a portable computer using DASYLab v.8 software via a FYLDE data acquisition module as shown in Figure 4-5. The data acquisition module operated at 10 V and is sampling rate was 5000 samples/s. A filter with a sampling rate of 30 samples s^{-1} (30 Hz) provided 166 samples s^{-1} (166 Hz). An average of a block of 50 samples is placed after the filter that provides 3.32 samples s^{-1} (3 Hz), the voltage was then transformed in force units from the calibration values of the transducers. The actual measurements were automatically saved to a file for further processing prior to the next experimental treatment. The calibration details of the draught force, vertical force and moment from the EORT and for torque and the rotational speed encoder are given in Appendix II.

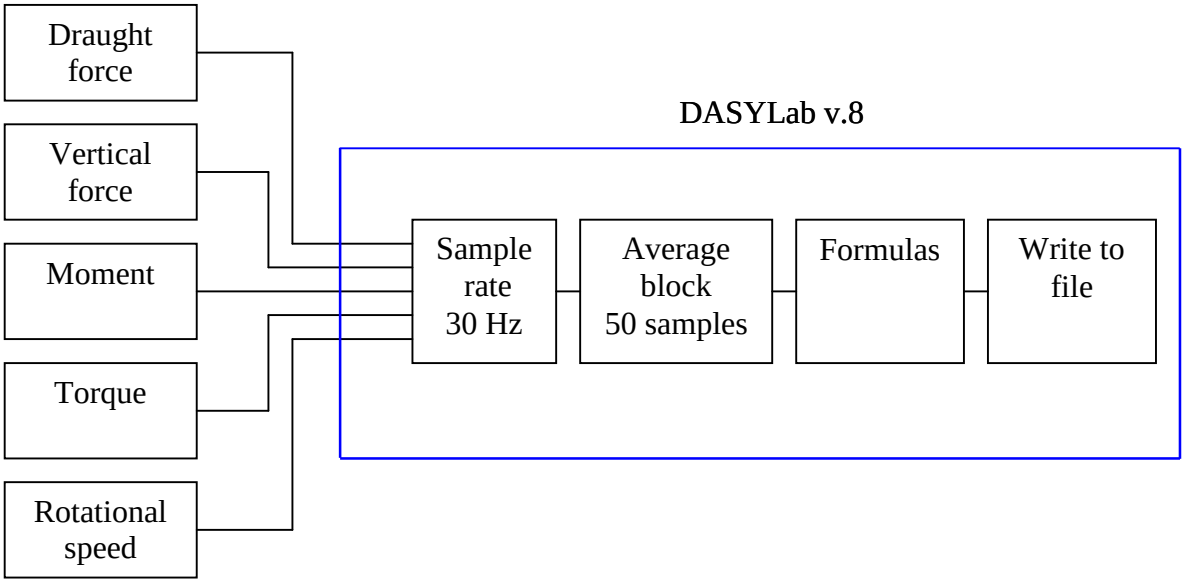

Figure 4-5 Details of instrumentation software system

4.4 Experiment design

The type and degree of soil disturbance is the prime factor when selecting tillage implements but this must be considered together with the draught and penetration force requirements for efficient operation (Godwin, 2007). The effect of working depth, inclination angle and disc geometry on draught and penetration force requirements for flat, convex and double cut-out (bowtie) discs (Figure 4-6) were assessed. Four inclination angles (0^o, 5^o, 10^o and 15^o) were examined at 0.5 m s^{-1} (1.8 km h^{-1}) forward speed and 1 rev s^{-1} rotational speed at 10 mm deep. Four depths (10, 15, 20 and 25 mm) were examined at 0.5 m s^{-1} driving speed and 1 rev s^{-1} rotational speed at 0^o inclination angle was tested under controlled conditions.

The soil was prepared in 50 mm layers in the soil bin laboratory. Water was sprayed on the surface following each layer of soil with two passes of a 700 kg roller for each layer to ensure uniform soil moisture content and compaction levels to minimise variability between treatments. This repeated twice giving uniform soil conditions to a depth of 100 mm, satisfying the requirements for maximum working depth of 25 mm. The experiments were conducted in a randomized block design, with each test being replicated three times. In total 72 experimental treatments were performed.

The soil type used was sandy loam, with 66%, 17%, and 17% percentage of sand, silt, and clay respectively. The mean soil moisture content was 9% with a standard deviation of 0.8%. The mean bulk density prior the treatment was 1530 kg m^{-3} with a standard deviation of 85 kg m^{-3}.

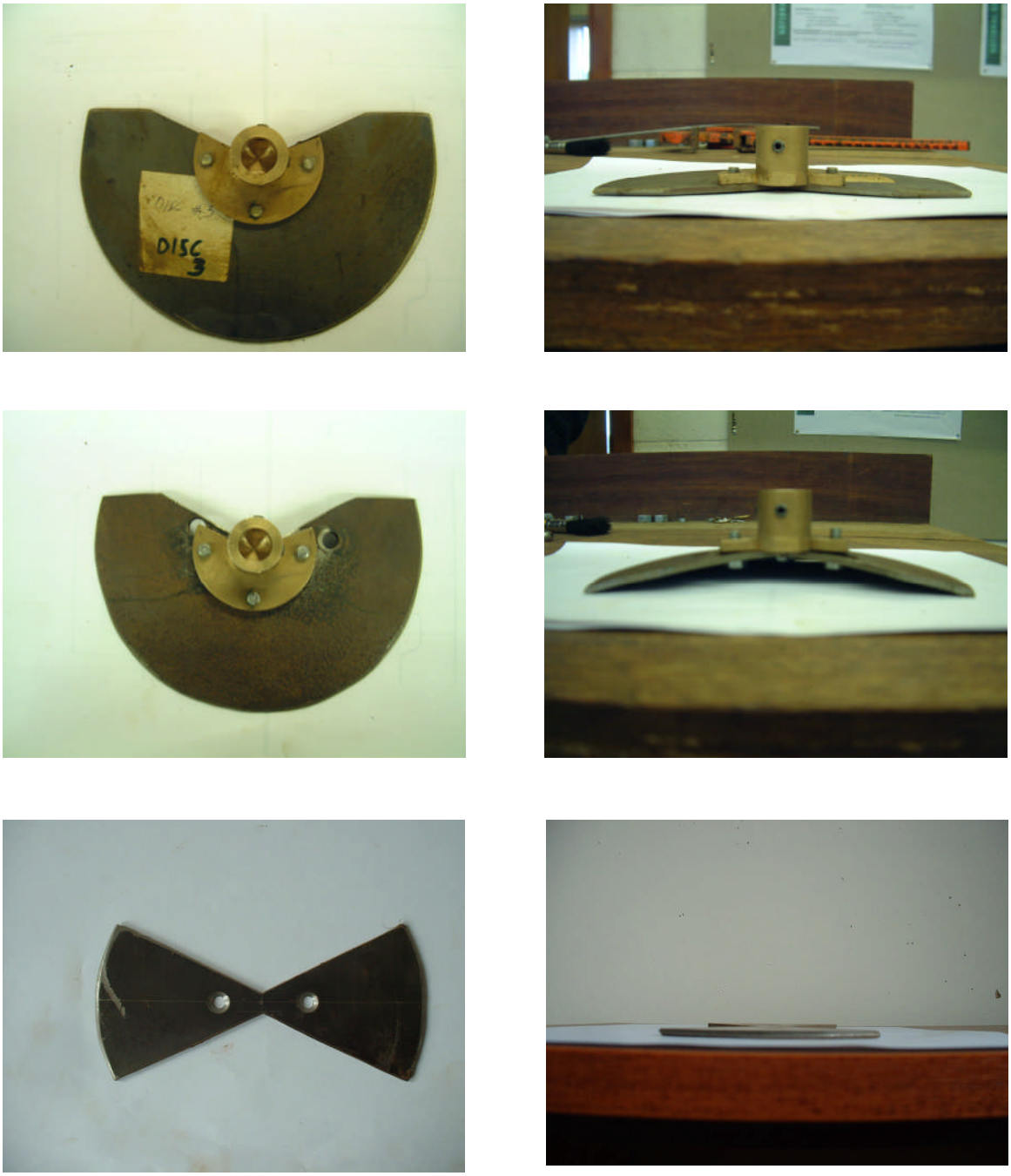

Figure 4-6 Disc geometries evaluated in the controlled laboratory experiments, flat (upper); convex (middle) and bowtie discs

4.5 Measurement technique

The same experimental technique for both the effects of inclination angle and depth experiment was used and was as follows:

1. The experimental equipment was attached to the EORT and all the transducers were connected to the data acquisition module.
2. The forwarded speed was set up at 0.5 m/s
3. The appropriate disc was attached to the shaft and the appropriate operated speed was selected via the control box.
4. The discs were operated over a 3 m length of uniformly prepared soil surface where the soil forces, torque and rotational speed were recorded.
5. The disturbed soil was excavated and three static profile measurements for each furrow created by the disc were taken.

4.6 Data analysis

The experimental data where exported into Microsoft Excel to be further analysed. The end effects of each experimental data set was removed (Figure 4-7, which shows a typical data set of draught and vertical forces) and a standard data length of 3 s (1.5 m) was selected for each of the transducer signal channels in order to maintain consistency and be able to further analyse the data with a statistical package.

The data were imported into GenStat v.8.1 and two analysis of variance (ANOVA) were performed one for the mean values and the second for the mean-max values as shown in Figure 4-7 (lower) for all transducer channels, for each of the inclination angle and depth effect experiment. For designing purposes the peak forces have to be accommodated to avoid failure.

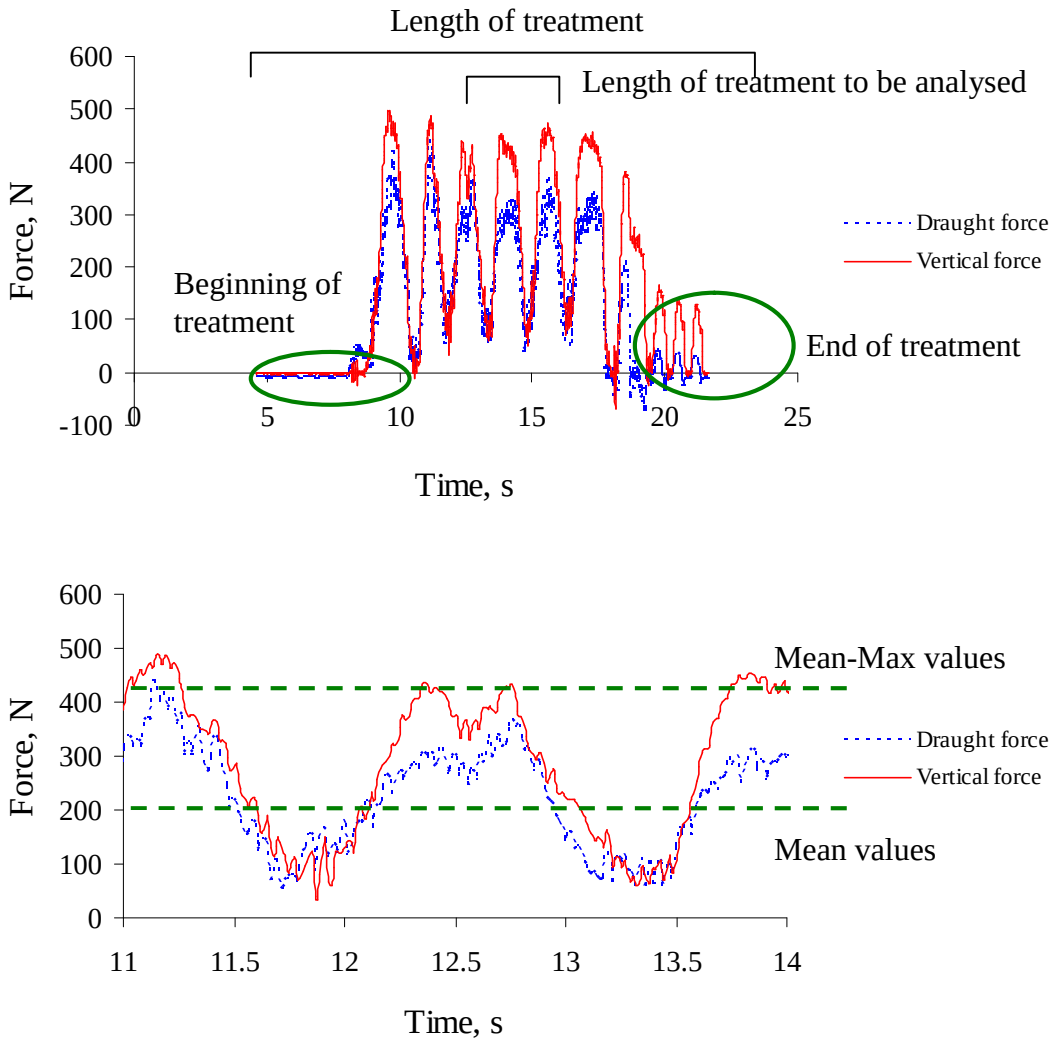

Figure 4-7 Typical data set from the EORT for draught and vertical force before the initial analysis (upper) and after the analysis (lower)

4.7 Results

All the results from the inclination angle and depth effect experiments for cut-out discs can be found in Appendix IV.

4.7.1 The effect of disc depth

The effect of working depth from 10 mm to 25 mm had a significant effect (5% level of significance) on the mean and the mean-max draught and vertical force for the three different disc geometries. The draught force increased with increasing working depth.

Figure 4-8 shows the effect of working depth for a convex, a flat, and a bowtie disc working at four depths, with a 0^o inclination angle, 0.5 m s^{-1} forward speed and 1 rev s^{-1} rotational speed for draught force. The mean draught force between the flat and the convex disc was not significantly different at 5% level of significance for depths from 10 mm to 25 mm. The draught force for the flat disc was 135 N to 264 N, for the convex disc was 185 N to 219 N and for the bowtie disc was 53 N to 132 N for depths from 10 mm to 25 mm. For depths from 20 mm to 25 mm there is a rapid increase in draught force for the flat and bowtie disc from 152 N to 264 N and from 90 N to 132 N respectively. The increase between 20 mm to 25 mm could be explained for the flat disc by the fact that the disc could be working below a critical depth, which relates the disc to the depth of work where soil failure approaches the bearing capacity failure both above and below the disc edge which in principle is similar to that described by Godwin and Spoor (1977) for narrow tines. This phenomenon increased the draught force by 84% from 20 mm to 25 mm for the flat disc. In order to help explain these results complementary experiments in a glass-sided soil bin were performed. These showed that the flat disc was cutting the soil by forming cracks on the top surface of the disc. The soil at the underside surface of the disc was smeared. The convex disc pushed the soil upwards and forwards, with cracks above and in front of the disc. No underside soil failure occurred. This is in accordance with the results obtained by Fielke (1996) which showed that sharp cutting edges on tillage tools cut the soil, while smearing the soil on the underside. The mean-max draught force for the flat and the convex disc is significantly greater at 5% level of significance than the equivalent bowtie disc for depths from 10 mm to 20 mm. At a depth of 25 mm there was a significant difference in the mean-max draught force between the flat and the convex disc. The mean-max draught force was 298 N to 310 N; 268 N to 394 N and 128 N to

176 N for the convex, the flat and the bowtie disc respectively. As mentioned earlier, the rapid increase in draught force for the flat and the bowtie disc can also be seen in the mean-max values when increasing the depth from 20 mm to 25 mm. The mean-max draught force is greater from the mean draught force by 70%; 50% and 100% for the flat, the convex and the bowtie disc respectively.

The direction of the vertical force (Figure 4-9) was upward and generally increased with working depth, thus tending to lift the disc out of the soil. The mean vertical force the flat, the convex and the bowtie disc required was 205 N to 290 N; 180 N to 208 N and 89 N to 134 N respectively for depths from 10 to 25 mm. There is a significant difference, at 5% level of significance in the mean vertical force at a depth of 25 mm between the flat and the bowtie disc. The mean-max vertical force was significantly different, at 5% level of significance for depths of 10 mm; 15 mm and 25 mm between all the disc geometries. At a depth of 20 mm the mean-max vertical force was significantly less for the bowtie disc compared with the equivalent flat disc.

Figure 4-10 shows the magnitude of torque versus depth for all the disc geometries. This shows that the mean torque required to rotate the convex disc is 66.7% more than for the flat disc. The torque for the convex disc is nearly uniform for the range of depths tested with the mean value of torque being 20 Nm. At depths of 10 mm to 25 mm the required mean torque was not significantly different for the flat and the bowtie disc. The mean torque for the convex disc was significantly greater for the convex disc than the equivalent flat disc at depths of 10 mm to 20 mm. The mean-max torque was significantly greater for the convex disc than the equivalent flat disc at depths of 10 mm to 20 mm. The torque increases with depth from 9.5 Nm to 15.8 Nm and from 9.1 Nm to 13.7 Nm over the 10 mm to 25 mm working depth range for the flat and bowtie disc respectively. The mean power needed was 126 Watt for a mean torque of 20 Nm, and it was within the range limits of the motor used in this study to rotate the discs (190 Watts).

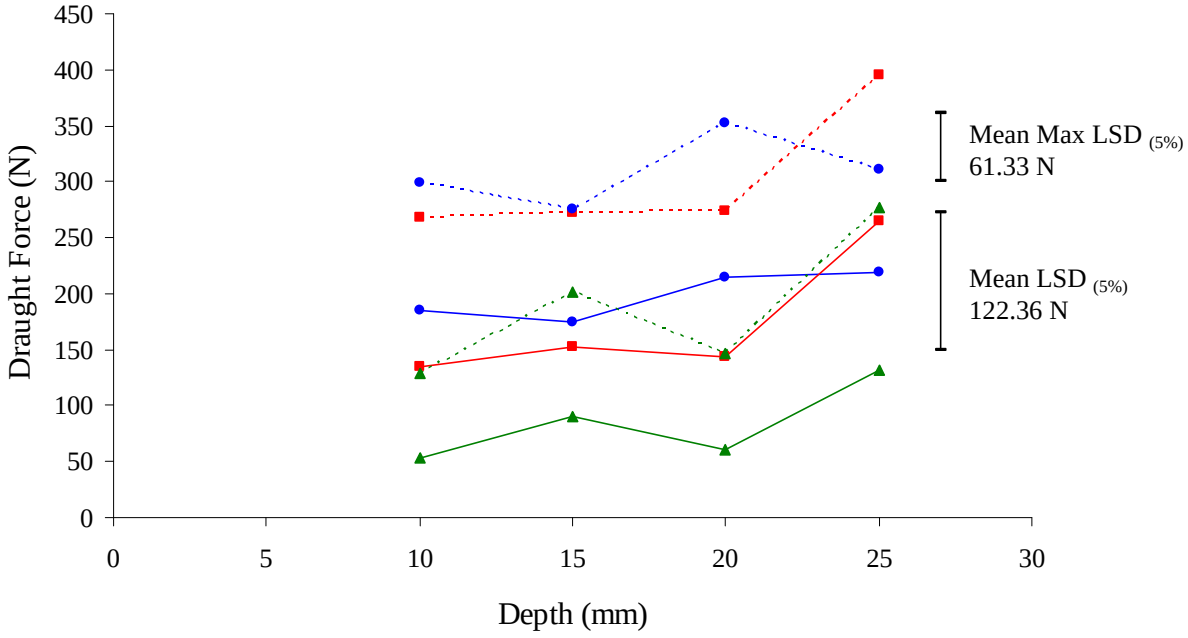

Figure 4-8 The effect of discs working depth on the mean (solid line) and mean max (broken line) draught force for flat, ■; convex, ● ; and bowtie, ▲, discs

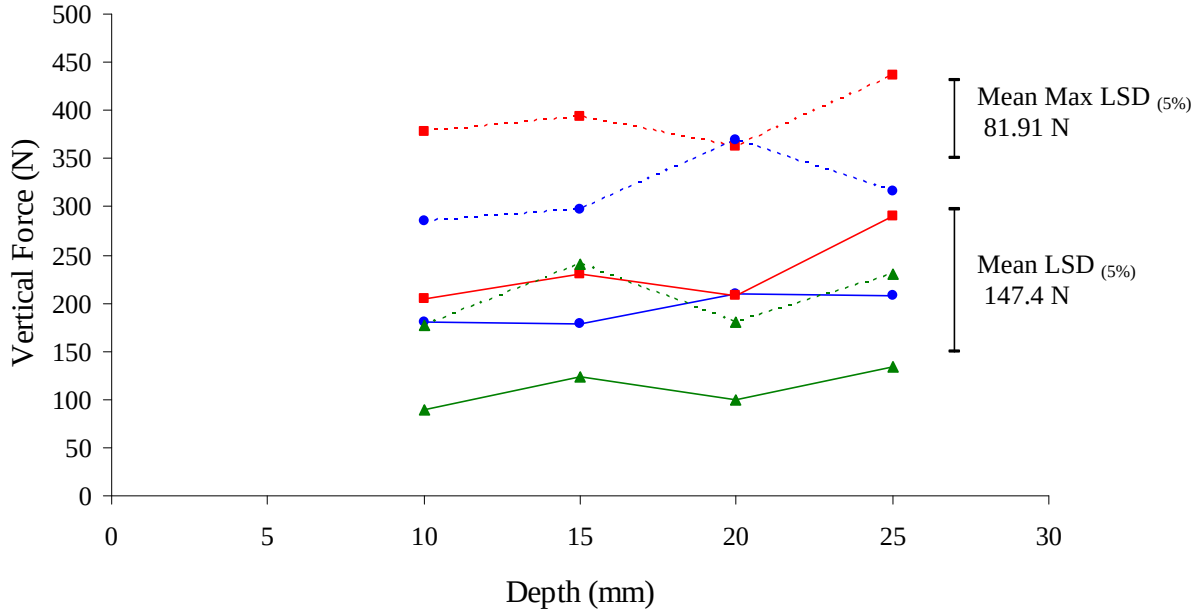

Figure 4-9 The effect of discs working depth on the mean (solid line) and mean max (broken line) vertical force for flat, ■; convex, ● ; and bowtie, ▲, discs

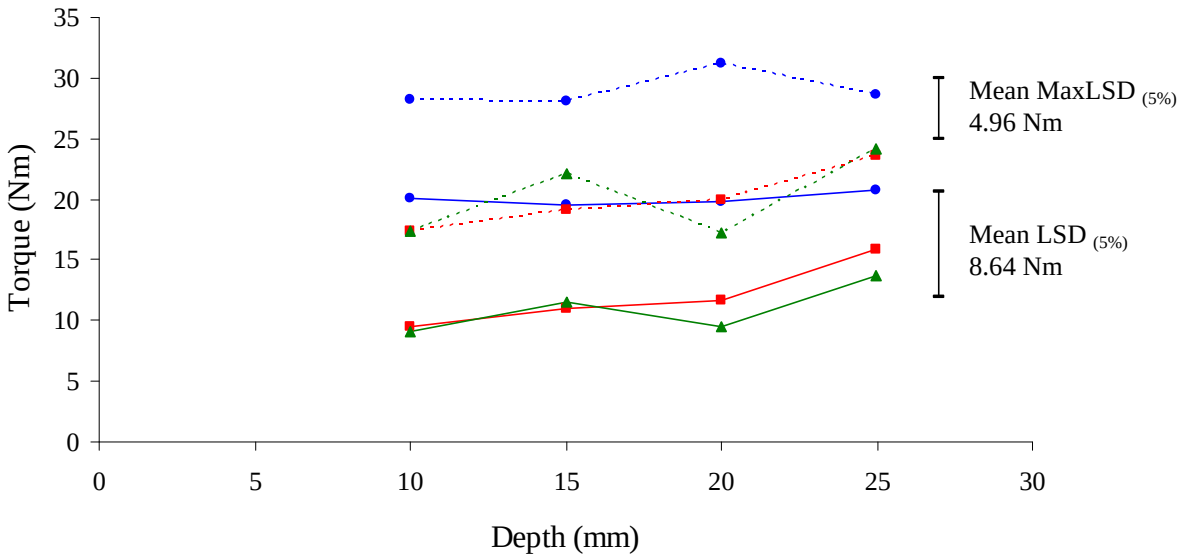

Figure 4-10 The effect of discs working depth on the mean (solid line) and mean max (broken line) torque for flat, ■; convex, ● ; and bowtie, ▲, discs

4.7.2 The effect of disc inclination angle

Increasing the inclination angle from 0^o to 15^o had a significant effect, at 5% level of significance on the mean and mean-max draught and vertical force for all three disc geometries. When the inclination angle is 0^o there is no clearance and scrubbing will occur on the underside of the disc so that the forces and torque requirements are high. Godwin (2007) states that for low draught force and good penetration implements should be designed with a low inclination angle but should have underside clearance.

Figure 4-11 shows that from 0^o to 5^o inclination angle there is a 74%, 69% and 71% reduction in draught force for the flat, the convex and the bowtie disc, respectively. This shows that even a very small inclination angle, 5^o provides sufficient clearance, so reducing the underside friction on the disc.

Figure 4-12 shows the effect of inclination angle for all the disc geometries for the mean and mean-max vertical force. This shows a similar effect for vertical force as for draught force with a reduction of 86%, 75% and 86% for the flat, convex and bowtie disc respectively, providing penetration of the disc, into the soil. There is a significant difference, at 5% level of significance between the flat the convex and the bowtie disc geometries for inclination angles of 0^o to 15^o.

Increasing the inclination angle from 0^o to 15^o had a significant effect, at 5% level of significance on the mean and mean-max torque for the convex and the bowtie disc due to the reduced contact area of the disc, i.e. there is clearance of the underside the discs so minimising the underside friction. Figure 4-13 shows a 55%, 50%, and 52% reduction for the convex, the flat and the bowtie disc, respectively, when increasing the inclination angle from 0^o to 5^o.

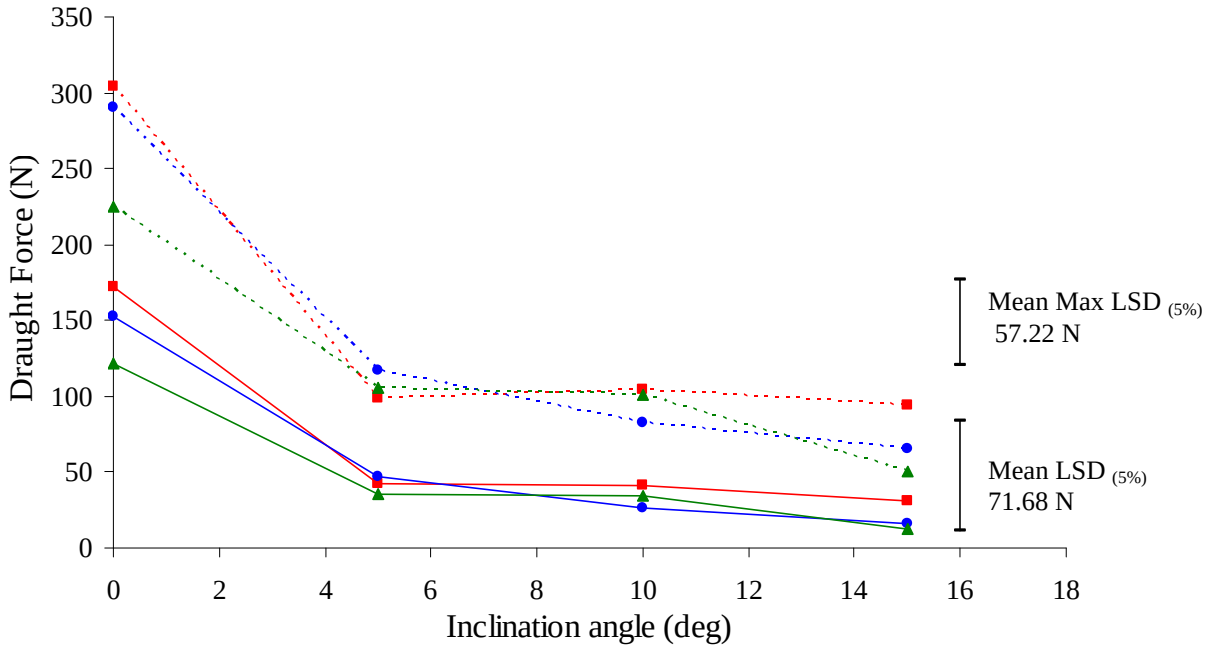

Figure 4-11 The effect of inclination angle on the mean (solid line) and mean max (broken line) draught force for flat, ■; convex, ● ; and bowtie, ▲, discs

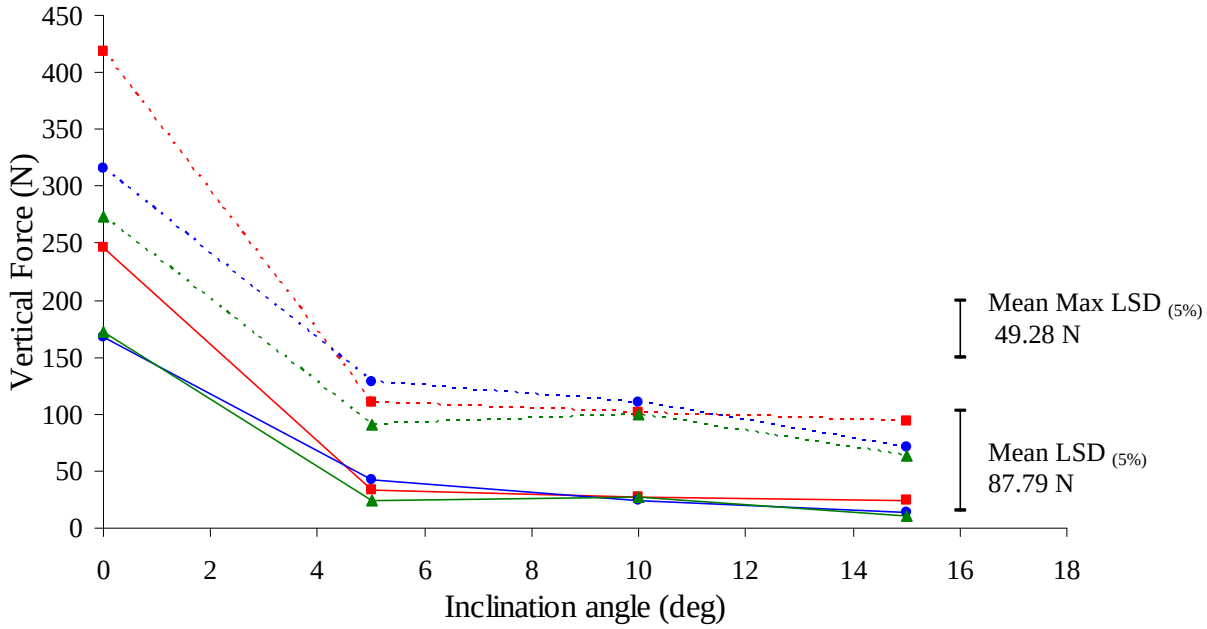

Figure 4-12 The effect of inclination angle on the mean (solid line) and mean max (broken line) vertical force for flat, ■; convex, ● ; and bowtie, ▲, discs

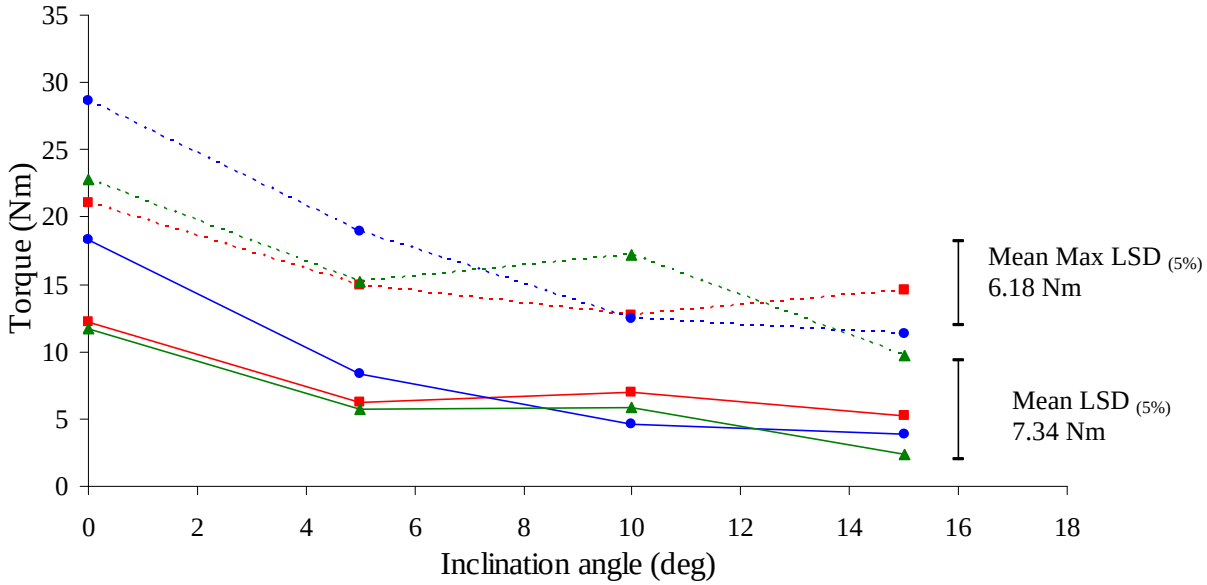

Figure 4-13 The effect of inclination angle on the mean (solid line) and mean max (broken line) torque for flat, ■; convex, ● ; and bowtie, ▲, discs

4.7.3 Dynamics of soil-disc interaction

Upadhyaya *et al.*, (1987) and Salokhe *et al.*, (1994) have found that simple tools acting in agricultural soils sustain horizontal forces which fluctuate in a periodic way. Analysis of the forces and torque results in this study showed a discrete complex wave form for draught, vertical force (Figure 4-14) and torque (Figure 4-15) which varies with respect to time.

Figure 4-14 shows that there is a discrete sinusoidal shape for draught and vertical force with a period of 0.90 s and amplitude of 200 N and 310 N, respectively. There is a sinusoidal increase and decrease in the forces with a peak draught and vertical force between 250 N and 400 N respectively. The minimum draught force is between 41 N and 81 N and between 90 N to 190 N for the vertical force. This fluctuation in the forces is due to the soil resistance of the cutting process. Forces increase as the disc cuts the soil and reaches a maximum point at the shear failure. As the disc is rotating and moving forwards part of the disc is now cutting disturbed soil and this results in the sinusoidal reduction of the forces, thus providing lower requirements for the draught and vertical force.

The disc is moving forward with 0.5 m s^{-1} and rotational speed of 1 rev s^{-1} in order to maintain the speed/plant spacing ratio to avoid the plants undisturbed zone. This shows the loading and unloading of the forces with time. A similar force-deformation curve employed by Upadhyaya *et al.*, (1987) for force versus soil displacement for the case when a tool moved rearward with respect to cutting front. Also from Figures 4-14 and 4-15 it can be seen that at the peak draught force torque also reaches its maximum value following the same shape as the soil forces. The result in torque (Figure 4-15) is an increase up to 21 Nm due to the resistance in the cut-out edge when rotating and cutting the soil, while at the minimum torque is lower at approximately 3 Nm. Because the period of each revolution is the same, the shape of the forces and torque are similar to the ones obtained by the simple harmonic motion. This comes in accordance with our results as the oscillation we obtained is sinusoidal. This variation in forces in torque is due to the cut-out sectors circular motion.

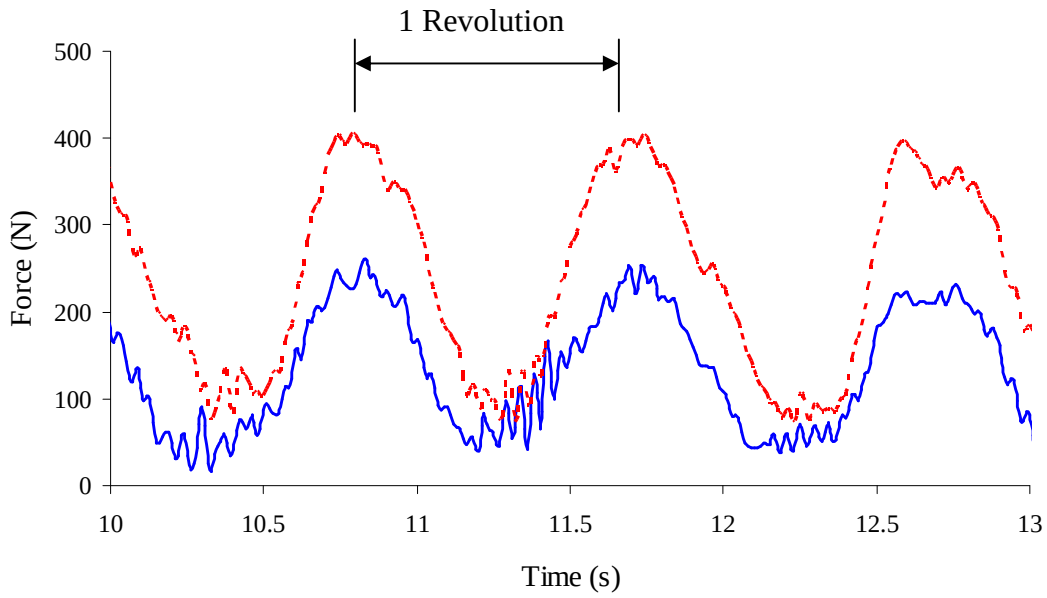

Figure 4-14 Draught and vertical force variation of a flat disc, draught (solid line) and vertical force (broken line) (inclination angle, 0^{o}; speed, 0.5 m s^{-1}; rotational speed 1 rev s^{-1}; working depth, 10 mm)

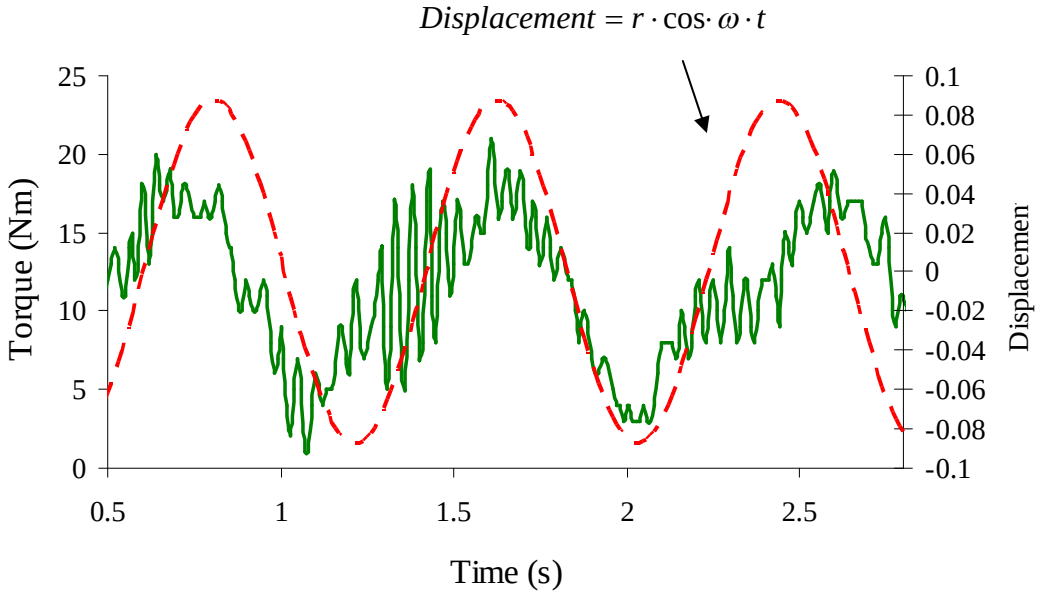

Figure 4-15 Torque variation for a flat disc (inclination angle, 0^{o}; speed, 0.5 m s^{-1}; rotational speed 1 rev s^{-1}; working depth, 10 mm)

Upadhyaya *et al.*, (1987) reported studies by Choa and Chancellor (1973) which showed that soil engaging tools that are forced to oscillate or resonate can cause the time-average draught to be less than that occurring when the tool is not reciprocating. In the present case this is been caused by the rotational action of the disc. Studies by Upadhyaya *et al.*, (1987) report that this effect occurs because the tool spends a period with a negative draught while reversing relative to the soil and a period at a low draught, when moving forward in previously cut soil.

Figure 4-16 shows the magnitude of draught force for a flat disc working at 0^o and 5^o inclination angles. The period and amplitude of, 0.04 s and 70 N respectively is significantly smaller with frequency of 25 Hz at 5^o inclination angle while for the same disc at 0^o the period and amplitude was 0.44 s and 177 N respectively with the frequency being 2.27 Hz. The reduction in force is due to the underside clearance which the 5^o inclination angle provides. The short period indicates that soil failure had smaller size aggregates producing a finer tilth than that produced when it was operated at 0^o inclination angle.

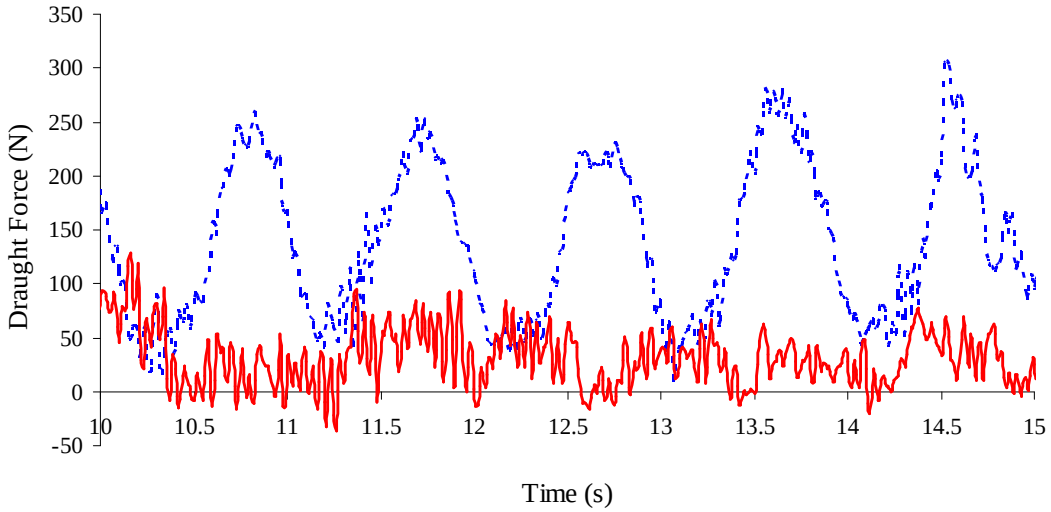

Figure 4-16 Draught force diagram for a flat disc working with 0^o (broken line) and 5^o (solid line) inclination angle (working speed, 0.5 m/s; rotational speed 1 rev/s; working depth, 10 mm)

During the controlled laboratory and field studies a different mode of soil failure was observed for the two discs. Figure 4-17 shows a two dimensional diagram for the two disc geometries of the resulting tilth. The convex disc created a fine tilth that was more uniform but for the flat disc larger aggregates were formed. Gill and Vanden Berg (1968) described a similar soil failure for plane tillage blades with a low inclination angle, with the same fundamental characteristic of a repeated failure of the soil by shear which forms small blocks of soil. Also the soil failure with the convex disc which leaves small regular aggregates can be related to the results of the same work where the size of the soil units is influenced by the height of lift of the cutter and in our case the effect of the concavity causes additional soil strain.

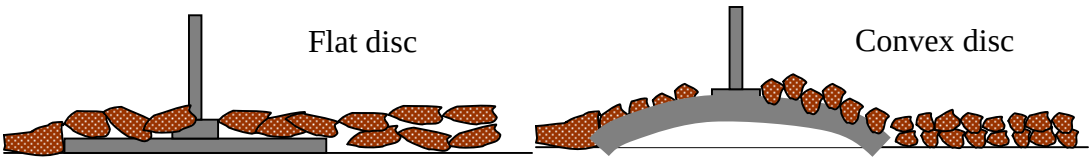

Figure 4-17 Representation of the mode of soil failure for the flat and convex disc

The inclined disc behaves like a shallow working, wide blade. When there is no inclination angle due to the small thickness (3 mm) of the disc the soil is undercut and, thus leaving big size aggregates. A similar conclusion made by Salokhe *et al.*, (1994) for driven disc tillers indicates that the wavelength of soil failure was longer in the case of unpowered disc tillers, which revealed that larger clods usually result from unpowered disc tillage. Their results indicate that the draught force and torque variations of driven powered disc tillers are periodic in nature due to discrete soil failure planes.

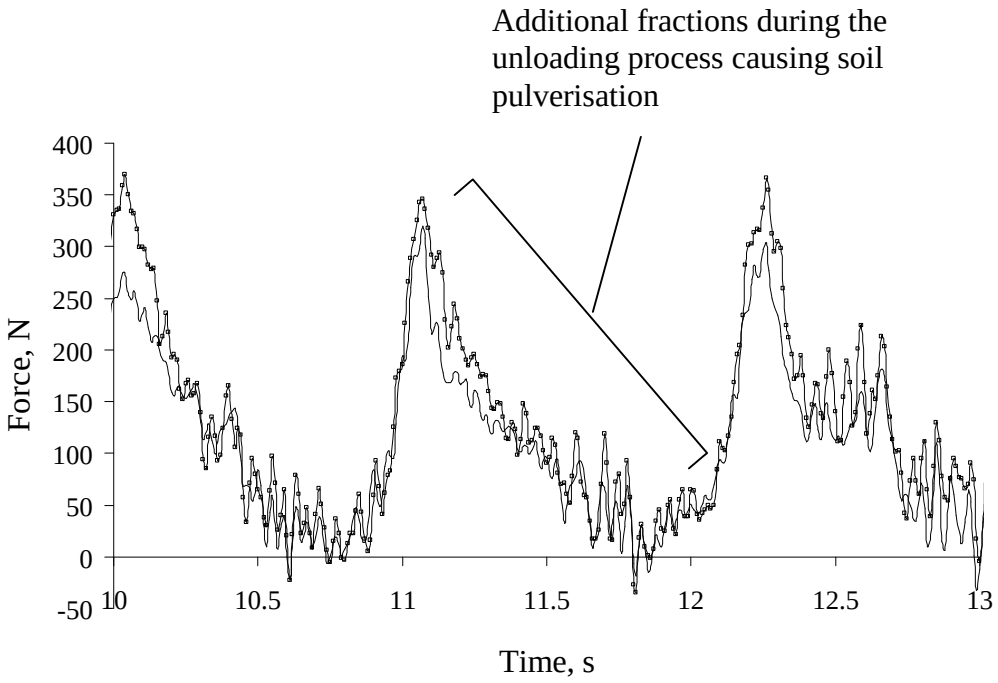

Figure 4-18 Draught (-) and vertical (□) force variation of a convex disc (inclination angle, 0^o; speed, 0.5 m/s; rotational speed 1 rev/s; working depth, 10 mm)

Figure 4-18 shows the soil forces with respect to time for a convex disc working with a 0^o inclination angle at, 0.5 m s^{-1} and 1 rev s^{-1} forward and rotational speed, respectively. The shapes of the soil forces have a saw tooth shape rather than a triangular one as in the case of the flat disc. If we study only one revolution in Figure 4-18 it shows a rapid increase in draught force and a slower reduction during the unloading process. Also the additional fluctuations within one period confirm the findings of Salokhe *et al.,* (1994).

Figure 4-19 shows the draught force variation in time for the flat and the bowtie disc working at 10 mm deep, with inclination angle of 0^o and forward and rotational speed of 0.5 m s^{-1} and 1.5 rev s^{-1} respectively. The period for a revolution is 1.5 s and 0.88 s for the flat and the bowtie disc respectively. For the same rotational speed the frequency is 0.66 Hz and 1.13 Hz. The frequency is generally double for the bowtie disc. This proves that the cut-out sector affects the sinusoidal shape of the force as

mentioned earlier on. The flat disc has one cut-out sector, and in the same period we can see from Figure 4-19 that the bowtie makes two revolutions.

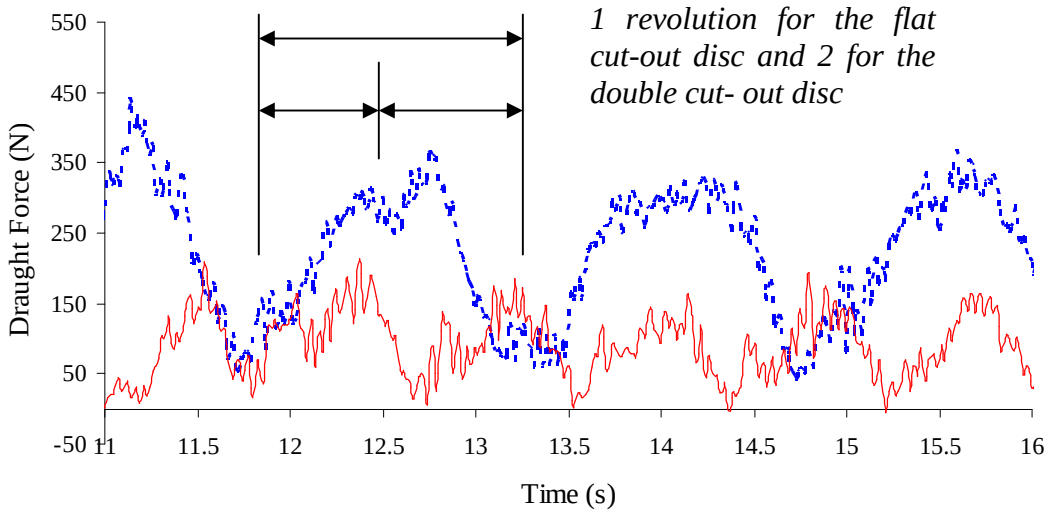

Figure 4-19 Draught force variation for the flat (broken line) and bowtie (solid line) discs (inclination angle, 0^{o}; speed, 0.5 m/s; rotational speed 1.5 rev/s; working depth, 10 mm)

4.7.4 Soil disturbance profile measurements

Analysis of the soil disturbance profile enables the absolute working depth to be found and enables measurement of the disturbed area. From this and the draught force measurements, the specific resistance can be calculated, providing useful information upon the most appropriate disc design and the working parameters, depth and inclination angle. After each test the surface disturbance created by the discs was excavated and the pattern the disc left after it had been through was measured with a profile meter across the width of the furrow. Each profile was traced on to paper and subsequently digitized.

Figure 4-20 shows how disc inclination angle and working depth can affect the soil disturbance with three different disc geometries in four different inclination angle positions and four depths. The analysis of variance for the inclination angle experiment (ANOVA) showed that there was a significance difference in the working depth with inclination angle. The mean working depth was -8.09 mm; -6.91 mm; -5.79 mm and -4.17 mm for inclination angles 0^o; 5^o; 10^o; and 15^o respectively with the least significant difference at 5% level of significance being 0.997 mm. The convex disc shows a tendency to disturb more soil with the mean disturbed area being 0.0022 m^2 while the flat and convex and the bowtie disc disturbed 0.0020 m^2 and 0.0019 m^2 respectively, with the least significant difference at 5% level of significance being 0.00044 m^2. Also the disturbed area decreased by increasing the inclination angle, being significant only between 0^o and 15^o.

The thickness of the flat disc is 3 mm and when in works at 10 mm deep with 0^o inclination angle, undercuts the soil. The convex disc because of its 17 mm concavity disturbs more soil in the same position, by lifting it after shear. As the inclination angle for the flat disc increases from 0^o to 10^o part of the disc is out of the soil and the disc behaves like a wide blade, and the disturbed area increases from 0.0021 m^2 to 0.0024 m^2.

The analysis of variance (ANOVA) for the working depth experiment showed that the disturbed area was significantly affected by the working depth. The disturbed area was 0.0027 m^2; 0.0033 m^2; 0.0041 m^2; and 0.0047 m^2 at depths 10 mm; 15 mm; 20 mm; and 25 mm respectively, with the least significant difference at 5% level of significance being 0.00045 m^2.

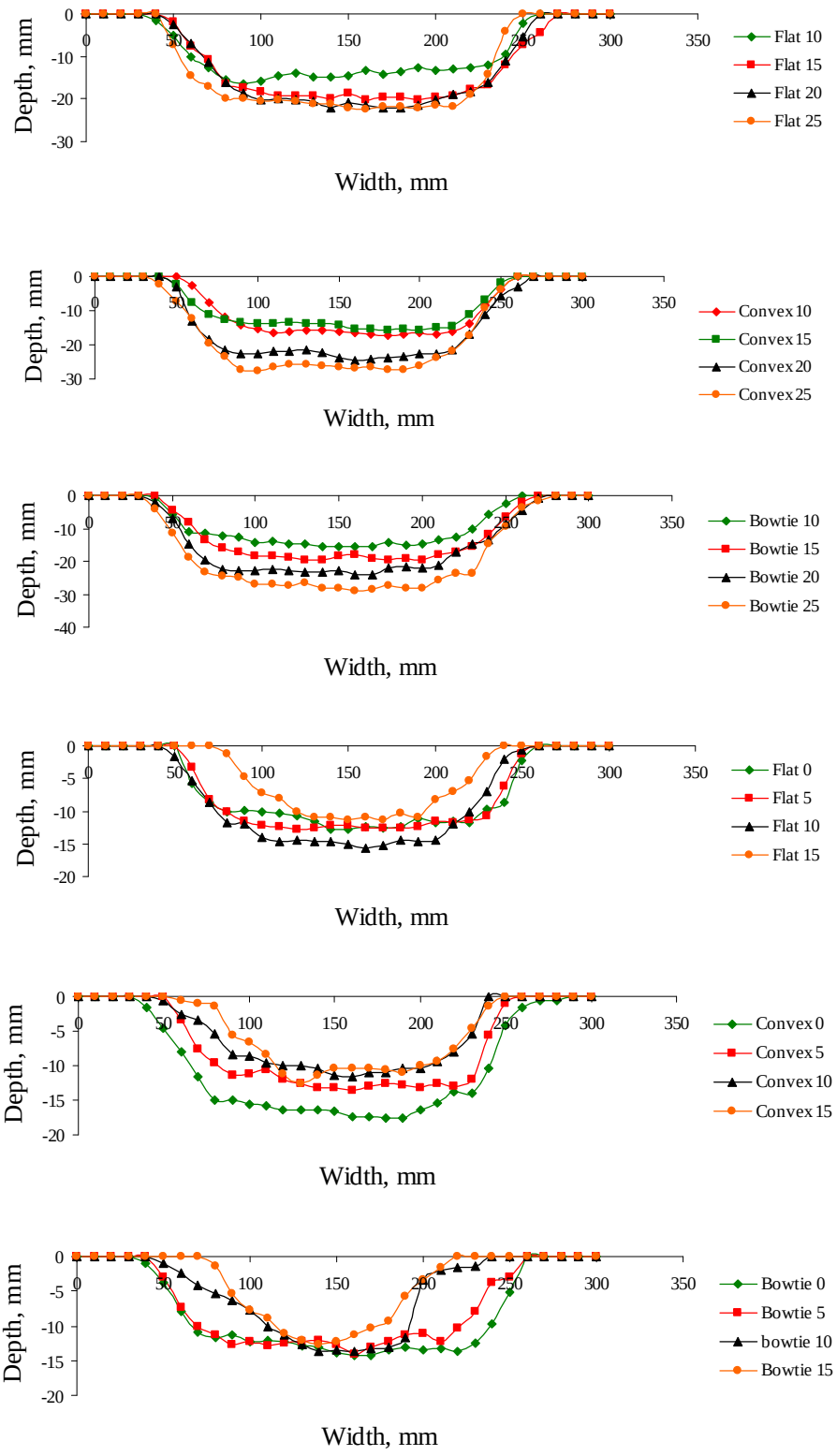

Figure 4-20 Static soil disturbance profile measurements for the three disc geometries for the depth and inclination angle effect

Table 4-1 summarises the draught force and the disturbed area for the flat and convex disc for the different depths and inclination angles examined and detailed in this Chapter. As it can be seen there is a difference in the specific resistance for both discs when increasing the inclination angle from 0^o to 5^o, from 81.905 kN m^{-2} and 46.061 kN m^{-2} to 22.341 kN m^{-2} and 11 kN m^{-2} for the flat and the convex disc respectively. The convex disc disturbes more soil than the equivalent flat disc for depths from 10 mm to 25 mm and is varying from 0.0029 m^2 to 0.0048 m^2.

Table 4-1 Specific resistance for the flat and convex disc

Inclination Angle (deg)	**Depth (mm)**	**Draught Force (kN)**		**Disturbed Area (m^2)**		**Specific Resistance (kN/m^2)**	
		Flat	Convex	Flat	Convex	Flat	Convex
0	10	0.172	0.152	0.0021	0.0033	81.905	46.061
5	10	0.043	0.048	0.0023	0.0023	18.722	20.652
10	10	0.040	0.026	0.0024	0.0018	16.529	14.689
15	10	0.031	0.017	0.0014	0.0015	22.341	11.000
0	10	0.135	0.185	0.0028	0.0029	48.214	63.793
0	15	0.152	0.174	0.0036	0.0028	42.222	62.143
0	20	0.143	0.214	0.0038	0.0043	37.632	49.767
0	25	0.264	0.219	0.0039	0.0048	67.692	45.625

In practice for a disc angle of 5^o or greater the mean-max draught force is equal to approximately 125 N which results in a power requirement for a five row machine of 1.25 kW for the rotating disc components, considering a safety factor equal to two.

4.8 Conclusions

A novel mechanical system for intra-row weed control was designed and evaluated in controlled laboratory studies. The following conclusions can be drawn:

- Inclination angle and disc geometry had a significant effect on disc forces and soil failure. A small increase in inclination angle to the direction of travel reduces the magnitude of draught and vertical force, 70% and 80% respectively in average for both disc geometries. The direction of vertical force is upward when all disc geometries work with 0^o inclination angle. The direction of vertical force is changing and assists the disc's penetration when the inclination angle is larger than 0^o.
- The disc geometry has a significant effect on soil failure and force direction and magnitude. The convex disc requires 15% less draught force than an equivalent flat disc.
- The mean and mean-max torque requirements for the effect of depth and inclination angle was generally 15 Nm and 25 Nm, the power requirements are 95 W and 157 W respectively.
- The convex disc created a tilth that was more uniform and had a regular disturbance pattern of smaller soil aggregates compared with an equivalent flat disc.
- The shape of the soil forces and torque is similar to the one obtained by the oscillation motion as the period of each revolution is the same. This results in the simple harmonic motion that has a sinusoidal shape.

Chapter 5

Soil Dynamics of Solid Discs

5 Controlled laboratory experiments into the soil dynamics of solid discs

This Chapter details experiments in controlled laboratory soil conditions of solid discs to investigate the soil forces as distribution on two different disc shapes, flat and convex as well at different operation modes, static and rotational. This would allow us to understand and quantify the dynamics of the soil-discs interactions and to develop a mathematical prediction model for the force and torque requirements. For that reason the experiment designed to include the effects of working depth, inclination angle and speed with both non-rotating and rotating solid discs. These studies are therefore focused very much at the fundamental shape than the actual practical discs of the earlier Chapter.

5.1 Experiment design

The experiments performed at the soil dynamics laboratory as described in Chapter 4, Section 4.1. The rotating disc hoe test apparatus (Section 4.2) was used to test these geometries using the same instrumentation software and hardware (Section 4.3).

The effect of working depth, inclination angle, speed and disc geometry on draught and penetration force requirements for flat and convex solid discs (Figure 5-1) in two different modes of operation static and rotational were assessed.

Four inclination angles (0^o; 5^o; 10^o; 15^o) were examined at 0.5 m/s (1.8 km/h) driving speed and 1 rev/s rotational speed at 10 mm deep. Four depths (10 mm; 15 mm; 20 mm; 25 mm) were examined at 0.5 m/s driving speed and 1 rev/s rotational speed at 0^o inclination angle. Four speeds (0.5 m/s, (1.8 km/h); 1 m/s, (3.6 km/h); 1.5 m/s, (5.4 km/h); 2 m/s, 7.2 km/h).

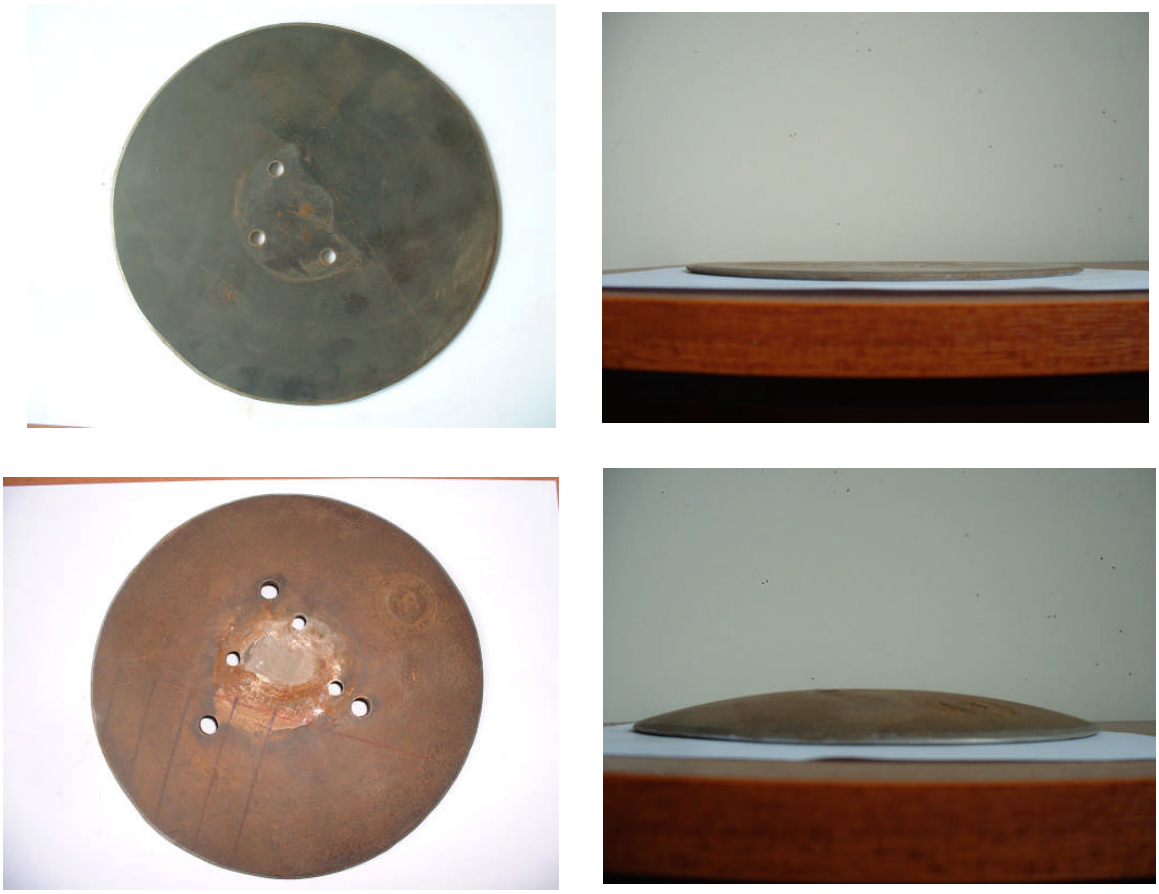

Figure 5-1 Disc geometries evaluated in the controlled laboratory experiments, flat (upper); convex (lower)

The soil was prepared as mentioned in Chapter 4, Section 4.4. The experiments were conducted in a randomized block design, each test being replicated three times. In total 144 experimental treatments were performed.

The soil type used was sandy loam, with 66%; 17%; and 17% of sand, silt and clay respectively. The mean soil moisture content was 8% with a standard deviation of

0.6%. The mean bulk density prior to the treatment was 1440 kg/m^3 with a standard deviation of 82 kg/m^3.

The measurement technique and the data analysis was performed as detailed in Chapter 4, Sections 4.5 and 4.6.

5.2 Results

All the results from inclination angle, depth and speed effect experiment for non-rotating and rotating solid discs can be found in Appendix IV.

5.2.1 The effect of depth on non-rotating solid discs

At a working depth of 15 mm and 25 mm there was a significant effect, at 5% level of significance on the measured mean and mean-max draught force for both disc geometries. The draught and vertical force increased with increasing working depth for the convex disc. Figure 5-2 shows the effect of working depth for a convex and a flat disc working at four depths with 0^o inclination angle and 0.5 m s^{-1} forward speed for the mean and mean-max draught force. Figure 5-3 shows the effect of working depth for a flat and a convex disc working at four depths with 0^o inclination angle and 0.5 m s^{-1} forward speed for the mean and mean-max vertical force.

The draught force for the flat disc is significantly greater than the equivalent convex disc for depths of 10 mm; 15 mm and 25 mm. The draught force for the convex disc is varying from 27 N to 119 N for depths from 10 mm to 25 mm. At a working depth of 10 mm there was a significant effect, at 5% level of significance on the mean and mean-max vertical force.

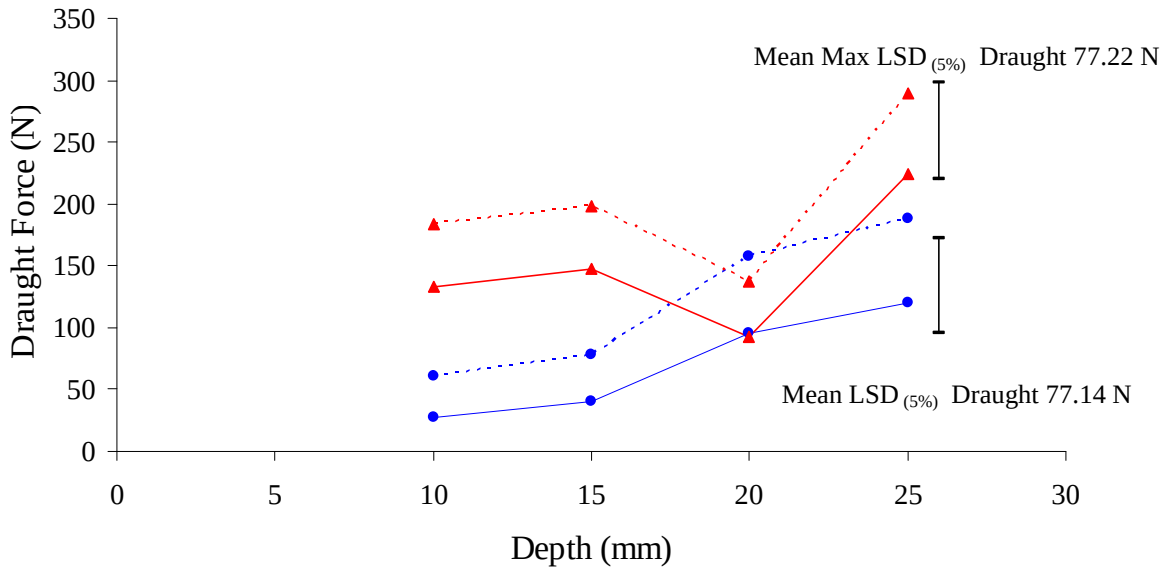

Figure 5-2 The effect of discs working depth on the mean (solid line) and mean-max (broken line) draught force for the convex (●) and flat (▲) disc (working speed, 0.5 m s^{-1}; inclination angle, 0^{o})

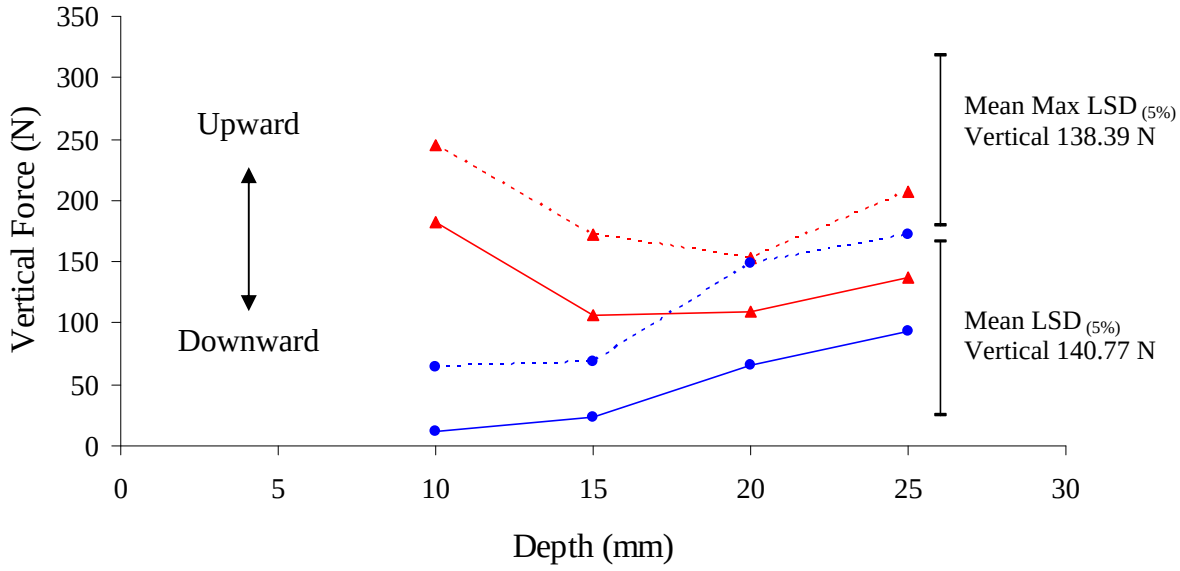

Figure 5-3 The effect of discs working depth on the mean (solid line) and mean-max (broken line) vertical force for the convex (●) and flat (▲) disc (working speed, 0.5 m s^{-1}; inclination angle, 0^{o})

For depths from 10 mm to 15 mm and 20 mm to 25 mm there is a 25% increase in draught force where from 15 mm to 20 mm there is greater increase of 58% for the convex disc. For the flat disc the draught force is varying from 132 N to 224 N for depths between 10 mm to 25 mm. In general it was found that the mean draught force in the range of the depths examined of the convex disc was half from the equivalent flat disc with the mean and mean-max draught force being 71 N and 149 N and 121 N and 202 N for the convex and flat disc respectively.

The vertical force for the flat disc was not significantly greater from the equivalent convex disc for depths from 15 mm to 25 mm. In general the mean vertical force for all the depths examined was 48 N and 133 N and the mean-max vertical force was 113 N and 194 N for the convex and flat disc respectively. The direction of the vertical force was upwards for the convex and downwards for the flat and increased with increasing working depth from 12 N to 94 N for the convex disc for depths of 10 mm to 25 mm. The direction of the vertical force for the flat disc showed a tenancy to move downward while increasing the working depth from 182 N to 137 N for depths of 10 mm to 25 mm. The mean-max vertical force was 30% and 60% greater than the mean vertical force for the flat and the convex disc respectively.

5.2.2 The effect of inclination angle on non-rotating solid discs

Increasing the inclination angle from 0^o to 15^o had not a significant effect on the mean and the mean-max draught force with the least significant difference at the 5% level of significance being 20.13 N and 20 N for the mean and mean-max draught force respectively. However when the inclination angle approached 0^o there was no clearance and scrubbing occured on the underside of the disc so that the forces increased. Figure 5-4 shows that from 0^o to 5^o inclination angle there is a 37% reduction in draught force for the convex disc. This shows that even a very small inclination angle, 5^o provides sufficient clearance, so reducing the underside friction on the disc. Figure 5-5 shows the mean and the mean-max vertical force for the flat and the convex disc. Increasing the inclination angle from 0^o to 15^o had a significant

effect on the mean-max vertical force for the convex disc. Also the increase in inclination angle changes the flat disc's vertical force direction. As it can be seen in Figure 5-5 at 15^{o} and at 10^{o} for the mean and the mean-max vertical force the direction is downwards for both discs. The mean vertical fore for inclination angles from 0^{o} to 15^{o} is varying from 8 N to -2.5 N and -1.08 N to -0.68 N, where the mean-max vertical force is varying from 56.8 N to 27.7 N and 31.7 N to 31.1 N for the convex and the flat disc respectively.

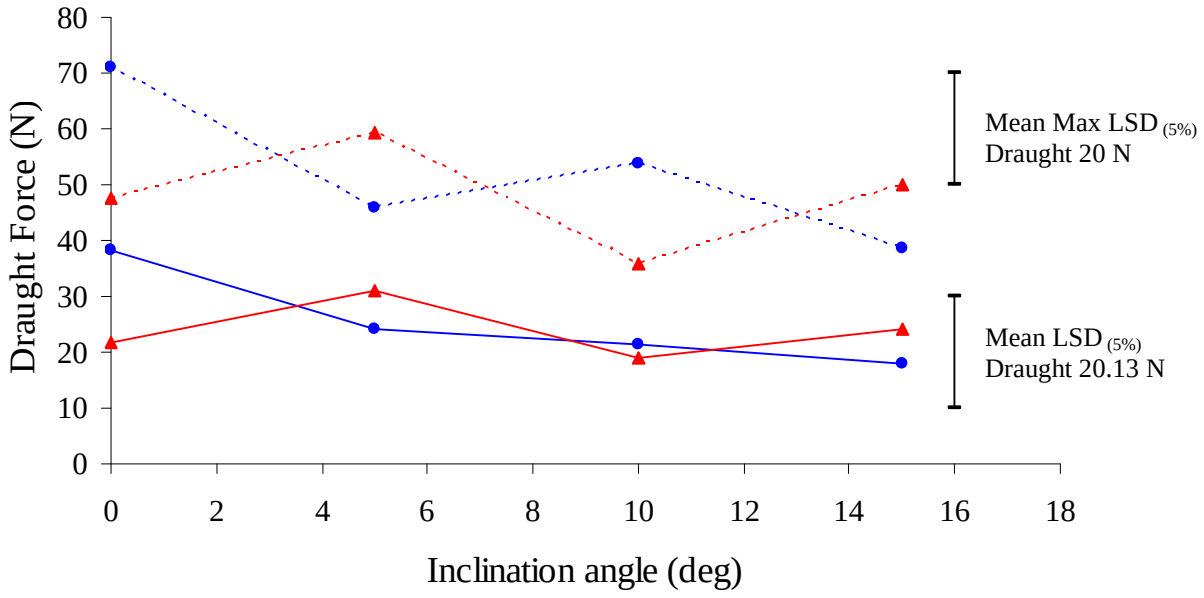

Figure 5-4 The effect of inclination angle on the mean (solid line) and mean-max (broken line) draught force for the convex (●) and flat (▲) disc (working speed, 0.5 m s^{-1}; working depth, 10 mm)

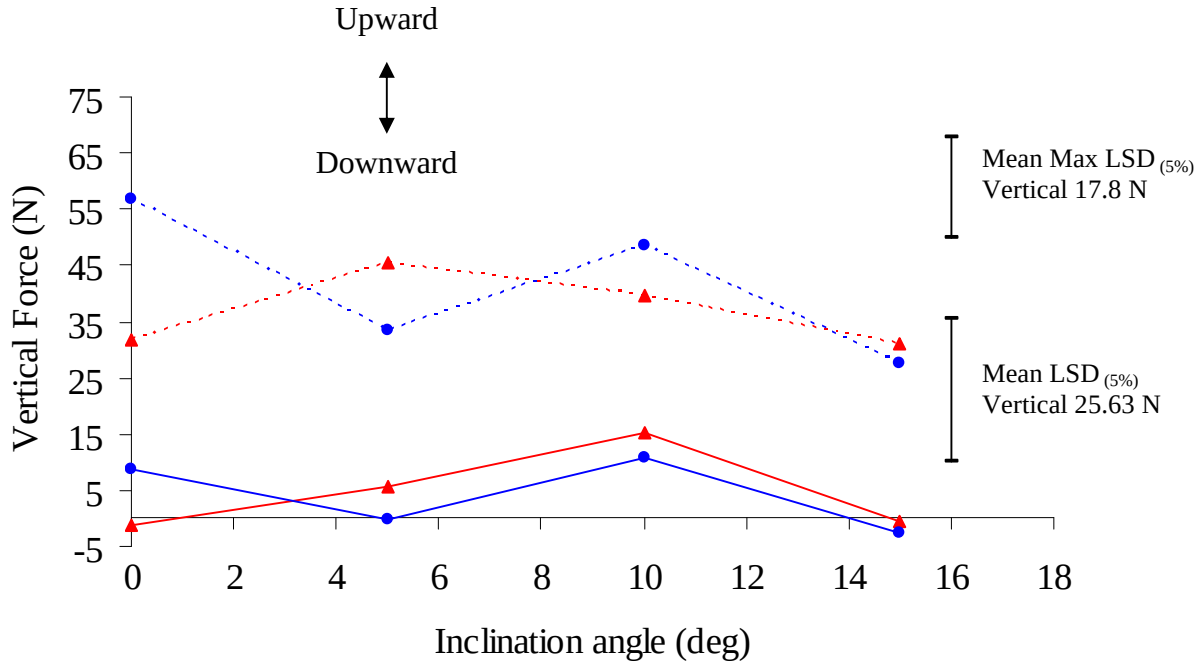

Figure 5-5 The effect of inclination angle on the mean (solid line) and mean-max (broken line) vertical force for the convex (●) and flat (▲) disc (working speed, 0.5 m s^{-1}; working depth, 10 mm)

5.2.3 The effect of forward speed on non-rotating solid discs

Figures 5-6 and 5-7 show the mean and mean-max draught and vertical force respectively. Increasing the forward speed from 0.5 m s^{-1} to 2 m s^{-1} had a significant effect on the mean and mean-max draught force for the convex disc. At 0.5 m s^{-1} the mean and the mean-max draught force was significantly greater, at 5% level of significance for the flat disc than the equivalent convex disc. Forward speed also effect the magnitude of the vertical force. At speeds from 0.5 m s^{-1} to 2 m s^{-1} had a significant effect on the mean and the mean-max vertical force for the flat and the convex disc. These results are similar to those found by Stafford (1979) and Wheeler and Godwin (1996) for narrow tillage tools working at 25 mm deep where the force increases with speed. Increasing the forward speed from 0.5 m s^{-1} to 2 m s^{-1} results in a 73% and 88% increase in draught and vertical force respectively. The results by

Wheeler and Godwin (1996) showed an increase in draught force for speeds from 0.5 m s^{-1} to 2.8 m s^{-1} of 43%. Also the increase in draught and vertical force in each speed increase of 0.5 m s^{-1} interval showed a mean increase of 35% and 50% for the draught and vertical force respectively.

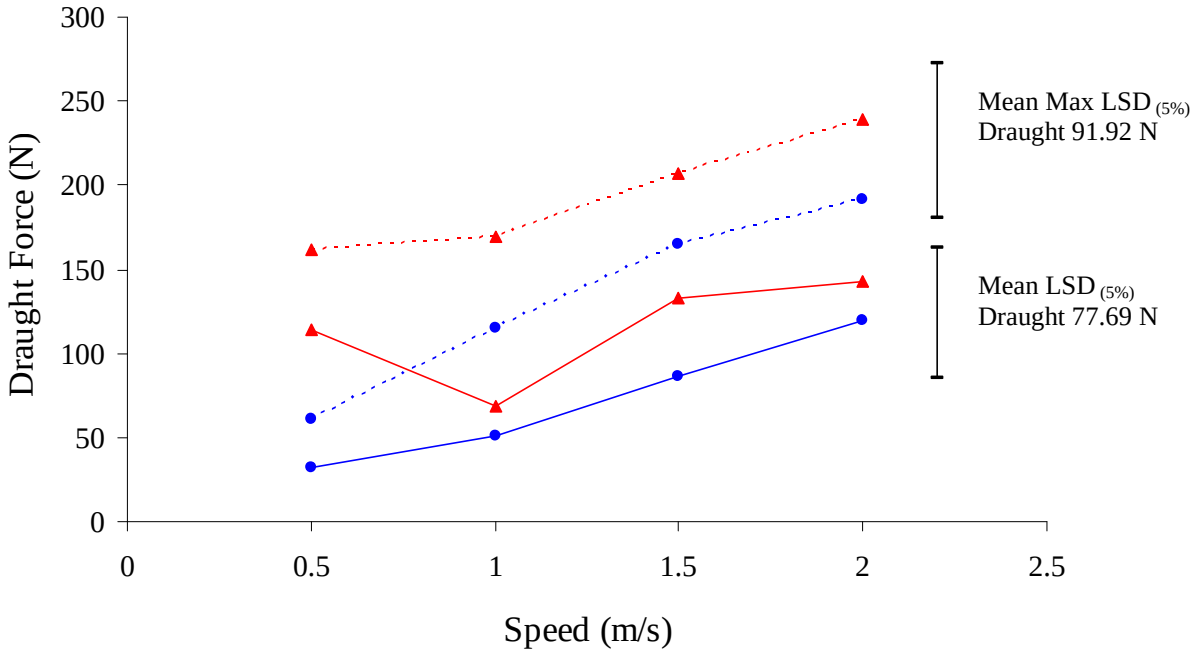

Figure 5-6 The effect of speed on the mean (solid line) and mean-max (broken line) draught force for the flat (●) and convex (▲) disc (inclination angle, 0^{o}; working depth, 10 mm)

Figure 5-7 shows the results on the mean and mean-max vertical force for a flat and a convex disc in the range of 0.5 m s^{-1} to 2 m s^{-1} forward speeds. As it can be seen the pattern obtained from the controlled laboratory studies is of unusual shape and such a pattern is mentioned in literature for soil engaging tillage tools. At speeds of 0.5 m s^{-1}; 1.5 m s^{-1} and 2 m s^{-1} there is a 10% increase in draught force for the flat disc. For forward speeds from 0.5 m s^{-1} to 1 m s^{-1} there is a 40% decrease in draught force. The apparent anomalies between 1 m s^{-1} and 1.5 m s^{-1} was thought to be due to an error in obtaining an absolute working depth of 10 mm.

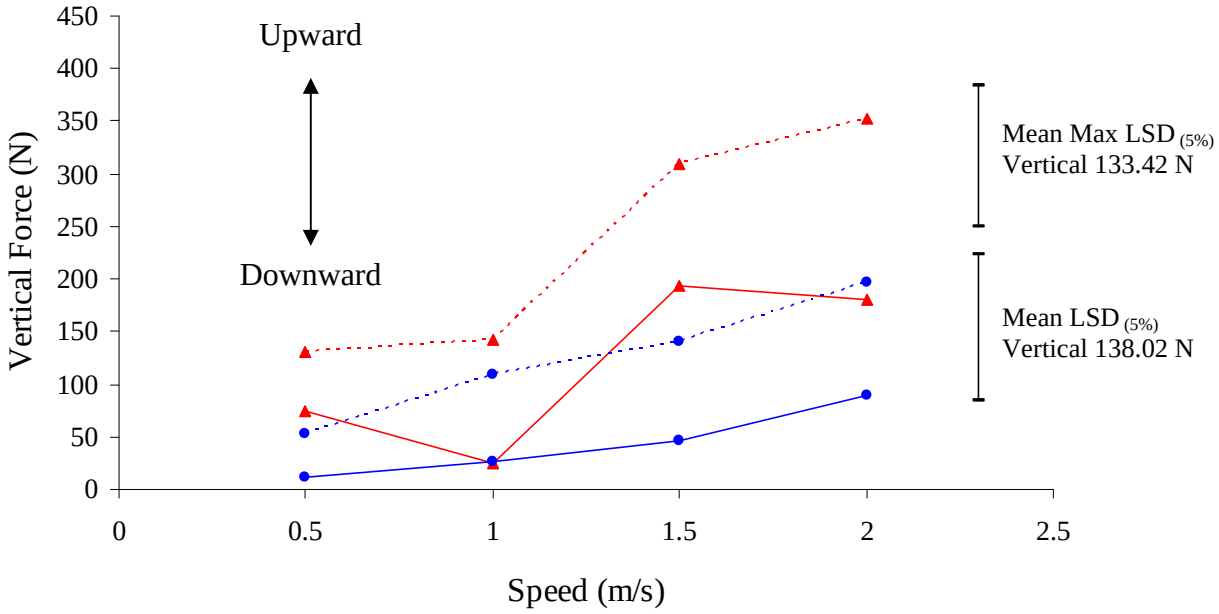

Figure 5-7 The effect of speed on the mean (solid line) and mean-max (broken line) vertical force for the convex (●) and flat (▲) disc (inclination angle, 0^{o}; working depth, 10 mm)

In order to help explain the force pattern of the flat disc an additional statistical analysis performed (ANOVA) using GenStat v.8.1 on the measured maximum values of draught force.

Figure 5-8 shows the increase in draught and vertical force on the mean-max values for both disc geometries over the range of speeds from 0.5 m s^{-1} to 2 m s^{-1}. The experimental data shown little deviation from a linear relationship, with the coefficient of determination (R^2) being 0.95 where the draught and vertical force effectively doubles and triples respectively from 0.5 m s^{-1} to 2 m s^{-1}. The results comes in accordance with those obtained from Wheeler and Godwin (1996) showing a linear relation and a significant increase in draught force.

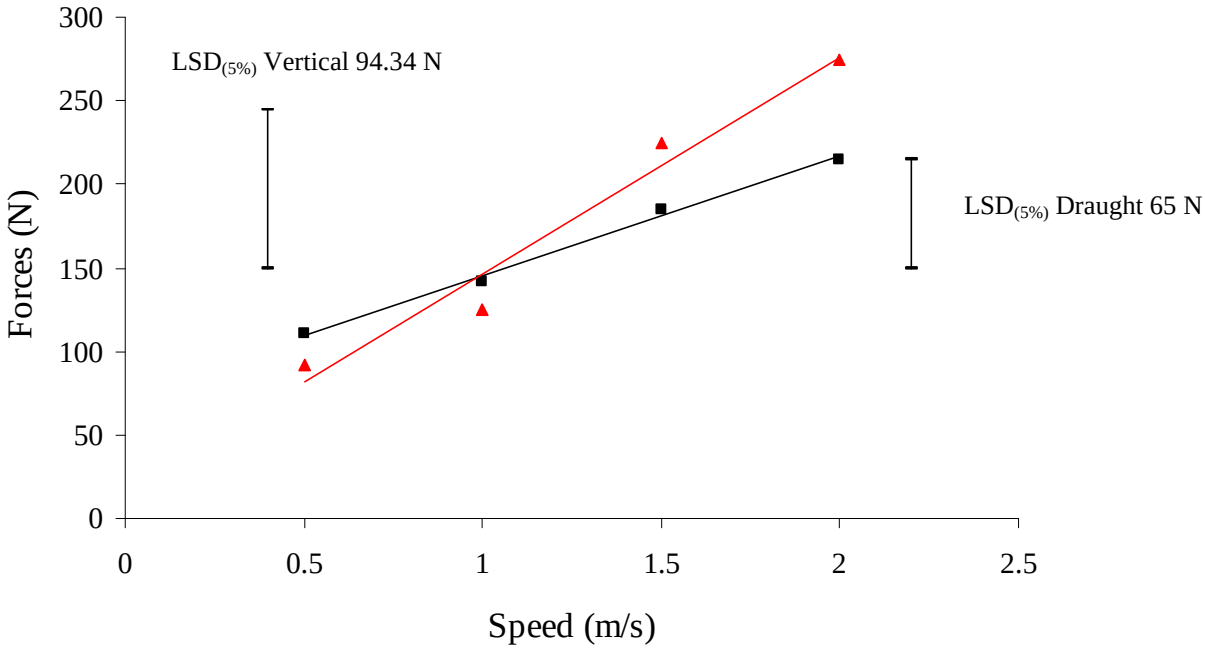

Figure 5-8 The effect of speed on the mean-max values for both disc geometries for draught (■) and vertical (▲) force

5.2.4 The effect of depth on rotating solid discs

Working depth from 10 mm to 25 mm had not a significant effect at a 5% level of significance on the mean measured draught and vertical force for the flat and convex disc. However working depth had a significant effect on the mean-max draught force for depths of 20 mm and 25 mm and for depths of 10 mm to 25 mm for the vertical force. Figures 5-9 and 5-10 show the mean and mean-max draught and vertical force for both disc geometries respectively.

Rotational speed increases the mean draught force by 24% and 5% for the convex and flat disc respectively. Also vertical force increased with the rotational speed by 46% and 36% for the convex and flat disc respectively. The draught force is varying from 59 N to 113 N and 109 N to 200 N for the convex and flat disc. For both discs the draught force doubles from 10 mm to 25 mm. The mean draught force is significantly

greater for the flat disc than the equivalent convex disc with the mean draught force through all the depths evaluated being 92 N and 156 N for the convex and flat disc respectively.

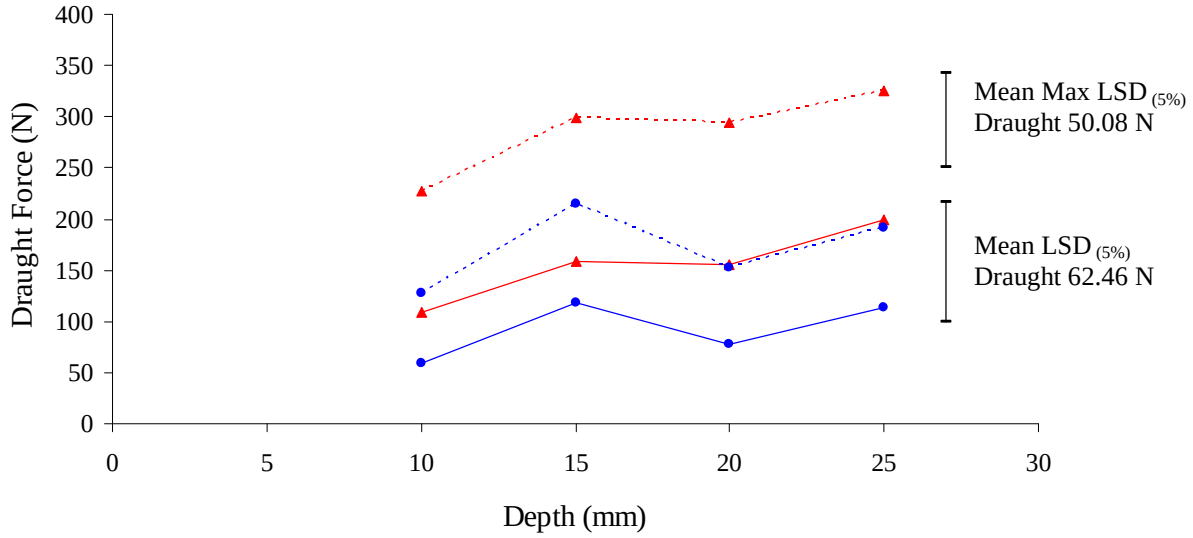

Figure 5-9 The effect of discs working depth on the mean (solid line) and mean-max (broken line) draught force for the convex (●) and flat disc (▲) (working speed, 0.5 m s^{-1}; inclination angle, 0^{o}; rotational speed, 1 rev s^{-1})

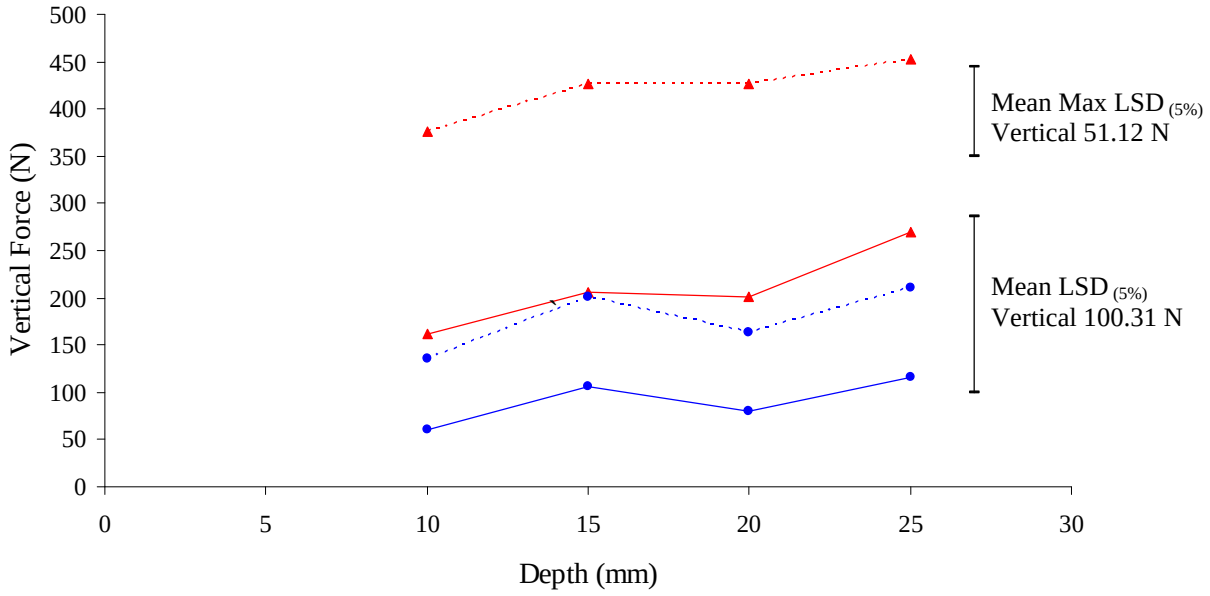

Figure 5-10 The effect of discs working depth on the mean (solid line) and mean-max (broken line) vertical force for the convex (●) and flat disc (▲) (working speed, 0.5 m s^{-1}; inclination angle, 0^{o}; rotational speed, 1 rev s^{-1})

The vertical force for the flat disc was significantly greater from the equivalent convex disc for depths from 10 mm to 25 mm. In general the mean vertical force for all the depths evaluated was 91 N and 201 N for the convex and flat disc respectively. The direction of the vertical force for both discs showed a tendency to move upwards. The mean torque required to rotate the convex and flat disc is 11 Nm and 12 Nm respectively Figure 5-11.

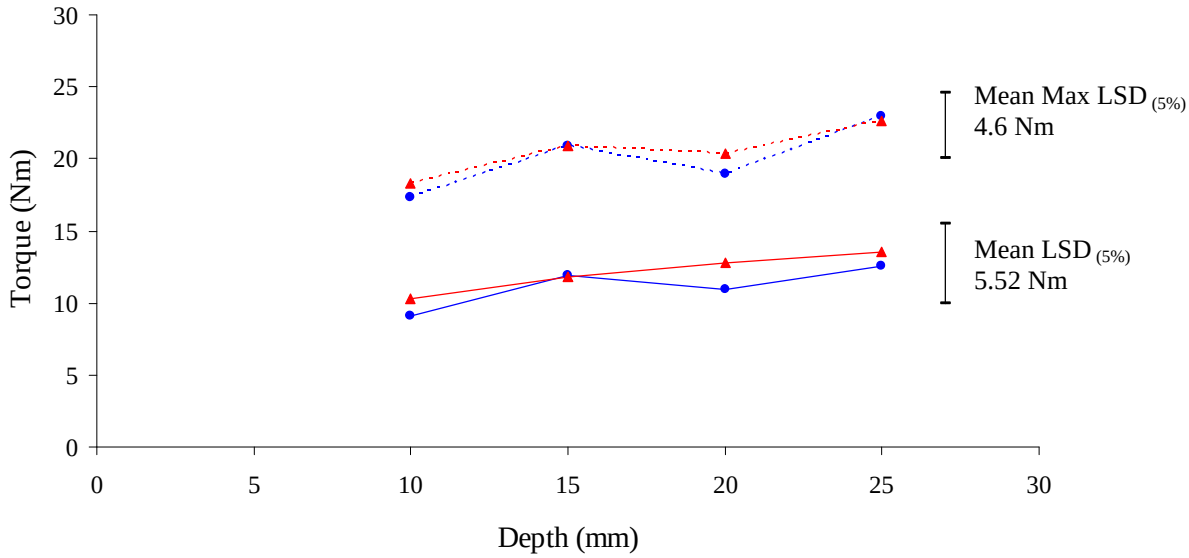

Figure 5-11 The effect of discs working depth on the mean (solid line) and mean-max (broken line) torque for the convex (●) and flat disc (▲) (working speed, 0.5 m s^{-1}; inclination angle, 0^o; rotational speed, 1 rev s^{-1})

5.2.5 The effect of inclination angle on rotating solid discs

Increasing the inclination angle from 0^o to 5^o had a significant effect at 5% level of significance on the mean draught and vertical force for the convex disc and the mean-max draught and vertical force for both disc geometries. Figures 5-12 and 5-13 show that a small increase in inclination angle from 0^o to 5^o had a significant effect on the magnitude of draught and vertical force. The mean and the mean-max reduction on draught force for both discs 65% and 63% and 48% for the flat and the convex disc

respectively. At inclination angles other than 0^o draught and vertical force had a uniform shape and magnitude up to 15^o inclination angle.

Torque was also reduced for both discs when the inclination angle increased from 0^o to 5^o due to the reduced contact area of the disc as mentioned in Section 4.7.3. The reduction in the magnitude of torque was of significance for the mean and the mean-max values of the convex disc. Figure 5-14 shows a 50% and 63% reduction in the mean torque and 25% and 40% in the mean-max torque for the flat and convex disc respectively for inclination angles, from 0^o to 5^o.

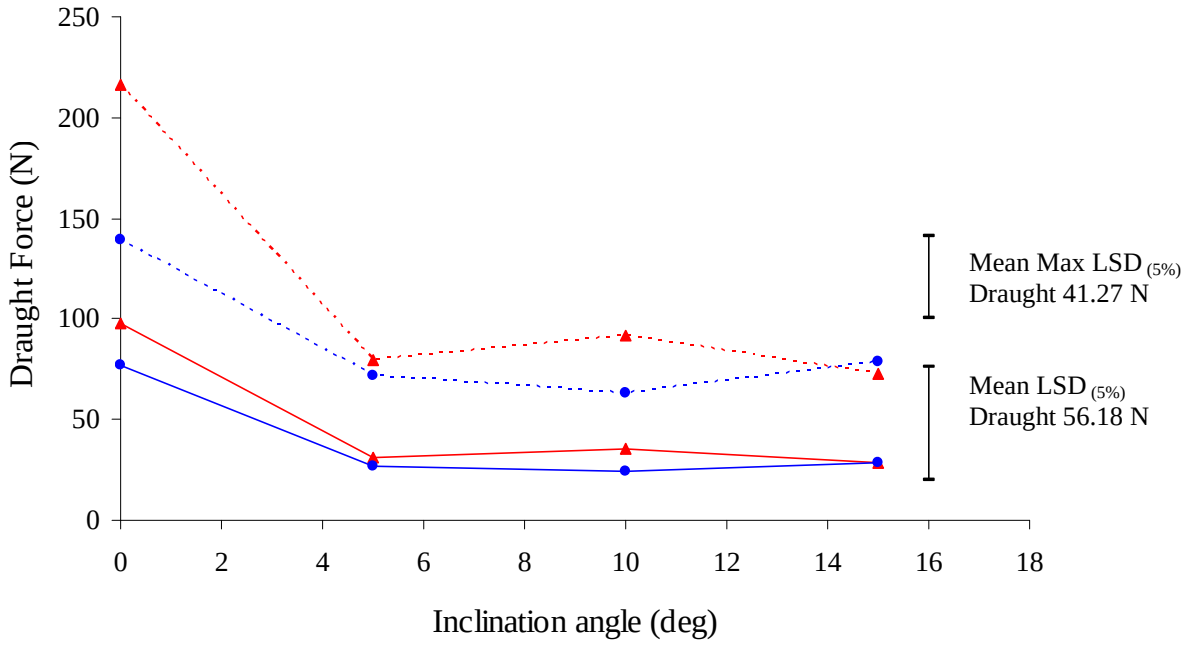

Figure 5-12 The effect of inclination angle on the mean (solid line) and mean-max (broken line) draught force for the convex (●) and flat, (▲), disc

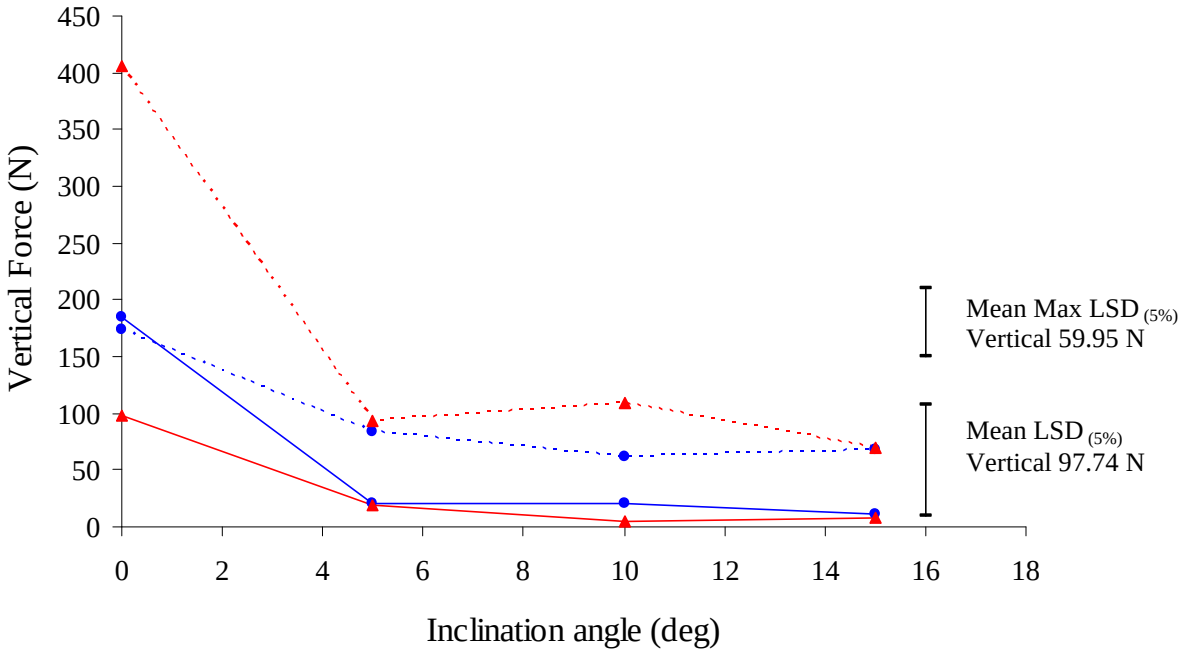

Figure 5-13 The effect of inclination angle on the mean (solid line) and mean-max (broken line) vertical force for the convex (●) and flat, (▲), disc

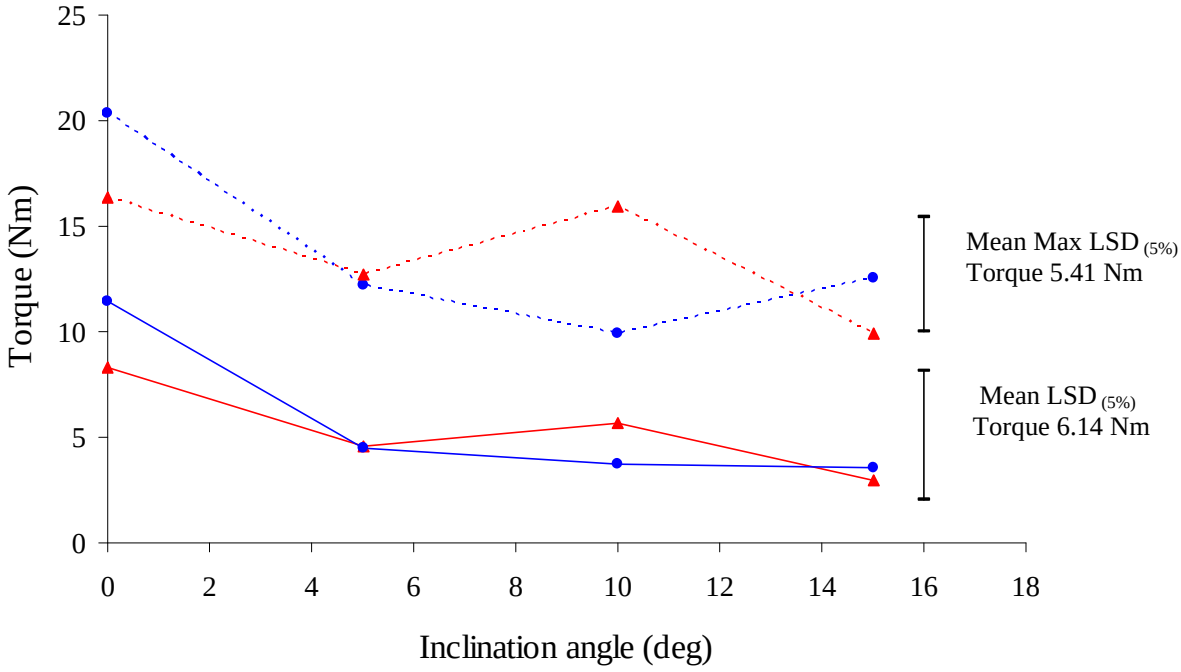

Figure 5-14 The effect of inclination angle on the mean (solid line) and mean-max (broken line) torque for the convex (●)and flat, (▲), disc (working speed, 0.5 m/s; rotational speed, 1 rev/s; working depth, 10 mm)

5.2.6 The effect of speed on rotating solid discs

Increasing the forward speed on rotating solid discs had the same effect on acting soil forces and torque as for the static solid discs, discussed in Section 5.2.3. Rotational speed from 1.6 rev s^{-1} to 6.6 rev s^{-1} for speeds of 0.5 m s^{-1} to 2 m s^{-1} increased the mean draught by 37% and 12% for the convex and flat disc respectively. Also the mean vertical force increased with speed by 62% and 45% for the convex and flat disc respectively.

Figure 5-15 shows the measured values for the mean and mean-max draught force for the convex and flat disc for forward speeds from 0.5 m s^{-1} to 2 m s^{-1}. At speeds from 1 m s^{-1} to 2 m s^{-1} there is a significant difference, at 5% level of significance for the mean-max draught force between the flat and the convex disc. Also from 0.5 m s^{-1} to 1 m s^{-1} the mean-max draught force increases significantly for the flat disc. The increase from 0.5 m s^{-1} to 2 m s^{-1} in draught force is less for the rotating solid discs for the equivalent discs in the static form that in the same range the draught force doubles (Section 5.2.3).

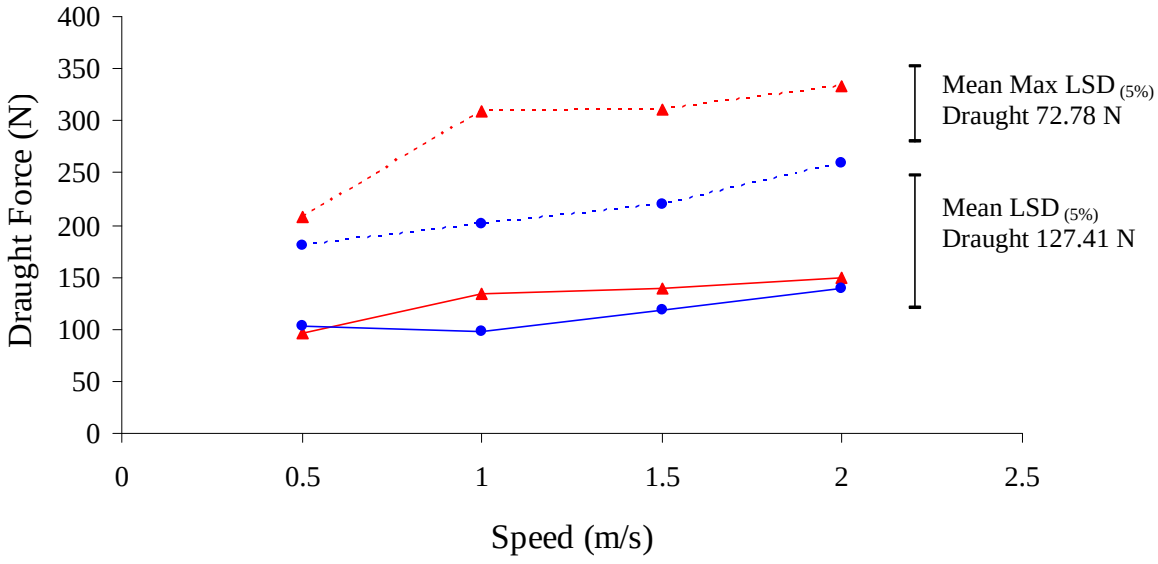

Figure 5-15 The effect of discs forward speed on the mean (solid line) and mean-max (broken line) draught force for the convex (●) and flat disc (▲) (working depth, 10 mm; inclination angle, 0^{o})

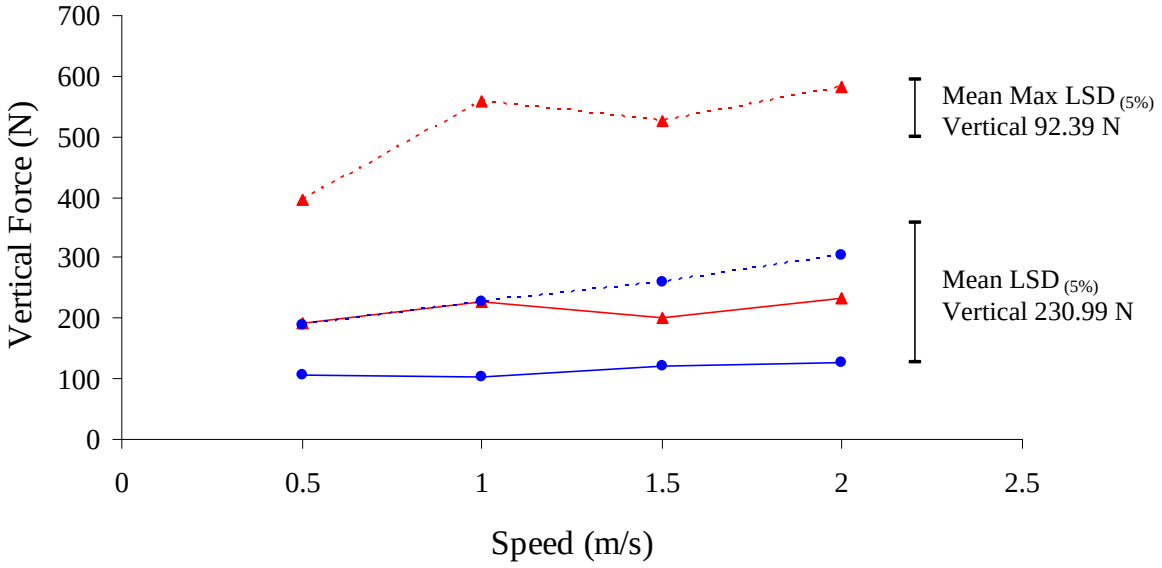

Figure 5-16 The effect of discs forward speed on the mean (solid line) and mean-max (broken line) vertical force for the convex (●) and flat disc (▲) (working depth, 10 mm; inclination angle, 0^{o})

Figure 5-16 shows the mean and the mean-max vertical force variation at different speeds for both disc geometries. As it can been seen there is a significant difference between the two discs with the magnitude of the mean-max vertical force for the flat disc being 50% greater than the equivalent convex disc. From 0.5 m s^{-1} to 2 m s^{-1} there is a 17% and 35% increase in the mean and mean-max vertical force for the convex and flat disc.

The mean and the mean-max torque for both discs were 12 Nm and 22 Nm respectively. Speed affected the mean-max torque for both disc geometries and it was of significance at speeds from 0.5 m s^{-1} to 2 m s^{-1} (Figure 5-17).

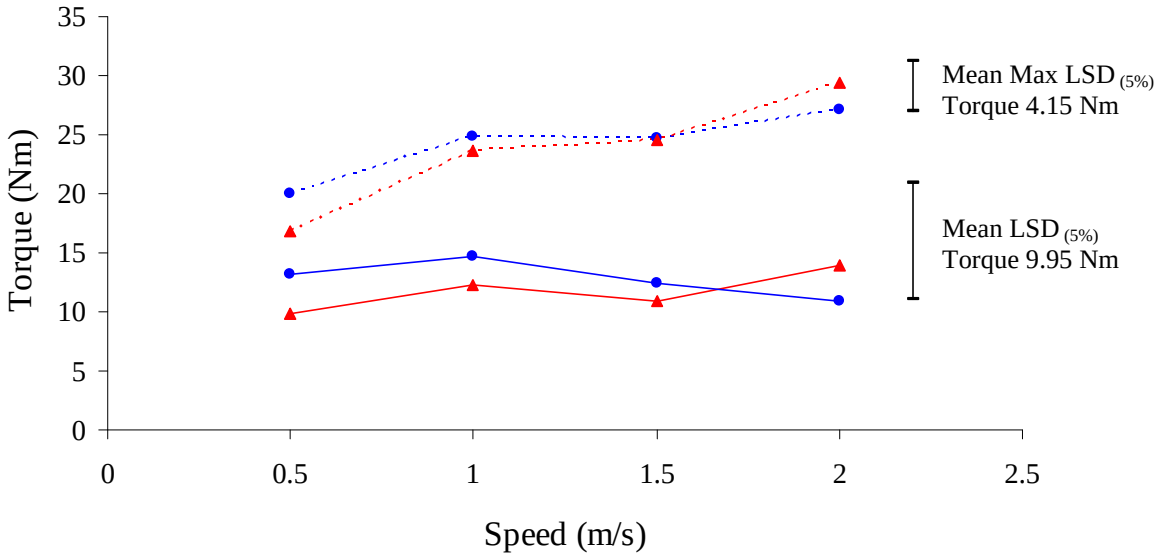

Figure 5-17 The effect of discs forward speed on the mean (solid line) and mean-max (broken line) torque for the convex (●) and flat disc (▲) (working depth, 10 mm; inclination angle, 0^{o})

5.3 Dynamics of soil-disc interactions

Analysis of the forces and torque results from the solid discs experiments showed a similar discrete complex wave form for draught, vertical force and torque which varies with respect to time as mentioned in Section 4.7.3. Figure 5-18 shows the draught force variation for a flat disc with 0^{o} inclination angle working 10 mm deep with forward and rotational speed of 0.5 m s^{-1} and 1.6 rev s^{-1} at three different working conditions, solid non-rotating, solid rotating and cut-out rotating discs. As it can be seen the magnitude of draught force increase for the solid disc when is rotating. Likewise there is an increase when a cut-out sector is removed from the disc due to the continues action of force in the cut-out sector of the disc. The mean-max draught force is generally 50 N, 150 N and 250 N for the flat non-rotating solid, flat rotating solid and flat cut-out rotating disc respectively.

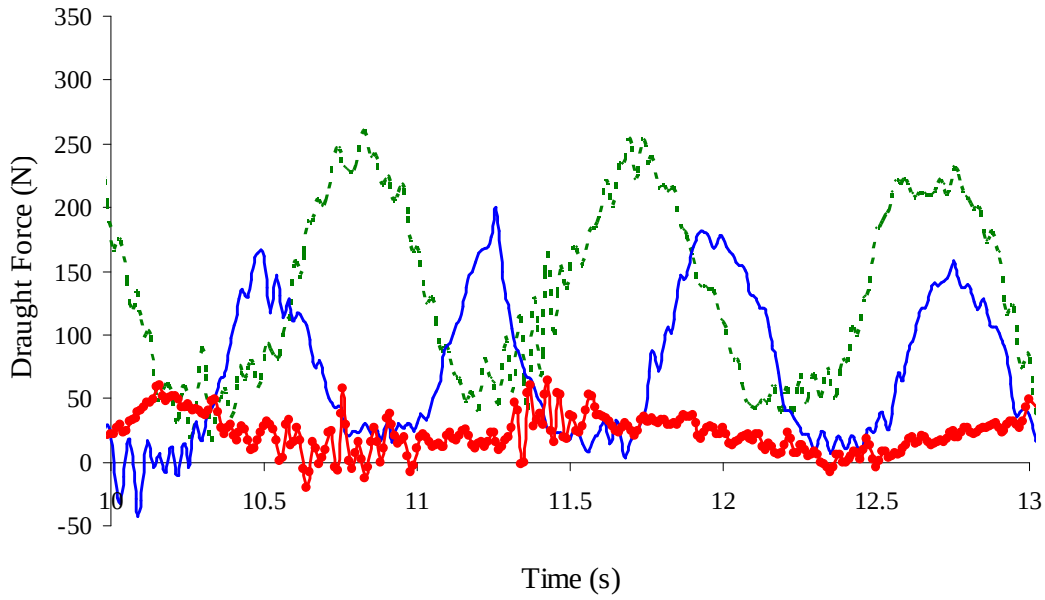

Figure 5-18 Draught force variation for a non-rotating solid (marked line) a rotating solid (solid line) and a rotating cut-out (broken line) disc (inclination angle, 0^{o}; speed, 0. 5 m s^{-1}; rotational speed, 1.6 rev s^{-1}; working depth, 10 mm)

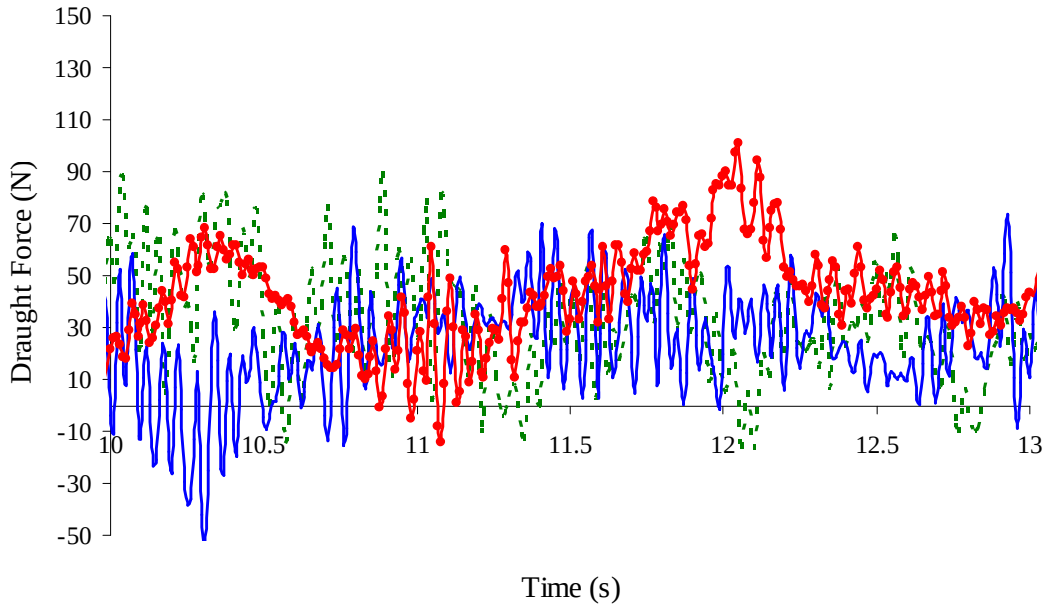

Figure 5-19 Draught force variation for a non-rotating solid (marked line) a rotating solid (solid line) and a rotating cut-out (broken line) disc (inclination angle, 5^{o}; speed, 0. 5 m s^{-1}; rotational speed, 1.6 rev s^{-1}; working depth, 10 mm)

Figure 5-19 shows the draught force variation for the flat disc in the same working conditions as mentioned earlier with 5^o inclination angle. As it can be seen the magnitude of draught force is smaller than when it was working with 0^o inclination angle and the shape of the force trace is similar for the non-rotating, rotating and cut-out disc.

The rotational speed for the rotating solid and cut-out disc was adjusted at 1.6 rev s^{-1}. When the discs engaged the soil it was observed that the actual rotational speed had a frequency of 1.06 Hz and 1.37 Hz for the cut-out and the rotating solid disc respectively due to the resistance in the cut-out edge when rotating and cutting the soil. The difference in the frequency between the rotating solid and cut-out disc confirms that the cut out sector affects the soil-disc interaction. Figure 5-20 shows the torque variation for the rotating solid and cut-out disc at difference inclination angles for the flat and the convex disc. As it can be seen torque increases for both discs when a cut-out sector is removed from the disc.

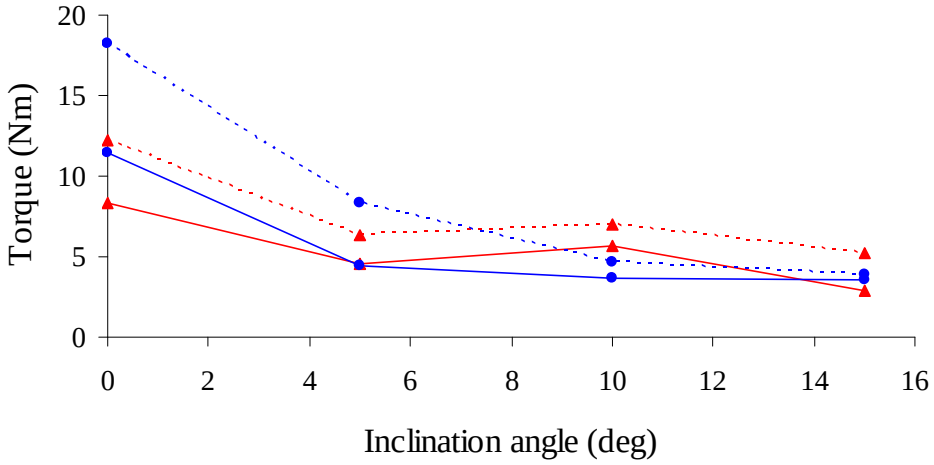

Figure 5-20 The effect of inclination angle on the mean torque for a rotating flat (▲) and a convex (●) disc without (solid line) and with (broken line) a cut-out sector

5.4 Soil failure and contact width of solid discs

During the soil force measurements on static and rotating solid discs it was found necessary to perform additional auxiliary measurements on the disc's contact width, the soil failure and form ahead of flat and convex discs in different inclination angles and depths under quasi-static conditions, that could be used for the development of the force prediction model and help to further understand the soil mechanics ahead of discs working close the horizontal plane. The soil type used was sandy loam and was the same used in the previous experiments, with 66%, 17%, and 17% percentage of sand, silt, and clay respectively. The mean soil moisture content was 7.5% with a standard deviation of 0.4%. The mean bulk density prior the treatment was 1400 kg m^{-3} with a standard deviation of 36 kg m^{-3}.

5.4.1 Rupture distance

Figure 5-21 shows the disturbed soil ahead of a flat disc at 15^{o} inclination angle. The schematic representation shows the measurements taken immediately after the disc had been through the soil. Two measurements performed:

1. The soil disturbed ahead of the disc up to the centre of the disc (R_l)
2. and then the soil was excavated and the distance between the discs edge to the undisturbed soil was measured (r_4; r_5; r_6) in the segmental area of the disc

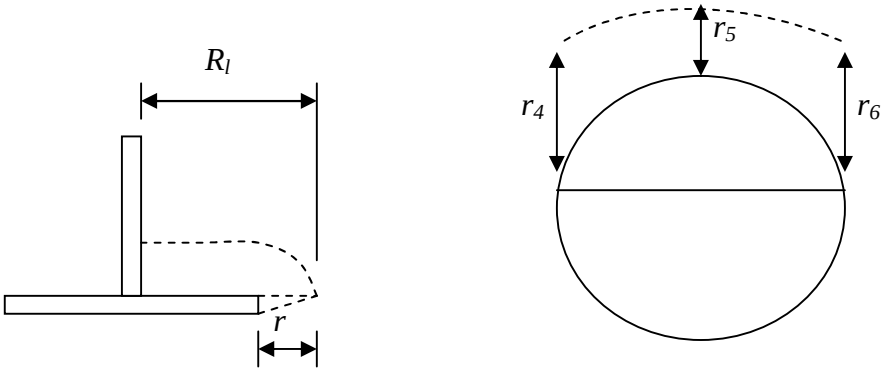

Figure 5-21 Static measurements on rupture distance ahead of a static flat disc

Figure 5-22 shows the results for the distance from the disc's edge to the undisturbed soil for both disc geometries. As it can be seen the rupture distance increases with inclination angle. From 0^o to 5^o and 15^o of inclination angle there is no significant difference at 5% level of significance. At an inclination angle of 10^o there is significant difference from the 0^o inclination angle.

Disc geometry had a significant effect on rupture distance with the flat disc having greater rupture distance than the equivalent convex disc at 5% level of significance. The rupture distance for the convex disc was 22 mm and 30 mm for the flat disc with the $LSD_{(5\%)}$ being 3.5 mm. At both depths, 20 mm and 25 mm the convex disc had a constant rupture distance of 22 mm where the flat disc had 28 mm and 32 mm for depths pf 10 mm and 15 mm respectively.

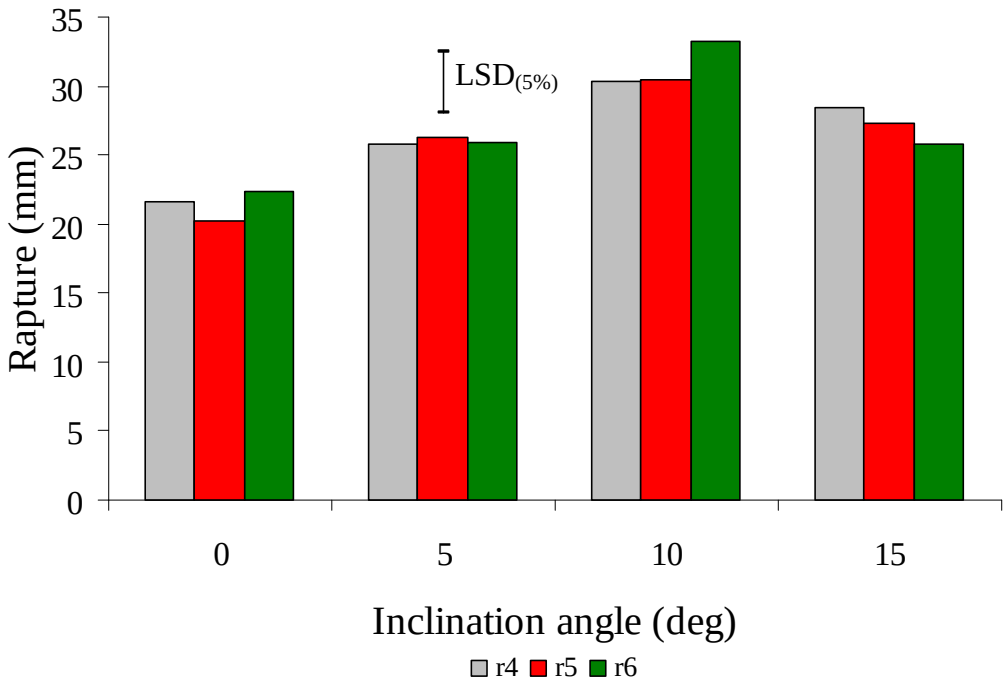

Figure 5-22 Rupture distance for both disc geometries, $LSD_{(5\%)}$ 4.5 mm

Table 5-1 shows the summary of results for the measurements of R_l for the flat and convex disc at depths of 10 mm and 15 mm and in four different inclination angles, 0^o; 5^o; 10^o and 15^o. As it can be seen there is no significant difference between the treatments.

Table 5-1 Summary of results for the soil disturbed from the edge to the centre of the disc for both disc geometries at two depths and four inclination angles

Inclination angle	Flat		Convex	
	10 mm	**15 mm**	**10 mm**	**15 mm**
0	139	145	145	150
5	138	122	135	112
10	150	147	152	147
15	144	128	143	132

5.4.2 Disc contact width

Figure 5-23 shows the measurement of the disc's contact width with soil at different inclination angles. These measurements will help us understand and quantify the percentage of reduction of the contact area of the disc with soil at different inclination angles, and will be incorporated in the force prediction model. The reduction of the disc's contact width will affect the amount of disturbed soil as well as the specific resistance (kN m^{-2}). Also the underside friction will be reduced as less part of the disc will be in contact with soil. These have an effect on the magnitude and direction of draught and vertical force as well as torque.

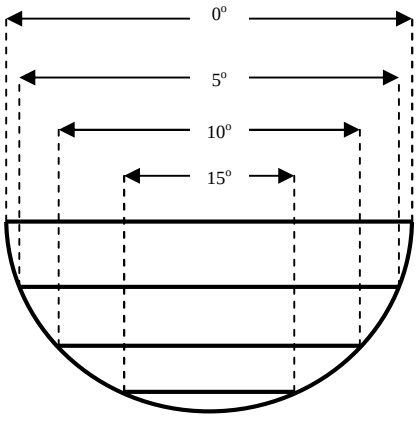

Figure 5-23 Static measurements of the disc contact width with soil

Figure 5-24 shows a linear reduction of disc's contact width by increasing the inclination angle from 0^o to 15^o. There is a 28%; 20% and 45% reduction in the flat disc's contact width from inclination angles from 0^o to 5^o; 5^o to 10^o and 10^o to 15^o respectively. For the equivalent convex disc there is a 31%; 13% and 27% for the same range of inclination angles. The reduction from 0^o to 15^o inclination angle is 68% and 57% for the flat and convex disc respectively.

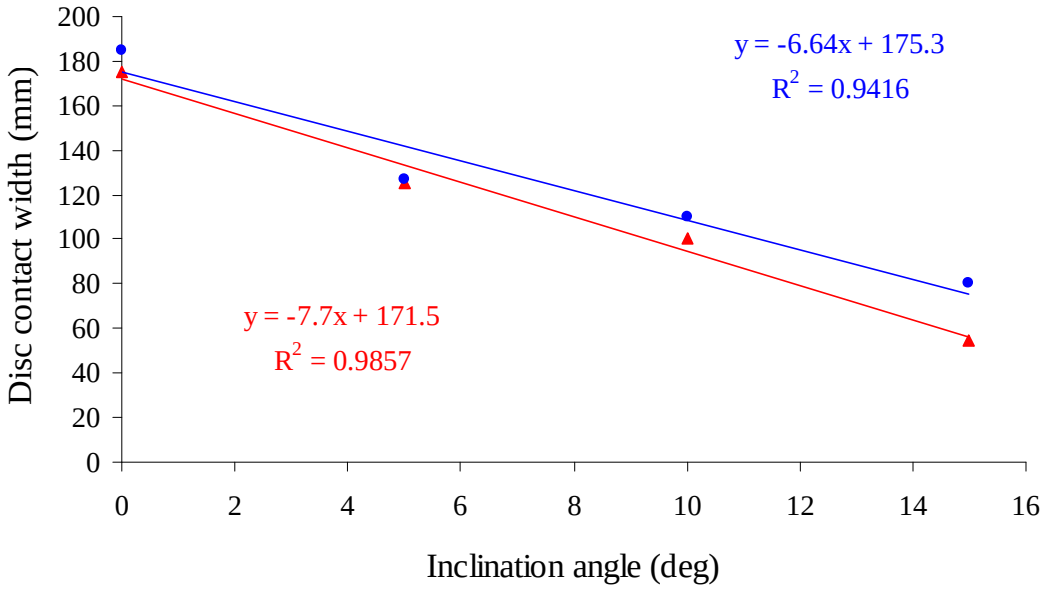

Figure 5-24 The contact width of the flat (▲) and convex (●) disc at four different inclination angles

5.5 Conclusions

The results from the controlled laboratory studies on static and rotating solid discs complement and confirm the results on rotating cut-out discs and provide us with important information for the force prediction model development. The following conclusions can be drawn:

- Inclination angle, working depth and disc geometry had a significant effect on the acting forces, coming in accordance with the findings of Chapter 4.
- The increase in draught force for every 0.5 m s^{-1} increase in forward speed is 30% and 15% for the convex and flat disc respectively.

- Rupture distance increase with inclination angle but it is not significant different at the 5% level of significance.
- The disc's contact width is reduced linearly with increasing inclination angle, 68% and 57% for the flat and convex disc respectively for inclination angles from 0^o to 5^o.
- The shape of the soil forces and torque is similar to the one obtained by the rotating cut-out discs described earlier by the oscillation motion as the period of each revolution is the same. This results in the simple harmonic motion that has a sinusoidal shape.
- The mean and the mean-max torque increases by 38%, 33% and 28%, 24% for the convex and flat disc respectively when a cut-out sector is removed from the discs. The mean and the mean-max torque for the solid rotating flat and convex disc and the rotating cut-out flat disc was generally the same and was 10 Nm and 20 Nm for a range of depths from 10 mm to 25 mm where for the rotating cut-out convex disc the mean and the mean-max torque was 20 Nm and 30 Nm.

Chapter 6

Force Prediction Mathematical Model

6 Force prediction mathematical models

This Chapter describes the methods and processes of the development of a prediction model that can be used to predict the acting forces and torques on non-rotating and rotating solid discs and the rotating cut-out discs proposed for mechanical weed control. The proposed model will consider the geometric parameters of the discs, the speed of operation, the working depth and the physical properties of soil based upon those required for the general soil mechanics equation (Hettiaratchi *et al.,* 1966) which obeys the Mohr-Coulomb failure criterion.

6.1 Introduction

According to Godwin (2007) the type and degree of soil disturbance is the prime factor when selecting tillage implements but this must be considered together with the draught and vertical force requirements for efficient operation. Also there are two major variables in the design and selection of the appropriate geometry for given tillage implements:

1. The depth, width ratio (*d/w*)
2. The rake angle (α)

The knowledge of the tool forces during soil working is of value to designers of cultivation equipment in relation to the design of the working elements and their supporting frames (Godwin & O'Dogherty, 2007). Understanding the forces, which act upon rotating asymmetric tools, enables suitable disc geometry to be specified together with optimum operating settings so as to enable intra-row weed control with minimum force and torque requirements. These relationships are valuable to designers and operators of cultivation equipment when selecting the optimal design of the soil working elements and their supporting frame. The right combination of inclination angle together with working depth and speed will increase the intra-row weed control area and minimize the soil thrown onto crop with the minimum force requirements (Dedousis *et al.,* 2007).

During the last four decades, several three dimensional analytical models have been developed for symmetric non-rotating tools based on the results from experimental work and Terzaghi's passive earth pressure theory. In these models, a soil failure pattern was proposed and soil force equations were derived from the proposed failure zones (Kushwaha *et al.,* 1993). Studies by Payne (1956) and Osman (1964) showed that by using the retaining wall and footing theories, predictions of soil failure for narrow tines and wide flat blades respectively can be achieved (Fielke & Riley, 1991). Reece (1965) assumed that the mechanics of soil cutting are similar to the bearing capacity mechanics of shallow foundations and presented an equation (Fundamental Equation of Earthmoving Mechanics) for the soil cutting force on a wide blade (Rajara & Erbach, 1996). The equation was of the same form with Terzhagi's (1943) bearing capacity equation for describing the soil failure force encountered by a tillage tool, incorporating an adhesion term.

Based on Reece's (1965) universal earthmoving equation several models were developed. Hettiaratchi *et al.,* (1966) presented a set of numerical charts utilizing the logarithmic spiral failure zone method of Sokolovski (1960) for a wide range of rake angles (α) and soil friction angles (φ). A three dimensional model was developed by Hettiaratchi and Reece (1967) to describe the soil failure caused by narrow blades having a width of about one sixth of the depth of operation. More realistic three dimensional models were developed by Godwin and Spoor (1977), McKyes and Ali (1977), Perumpral *et al.,* (1983) and Zeng-Yao (1992) accounting for both crescent and lateral soil failure. A detailed review of the prediction models can be found to Kushwaha *et al.,* (1993) and Shien and Kushwaha (1998). Work by Godwin and O'Dogherty (2007) integrates soil tillage force prediction models for a range of implements from narrow tines to land anhcros and includes a simple spreadsheet for quick calculations. A comparative description of the models can be found in McKyes (1985).

Numerous studies have been conducted to evaluate the force mechanics of freely rotating discs working vertically to the soil, Gill *et al.,* (1980), Abo El Ees and Wills (1986), Godwin *et al.,* (1987), O'Dogherty *et al.,* (1996) and Hettiaratchi and Alam

(1997). Gill and Hendrick (1976) and Hann and Giessibl (1998) measured the forces on driven discs without the development of a theory and an analytical model to predict the forces on driven discs. Soehne and Eggenmueller (1959) investigated fast running rotary cultivators and slow running diggers. Thakur and Godwin (1990) studied the tip effect phenomenon of rotary tillage tools while cutting a two dimensional soil slice with a wire under quasi-static conditions and developed a force prediction model based on Mohr-Coulomb soil mechanics. Upadhyaya *et al.,* (1987) and Gupta and Rajput (1993) studied the dynamics of soil-tool interactions for oscillating tools without the development of theory on predicting the forces. Albuquerque and Hettiaratchi (1980) presented an approximate method for the rapid evaluation of the passive soil thrust for sub-surface cutting blades using non-dimensional earth resistance coefficients.

The author was unable to locate in the literature an analytical model to predict the forces acting on very shallow asymmetric non-rotating or rotating discs (about a vertical axis) with a depth, ratio d/w of < 0.15 with inclination angles varying from 0^o to 15^o approaching the horizontal.

6.2 Sub-surface model evaluation

An interactive spreadsheet based on Albuquerque's and Hettiaratchi's (1980) mathematical model on sub-surface cutting blade theory was developed in order to investigate if the model can predict the forces acting on shallow working freely rotate discs.

The mathematical model is based on the general soil resistance equation developed by Hettiaratchi and Reece, (1974, 1975). Albuquerque & Hettiaratchi (1980) calculated the earth resistance coefficients, N by combining Sokolovski's (1960) type slip-line fields with a special modified Rankine plane shear zone.

In order to use the soil resistance coefficients the boundary wedge limit angle α_w has to be bigger than the rake angle α. The boundary wedge limit α_w is given by the following equation:

$$\alpha_w = 135^o - \frac{1}{2}\cdot\varphi - \frac{1}{2}\cdot\delta_\varphi - \frac{1}{2}\cdot\Delta_f + \beta \quad (1)$$

where:

Rearranging the aforementioned equation we get:

$$\alpha_w = 135^o - \frac{1}{2}\cdot\left[\varphi + \delta + \sin^{-1}\cdot\left(\frac{\sin\delta}{\sin\varphi}\right)\right] + \beta \quad (2)$$

where:

φ is the angle of friction

δ_φ is the limiting value of the mobilized friction angle

Δ_f is $\sin^{-1}\cdot\left(\sin\delta_\varphi / \sin\varphi\right)$

β is the direction of motion of interface with horizontal

In our case $\alpha > \alpha_w$ so the model cannot be used. As the difference was only 2.5° (α, 90°, α_w, 87.5°) the boundary wedge limit was overlooked.

The soil reaction P acting at δ with the normal to the interface and the adhesive force A acting along the interface are given by

$$P = \gamma\cdot z^2\cdot K_\gamma + c\cdot z\cdot K_{ca} \quad (3)$$

$$A = \alpha\cdot z\cdot \cos ec\cdot a \quad (4)$$

where:

K is the dimensionless soil resistance coefficient

z is the vertical reach of interface

The total soil reaction on the interface is been calculated by:

$$R = b \cdot \left(P^2 + A^2 + 2 \cdot P \cdot A \cdot \sin\delta\right)^{\frac{1}{2}} \quad (5)$$

This force acts at an angle δ_r with the normal to the interface and is calculated by:

$$\delta_r = \delta + \sin^{-1} \cdot \left[\frac{\left(b \cdot A \cdot \cos\delta\right)}{R}\right] \quad (6)$$

The following values used for the evaluation of the sub-surface and blade theory:

φ, 37°; δ, 22°; γ, 15.5 kN m^{-3}; d, 0.01 m to 0.025 m, K_γ, 10.98; c, 4.7 kN m^{-2}; K_{ca}, 11.15; α, 90°

The mean measured draught force for the convex disc was 27 N, 40 N, 95 N and 119 N for 0.01 m, 0.015 m, 0.02 m and 0.025 m depth respectively with the least significant difference at 5% level of significance being 77.14 N. The model over predicts (Figure 6-1) and the theoretical values were 90 N, 140 N, 200 N and 250 N for 0.01 m, 0.015 m, 0.02 m and 0.025 m depth respectively. The performance of the model in predicting the experimental results was evaluating by plotting graphs of the draught force for different depths. In addition the deviation (%) of the predicted values from the experimental ones was obtained.

$$Deviation(\%) = \left[\frac{Experimental - \Pr edicted}{Experimental}\right] \cdot 100 \quad (7)$$

The mean deviation of the predicted values was -176%. The mean draught force for the flat disc was 133, 148, 190 and 224 N for 0.01 m, 0.015 m, 0.02 m and 0.025 m depth respectively. The predicted values were 90 N, 140 N, 200 N and 250 N for the

four depths as mentioned above. The mean deviation of the predicted values was 5.14% and the model enables an acceptable fit to the experimental values. Figure 6-1 shows the mean experimental values compared with the theoretical values. The model can predict the 90% of the experimental values.

The model is not enabling the prediction of draught force due to the variations with different rake angle and speed combinations.

The soil resistance coefficients Albuquerque and Hettiaratchi (1980) incorporated in the model were K_{γ}=10.98 and K_{ca}=11.15 (*N* factors)

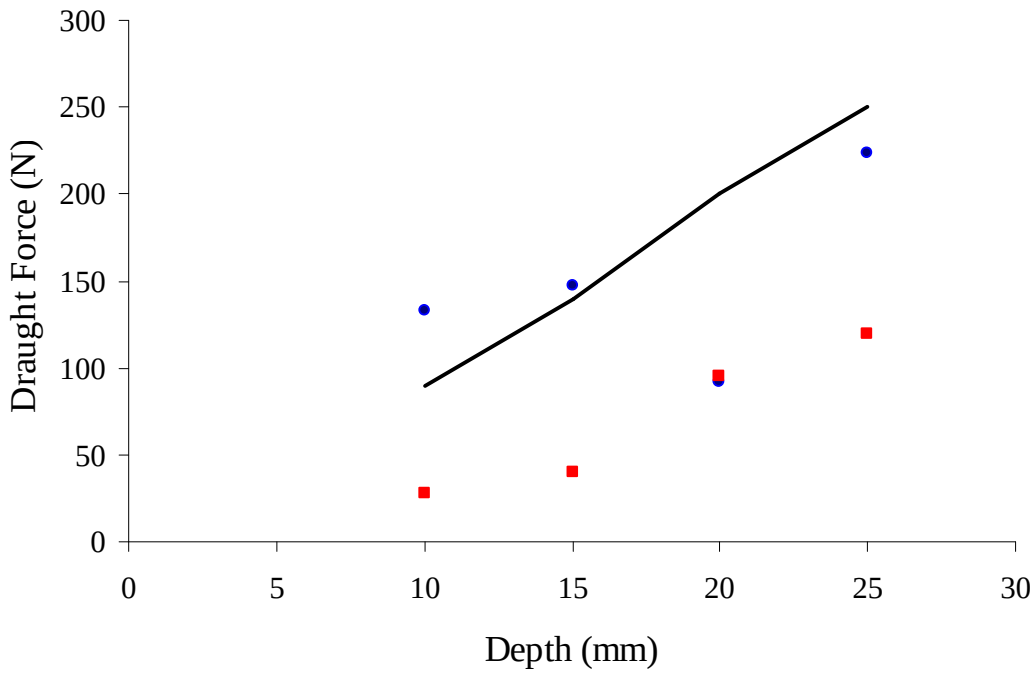

Figure 6-1 The effect of disc's working depth on the measured values for the flat (●) and convex (■) disc and the predicted (solid line) using the Albuquerque and Hettiaratchi (1980) prediction model

6.3 Blade model evaluation

Godwin and Spoor (1977) predicted the passive force above the critical depth by modifying equation (8) developed by Hettiaratchi *et al.,* (1966) and Hettiaratchi and Reece (1974) to take into account the crescent shape failure patterns.

$$P = \left(\gamma \cdot d^2 \cdot N_\gamma + c \cdot d \cdot N_c + c_a \cdot d \cdot N_{ca} + q \cdot d \cdot N_q\right) \cdot w \tag{8}$$

The prediction equations developed further by Godwin et al., (1984) and are:

$$H = \left(\gamma \cdot d_c^2 \cdot N_\gamma + c \cdot d_c \cdot N_c + q \cdot d_c \cdot N_q\right) \cdot \left[w + d \cdot \left\{m - \frac{1}{3} \cdot (m-1)\right\}\right] \cdot \sin(\alpha + \delta) \tag{9}$$

The term $\left\{m - \frac{1}{3} \cdot (m-1)\right\}$ represents the effect of tine width of the crescent flanks of the soil failure pattern. The soil below the critical depth (Godwin & Spoor, 1977 and Godwin & O'Dogherty, 2007) is assumed to fail two-dimensionally in a horizontal plane, independently of rake angle. The lateral force component is calculated from the logarithmic spiral method for the bearing capacity of a deep narrow footing developed by Meyerhof (1951). This resulted in equation (10) for the lateral failure force (*Q*), acting horizontally:

$$Q = w \cdot c \cdot N_c^{'} \cdot (d - d_c) + 0.5 \cdot (1 - \sin\phi) \cdot \gamma \cdot w \cdot N_q^{'} \cdot \left(d^2 - d_c^2\right) \tag{10}$$

The values for the factors $N_c^{'}$ and $N_q^{'}$ are calculated from Meyerhof's (1951) equations which are:

$$N_c^{'} = \cot\phi \cdot \left[\frac{(1 + \sin\phi) \cdot e^{2 \cdot \theta \cdot \tan\phi}}{(1 - \sin\phi \cdot \sin(2 \cdot \eta + \phi))} - 1\right] \tag{11}$$

$$N_q^{'} = \frac{(1 + \sin\phi) \cdot e^{2 \cdot \theta \cdot \tan\phi}}{(1 - \sin\phi \cdot \sin(2 \cdot \eta + \phi))} \tag{12}$$

The total draught force (H_T) acting on narrow and very narrow tines is given by incorporating equations (9) and (10) which give us:

$$H_T = H + Q \tag{13}$$

The discs will work in the field at a maximum depth of 0.025 m. A low rake angle will be given to the discs in order to reduce the magnitude of the draught force (Godwin & O'Dogherty, 2007). Based on such a configuration part of the disc will be out of the soil, thus behaving as a blade (d/w<0.5) with d/w varying from 0.057 to 0.14 based on the working depth from 0.01 m to 0.025 in 0.005 m intervals and for a disc diameter of 0.175 m.
In order to investigate the performance of the prediction model reported by Godwin and O'Dogherty (2007) incorporating the rupture distance and speed effects the experimental values were plotted compared with the theoretical values.

Figure 6-2 shows the configuration of the convex and flat disc. In order to able to use the soil resistance coefficients calculated by Hettiaratchi (1969) for 0^o rake angle, an assumption made based on the angle the shaft has were the disc is engaged with the soil.

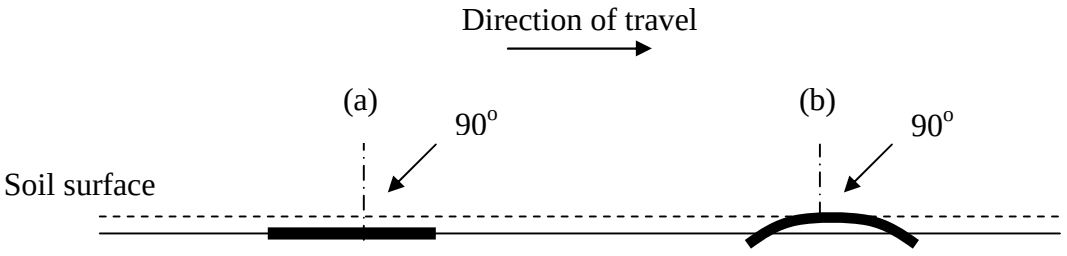

Figure 6-2 Rake angle configuration for the flat (a) and convex (b) disc.

The predicted draught force for the flat and the convex disc was 70 N, 100 N, 150 N and 190 N for 0.01 m, 0.015 m, 0.020 m and 0.025 m depth respectively and the magnitude is similar to the one predicted by Albuquerque and Hettiaratchi (1980) that

predicts 25% more than Godwin's model. The deviation of the predicted values was 28.95% (Figure 6-3).

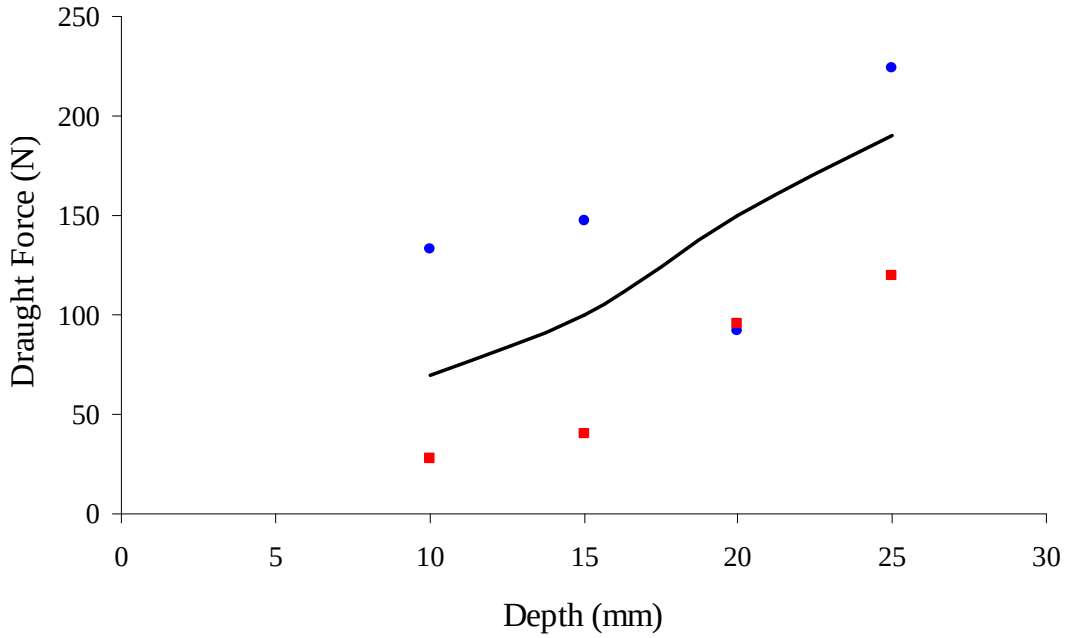

Figure 6-3 The effect of disc's working depth on the measured values for the flat (●) and convex (■) disc and the predicted using the Godwin and Spoor (1977) prediction model

From this study the following conclusions can be made regarding the selection of the most appropriate mathematical model and theory between sub-surface cutting theory and blade theory for use in the mathematical prediction model for shallow working implements with depth/width ratio d/w of < 0.15. These are as follows:

- Godwin's model and soil failure theory predicted the draught force with smaller deviation between predicted and measured than Albuquerque and Hettiaratchi's model.
- The vertical force component is missing from Albuquerque & Hettiaratchi model.
- Forward speed and rake angle variations are not incorporated in Albuquerque and Hettiaratchi model.

- The discs will work in the field with low rake angle varying from 5 to 10^{o}. As part of the disc will be out of soil and after the development of the descriptive soil failure mechanism theory it was concluded that blade theory applies better in order to be used with the necessary modifications in order to predict the forces on shallow working implements with $d/w < 0.15$.

6.4 Disc model development

The results from this study indicated that a model is necessary to predict the magnitude of shallow working implements that are working in the vertical axis. The results from the analysis of the models based on sub-surface cutting theory by Albuquerque and Hettiaratchi (1980) and Godwin and O'Dogherty (2007) blade theory was chosen to used as a basis of a new model. For the disc model development the prediction model developed by Godwin and Spoor (1977) and further developed by Godwin *et al.,* (1984) and summarized in Godwin and O'Dogherty (2007) will be used as a starting point in order to develop a force prediction model for shallow working discs.

This prediction model applies for wide tools working very shallow to the soil with or without rotational speed. The draught force can be calculated using the geometric parameters of the disc, the working speed and the physical properties of the soil. The model was evaluated versus measured values gathered from controlled laboratory experiments in three different operating modes:

(i) Solid discs with no rotation,
(ii) Solid discs with rotation and
(iii) Discs incorporating a cut out sector with rotation.

The development of the model is based on the principles of Mohr-Coulomb soil mechanics for blade and tine theory primarily form the work of Godwin and Spoor (1977), Godwin *et al.,* (1984), Wheeler and Godwin (1996), Godwin and O'Dogherty (2007) and Godwin *et al*, (2007) and Godwin (2007).

6.4.1 Approach

Figure 6-4 shows a conceptual diagram of the disc incorporating a cut-out sector engaged with soil

where:

D is the working depth

α is the inclination angle

l is the contact length of the disc with the soil

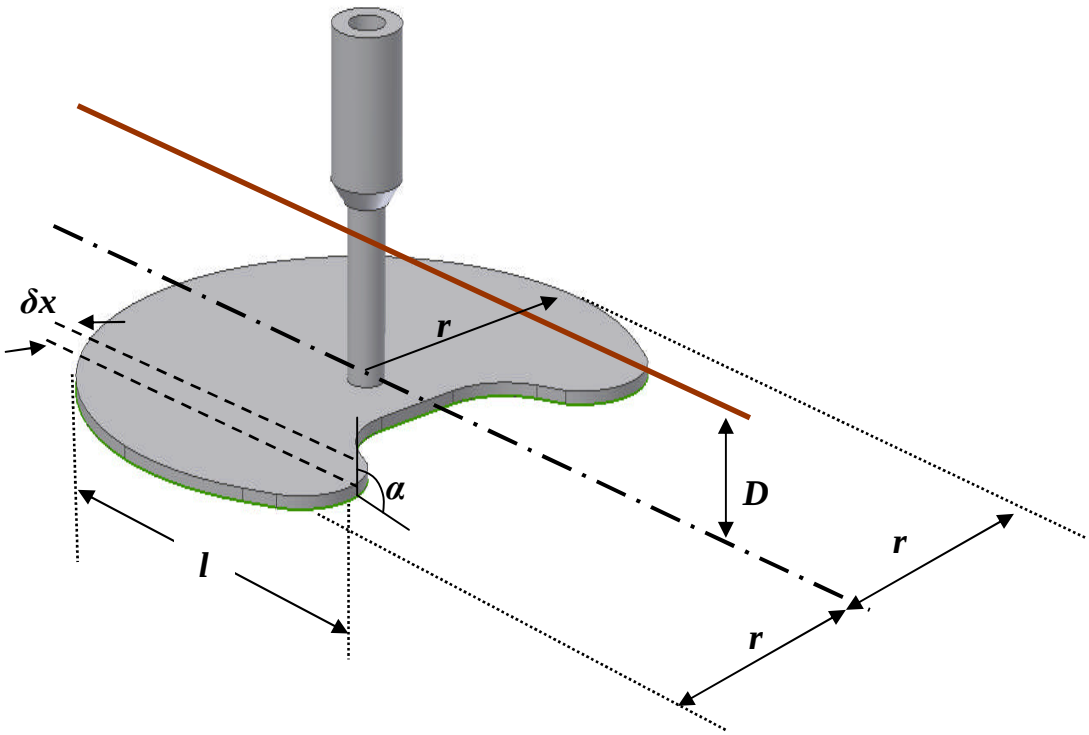

Figure 6-4 Conceptual diagram of the cut-out disc

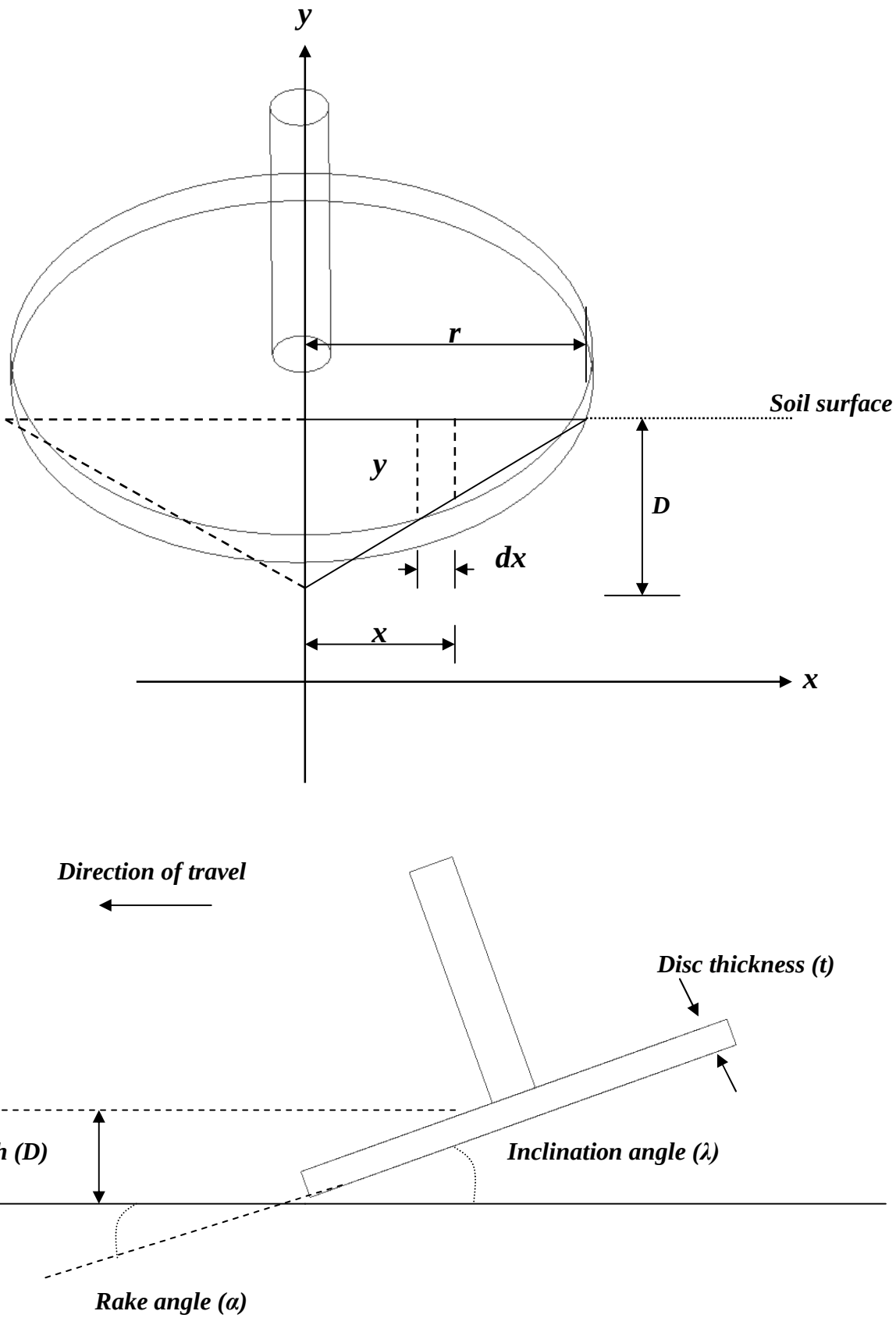

Figure 6-5 Width-depth relationship for inclined disc

Equation (14) gives the width-depth linear reletionship that developed based on Figure 6-5.

$$y = \frac{D \cdot (r - x)}{r} \tag{14}$$

Equation (8) developed by Hettiaratchi *et al.,* (1966) and Hettiaratchi and Reece (1974) will be used to start with the disc force prediction model. The adhesion term will be excluded and a velocity factor will be included based on McKeys (1985) as used by Wheeler and Godwin (1996). The velocity factor is given by:

$$\frac{\gamma \cdot v^2 \cdot N_\alpha \cdot y}{g} \tag{15}$$

Equation (8) takes the form of:

$$\delta H = \left(\gamma \cdot y^2 \cdot N_\gamma + c \cdot y \cdot N_c + q \cdot y \cdot N_q + \frac{\gamma \cdot v^2 \cdot N_\alpha \cdot y}{g} \right) \cdot \delta x \tag{16}$$

where:

γ is the bulk unit weight

y is the linear relationship as given in equation (14)

N_γ; N_c; N_q; N_α dimensionless soil resistance coefficients

c is cohesion

q is surcharge due to the weight of soil on the disc

v is forward speed

g acceleration due to gravity

The dimensionless factor N_a is a function of α, δ, φ and m, is given by:

$$N_\alpha = \frac{\tan\beta + \cot(\beta+\phi)}{[\cos\cdot(\alpha+\delta)+\sin\cdot(\alpha+\delta)\cdot\cot\cdot(\beta+\phi)]\cdot(1+\tan\beta\cdot\cot\alpha)} \qquad (17)$$

where

$$\tan\beta = \frac{1}{m-\cot\alpha} \qquad (18)$$

The dimensionless soil resistance coefficients N_γ; N_c and N_q are represented by two families of curves, one for a perfectly smooth interface (δ = 0) and the other for a perfectly rough interface ($\delta = \varphi$) (Hettiaratchi *et al.*, 1966). All the curves presented are for evaluating the resultant soil reaction per unit width of the interface and act at an angle δ with the normal interface.

Once the values for the dimensionless soil resistance coefficient have been extracted from the curves proposed by Hettiaratchi *et al.*, (1966) the following relationship can be used to calculate N_γ; N_c and N_q:

$$N_\delta = (N_\delta)_{\delta=0}\cdot\left[\frac{(N_{\gamma,c,q})_{\delta=\varphi}}{(N_{\gamma,c,q})_{\delta=0}}\right]^{\frac{\delta}{\varphi}} \qquad (19)$$

Integrating equation (14) into equation (16) gives *H* and *V* for the calculation of draught and vertical force respectively

$$H = \left[\left(2 \cdot \gamma \cdot \frac{D^2 \cdot r}{3} \cdot N_\gamma \right) + \left(c \cdot D \cdot r \cdot N_c \right) + \left(q \cdot D \cdot r \cdot N_q \right) - \right.$$

$$\left. + \left(\frac{\gamma \cdot v^2 \cdot N_\alpha}{g} \cdot D \cdot r \right) \right] \cdot \sin(\alpha + \delta) \qquad (20)$$

$$V = \left[\left(2 \cdot \gamma \cdot \frac{D^2 \cdot r}{3} \cdot N_\gamma \right) + \left(c \cdot D \cdot r \cdot N_c \right) + \left(q \cdot D \cdot r \cdot N_q \right) - \right.$$

$$\left. + \left(\frac{\gamma \cdot v^2 \cdot N_\alpha}{g} \cdot D \cdot r \right) \right] \cdot \cos(\alpha + \delta) \qquad (21)$$

H is the force in the tip of the disc (Figure 6-6). When the disc works at an inclination angle of 0^o there is a high bottom surface friction. It was found necessary to add the effects of bottom surface friction, top surface friction and the reaction from the upward soil throwing. An explanation of these additional force components are represented diametrically in Figure 6-6.

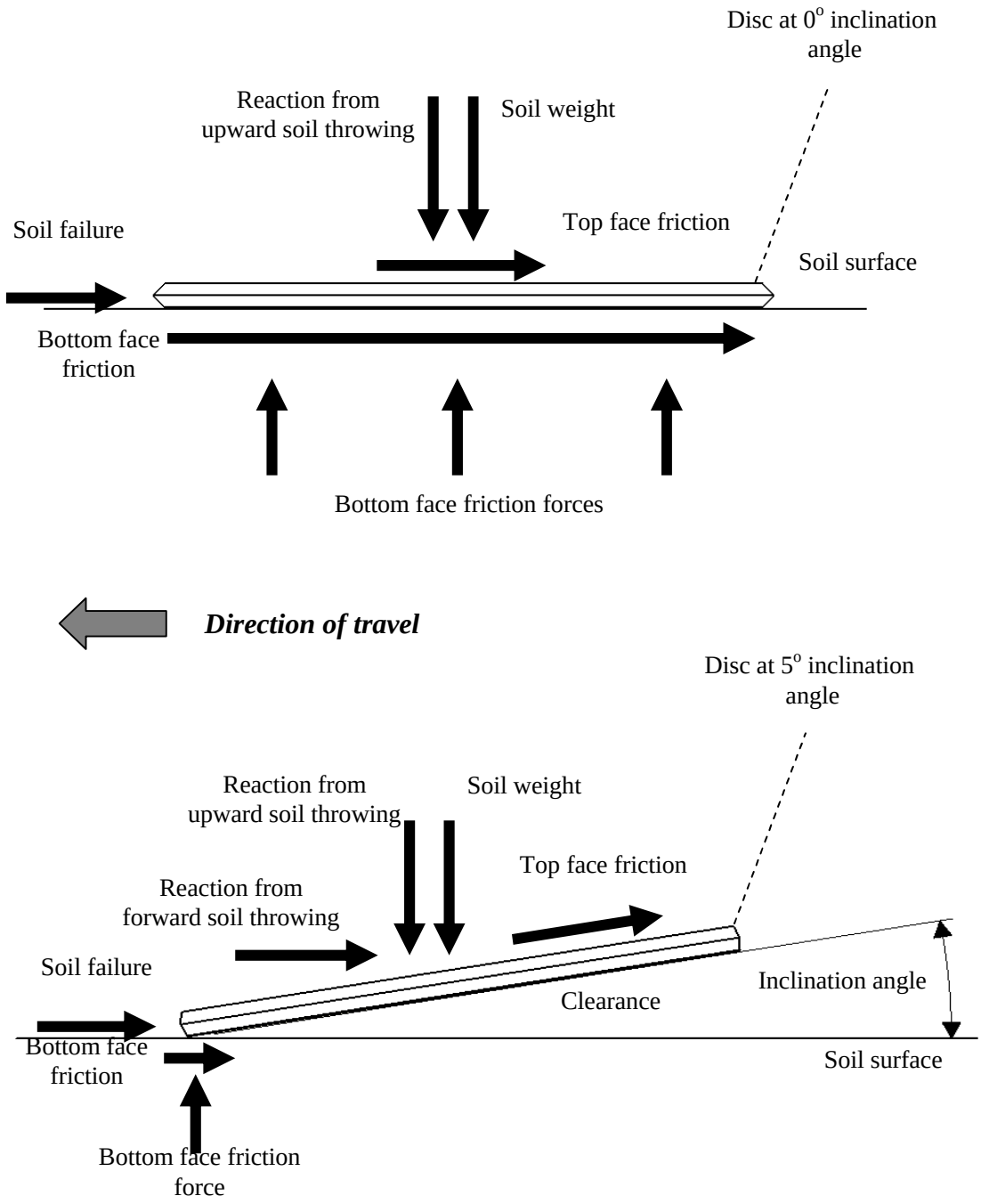

Figure 6-6 Two dimensional model of forces acting on the disc (upper) with 0^o; and (lower) 5^o inclination angle (Adopted and modified by Fielke, 1988)

The equation of bottom surface friction is the multiplication of vertical force, V with the coefficient of friction, μ and is given below:

$$H_{bf} = V \cdot \tan\delta \tag{22}$$

The top surface friction is calculated by:

$$H_{tf} = \gamma \cdot \pi \cdot r^2 \cdot D \cdot \tan\delta \tag{23}$$

The reaction from the upward soil throwing is calculated by:

$$H_e = \gamma \cdot \pi \cdot r^2 \cdot D \cdot t \tag{24}$$

where t is the disc thickness in m

The total draught force is the sum of all the individual components as given in Equations 20 to 24:

$$H_{TOTAL} = H + H_{bf} + H_{tf} + H_e \tag{25}$$

The aforementioned Equations are predicting the forces acting on non-rotating solid discs. In order to take into account the effect of rotational speed and the cut-out sector the following equations developed:
For the rotating solid disc the torque is been calculated by:

$$T_D = \mu \cdot r \cdot H_{TOTAL} \tag{26}$$

where:
μ is the coefficient of friction (tanδ)
r is the disc radius
H_{TOTAL} is the predicted draught force

The additional draught force for the rotating solid disc is given by:

$$H_T = \frac{2 \cdot \pi \cdot \mu \cdot r}{d} \cdot H_{TOTAL} \tag{27}$$

where:

d is the crop spacing

So the total draught force is $H_{TOTAL}+H_T$

$$H_R = \left(1 + \frac{2 \cdot \pi \cdot \mu \cdot r}{d}\right) \cdot H_{TOTAL} \tag{28}$$

For the rotating disc with the cut-out sector the torque is calculated by:

$$T_C = H_{TOTAL} \cdot \frac{r}{2} = \frac{H_{TOTAL} \cdot r}{2} \tag{29}$$

where:

H_C is the cut-out sector draught force

It is assumed that H_C acts at the midpoint of the cut-out of a revolution

The increase in draught force is given by:

$$F_C = \frac{\pi \cdot r}{d} \cdot H_{TOTAL} \tag{30}$$

and the total draught force is $H_{TOTAL}+H_C$

$$H_S = \left(1 + \frac{\pi \cdot r}{d}\right) \cdot H_{TOTAL} \tag{31}$$

The total torque is given by:

$$T_r = \mu \cdot r \cdot H_{TOTAL} + 1 \cdot H_{TOTAL} \cdot r \tag{32}$$

The total draught force is given by:

$$F_o = \left[\left(1 + \frac{2 \cdot \pi \cdot \mu \cdot r}{d} \right) \cdot H_{TOTAL} + \left(1 + \frac{\pi \cdot r}{d} \right) \cdot H_{TOTAL} \right] \tag{33}$$

6.4.2 Evaluation of the disc model

The predicted forces from the model were compared to the results from the controlled laboratory experiments for rotating cut-out discs and non-rotating and rotating solid discs and can be found in Chapters 4 and 5 respectively. Table 6-1 summarises the laboratory soil conditions. Also it was found necessary to predict the draught force incorporating the variation in depth and inclination angle due to the shaft deflection when working at inclination angle of 0^o.

Table 6-1 Laboratory soil conditions

Soil texture: sandy-loam (66% sand, 17% silt, 17% clay) Bulk unit weight, γ: 1530 kN m^{-3} Soil moisture content, MC: 9% Mechanical properties	
Cohesion, c	4.7 kN m^{-2}
Soil internal friction angle, φ	37^o
Soil-tool interface friction angle, δ	22^o
Adhesion, c_a	0 kN m^{-2}

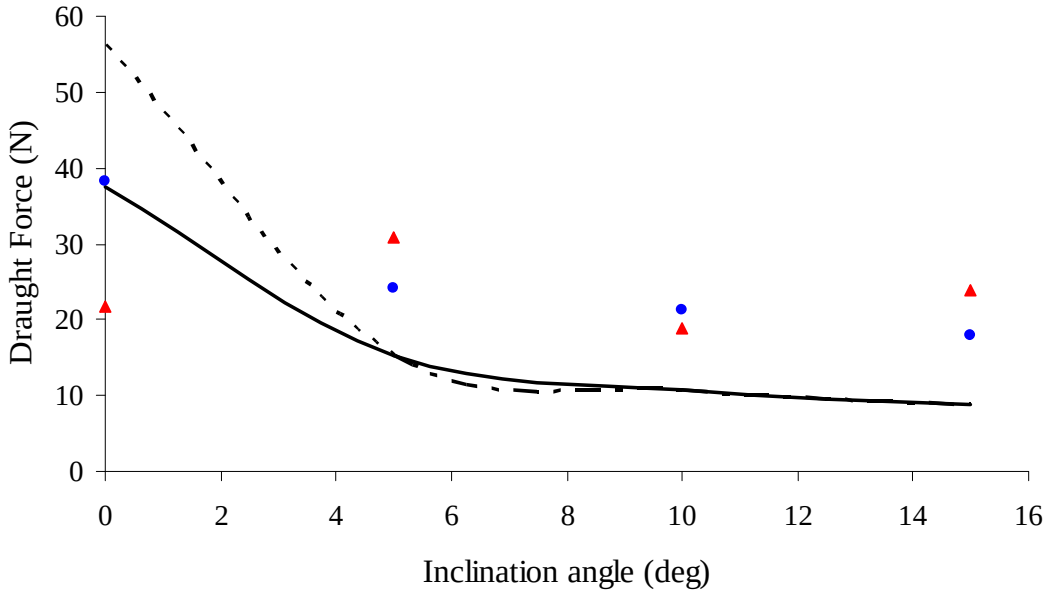

Figure 6-7 Measured draught force for the flat (▲) and the convex (●) disc and predicted values without (solid line) and with the deflection effect (broken line) for the effect of inclination angle on non-rotating solid discs

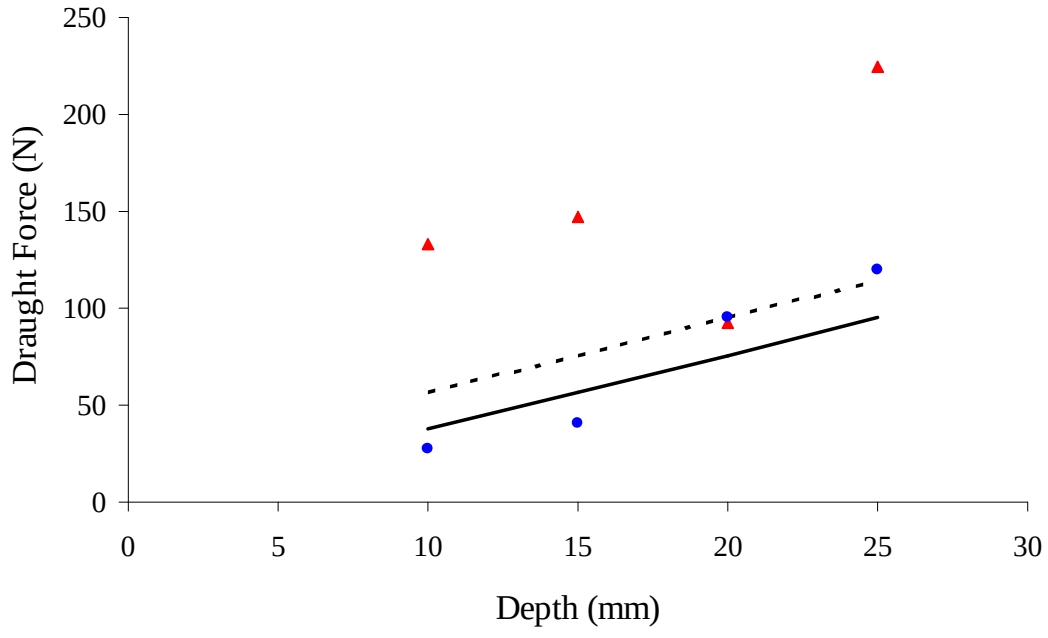

Figure 6-8 Measured draught force for the flat (▲) and the convex (●) disc and predicted values without (solid line) and with the deflection effect (broken line) for the effect of depth on non-rotating solid discs

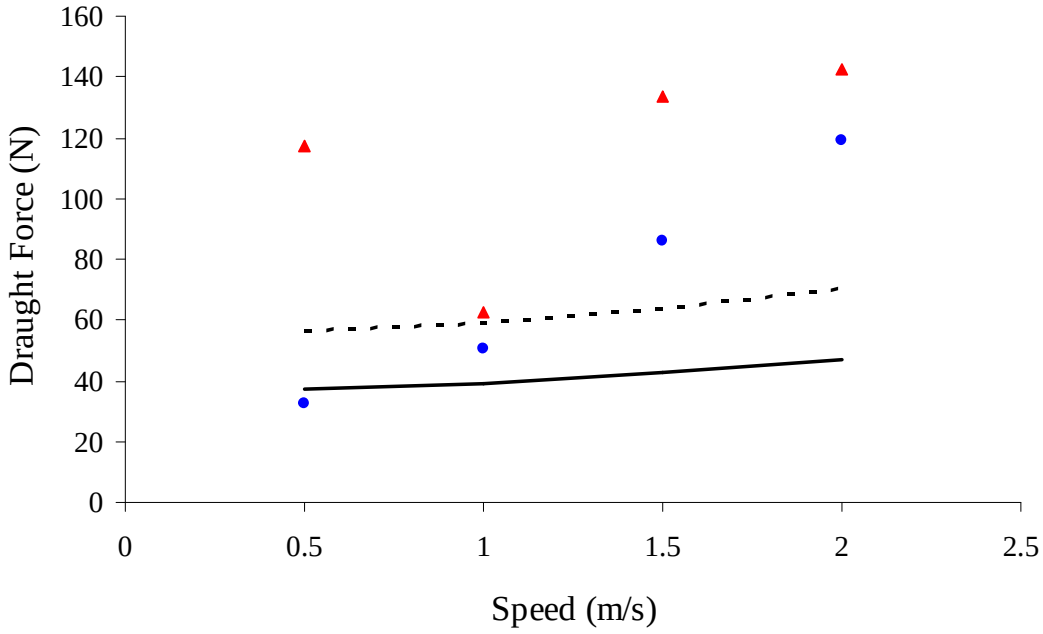

Figure 6-9 Measured draught force for the flat (▲) and the convex (●) disc and predicted values without (solid line) and with the deflection effect (broken line) for the effect of speed on non-rotating solid discs

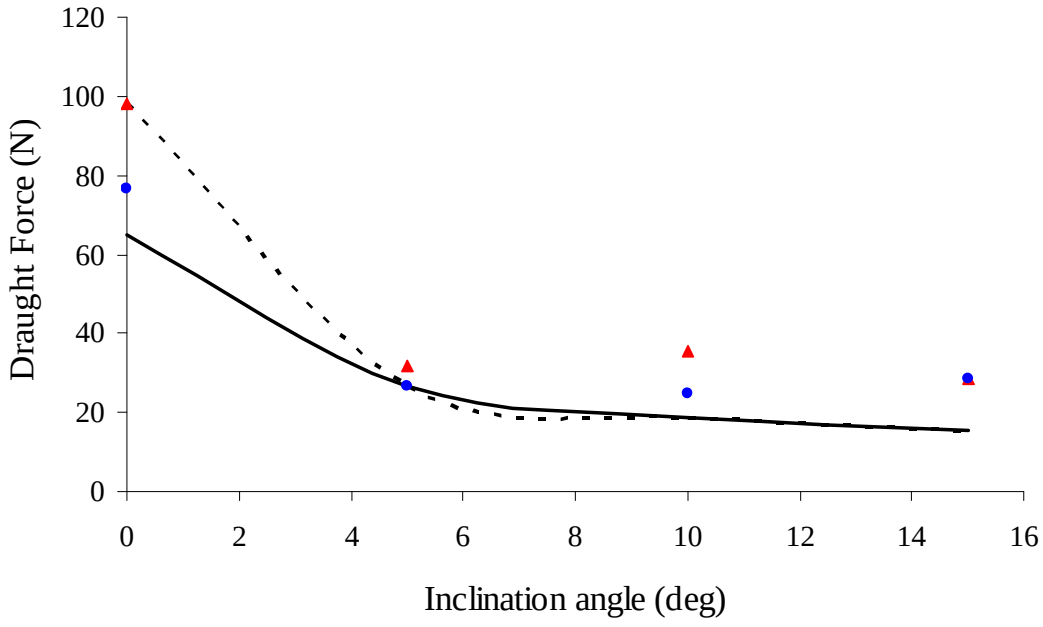

Figure 6-10 Measured draught force for the flat (▲) and the convex (●) disc and predicted values without (solid line) and with the deflection effect (broken line) for the effect of inclination angle on rotating solid discs

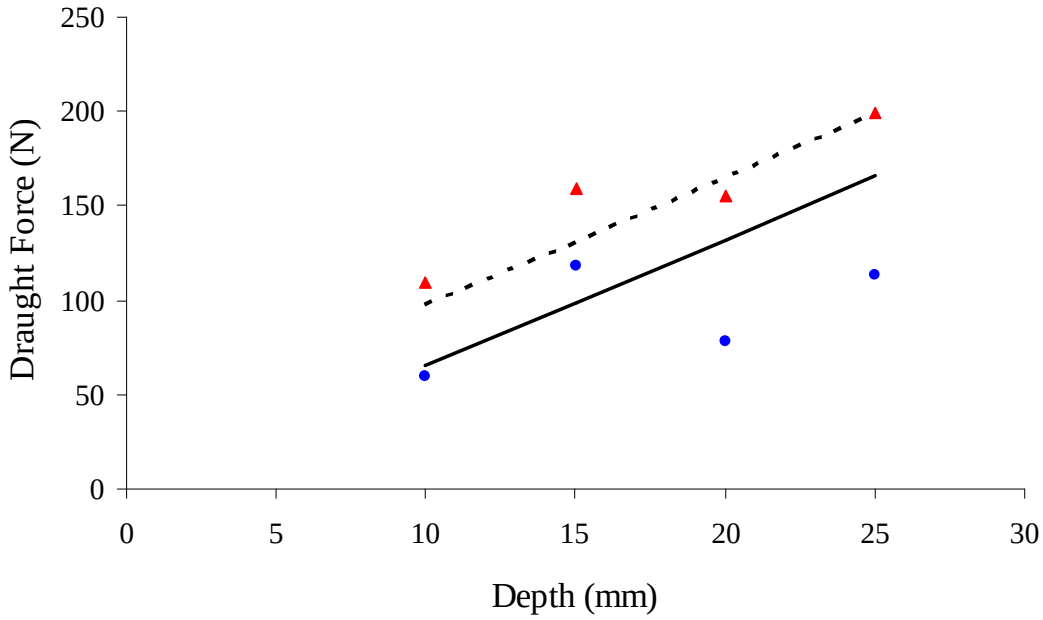

Figure 6-11 Measured draught force for the flat (▲) and the convex (●) disc and predicted values without (solid line) and with the deflection effect (broken line) for the effect of depth on rotating solid discs

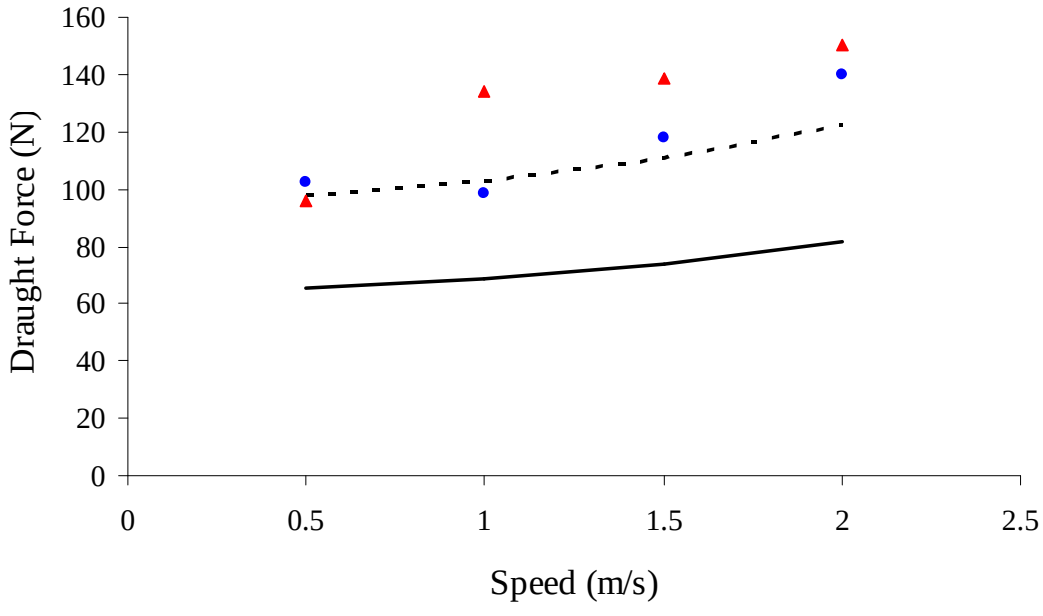

Figure 6-12 Measured draught force for the flat (▲) and the convex (●) disc and predicted values without (solid line) and with the deflection effect (broken line) for the effect of speed on rotating solid discs

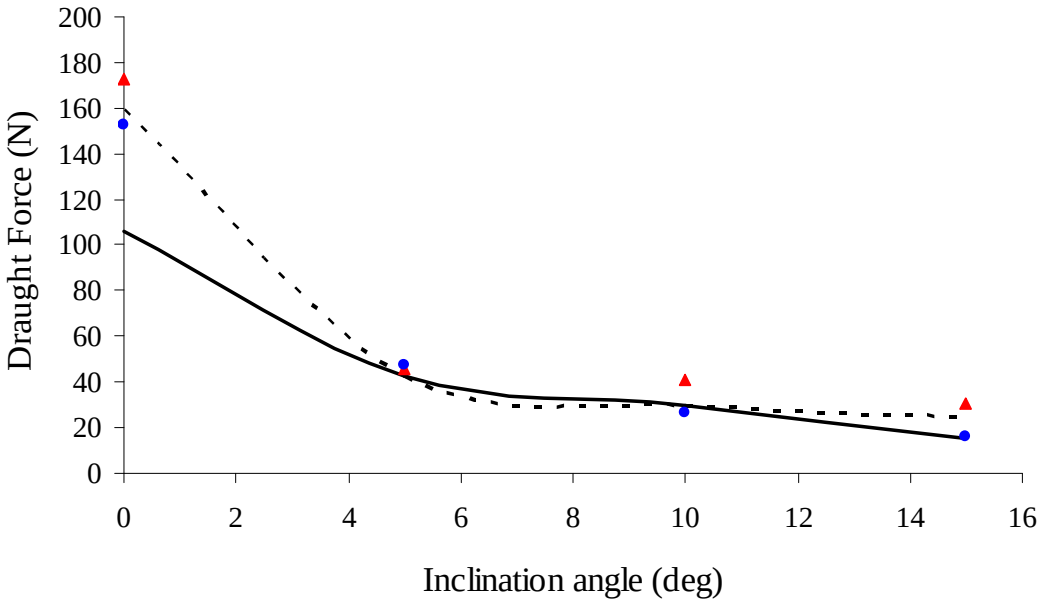

Figure 6-13 Measured draught force for the flat (▲) and the convex (●) disc and predicted values without (solid line) and with the deflection effect (broken line) for the effect of inclination angle on rotating cut-out discs

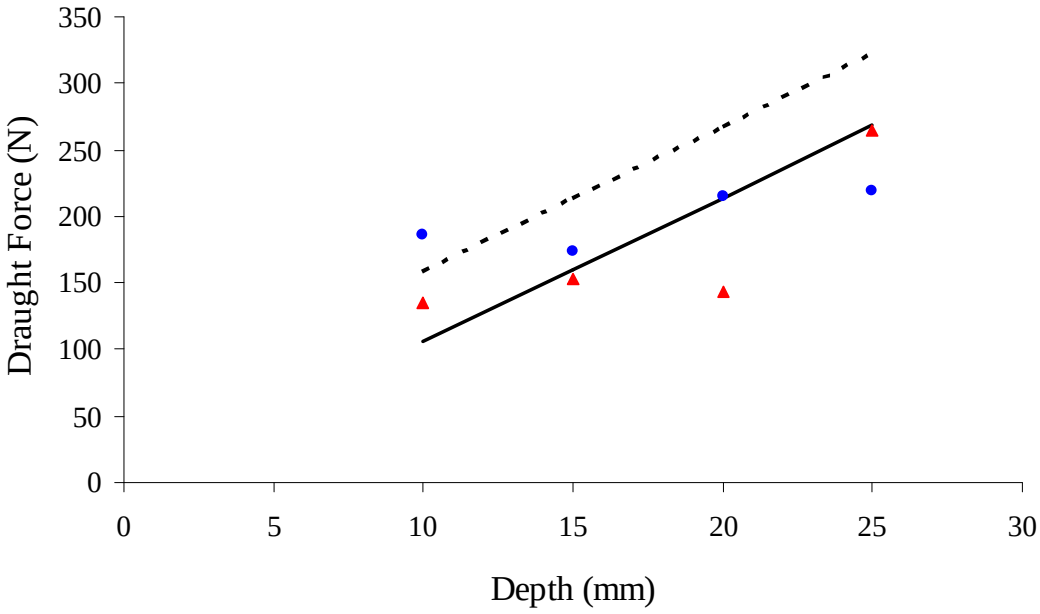

Figure 6-14 Measured draught force for the flat (▲) and the convex (●) disc and predicted values without (solid line) and with the deflection effect (broken line) for the effect of depth angle on rotating cut-out discs

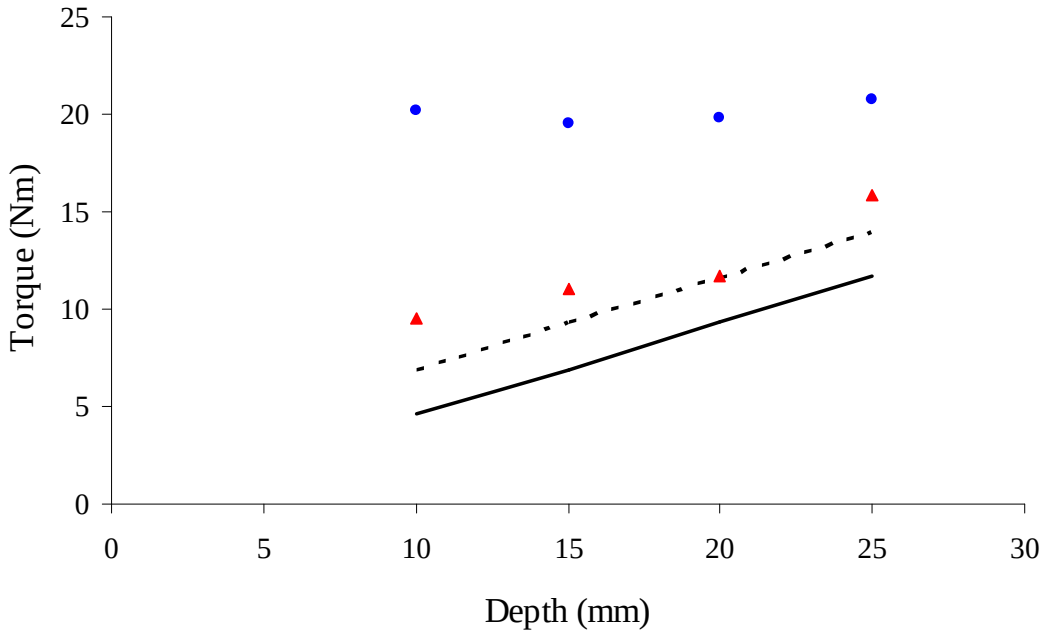

Figure 6-15 Measured torque for the flat (▲) and the convex (●) disc and predicted values without (solid line) and with the deflection effect (broken line) for the effect of depth on rotating cut-out discs

The results of the prediction model together with the measured values from the controlled laboratory experiments are presented in Figure 6-7 through Figure 6-16. The predicted forces without and with the deflection effect from the model are plotted against the measured forces for the convex, the flat disc and both disc geometries in Figures 6-17 and 6-18 respectively for all that acquired in the soil bin studies. A regression line fitted to the results shows that the model under predicts the draught force by 17%; 36% and 31% for the convex, the flat and both disc geometries respectively. Considering the individual data points it was found that 68%; 62% and 55% were within bounds of ± 25%. For the predicted forces with the deflection effect (Figure 6-18) the regression line fitted to the results showed that the model over predicts by 14% and 3.5% the measured draught force for the convex disc and overall prediction for both disc geometries respectively and under predicts by 10% for the flat disc. Also 60%; 69% and 61% of the individual data points lie within bounds of ± 25% for the convex, the flat disc and both disc geometries respectively.

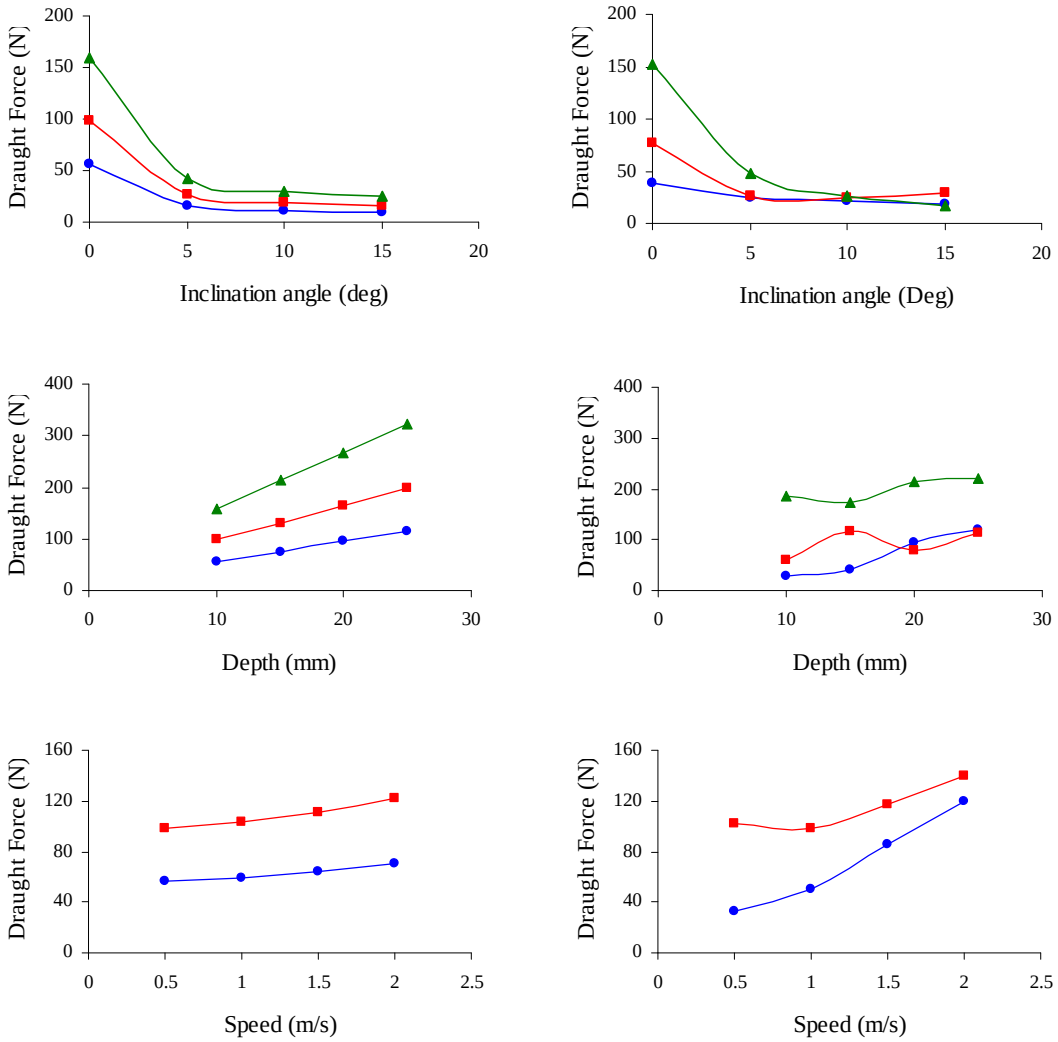

Figure 6-16 Comparison of the predicted values (left side) with the measured values (right side) of the convex disc for non-rotating solid discs (●); rotating solid discs (■) and cut-out rotating discs (▲)

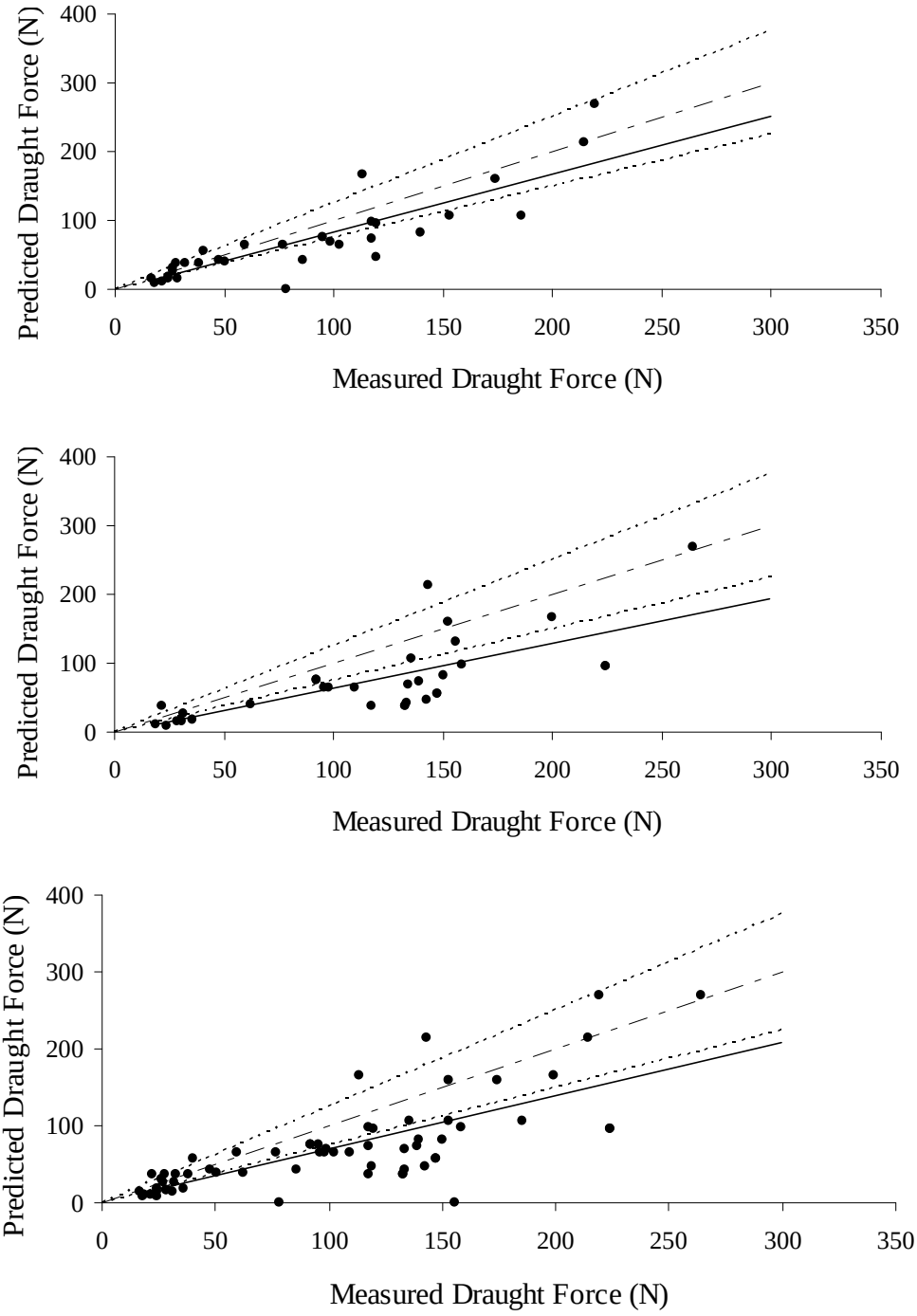

Figure 6-17 Comparison between measured and predicted draught forces in laboratory conditions for the (a) convex, the (b) the flat and (c) both disc geometries with regression line through the origin (solid line), line of equal magnitude (long dashed line) and ± 25% limits (broken lines)

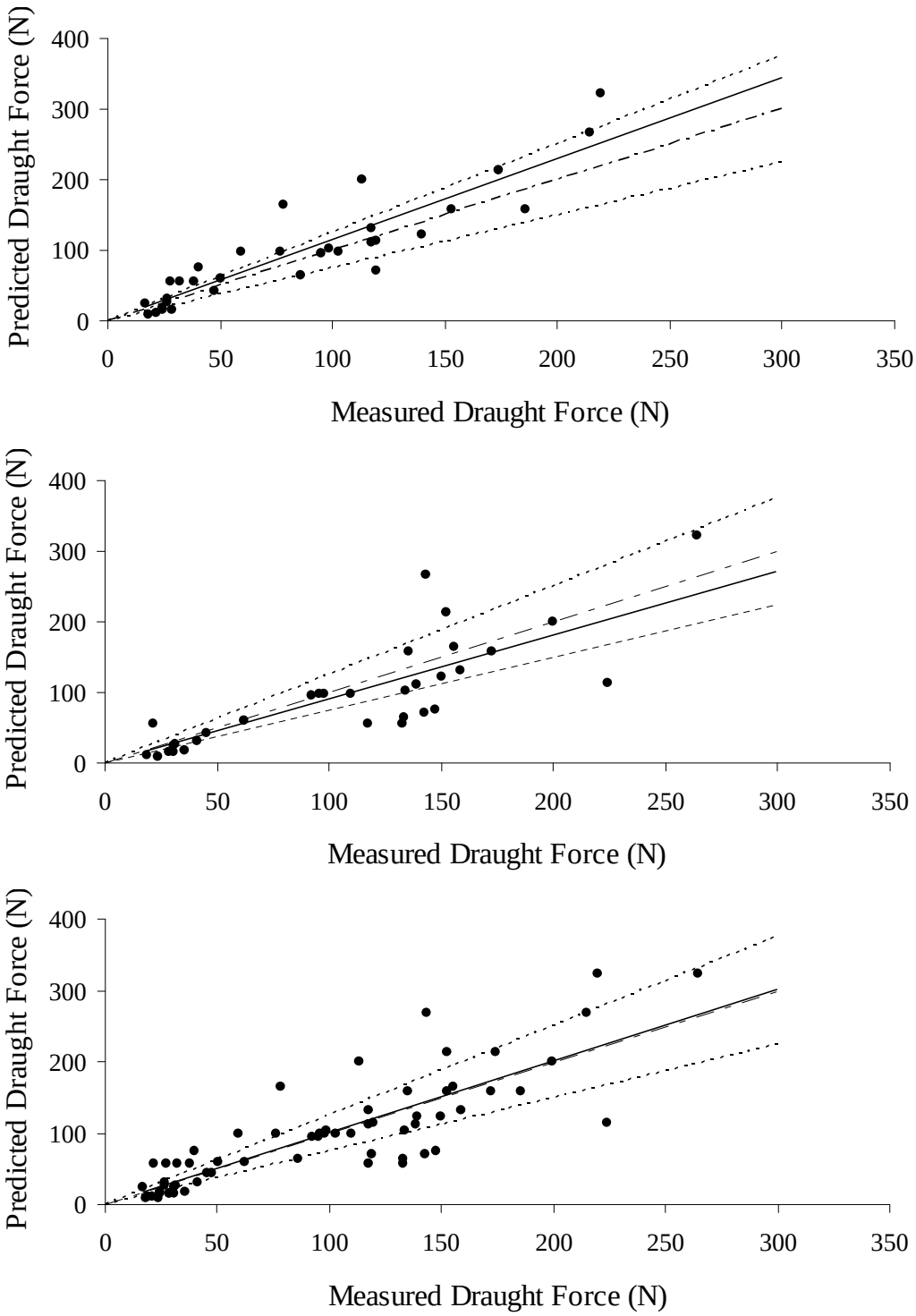

Figure 6-18 Comparison between measured and predicted draught forces with the deflection effect in laboratory conditions for the (a) convex, the (b) the flat and (c) both disc geometries with regression line through the origin (solid line), line of equal magnitude (long dashed line) and ± 25% limits (broken lines)

6.5 Conclusions

- A force prediction model for shallow asymmetric non-rotating and rotating discs (about a vertical axis) developed to predict the forces on two different working conditions, non-rotating and rotating. The model takes into account the geometric parameters of the discs, the speed of operation, the working depth and the physical properties of the soil based upon those required for the general soil mechanics equation which obeys the Mohr-Coulomb failure criterion.
- Experiments were conducted to verify the draught force predictions of the model, using four disc geometries, flat and convex with and without a cut-out sector. Measurements were made in a laboratory soil bin in a sandy loam soil, at depths from 10 mm to 25 m, inclination angles from 0^o to 15^o over a range of speeds from 0. 5 m s^{-1} to 2 m s^{-1}.
- For the convex disc the values of the predicted forces in the laboratory experiments of the depth, inclination angle and speed effect were overall 17% less than the measured values (with a coefficient of determination of 0.75) with the majority of the values within bounds of ± 25% a line of equal magnitude. For the flat disc there was not a good overall agreement with the predicted forces be 36% less than the measured forces (with a coefficient of determination of 0.53) with the majority of the values within bounds of ± 25% a line of equal magnitude.
- A comparison of all experimental work encompassing the laboratory experiments with non-rotating and rotating discs, incorporating the deflection effect of the shaft when working at 0^o inclination angle showed that the model is able to predict the draught force with good accuracy. The predicted forces were 3.5% more than the measured forces overall for a linear regression line (with a coefficient of determination of 0.7) and 61% of the data were within bounds of ± 25% a line of equal magnitude. The model showed a sensitivity in depth and the scatter distribution of the measured values is due to soil variability as the disc were working very shallow (maximum depth of 25 mm).

- The increase in the total draught force from the non-rotating to the rotating solid discs and the rotating cut-out discs was constant and was generally 45% greater.
- The practical value of this model is that it stands as a starting point for the prediction of draught force for shallow asymmetric non-rotating and rotating discs. With the necessary modifications in implement geometry the proposed force prediction model can be used for a wide range of shallow working implements with low inclination angles.

Chapter 7

Field Performance and Economic Analysis

7. Field performance and economic analysis

The aim of this experiment was to investigate the working parameters of the rotating disc hoe upon its performance in the field. A novel inter and intra-row weeder was designed and constructed targeting transplanted high value crops (i.e. brassicas and headed lettuce) by Garford Farm Machinery (See Appendix III) for within-the-row weed control using computer vision to locate the plants. The minimum intra-row spacing was 300 mm.

7.1 Rotating disc hoe prototype

An experimental implement was constructed by Garford Farm Machinery based on a standard vision guided inter-row steerage hoe equipped with conventional inter-row cultivation blades. The implement was mounted in the front three-point linkage of the tractor (Figure 7-1). A camera was mounted in the centre of the implement at 1.7 m from the soil surface looking ahead and down in order to view the bottom of the field vertically and be able to view the full width of the bed at a width of 2.5 m.

Figure 7-1 The prototype guided rotating disc hoe with one disc attached and a camera mounted 1.7 m from the soil surface

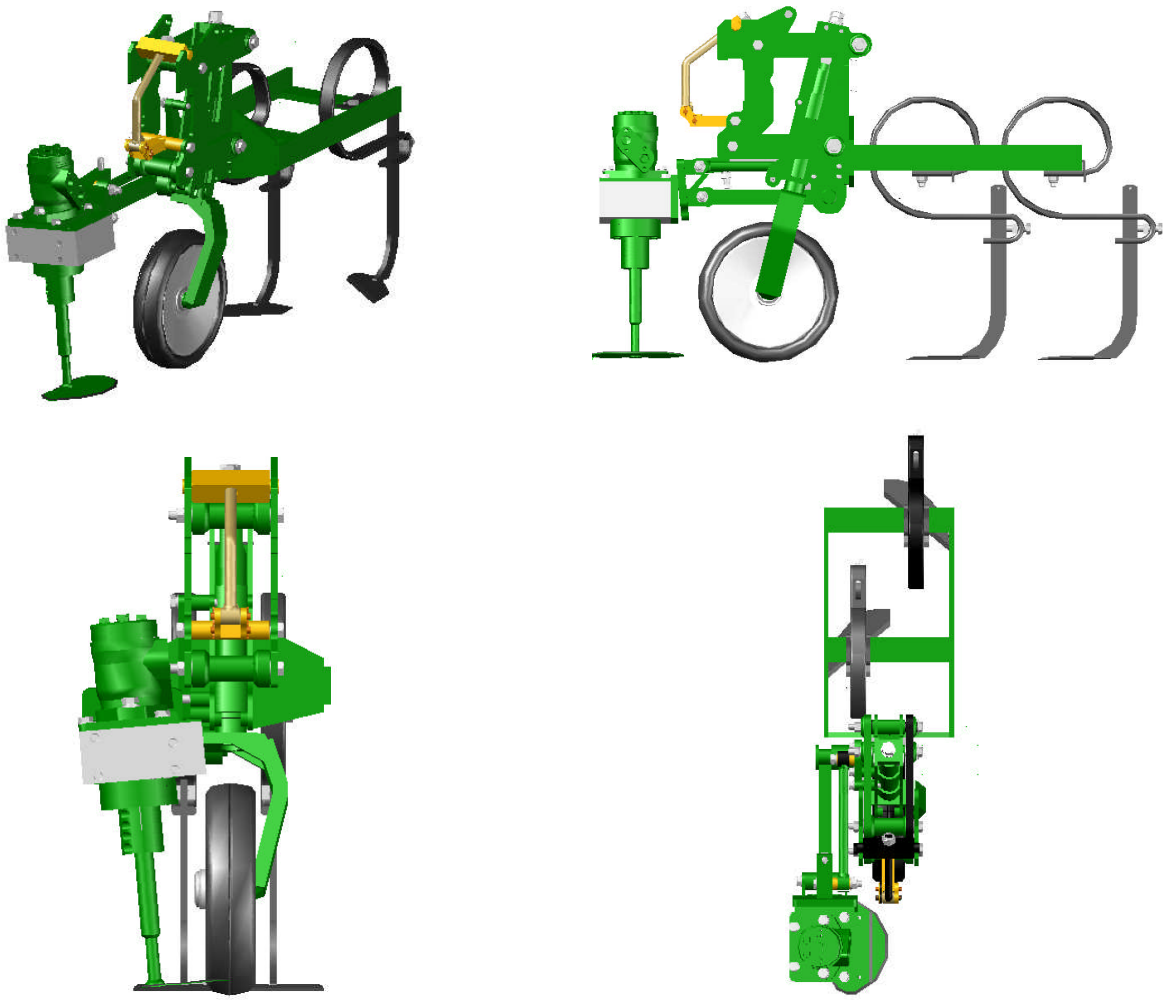

Figure 7-2 Different views of one unit showing the rotating disc, the motor, the depth wheel and the inter-row blades

Soil engaging implements working shallow ground face problems in maintaining a constant depth through the working process. Kurstjens *et al.*, (2000) in his study for weed harrowing reported that "to exploit uprooting selectivity, working depth should be shallow, spatially homogenous and precisely controlled". In order the maintain a constant depth of around 20 mm each rotating disc was mounted to a depth wheel attached to the implement so that cultivation depth could be consistently maintained

(Figure 7-2). Also the depth wheels had frames in the back providing mounting points for standard inter-row cultivation blades (Figure 7-2). The prototype rotating disc hoe designed to accommodate five intra-row units, but only one was used in the field experiment.

The rotary disc unit consisted of an orbital hydraulic motor attached to a bearing housing with a straight through shaft to the disc (Tillett *et al.*, 2007). At early weeding treatments no problems occurred with the straight shaft, but foliage potential damage observed from the shaft as the plants will grow. In order to overcome this limitation a crankshaft shape was attached with the motor in order to avoid the leaf area of the crop (Figure 7-3).

Consequently for the final experimental treatment the straight shaft was replaced with the crank type shaft that had the same centre of rotation, but moved the connection point away from the plant. Within the bearing housing a toothed belt drove an incremental encoder measuring the revolutions on the shaft. An inductive index sensor picked up on a plate rotating with the shaft to provide registration every revolution. Also a lightweight pointer was attached to the shaft to aid visual inspection of performance when the disc was soil engaged (Tillett *et al.*, 2007).

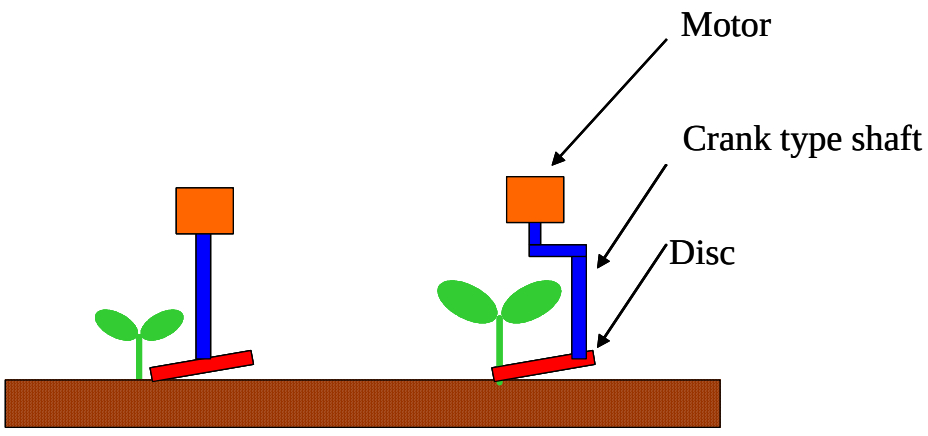

Figure 7-3 Drawing illustrating the straight and crank type shaft at two different crop growing stages

7.2 Re-design of disc geometry for commercial use

In the mathematical model study the tolerance of the disc due to lateral and angular misalignment was not taken into account. The tolerance in the mathematical model can be incorporated by reducing by 20% the angle (θ), so for a 130^o cut-out sector angle ($\theta = 25^o$) a 20% reduction results in a 156^o cut-out sector angle ($\theta = 12^o$). Figure 7-4 shows the results from the kinematic analysis of the disc geometry proposed by O'Dogherty *et al.,* (2007 a) with and without tolerance. It can be seen that if we use the disc proposed by O'Dogherty *et al.,* (2007 a) , with an angular misalignment of 12.5 mm in both directions the disc will penetrate the plant's undisturbed zone (Figure 7-4 (a)). Figure 7-4 (b) shows the disc of Figure 7-4 (a) with a 20% reduction in angle (θ) that is 12^o. As it can be seen the disc now avoids the plant's undisturbed zone in case they are mis-placed in the intra-row area. In case of the plants not being in a straight line within the crop row the system will move laterally up to 20 mm (Figure 7-4 (c)) providing enough clearance to avoid the plants.

Trials from Tillett *et al.,* (2007) and Tillett and Hague (2006) indicated a 10 mm and 10^o lateral and angular misalignment respectively. The design of the disc diameter and cut-out sector angle will have to change and a compromise should be made between maximising the cultivated area and providing adequate tolerance to lateral and angular misalignment which if insufficient might have led to crop damage (Tillett *et al.,* 2007) in order to be used in commercial farming. The tolerance required depended on the dynamic performance of the system as a whole and the growth habit of the crop plants (Tillett *et al.,* 2007). A 25 mm and 25^o lateral and angular misalignment will provide adequate tolerance under commercial farming. The rotating disc hoe has a limitation at intra-row crop spacing of less than 300 mm. Figure 7-5 shows a proposed disc design that can be used for intra-row crop spacing from 300 mm onwards. To maintain the effect of the 87.5 mm disc radius r must be equal to (37.5+a) for any value of a.

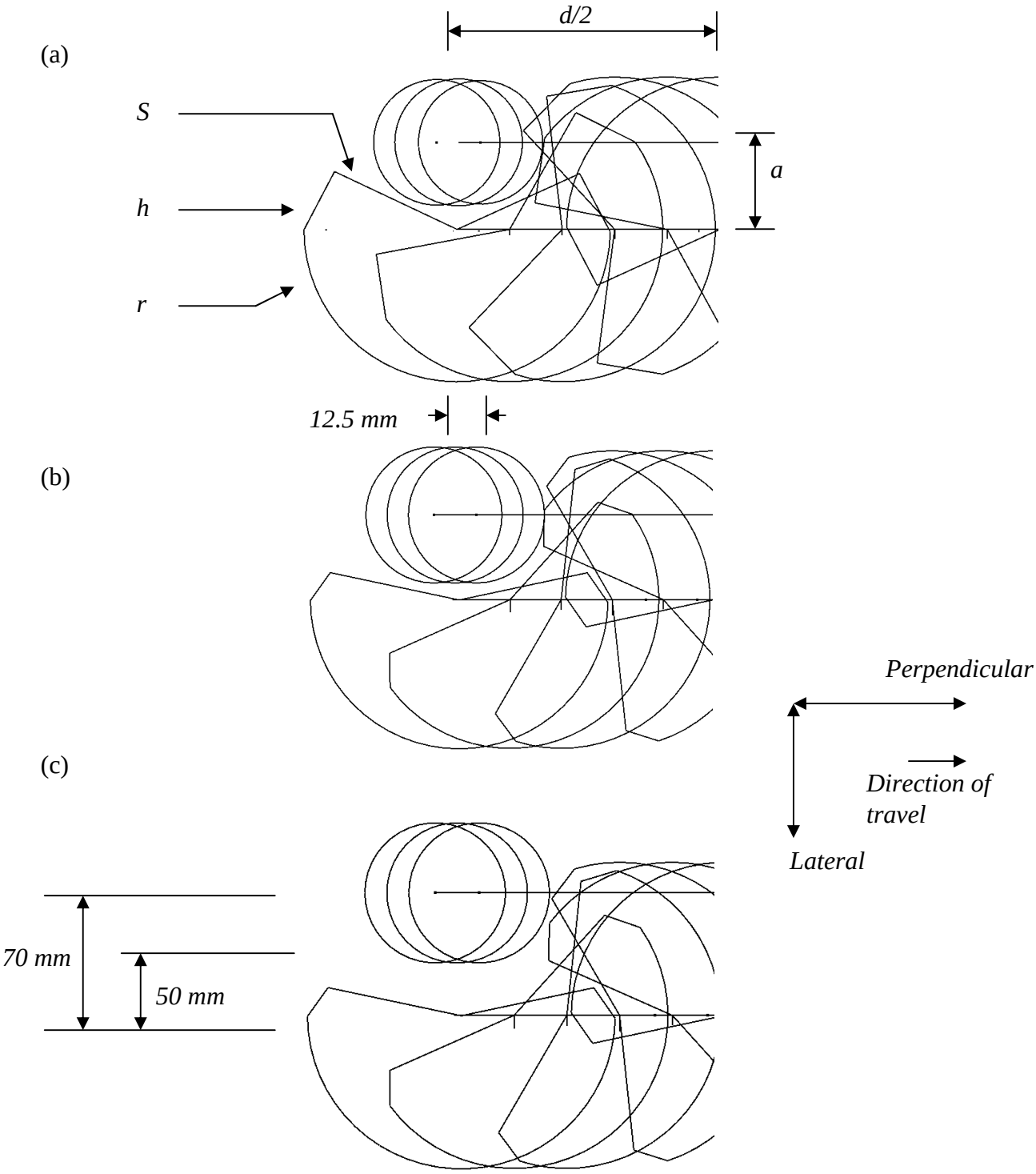

Figure 7-4 (a) Proposed disc geometry based on the mathematical model (*h*, 33 mm; θ, 25^{o}; *S*, 70 mm; *r*, 87.5 mm; *a*, 50 mm) (b) Modified disc geometry to incorporate tolerance (*h*, 12 mm; θ, 12^{o}; *S*, 75 mm; *r*, 87.5 mm; *a*, 50 mm) (c) Lateral movement of 20 mm of the modified disc from the plant centre (*a*, 70 mm)

The parameters that have to be considered to design a disc for inter and intra-row weed control are:

i) inter and intra-row crop spacing
ii) crops undisturbed zone diameter
iii) distance of disc centre from crops undisturbed circle centre
iv) cut-out sector angle
v) bevel edges dimensions
vi) required tolerance dependent upon the growth habit of the crop plants

For that purpose it was found necessary to give the guidelines for designing a disc based upon the individual requirements of the user.

1) First the crops undisturbed circle has to be designed
2) The tolerance required also has to be designed due to the crop not being in the right position.
3) Design the offset line that the disc will work from the centre of the crop row
4) The disc radius will be equal to ((37.5+*a*)-*tolerance*) in mm.
5) A length of sector equal to the undisturbed circle diameter will be designed from the centre of the disc.
6) At an angle of 150 deg from the centre of the disc and of 20 mm length the bevel is placed of 15 mm length.

Figure 7-5 shows the proposed disc design produced used the aforementioned methodology.

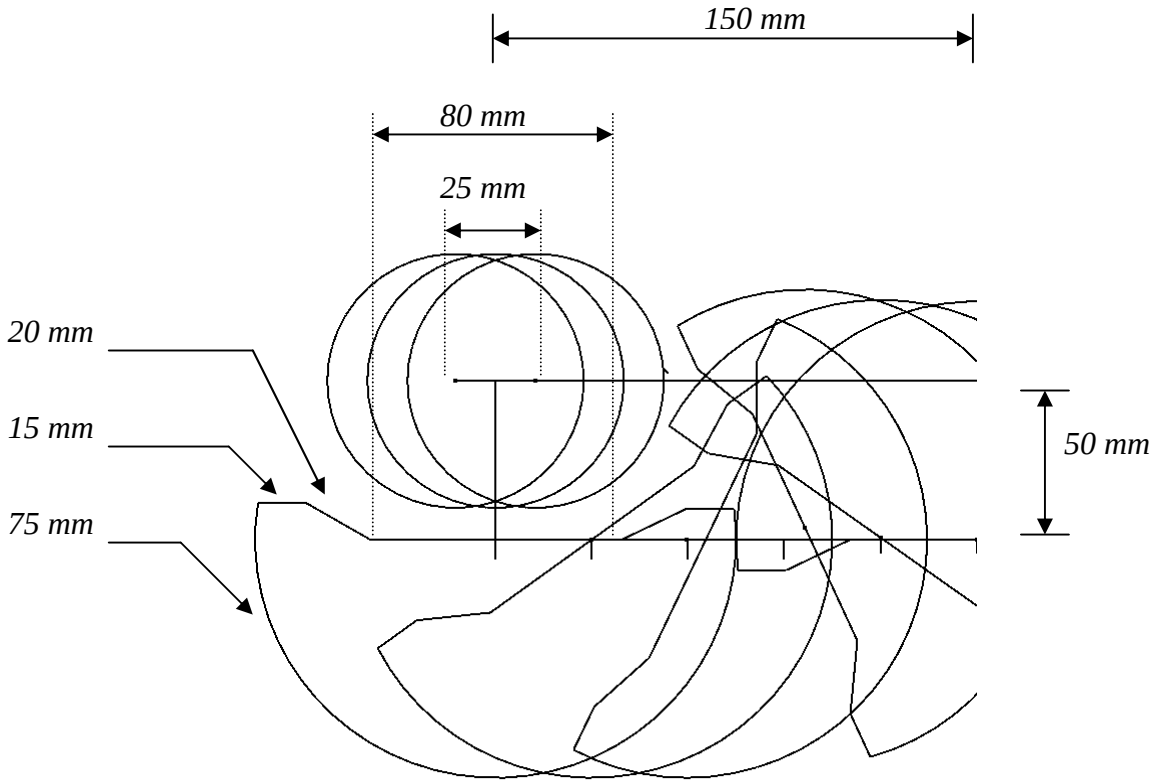

Figure 7-5 Disc geometric characteristics for 300 mm intra-row spacing

The crop used in the field experiment was cabbage with an inter- and intra-row plant spacing of 500 mm. In order to treat the intra-row weeds at a distance of 500 mm and with crops undisturbed circle of 40 mm radius a 110 mm radius disc was designed with round edges to give adequate clearance in the field to accommodate variation in plant spacing (Figure 7-6). This design is a compromise between maximum cultivation is with adequate tolerance to angular and lateral misalignment, which if insufficient might lead to crop damage. The tolerance required depended on the dynamic performance of the system as a whole and the growth habit of the crop plants (Tillett *et al.*, 2007).

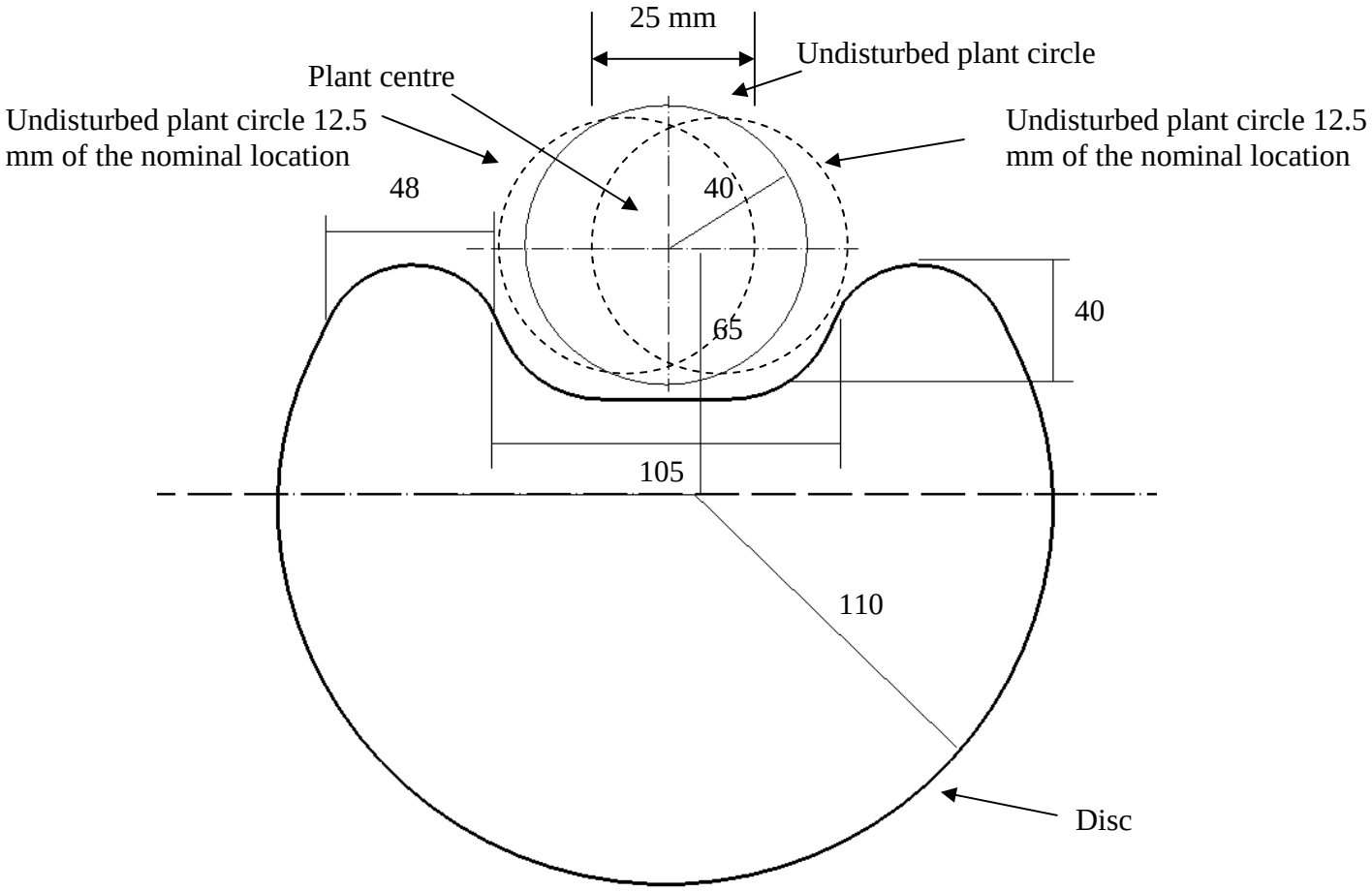

(a)

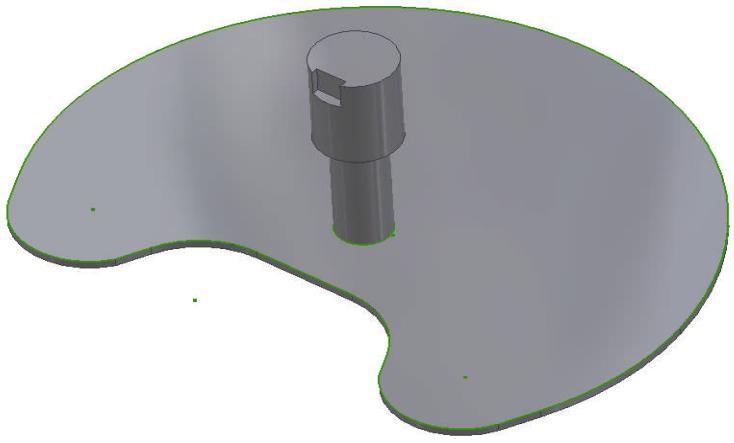

(b)

Figure 7-6 (a) Disc design characteristics to provide clearance from the non-tilled area, for 500 mm plant spacing and (b) 3D model of the disc

Variability in plant spacing along the row was accommodated by making small adjustments to the rotational speed of the disc via a phase lock loop. This mechanism minimised the relative speed between the cultivation device and the soil, thus reducing soil throw and possible crop contamination. The mechanism also reduced machine wear by avoiding the need for very high accelerations, such as those required by reciprocating mechanisms as the ones proposed by Home (2003).

Field pilot studies indicated that angular control phase errors were usually within 10^{o}. Earlier work by Tillett and Hague (2006) had shown that lateral error perpendicular to crop rows would have had a standard deviation of within 10 mm. Visual observations of the system performance suggested that in this case the potential error parallel with crop rows was similar in magnitude. However, these were not the only factors that needed to be taken into account. Most brassica transplants plants do not grow vertically out of their modules. They are inclined to grow a hooked stem offsetting the centre of the foliage, as located by the vision system, from the centre of the root system, which must be avoided by the disc (Tillett *et al.*, 2007). The magnitude of this offset varies with variety, season and growing regime. The standard deviation in offset in our experimental cabbage crop was measured as 19mm with no significant bias. Lettuce on the other hand can be considered as growing vertically out of the module. The disc profile (Figure 7-6) for this experimental work conducted on cabbage was based on a 80mm diameter of undisturbed zone with a cut out designed to avoid that area with angular and lateral errors of up to 20° and 20 mm respectively (Figures 7-6 and 7-7).

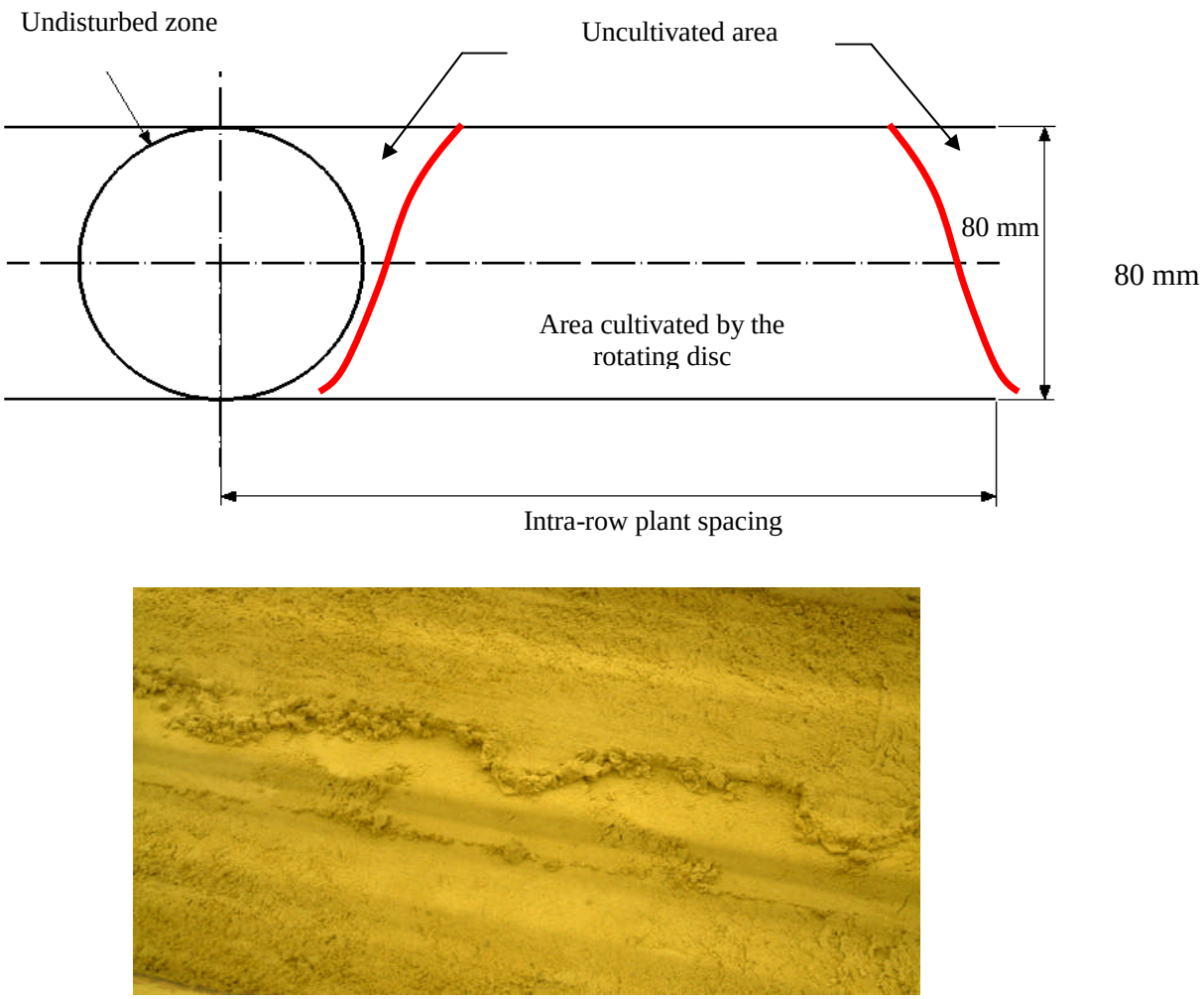

Figure 7-7 Illustration of cultivated area with a rotating disc with angular and lateral misalignment of not less than 20° and 20 mm for a 500 mm intra-row plant spacing (upper) and photograph of soil disturbance (lower).

Inter- and intra-row cultivation had an overall coverage of 95% excluding the undisturbed circle surrounding the crop plants. The treated area could be increased by cultivation from both sides for each row either with two rotating discs per row, or by making two passes.

The disc was a convex one and had an inclination angle of 5° in order to minimise the draught and vertical force, as well torque (Dedousis *et al.*, 2006 and 2007). The disc was also inclined towards the crop row at an angle of 5° laterally.

7.3 Computer vision guidance

The position of the plants and their phase relative to the rotating disc was detected using computer vision. The tracking algorithm was developed by Tillett & Hague Technology Ltd as part of a HortLink project funded by the Department of Food Environment and Rural Affairs (DEFRA), UK (project code: HL0173LFV). Details on the computer vision guidance software and hardware can be found in Appendix VII and in Tillett *et al.*, 2007 a and b.

7.4 Design of field experiment

The crop selected for the experiment was cabbage and was transplanted in early September, 2006. The fast growing variety Elisa was chosen and transplanted slightly larger than normal in order to ensure good establishment. In total 1600 cabbage plants was manually transplanted. The crop was planted at Cranfield University's research farm at Silsoe in a 0.2 ha field area. The cabbages were transplanted into a seedbed that had been prepared three weeks earlier to ensure that the relative sizes of the crop and weeds were typical of a normal cropping system. No herbicide was used on this relatively weedy site and the weed pressure was high. The site was judged to have a reasonable representative sample of weed species experience in commercial vegetable production including *Tripleurospermum inodorum* (Mayweed), *Capsella bursa-pastoris* (shepherds purse) and Stellaria media (Chickweed) amongst others. Figure 7-8 shows the layout of the field experiment.

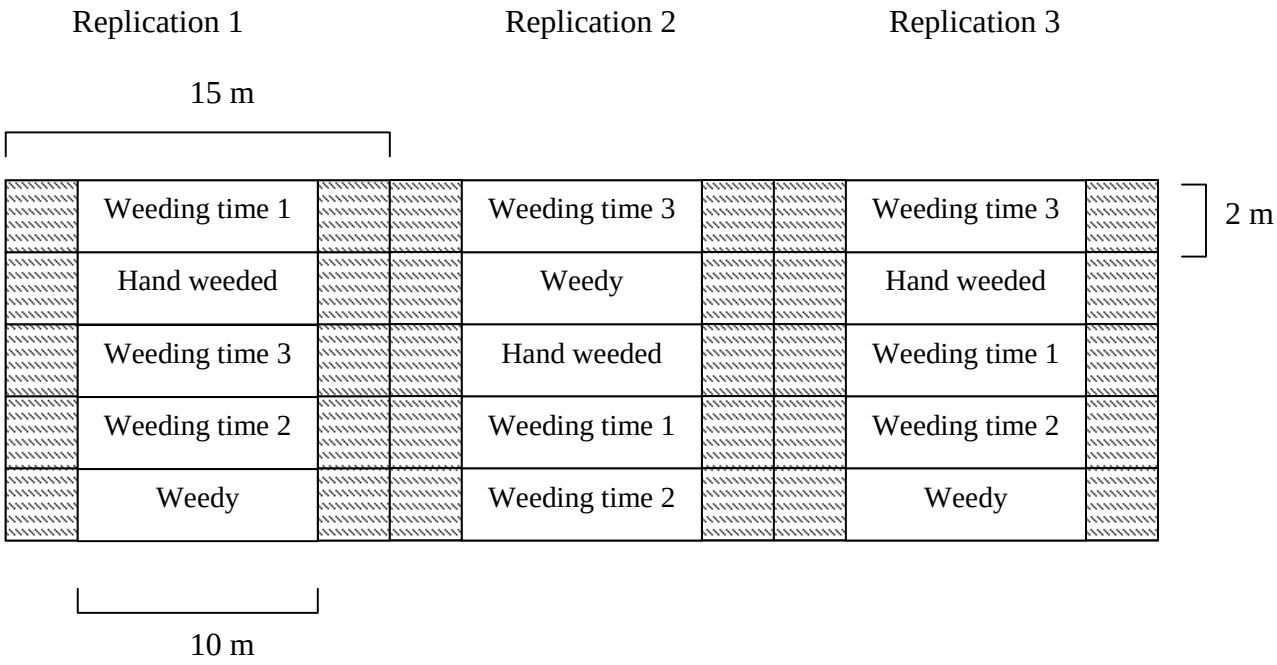

Figure 7-8 Field experiment layout

Three weeding treatments were conducted at 16 days, 23 days and 33 days after transplanting. The first treatment was timed to coincide with the "white thread" stage when weed seedlings are extremely sensitive to mechanical weed control. The last treatment was beyond that which would normally be considered realistic for a mechanical weeding operation. Thus these timings tested the system over and perhaps beyond the normal weeding window. Each treatment had three replicates. Weed free (hand weeded) and untreated plots were included for comparison. All treatments were conducted at 1.8 km h^{-1}. The tool frame was equipped with both inter-row and in-row cultivators so that both zones were cultivated in one pass.

Within each plot eight crop plants were selected and weed numbers counted in three annular areas (radii of 0-80mm, 80-160mm and 160-240mm) centered on those plants. Figure 7-9 shows three different cabbage growing stages in different weed infestation levels. Weed counts were performed immediately before and after each treatment, and again two weeks after treatment. The eight crop plants on each plot were also assessed for any damage inflicted by the equipment.

(a) (b) (c)

Figure 7-9 (a) First weeding treatment (b) Hand weeded two weeks after (c) Weedy two weeks after

7.5 Rotating disc hoe performance

The experimental equipment performed well in the first two treatments with no gross errors in crop plant identification and tracking. Logged data from the control system suggested that angular errors were normally within 10°. By the time the third treatment was conducted the weed infestation had reached the point in many places that coverage was complete (Figure 7-10). At this stage weeds had started to compete with the crop and indeed themselves as can be seen in the lower weed densities prior to the third treatment. As the vision system relies on identifying plant material from a soil background it is not surprising that in some cases tracking was poor. These observations of engineering performance are borne out by the crop damage record. Assessment two weeks after treatment for the first two treatments showed no visible damage to the sample crop plants. However, minor damage had been noted immediately after treatment on one plant at treatment one and on two plants at treatment two. Two of the sample plants at treatment three were killed by the machine. It should be noted that the level of weed infestation experienced during the second treatment would normally be regarded as an upper limit for commercial production.

An additional factor in the apparent increase in crop damage with treatment timing was the size of the crop plants. As the plants grew the physical margin between blade and crop was reduced making the system less tolerant to misalignment. Comparison between weed populations in the three annular assessment areas pre treatment illustrated in Figures 7-11 to 7-13 suggest that the crop has some ability to suppress weeds within an 80mm radius. It might therefore be a better compromise between crop damage and weeding efficacy if the uncultivated crop plant zone were increased in diameter at more advanced growth stages. This balance is affected by a complex interaction between factors that include crop competitiveness, weed species and commercial considerations that are beyond the scope of this project, but which would be worthy of further consideration.

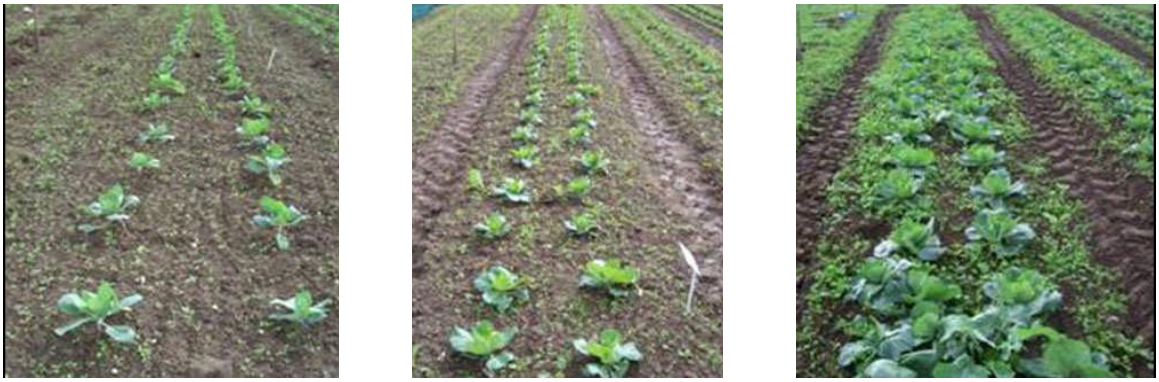

Figure 7-10 Typical weed levels experienced during treatments one, two and three on the 27 September, 4 October and 17 October respectively.

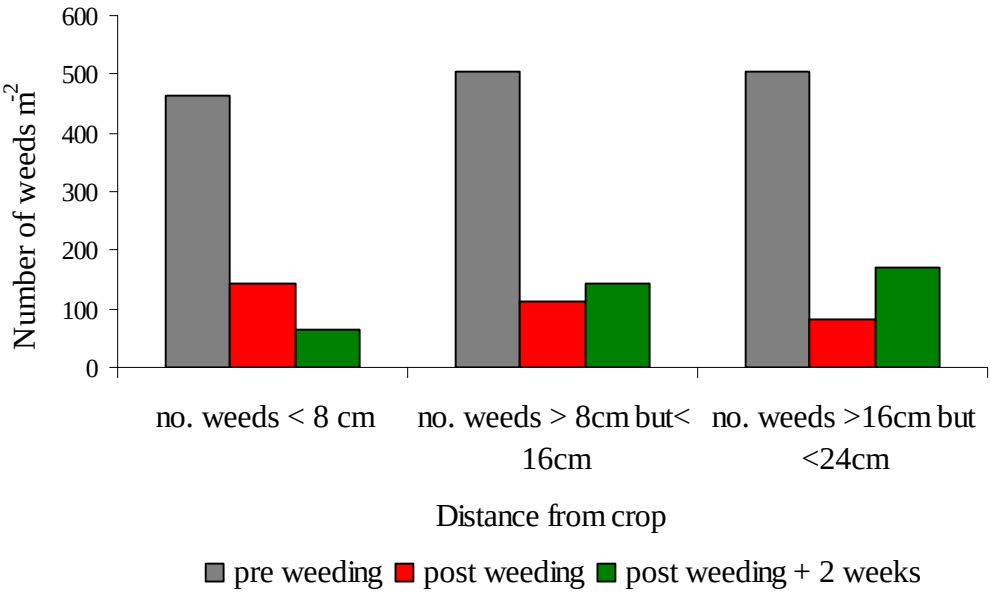

Figure 7-11 Field experiments results of weeding treatment 1

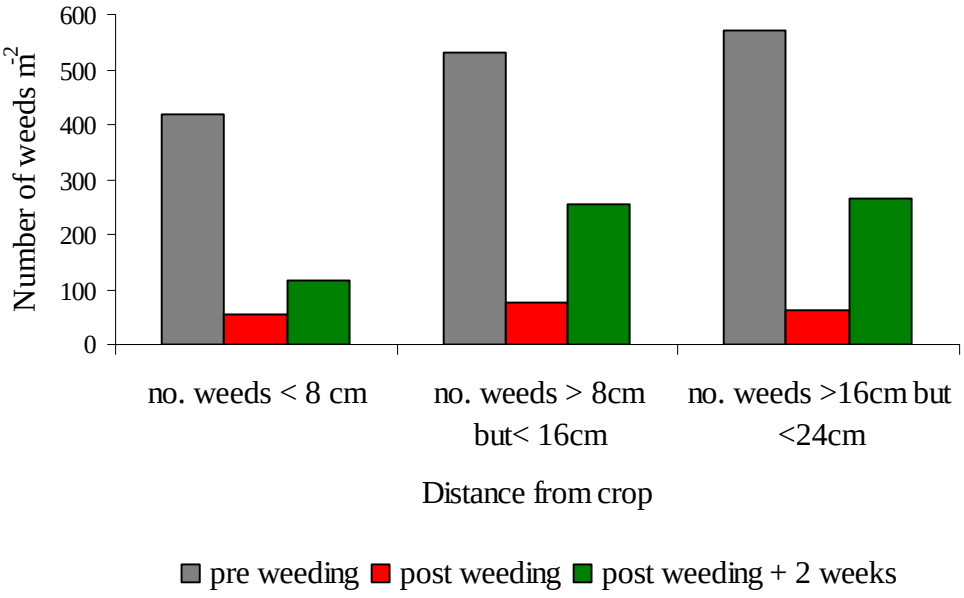

Figure 7-12 Field experiments results of weeding treatment 2

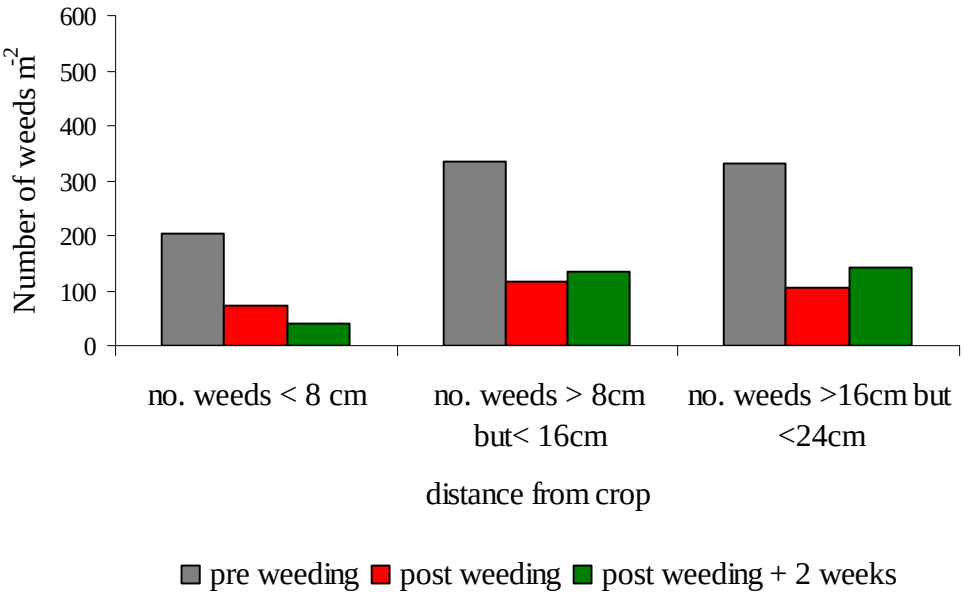

Figure 7-13 Field experiments results of weeding treatment 3

The efficiency of weed control was at its best during treatments one (Figure 7-11) and two (Figure 7-12) with initial weed numbers immediately after treatment reduced by 77% and 87%. Subsequent re-growth and new germination in the two weeks after treatment reduced those figures to 74% and 66% of the original weed numbers. Whilst rainfall was marginally higher in the two weeks after the second treatment (13mm) than in the two weeks after the first (9mm), this is unlikely to have accounted for the higher recovery in weed numbers seen after the second treatment. It is thought that the greater susceptibility of weeds to mechanical damage at the earlier treatment was a more significant factor. By the third treatment overall weed numbers pre treatment were lower, but those that remained had grown to be larger and more robust. This combined with the difficulty in tracking reduced the initial reduction in weed numbers to only 65% (Figure 7-13). However, there was no significant recovery in weed numbers over the subsequent two weeks possibly due to the late stage in the season not being suitable for further weed germination.

7.6 Economic analysis

An economic analysis was performed for the proposed inter- and intra-row weed control system aiming to evaluate and compare the cost of different weed control strategies for organic as well conventional farming.

The rotating disc-hoe main target is organic farms with high value products (i.e. vegetables) and the difference that this system will make is the availability, amount and cost of labour requirements resulting in the final value of the marketable product. Furthermore the rotating disc-hoe can be used in conventional farming, in order to overcome and treat the chemical-tolerant weeds.

Figure 7-14 shows a three dimensional conceptual model of the rotating disc-hoe for a spanning bed of 1.8 m showing with five intra-row units (rotating discs) as well inter-row blades to treat the weeds between the crop rows to fulfil typical transplanted lettuce configuration.

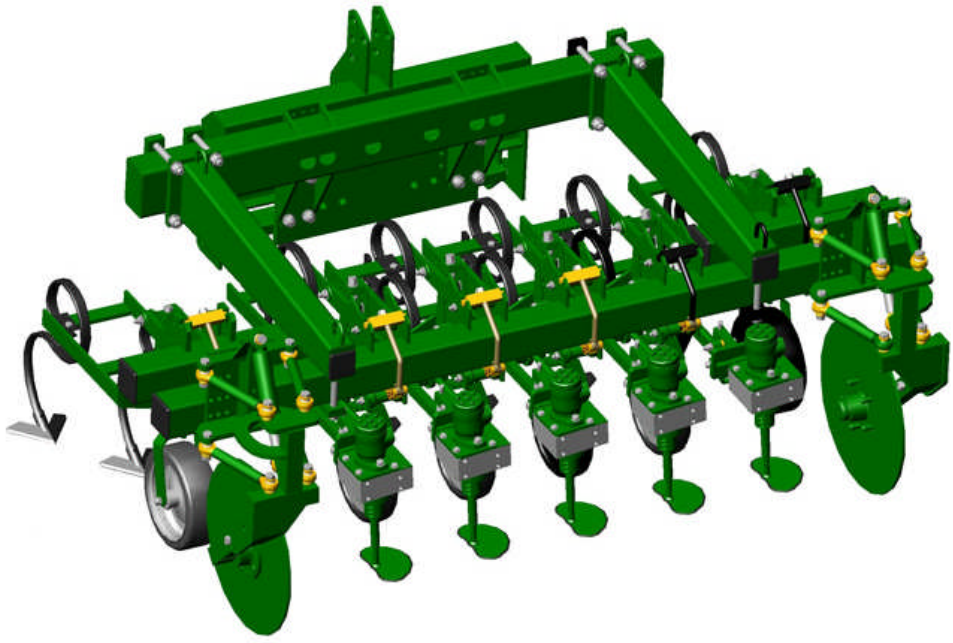

Figure 7-14 Five unit inter- and intra-row weeding concept

7.6.1 Economic cost calculator

The economic analysis of the different weeding strategies presented in this chapter performed with an economic cost calculator software developed by Home (2003). The calculator has over 50 implement selections and more can be easily added for different economic comparisons. Figure 7-15 shows a screen image of the cost calculator.

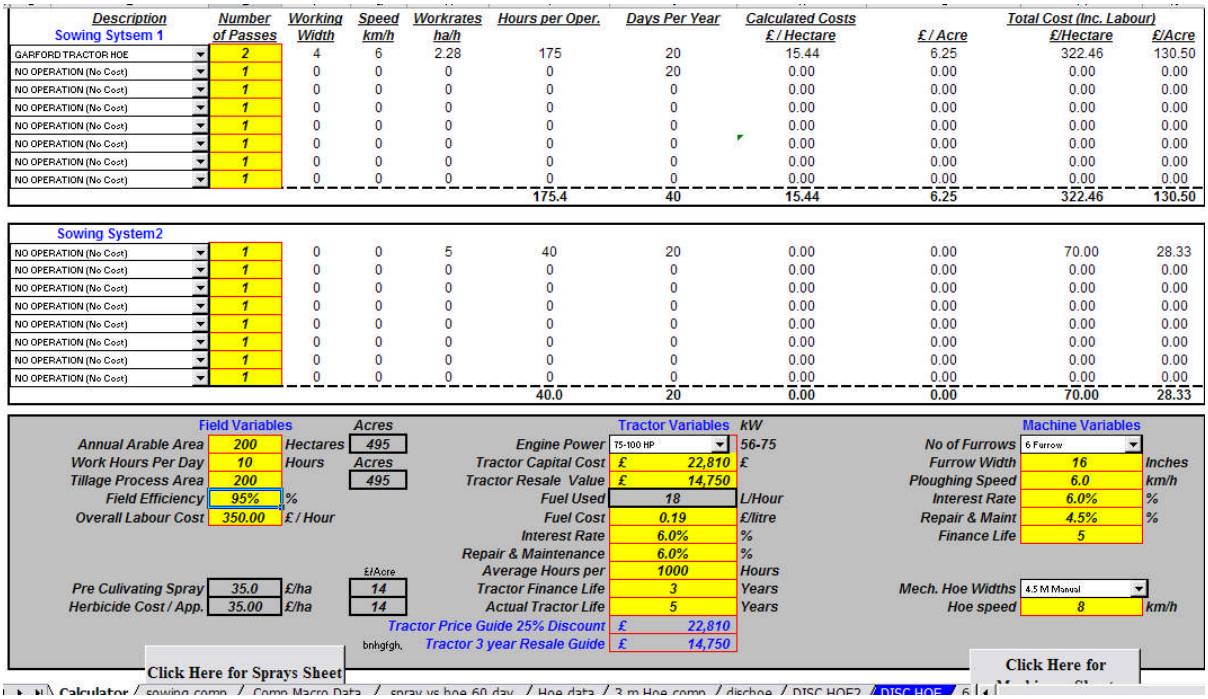

Figure 7-15 Screen image of the cost calculator

7.6.1.1 Machinery variables

The selection of machinery as well as the required number of passes of each treatment can be made by the drop down boxes. The cost calculator based on the data we have entered on a linked sheet for the machinery properties such as implement width, working speed, capital cost and residual values based on depreciation factors based on Nix (2006) calculates the work rate in ha/h and the cost of each treatment in £/ha.

7.6.1.2 Field variables

After had selected the machinery required the field variables has to be entered. The required fields are the annual arable area in ha, the working hours per day in h, the tilled processed area, the field efficiency of the operation and the overall labour cost in £/ha based on the minimum wage for a farm worker in the UK. This will provide as with a cost calculation for a specific weed control strategy.

7.6.1.3 Tractor variables

After had selected the machinery required and the field variables the tractor that will be used to carry out the field operations has to be selected. By selecting the tractor engine power, the economic cost calculator automatically generates the mean fuel consumption based on manufactures specifications which enables the calculation of the fuel use for each operation (Home, 2003). For new tractors an interest rate of 5% over a three year of finance has been incorporated in the cost calculator.

7.6.1.4 Implement variables

The implement variable section is the last to be completed on the economic cost calculator. The required fields entered by the user are, the implement width, the interest rate, the repair and maintenance rate and the finance life of the implement.

Further details on the economic cost calculator as well the application on mechanical weeding and ploughing can be found in Home (2003) and Saunders (2002) respectively.

7.6.2 Cost analysis

The crop selected for this analysis is cabbage, and two passes were encountered for each treatment. Table 1 show the proposed strategies compared in this analysis.

Table 7-1 Weeding systems compared in this analysis

		Disc-hoe	Sprayer	Inter-row and Hand weeding	Hand weeding
Width	(m)	4	24	4	6
Speed	(km h^{-1})	3	8	6/2	2
Work rate	(ha h^{-1})	1.14	9.12	2.28	1.14
Capital cost	(£)	34000	12750	9700	N/A
Residual value*	(£)	18000	1500	4000	N/A
Life before change	(Years)	5	5	5	N/A
Minimum payment wage	(£ h^{-1})				5.75

* Depreciation value: 15% $year^{-1}$ (Nix 2006)

Figure 7-16 shows the comparative cost per hectare of the four weeding strategies. Each treatment has been undertaken twice as cabbage has a longer growing period than salads and more than one treatment is required for efficient weed control. This shows that for 10 ha the most expensive treatment is the rotating disc-hoe with £703 ha^{-1} and a work rate of 1.14 ha h^{-1}. The cost for the six mean hand weeding gang is £690 ha^{-1} with a minimum cost per worker of £5.75 h^{-1}, Nix (2006) and work rate of 1.14 ha h^{-1}. The cost of the 24 m tractor mounted sprayer is £436 ha^{-1} with a work rate of 18.24 ha h^{-1}. The cost for the combination of inter-row hoeing and intra-row manual weeding is £337 ha^{-1} with a workrate of 2.28 ha h^{-1} nad 1.14 ha h^{-1} for the inter-row hoe and the six men gang respectively. At 50 ha the cost is significantly lower for all the mechanized treatments at a common cost of £156 ha^{-1}, which represent a reduction of 77%; 67%; and 51%, for the disc-hoe, the tractor mounted sprayer and the inter-row hoe and hand weeding combination respectively. For areas greater than 50 ha the disc-hoe is the cheapest strategy. For a 125 ha treated area the disc hoe cost is £81 ha^{-1} while the tractor mounted sprayer and the inter-row hoe and hand weeding combination is £100 ha^{-1} and £139 ha^{-1}, respectively.

This analysis shows that the disc hoe has potential advantage for organic as well as conventional farming as the total cost per hectare is less in farm sizes greater than 50 ha. In relation to organic farming the biggest benefit of the machine is the significant reduction of labour needs and cost. For hand weeding a six men gang is needed to treat the intra-row weeds at a cost of £35 h^{-1} and the disc hoe needs only one person to drive the tractor at a cost of £10 h^{-1}. For conventional farming this may prove to be a solution to eliminate weeds that have a great tolerance to current herbicides. Also concerning both farming systems the use of such machines will help to improve the final value of the marketable product.

This work clearly demonstrates that the rotating disc-hoe, apart from the environmental benefits that it has due to the reduced herbicide use, decreases significantly the cost of weeding increasing the potential for organic farming production.

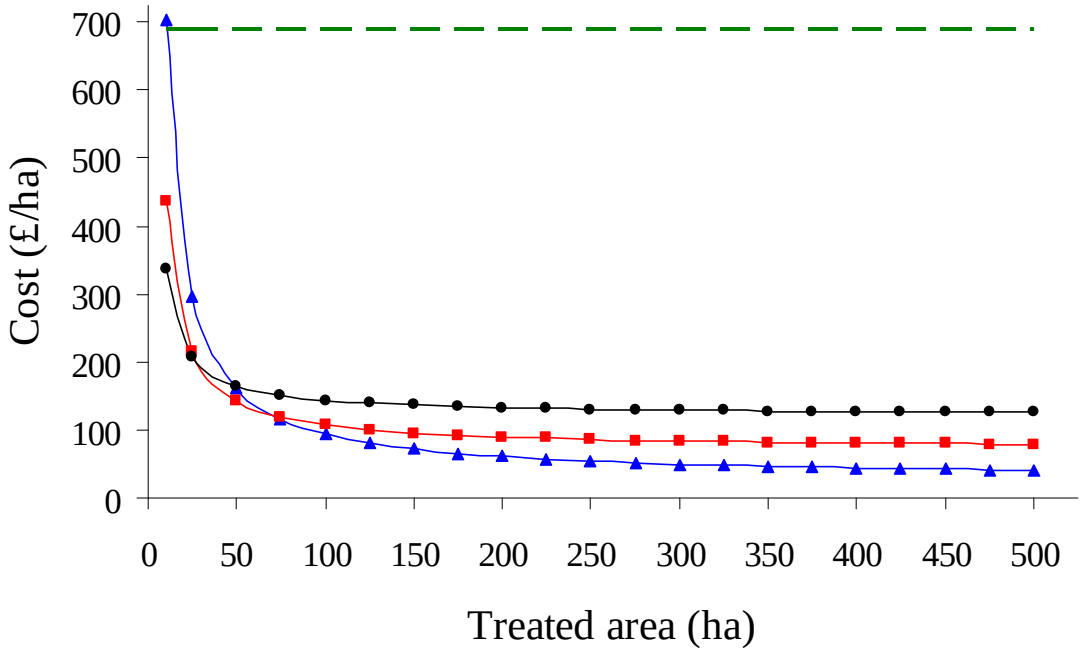

Figure 7-16 Comparative cost of four different weed control strategies, six men hand weeding (---); rotating disc hoe (▲); mounted sprayer (■); and inter-row and hand weeding combination (●)

In practice for a 100 ha target giving a 10 day window for the hoeing operation the disc-hoe will cover 11.4 ha for a 10 hour day and therefore will carry out the operation in 8.77 days. Hence the hoe is able to meet the 10 day window with 1.23 days to spare.

7.7 Conclusions

- The crop location and tracking algorithm performed well under normal commercial weed infestation levels.
- The hydraulic disc control system maintained angular alignment within 10° of the demanded value.
- The convex rotating cut out disc cultivator was effective in removing weeds within crop rows and the soil tilth was similar to the one observed during the controlled laboratory experiment.
- Combined in-row with inter-row cultivation typically removes 80% of weeds, though some re-growth and new germination can be expected.
- Crop damage was low with no plants killed when operating within normal commercial weed levels.
- The disc-hoe is a lower cost mechanical weed control system especially for organic farmers with a cost for 125 ha of £81 ha^{-1}, £139 ha^{-1} for the inter-row and hand weeding combination and £690 ha^{-1} for a six man gang manual intra-row weeding, for two passes. It is also cheaper for non-organic farmers compared to the cost of the 24 m tractor mounted sprayer of £100 ha^{-1}

Chapter 8

Conclusions and Recommendations

8. Conclusions and Recommendations

8.1 Conclusions

This study has reviewed current systems for non-chemical weed control in order to develop a novel system for inter- and intra-row weed control to reduce the environmental loading of agrochemicals. The approach taken has investigated the kinematics of different geometries discs with computer simulation graphical tools as well validated these with a mathematical model for the kinematics of rotating discs. This enables a suitable geometry to be specified for a disc to enable it to achieve intra-row weed control without disturbing the no-till area that surrounds the crop. Laboratory investigations into the soil dynamics of working discs has enabled the optimum setting properties to specified for a disc to weed with the minimum force requirements and the maximum disturbed area. Field investigations enabled the agronomic evaluation of pre-production prototype on mechanical weed control efficiency. From this study's investigations it has been seen that the rotating disc-hoe has the potential to address the issues facing inter- and intra-row weed control in widely spaced field vegetables.

The following conclusions can be made:

- A novel prototype inter- and intra-row weeding mechanism has been shown to operate successfully at speeds up to 1.4 m/s (5 km/h) at commercial planted vegetables, inter- and intra-row plant spacing, 300 and 500 mm. The principles developed in this could be applied to the design of machines for other agricultural row crops.

- A convex disc with an 156 deg cut-out sector angle working 15 mm deep with forward speed of 1 m/s and an inclination angle varying from $5 \leq \alpha < 10$ deg is the most appropriate combination to eliminate the weeds up to seven weeks after planting.

- Investigations showed that for different disc geometries different modes of soil failure could occur. Flat disc has a tear failure mode, thus leaving larger irregular aggregates; the convex disc had a shear failure mode, leaving a more uniform clod size, and an improved quality of tilth.

- A theoretical model was developed for shallow working rotating discs identifying the soil failure mechanisms, based on sub-emerged and blade theory. Also a mathematical prediction model developed based upon Mohr-Coulomb soil mechanics theory for the disc geometries. A comparison of all experimental work encompassing the laboratory experiments with non-rotating and rotating discs, incorporating the deflection effect of the shaft when working at 0^o inclination angle showed that the model is able to predict the draught force with good accuracy. The predicted forces were 3.5% more than the measured forces overall for a linear regression line (with a coefficient of determination of 0.7) and 61% of the data were within bounds of $\pm$ 25% a line of equal magnitude. The model showed a sensitivity in depth and the scatter distribution of the measured values is due to soil variability as the disc were working very shallow (maximum depth of 25 mm).

- The mathematical model for the disc kinematics of rotating discs based on co-ordinate geometry enables the specification of suitable geometries for a range of crops and operations and reduces significantly the time required to optimize the geometry in comparison with empirical methods.

- A reduction in plant spacing results in a linear reduction in the minimum distance from the plant centre to approximately 10 mm at a spacing of 200 mm. There is intrusion of the disc cut-out into the no-till circle at smaller plant spacing and modification of the disc design for a 300 mm plant spacing is required.

- The percentage of the intra-row area hoed increases from 83% to 95% when the plant spacing is increasing from 200 mm to 500 mm. Also the double cut-out disc (bowtie) can be used at plant spacing down to 150 mm. Combined in-row with inter-row cultivation typically removes 80% of weeds, though some re-growth and new germination can be expected. Crop damage was low with no plants killed when operating within normal commercial weed levels.

- The disc-hoe is a lower cost mechanical weed control system especially suitable for organic farmers with a cost for 125 ha of £81 ha^{-1}, £139 ha^{-1} for the inter-row and hand weeding combination and £690 ha^{-1} for a six man gang manual intra-row weeding, for two passes. It is also cheaper for non-organic farmers compared to the cost of the 24 m tractor mounted sprayer of £100 ha^{-1}

8.2 Recommendations

- Detailed investigations on the forward and lateral translocation as proposed by Sharifat & Kushwaha 2000 as well as the flow of soil (Hanna *et al.,* 1993 (a) and (b)) over the discs in controlled laboratory and field experiments will help understand the soil aggregate formation and soil failure. This would allow the determination of improved cutting and burial weed control techniques.

- Field investigations with commercial intra-row weeders (torsion, finger) and the rotating disc-hoe in order to quantify and evaluate them upon their performance.

- The future of agricultural production requires machinery that is not making permanent damage to the soil that requires minimum amount of energy. This would be an autonomous platform of a robot that will have attached a set of discs for weed control. This would provide us with a robot that will be able to work 24 hours 7 days a week, and help minimise problems caused by the frequent upper soil layer disturbance and subsoil compaction.

- An investigation into other possible ways to use the rotating disc in conservation agriculture. The disc can be used as a shallow plough (25 mm deep) or cultivator using the same theory-philosophy with larger diameter convex discs with low inclination and sweep angle.

Chapter 9

References

9. References

1. Aastrand B. & Baerveldt A.J. (2002) An agricultural mobile robot with vision-based perception for mechanical weed control. *Autonomous Robots,* 13, 21-35.

2. Aastrand B. & Baerveldt A.J. (2005) A vision based row-following system for agricultural field machinery. *Mechatronics,* 15 (2), 251-269.

3. Abo El Ees N. A. E. H. & Wills B. M. D. (1986) An analysis of the geometric and soil working parameters of a curved vertical disc. *Journal of Agricultural Engineering Research,* 35, 277-286.

4. Albuquerque De J.C.D. & Hettiaratchi D. R. P. (1980) Theoretical mechanics of sub-surface cutting blades and buried anchros. *Journal of Agricultural Engineering Research,* 25, 121-144.

5. Ascard J. (1990) Thermal weed control with flaming in onions. *In*: Proceedings of the *3rd International conference IFOAM, Non-chemical weed control,* Linz, Austria.

6. Ascard J. (1994) Dose response models for flame weeding in relation to plant size and machinery. *Weed Research,* 34 (5), 377-385.

7. Ascard J. (1995) Effects of flame weeding on weed species at different developmental stages. *Weed Research,* 35 (5), 397-411.

8. Ascard J. (1998) Mechanical intra-row weed control techniques in row crops. *In*: Proceedings of the *3rd EWRS Workshop on physical weed control,* European Weed Research Society, Wye college, UK.

9. Ascard J. (2007) Why are some non-chemical weed control methods adopted in practice and others not, and what can we learn from this? *In*: Proceedings of the *7th European Weed Research Society workshop on physical and cultural weed control,* Salem, Germany,

10. Bakker T. (2003) *Autonomous weeding literature review*. SCO Report 03-01, Wageningen University: Systems and Control Group.

11. Bar-Shalom Y. & Fortmann T. (1988) Tracking and data association. *New York,* Academin Press

12. Bellinder R. Cultivation tools for mechanical weed control in vegetables. (1997) Cornell University, Ithaca, NY. 97.

13. Blackmore S. & Griepentrog H. (2002) A future view of precision farming. *In*: Proceedings of the *Precision Agriculture Tage,* Bonn, Germany,

14. Blasco J., Aleixos N., Roger J., Rabatel E. & Molto E. (2002) Robotic weed control using machine vision. *Biosystems Engineering,* 83 (2), 149-157.

15. Bleeker P. (2005) First experiments with intra-row weed control with a camera. *In*: Proceedings of the *Spatial and dynamic weed measurements and innovative weeding technologies,* Bygholm, Denmark, European Weed Research Society,

16. Bleeker P. (2007) Personal communication.

17. Bleeker P. & Weide R. (1998) Possibilities of finger weeders. *In*: Proceedings of the *3rd EWRS Workshop on physical weed control,* Wye college, UK, European Weed Research Society,

18. Bleeker P., Weide R. & Kurstjens D. (2002) Experiences and experiments with new intra-row weeders. *In*: Proceedings of the *5th EWRS workshop on Physical weed control,* Pisa, Italy, European Weed Research Society,

19. Bleeker P. & Weide van der R. (2007) Personal communication.

20. Bond W. & Grundy A.C. (2001) Non-chemical weed management in organic farming systems. *Weed Research,* 41 (5), 383-405.

21. Bontsema J., Asselt C.J. & Vermuelen G.D. (2000) Intra-row weed control. *In*: Proceedings of the *4th EWRS workshop on Physical weed control*, Elspeet, The Netherlands, European Weed Research Society,

22. Bontsema J., Asselt van C.J., Lempens P.W.J. & Straten van G. (1998) Intra-row weed control: Amechatronics approach. *In*: Proceedings of the *Control Applications and Ergonomics in Agriculture*, Athens, Greece,

23. Bowman G. (1997) *Steel in the field - A farmers guide to weed management tools*.

24. Cavalieri A., Janssen S., Smithnson A. & Buisman T. (2001) *Economic viability of weeding strategies in organically grown sugar beets*. KVL The Royal Veterinary and Agricultural University, Denmark.

25. Choa S. L. & Chancellor W. J. (1973) Optimum design and operation parameters for a resonant oscillating subsoiler. *Transactions of the ASAE*, 16 (6), 1200-1208.

26. Davis M. (2005) *Scientific papers and presentations*. 2 ed. Academic Press, An imprint of Elsevier.

27. Dedousis A. P. (2003) Development of high density energy techniques in robotic weeding. MSc Thesis. Wageningen University.

28. Dedousis A.P. & Godwin R.J. (2005) Precision mechanical weed control. *In*: Proceedings of the *13th European Weed Research Society Symposium*, Bari, Italy,

29. Dedousis A.P., Godwin R.J., O'Dogherty M.J., Tillett N.D. & Brighton J.L. (2005) An investigation into the design and performance of a novel mechanical system for inter and intr-row weed control. *In*: Proceedings of the *Brighton Crop Protection Conference*, Glasgow, Scotland, Vol. 2.

30. Dedousis A.P., Godwin R.J., O'Dogherty M.J., Tillett N.D. & Brighton J.L. (2006) Effect of implement geometry and inclination angle on soil failure and forces acting on a shallow rotating disc for inter and intra-row hoeing. *In*: Proceedings of the *17th Triennial Conference of the International Soil Tillage Research Organisation* , Kiel, Germany,

31. Dedousis A.P., Godwin R. J., O'Dogherty M. J., Tillett N.D. & Grundy A.C. (2007) Inter and intra-row mechanical weed control with rotating discs. *In*: *Precision Agriculture 07*. Editor J. V. Stafford, Wageningen Academic Publishers, 493-498.

32. Dedousis A.P., O'Dogherty M J., Godwin R J, Tillett N.D. & Brighton J.L. (2006) A novel approach to precision mechanical weed control with a rotating disc for inter and intra-row weed hoeing. *In*: Proceedings of the *17th Triennial Conference of the International Soil Tillage Research Organisation* , Kiel, Germany,

33. Dekker E., Pute K., Smit J. & Wilbrink R. (2002) Agricultural engineering as backbone in agriculture. *In*: Proceedings of the *European Agricultural Engineering Society,* Budapest,

34. Eatough K. (2002) *Tractive performance of 4x4 tyre treads on pure sand*. EngD thesis, Cranfield University, Silsoe.

35. Ees A. & Wills D. (1986) An analysis of the geometric and soil working parameters of a curved vertical disc. *Journal of Agricultural Engineering Research,* 35, 277-286.

36. Fielke J. M. (1988) The influence of the geometry of chisel plough share wings on tillage forces in sandy loam soil. University of Melbourne, Australia.

37. Fielke J. M. (1996) Interactions of the cutting edge of tillage implements with soil. *Journal of Agricultural Engineering Research,* 63 (1), 61-71.

38. Fielke J. M. & Riley T. W. (1991) The universal eartmoving equation applied to chisel plough wings. *Journal of Terramechanics,* 28 (1), 11-19.

39. Fogelberg F. (2007) Reduction of manual weeding labour in vegetable crops - what can we expect from torsion weeding and weed harrowing. *In*: Proceedings of the *7th European Weed Research Society workshop on physical and cultural weed control,* Salem, Germany,

40. Fogelberg F. & Kritz G. (1999) Intra-row weeding with brushes on vertical axes-factors influencing in-row soil height. *Soil & Tillage Research,* 50, 149-157.

41. Gill W. R. & Hendrick J. G. (1976) The irregularity of soil disturbance depth by circular and rotating tillage tools. *Transactions of the ASAE,* 230-233.

42. Gill W.R., Reaves C.A. & Bailey A.C. (1980) The effect of geometric parameters on disk forces. *Transactions of the ASAE,* 266-269.

43. Gill W. R. & Vanden Berg G. E. (1968) *Soil dynamics in tillage and traction*. Agriculture Research Service, US Department of Agriculture, Washington, DC.

44. Gobor Z. & Lammers P. S. (2006) Concept and virtual prototype of a rotary hoe for intra-row weed control in row crops. *In*: Proceedings of the *European Agricultural Engineering Society International Conference*, Bonn, Germany,

45. Gobor Z. & Lammers P. S. (2007) Mechanical weeding of the intra-row area in row crops with rotary hoe. *In*: Proceedings of the *7th European Weed Research Society workshop on physical and cultural weed control,* Salem, Germany,

46. Godwin R., Seig D. & Allott M. (1987) Soil failure and force prediction for soil engaging discs. *Soil Use and Management,* 3 (3), 106-114.

47. Godwin R. & Spoor G. (1977) Soil failure with narrow tines. *Journal of Agricultural Engineering Research,* 22, 213-228.

48. Godwin R., Spoor G. & Soomro M. (1984) The effect of tine arrangement on soil forces and disturbance. *Journal of Agricultural Engineering Research,* 30, 47-56.

49. Godwin R. J. (1975) An extended octagonal ring transducer for use in tillage studies . *Journal of Agricultural Engineering Research,* 20, 347-352.

50. Godwin R.J. (2007) A review of the effect of implement geometry on soil failure and implement forces. *Soil & Tillage Research,*

51. Godwin R.J. & O'Dogherty M.J. (2007) Integrated soil tillage force prediction models. *Journal of Terramechanics,* 44, 3-14.

52. Godwin R. J. , O'Dogherty M. J., Saunders C. & Balafoutis A. T. (2007) A force prediction model for mouldboard ploughs incorporating the effects of soil characteristic properties, plough geometric factors and ploughing speed. *Biosystems Engineering,* 97, 117-129.

53. Godwin R.J., Reynolds A.J., O'Dogherty M.J. & Al-Ghazal A.A. (1993) A triaxial dynamometer for force and moment measurements on tillage implements. *Journal of Agricultural Engineering Research,* 55, 189-205.

54. Godwin R.J. & Spoor G. (1977) Soil Failure with Narrow Tines. *Journal of Agricultural Engineering Research,* (22), 213-228.

55. Griepentrog H. W., Gulhom-Hansen T. & Nielsen J. (2007) First field results from intra-row rotor weeding. *In*: Proceedings of the *7th European Weed Research Society workshop on physical and cultural weed control,* Salem, Germany,

56. Griepentrog H. W., Norremark M. & Nielsen J. (2006) Autonomous intra-row weeding based on GPS. *In*: Proceedings of the *Agricultural*

Engineering World Congress, Bonn, Germany,

57. Griepentrog H. W., Norremark M., Nielsen J. & Blackmore B. S. (2005) Seed mapping of sugar beet. *Precision Agriculture,* 2 (6), 157-165.

58. Gupta C.P. & Rajput D.S. (1993) Effect of amplitude and frequency on soil break-up by an oscillating tillage tool in a soil bin experiment. *Soil & Tillage Research,* 25, 329-338.

59. Hague, T. & Tillett N. (2001) A bandpass filter-based approach to crop row location and tracking. *Mechatronics*, 11, 1-12.

60. Hann M.J. & Giessibel J. (1998) Force measurements on driven discs. *Journal of Agricultural Engineering Research,* 69 (2), 149-158.

61. Hanna H. M., Erbach D. C., Marley S. J. & Melvin S. W. (1993a) Comparison of the goryachkin theory to soil flow on a sweep. *Transactions of the ASAE,* 36 (2), 293-299.

62. Hanna H. M., Marley S. J., Erbach D. C. & Melvin S. W. (1993b) Change in soil microtopography by tillage with a sweep. *Transactions of the ASAE,* 36 (2), 301-307.

63. Hansson D. & Svensson S. E. (2007) Steaming soil in narrow bands to control weeds in row crops. *In*: Proceedings of the *7th European Weed Research Society workshop on physical and cultural weed control,* Salem, Germany,

64. Hettiaratchi D. R. P. (1969) The calculation of passive earth pressure. University of Newcastle-upon-Tyne, UK.

65. Hettiaratchi D. R. P. & Alam M. M. (1997) Calculation, validation and simulation of soil reactions on concave agricultural discs. *Journal of Agricultural Engineering Research,* 68, 63-75.

66. Hettiaratchi D. R. P. & Reece A. R. (1974) The calculation of passive soil resistance . *Geotechnique,* 24 (3), 289-310.

67. Hettiaratchi D. R. P. & Reece A. R. (1975) Boundary wedges in two dimensional passive soil failure. *Geotechnique,* 25 (2), 197-220.

68. Hettiaratchi D. R. P., Witney, B.D. & Reece A. R. (1966) The calculation of passive pressure in two-dimesnional soil failure. *Journal of Agricultural Engineering Research,* 11 (2), 89-107.

69. Hettiaratchi P (1987) A critical state soil mechanics model for agricultural soils. *Soil use and management,* 3 (3), 94-105.

70. Hettiaratchi P. & Reece R. (1967) Symmetrical three-dimensional soil failure. *Journal of terramechanics,* 4 (3), 45-67.

71. Home M. (2003) An investigation into the design of cultivation systems for inter-and intra-row weed control. EngD thesis. Cranfield University, Silsoe.

72. Home M., Tillett N. & Godwin R.J. (2001) What lateral accuracy is required for weed control by inter-row cultivation? *In*: Proceedings of the *The BCPC conference-Weed 2001,*

73. Hoogmoed W.B. (2002) No-tillage. Anonymous Wageningen University.

74. Jones P.A., Blair A.M. & Orson J.H. (1995) The effect of different types of psysical damage to four weed species. *In*: Proceedings of the *Brighton crop protection conference-weeds,*

75. Jones P.A., Blair A.M. & Orson J.H. (1996) Mechanical damage to kill weeds. *In*: Proceedings of the *Second international weed control congress,* Copenhagen, Denmark.

76. Kouwenhoven J. K. (1997) Intra-row mechanical weed control-possibilities and problems. *Soil & Tillage Research,* 41, 87-104.

77. Kouwenhoven J.K. (1998) Finger weeders for future intra-row weed control. *In*: Proceedings of the *3rd EWRS Workshop on physical weed control*, Wye college, UK, European Weed Research Society,

78. Kouwenhoven J.K., Wevers J.D.A. & Post B.J. (1991) Possibilities of mechanical post-emergence weed control in sugar beet. *Soil & Tillage Research,* 21 (1), 85-95.

79. Kurstjens D. (2002) Mechanisms of selective mechanical weed control by harrowing. PhD Thesis. Wageningen University.

80. Kurstjens D. & Bleeker P. (2000) Optimising torsion weeders and finger weeders. *In*: Proceedings of the *4th EWRS workshop on Physical weed control*, Elspeet, The Netherlands, Elspeet, The Netherlands: European Weed Research Society,

81. Kurstjens D., Perdok U. & Goense D. (2000) Selective uprooting by weed harrowing on sandy soils. *Weed research,* 40, 431-447.

82. Kurstjens D. A. G. & Perdok U. D. (2000) The selective soil covering mechanism of weed harrows on sandy soils. *Soil & Tillage Research,* (55), 193-206.

83. Kushwaha R. L., Chi L. & Shen J. (1993) Analytical and numerical models for predicting soil forces on narrow tillage tools-A review. *Canadian Agricultural Engineering,* 35 (3), 183-193.

84. Lee W.S., Slaughter D.C. & Giles D.K. (1999) Robotic weed control system for tomatoes. *Precision Agriculture,* 1, 95-113.

85. Leinonen P., Saastamoinen A. & Vilmunen J. (2004) Finger weeder for cabbage and lettuce cultures. *In*: Proceedings of the *6th EWRS Workshop on Physical and cultural weed control* , Lillehamer, Norway, Lillehammer, Norway: European Weed Research Society,

86. Lempens P.W.J., Bontsema J., Asselt C.J. & Straten van G. inventors (1996) Actuator for use in an agricultural meachinery for cultivation of crops growing in rows. The Netherlands. OA 1004479.

87. Mattsson B., Nylander C. & Ascard J. (1990) Comparison of seven inter-row weeders. *In*: Proceedings of the *Veroffentlichungen bundesanstalt fur agrarbiologie,* Linz, Donau.

88. McKyes E. 1985) *Soil Cutting and Tillage*. Elsevier.

89. McKyes E. & Ali O. S. (1977) The cutting of soil by narrow blades. *Journal of Terramechanics,* 14 (2), 43-58.

90. Melander B. & Hartvig P. (1997) Yield responses of weed-free seeded onions [Allium cepa(L.)] to hoeing close to the row. *Crop Protection,* 16 (7), 687-691.

91. Melander B. & Rasmussen G. (2001) Effects of cultural methods and physical weed control on intrarow weed numbers, manual weeding and marketable yield in direct-sown leek and bulb onion. *Weed Research,* 41 (6), 491-508.

92. Meyer J., Laun N. & Lenski B. (2002) Evaluation of physical weeders. *In* : Proceedings of the *5th EWRS workshop on Physical weed control*, Pisa, Italy, European Weed Research Society,

93. Meyerhof G. G. (1951) The ultimate bearing capacity of foundations. *Geotechnique,* 2 (4), 301-332.

94. Montgomery D. C. 2001) *Design and anaysis of experiments*. 5 ed. John Wiley & Sons, Inc.

95. Nix J. (2006) *Farm management pocketbook.* 37 ed. Imperial College London, Wye campus.

96. O'Dogherty M., Godwin R., Hann M. & Al-Ghazal A. (1996) A geometrical analysis of inclined and tilted spherical plough discs. *Journal of Agricultural Engineering Research,* 63, 205-218.

97. O'Dogherty M.J. (1975) A dynamometer to measure the forces on a sugar beet topping knife. *Journal of Agricultural Engineering Research,* 20 (4), 339-345.

98. O'Dogherty M.J. (1996) The design of octagonal ring dynamometers. *Journal of Agricultural Engineering Research,* 63, 9-18.

99. O'Dogherty M.J., Godwin R.J., Dedousis A.P., Brighton J.L. & Tillett N.D. (2007a) A mathematical model of the kinematics of a rotating disc for inter- and intra-row hoeing. *Biosystems Engineering,* 96 (2), 169-179.

100. O'Dogherty M. J., Godwin R. J., Dedousis A.P., Brighton J.L. & Tillett N.D. (2007b) A mathematical model to examine the kinematics of a rotating disc with a cut-out sector for use as an inter- and intra-row hoeing device. *In*: Proceedings of the *6th European Conference in Precision Agriculture,* Skiathos island, Greece,

101. Osman M.S. (1964) The mechanics of soil cutting blades. Durham University.

102. Parish S. (1990) A review of non-chemical weed control techniques. *Biological Agriculture and Horticulture,* 7, 117-137.

103. Payne P. (1956) The relationship between the mechanical properties of soil and the performance of simple cultivation implements. *Journal of Agricultural Engineering Research,* 1 (1), 1-23.

104. Payne P.C.J. (1956) The Relationship between the Mechanical Properties of Soil and The Performanc of Simple Cultivation Implements. *Journal of Agricultural Engineering Research,* (1), 1-23.

105. Perumpral J. V., Grisso R. D. & Desai C.S. (1983) A soil-tool model based on limit equilibrium analysis. *Transactions of the ASAE,* 26 (4), 991-995.

106. Peruzzi A. (2005) *La gestione fisica delle infestanti su carota biologica*. CIRRA.

107. Peruzzi A. (2006) *Il controllo fisico delle infestanti su spinacio in coltovazione biological ed integrata nella bassa valle del serchio*. CIRAA.

108. Peruzzi A, Ginanni M, Raffaelli M. & Di Ciolo S. (2005) The rolling harrow:a new implement for physical pre-and post emergence weed control. *In*: Proceedings of the *13th European Weed Research Society Symposium*, Bari, Italy,

109. Peruzzi A., Raffaelli M., Barberi P. & Silvestri N. (1998) Experimental tests of weed control by means of finger harrowing in durum wheat. *In*: Proceedings of the *3rd EWRS Workshop on physical weed control*, Wye college, UK, Wye college, UK: European Weed Research Society,

110. Pullen D. (1995) A high-speed automatically guided mechanical inter row weeder for arable crops. PhD Thesis. Cranfield University, Silsoe.

111. Pullen D. & Cowell P. (1997) An evaluation of the performance of mechanical weeding mechanisms for use in high speed inter-row weeding for arable crops. *Journal of Agricultural Engineering Research*, 67, 27-34.

112. Rajaram G. & Erbach D. C. (1996) Soil falure by shear versus modification by tillage: A review. *Journal of Terramechanics*, 33 (6), 265-272.

113. Rasmussen J. (1990) Selectivity. An important parameter on establishing the optimum harrowing technique for weed control in growing cereals. *In*: Proceedings of the *EWRS symposium, Integrated weed management in cereals*, European Weed Research Society,

114. Rasmussen J. (2003) Punch planting, flame weeding and stale seedbed for weed control in row crops. *Weed Research*, 43, 393-403.

115. Rasmussen K. (2002) Weed control by a rooling cultivator in potatoes. *In*: Proceedings of the *5th EWRS workshop on Physical weed control*, Pisa, Italy, European Weed Research Society,

116. Reece A. R. (1965) The fundamental equation of earth-moving mechanics. *In*: Proceedings of the *Symposium on Earth-moving Machinery*, Vol. 2, 8-14.

117. Salokhe V. M., Islam M. S. & Sakalaine M. N. (1994) Power spectral density analysis of draft and torque fluctuations of a PTO powered disc tiller. *Journal of Terramechanics*, 31 (3), 163-171.

118. Saunders C. (2002) *Optimising the performance of shallow, high-speed moulboard ploughs*. PhD Thesis, Cranfield University, Silsoe.

119. Shen J. & Kushwaha R. L. (1998) *Soil-Machine Interactions, a finate element perspective* . Marcel Dekker.

120. Slaughter D.C., Giles D.K., Lamm R.D. & Lee W.S. (2000) Robotic weed control systems for california row crops. *In*: Proceedings of the *AgEng 2000*, Warwick, UK, European Agricultural Engineering Society,

121. Sogaard H.T. (1998) Automatic control of a finger weeder with respect to the harrowing intensity at varying soil structures. *Journal of Agricultural Engineering Research*, 70, 157-163.

122. Söhne W. & Eggenmüller A. (1959) Fast-running rotary cultivators and slow-running rotatry diggers. Investigations on individual tools. *Grundlagen der Landtechnick*, 11, 72-80.

123. Sokolovski V. V. (1960) *Statics of soil media*. Oxford: Butterworths scientific publications Oxford.

124. Spoor G. & Godwin R.J. (1978) An Experimental Investigation into the Deep Loosening of Soil by Rigid Tines. *Journal of Agricultural Engineering Research*, (23), 243-258.

125. Stafford J. V. (1979) The performance of a rigid tine in relation to soil properties and speed. *Journal of Agricultural Engineering Research*, 24, 41-56.

126. Stroud K. A. (2001) *Engineering Mathematics*. 5 ed. Palgrave macmillan.

127. Tei F., Stagnari F. & Granier A. (2002) Preliminary results on physical weed control in processing spinach. *In*: Proceedings of the *5th EWRS workshop on Physical weed control*, Pisa, Italy, European Weed Research Society,

128. Terpstra R. & Kouwenhoven J.K. (1981) Inter-row and intra-row weed control with a hoe-ridger. *Journal of Agricultural Engineering Research*, 26, 127-134.

129. Terzaghi K. (1943) *Theoretical soil mechanics*. J. Willey & Sons, Inc., N.Y.

130. Thakur T.C. & Godwin R. J. (1990) The mechanics of soil cutting by a rotating wire. *Journal of Terramechanics*, 27 (4), 291-305.

131. Tillett N. & Hague T (2004) Vision guidance for increasing inter-row cultivation work rate in arable crops. *In*: Proceedings of the *AgEng, 2004*, Leuven, Belgioum, European Agricultural Engineering Society,

132. Tillett N.D. & Hague T. (2006) Increasing work rate in vision guided precision banded operations. *Biosystems Engineering*, 94 (4), 487-494.

133. Tillett N.D., Hague T., Grundy A.C. & Dedousis A.P. (2007) A vision guided system using rotating discs for within-row mechanical weed control. *In*: Proceedings of the *6th European Conference in Precision Agriculture*, Skiathos island, Greece,

134. Tillett N.D., Hague T. & Marchant J. A. (1998) A robotic system for plant-scale husbandry. *Journal of Agricultural Engineering Research*, 69 (2), 169-178.

135. Tillett N.D., Hague T. & Miles S.J. (2002) Inter-row vision guidance for mechanical weed control in sugar beet. *Computers and Electronics in Agriculture,* 33 (3), 163-177.

136. Upadhyaya S. K., Ma T.X., Chancellor W.J. & Zhao Y.M. (1987) Dynamics of soil-tool interaction. *Soil & Tillage Research,* 9, 187-206.

137. Van Zuydam R.P., Sonneveld C. & Naber H. (1995) Weed control in sugar beet by precision guided implements. *Crop Protection,* 14 (4), 335-340.

138. Watson R. T. *Data management, databases and organisations*. 3 ed. John Wiley & Sons, Inc.

139. Weide van der A., Beulens A. & Dijk van S. 2003) *Project planning and management*. Lemma Publishers.

140. Wheeler, P.N. & Godwin R.J. (1996) Soil Dynamics of Single and Multiple Tines at Speeds up to 20 km/h. *Journal of Agricultural Engineering Research,* (63), 243-250.

141. Wiltshire J.J.J., Tillett N.D. & Hague T. (2003) Agronomic evaluation of precise mechanical hoeing and chemical weed control in sugar beet. *Weed research,* 43, 236-244.

142. Zeng D. & Yao Y. (1992) A dynamic model for soil cutting by blade and tine. *Journal of Terramechanics,* 29 (3), 317-327.

Appendices

Appendix I Model of disc kinematics

The mathematical model of the disc kinematics presented in this Thesis was extracted from the paper:
O'Dogherty M.J., Godwin R.J., Dedousis A.P., Brighton J.L. & Tillett N.D. (2007) A mathematical model of the kinematics of a rotating disc for inter- and intra-row hoeing. *Biosystems Engineering*, 96 (2), 169-179.

I.1 Disc rotational speed

The time t in s for the disc centre to travel between plant centres along its line of motion parallel to the plant row is given by:

$$t = \frac{d}{v} \tag{1}$$

where: d is the distance in m between plant centres; and v is the disc forward speed in m s^{-1}.
In this time, the disc must rotate by one revolution, so that its rotational speed, R in s^{-1} is given by:

$$R = \frac{v}{d} \tag{2}$$

The angular velocity ω in rad/s of the disc, therefore, is:

$$\omega = \frac{2\pi v}{d} \tag{3}$$

I.2 Angle of disc rotation

If the disc centre moves a distance p in m from a point directly opposite the centre of a plant stem (*Fig. I-1*), the time t^1 in s taken to travel this distance is:

$$t^1 = \frac{p}{v} \tag{4}$$

In this time, the leading edge of the cut-out sector of the disc will rotate by an angle β in rad given by:

$$\beta = \omega t^{1} \tag{5}$$

Substituting Eqns (3) and (4) into Eqn (5) gives:

$$\beta = \frac{2\pi p}{d} \tag{6}$$

so that the value of β is 2π when p equals d.

If θ is the initial angle in rad made by the leading edge of the cut-out sector with the direction of motion of the disc centre, then the total angle ϕ in rad (*Fig. I-1*) made by the leading edge as the disc moves parallel to the row is:

$$\phi = \theta + \beta$$

i.e.

$$\phi = \theta + \frac{2\pi p}{d} \tag{7}$$

The angle θ is given by:

$$\theta = \tfrac{1}{2}(\pi - \alpha) \tag{8}$$

where α is the included angle in rad of the cut-out sector.

I.3 Analysis of disc rotation

Consider co-ordinate axes OX along the line of motion of the disc centre at a distance *a* in m from the centres of the plant stems and OY through the centre of a particular plant stem (see Fig. I-1). The centre of the initial plant stem is the point P, and the no-till zone is taken as a circle of radius *c* about P.

If the centre of the disc A moves a distance *p* from the origin O along the X axis, the leading edge of a complete cut-out sector takes up a position represented by AB at an angle ϕ given by Eqn (7); and AB is equal to *r* the disc radius in m. The co-ordinates of P are (0 ,*a*), those of A are (*p*,0) and those of B are ($p + r\cos\phi$, $r\sin\phi$).

The important requirement of the disc geometry is that as its centre moves between the plant centres along the X axis, no point on the cut-out edge AB must enter the no-till circle of radius *c* in m.

To examine this condition two lines from P onto AB are considered. The line PC is a line perpendicular to AB of length *l* in m. The line PB is that joining the points P and B of length in m. This means that neither the point C which changes its position as the disc moves, nor the fixed point B must enter the circle. This gives rise to the following criteria:

$$l \geq c \tag{9}$$

$$m \geq c \tag{10}$$

The equation for the line AB is:

$$y = (x - p)\tan\phi$$

which can be written,

$$x\tan\phi - y - p\tan\phi = 0 \tag{11}$$

The length of the perpendicular PC from P to AB is then given by:

$$l = \pm(-a - p\tan\phi)\cos\phi \tag{12}$$

The length of *l* will be positive or negative depending on whether the centre of the plant P, and the origin O, are on the same or opposite sides of the line represented by

the edge of the cut-out sector. This necessitates taking the modulus of the length *l* and length of the perpendicular can be expressed as:

$$l = \left| a\cos\phi + p\sin\phi \right| \tag{13}$$

and from Eqn (9), $l \geq c$ to preclude entry of the leading edge into the no-till zone. The length of the line PB from P to B is given by:

$$m = \sqrt{\left(p + r\cos\phi\right)^2 + \left(r\sin\phi - a\right)^2} \tag{14}$$

Taking the positive sign for the square root and from Eqn (10), $m \geq c$ to avoid the circumferential end of the leading edge entering the no-till zone.

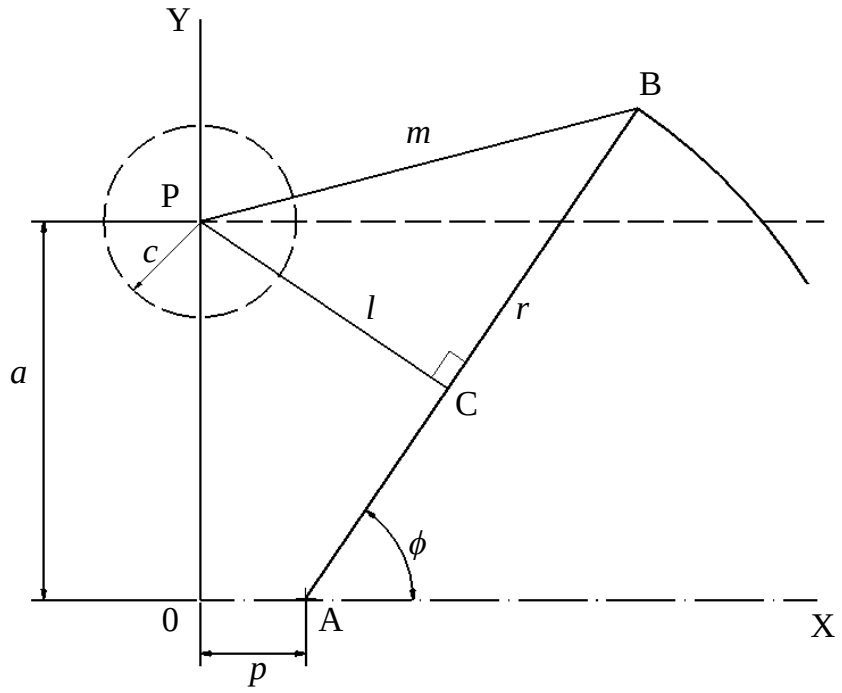

Figure I-1 Co-ordinate system for analysis of the position of any point on the cut-out sector edge in relation to the no-till circle (a, distance of disc line of motion from plant row; c, radius of no-till circle; r; radius of disc; ϕ, angle of cut-out sector edge to line of disc motion; p, distance moved by disc centre from initial point 0 opposite plant centre P; l, length of perpendicular from plant centre to cut-out sector edge; m, length from plant centre to circumferential end point of cut-out sector edge)

I.4 Transition between criteria for avoidance of undisturbed circle

If the point C lies between A and B then the criterion for the length PC applies, given by Eqn (9). In some cases, however, C lies on or beyond the point B and the criterion given by Eqn (10) must be adopted.

It is necessary to apply a test for the transition point and this can be done by considering the *y* co-ordinates for the points C and B.

The co-ordinate *y* of B is given by:

$$y_B = r\sin\phi \tag{15}$$

The co-ordinate *y* of C can be found by considering the equations of the lines PC and AB.

The equation of AB is:

$$y = (x - p)\tan\phi \tag{16}$$

and the equation of PC is:

$$y = a - x\cot\phi \tag{17}$$

Equations (16) and (17) can be solved for the *y* co-ordinate for the point C, giving:

$$y_C = \frac{a\tan\phi - p}{\tan\phi + \cot\phi} \tag{18}$$

The transition point between the criteria occurs when $y_B = y_C$, *i.e.*, for the angle ϕ given by:

$$\frac{a\tan\phi - p}{\tan\phi + \cot\phi} = r\sin\phi \qquad (19)$$

where $\phi = \theta + \frac{2\pi p}{d}$ from Eqn (7).

I.5 Bevelled disc

Modifications can be made to the disc by providing a bevelled edge to avoid the points at the circumference of the edge of the cut-out sector entering the no-till zone. Two cases as shown in *Fig. I-2* are considered below in terms of the disc geometry:

(1) a bevel from a point on the cut-out sector parallel to the disc diameter of the uncut semicircle of the disc *Fig I-2 (a)*; and

(2) a bevel from a point on the cut-out sector to a point at the circumference of the disc *(Fig I-2 (b)).*

I.6 Straight bevel

Figure I-2 (*a*) shows the bevel from a point U on the sector edge to where it meets the disc circumference at the point T. In order to analyse the path of the point T, it is necessary to determine the angle γ in rad between AU and AT so as to calculate the angle ϕ (Eqn 7).

The angle γ can be determined from the triangle ATU and is given by:

$$\gamma = \theta - \sin^{-1}\left\{\frac{s\sin\theta}{r}\right\} \qquad (20)$$

where *s* is the length in m of the cut-out sector edge.

This means that the initial angle made by the radius AU to the X axis is (θ -γ) instead of θ, so that the expression for the angle ϕ in Eqn (7) is modified to:

$$\phi = \sin^{-1}\left\{\frac{s\sin\theta}{r}\right\} + \frac{2\pi p}{d} \tag{21}$$

The length e in m of the bevelled edge UT can be found from the triangle ATU if the length of the edge of the cut-out sector AU is specified, which determines the value of the angle γ. The value of e is given by:

$$e = \frac{r\sin\gamma}{\sin\theta} \tag{22}$$

The length q in m of a line AV from A to any point on the bevel edge UT, making an angle λ with the edge AU is given by the expression:

$$q = \frac{s\sin\theta}{\sin(\theta - \lambda)} \tag{23}$$

In this case, ϕ is equal to (θ - λ) and, for any line AV of length q, values of m can be calculated from Eqn (14) using appropriate values of q in place of r for values of λ up to a maximum of γ. The minimum value of m can then be found to examine whether any point on the bevel edge will enter the no-till circle.

Examination of the effect of the position of a point on the bevel, however, has shown that the minimum distance of the end point T of the bevel is a sufficient criterion to determine whether there is entry into the no-till circle. In this case, a value for q equal to r is used together with a value of ϕ equal to (θ -γ) to determine a minimum value of m from Eqn (14).

I.7 Angled bevel

Figure I-2 (b) shows the angled bevel from a point Q on the sector edge to the point S on the circumference of the disc. The disc radius AS (of length *r*) makes an angle γ with the edge of the cut-out sector.

A general analysis for the length *q* of a line AW to a point W on the bevel edge was made as for the straight bevel in Section I.3 In this case, if the line AW makes an angle λ with the cut-out edge AQ, the value of *q* is given by:

$$q = \frac{s \sin \delta}{\sin(\lambda + \delta)} \tag{24}$$

where the angle δ in rad which the bevelled edge makes with the edge of the cut-out sector can be found from the angle AQS and is given by:

$$\delta = \sin^{-1}\left(\frac{r \sin \gamma}{h}\right) \tag{25}$$

The length of the bevelled edge *h* in m in this case can be found from triangle AQS and is given by:

$$h = \sqrt{r^2 + s^2 - 2rs \cos \gamma} \tag{26}$$

To determine whether any point on the bevel will intrude into the no-till circle, the minimum value of *m* in Eqn (14) can be found for a series of values of *q* in place of *r* and for values of ϕ equal to (θ -λ) for a range of λ from *0* to γ. However, it was found that the use of the circumferential point S was a sufficient criterion and the minimum value of *m* can be found by using values of *q* equal to *r* and ϕ equal to (θ -γ) in Eqn (14).

(a)

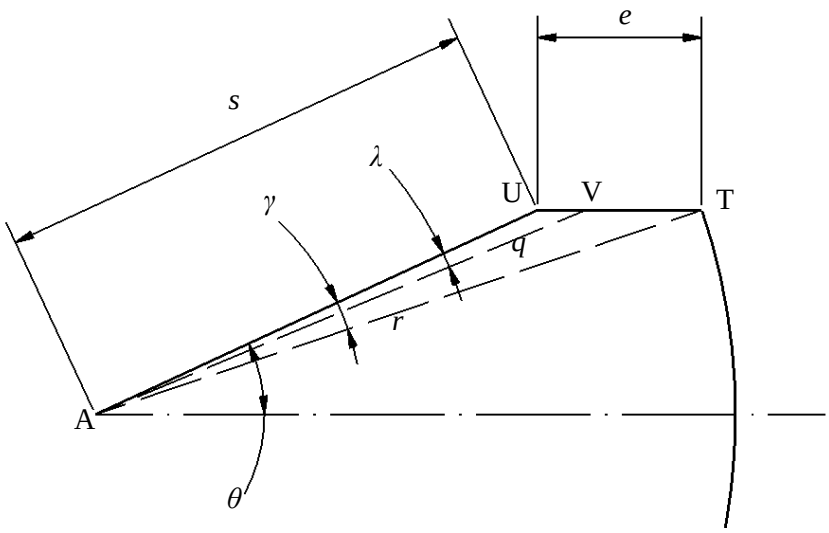

(b)

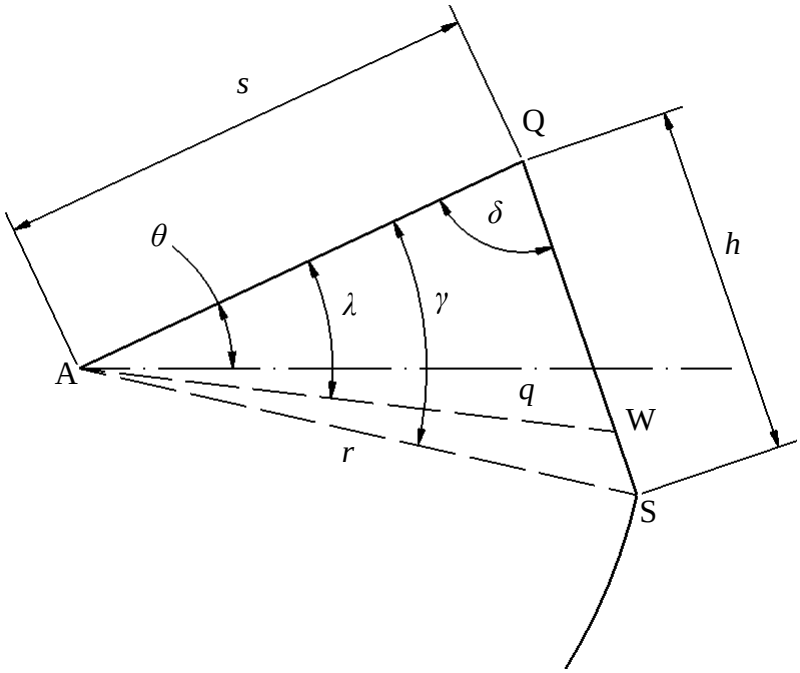

Figure I-2 Principal geometric parameters of bevelled discs: (a) straight bevel ; (b) angled bevel

Appendix II Instrumentation calibration

II.1 EORT calibration

Static calibration test were carried out to determine the measurement linearity and accuracy between applied load with the measured output strain and accuracy between applied loads with the measured loads. The calibration of the EORT was measured by applying known load and recording the electrical gain response. To measure the vertical force (Fx) and the moment (My) the EORT was bolted vertical to the ground at the soil bin processor.

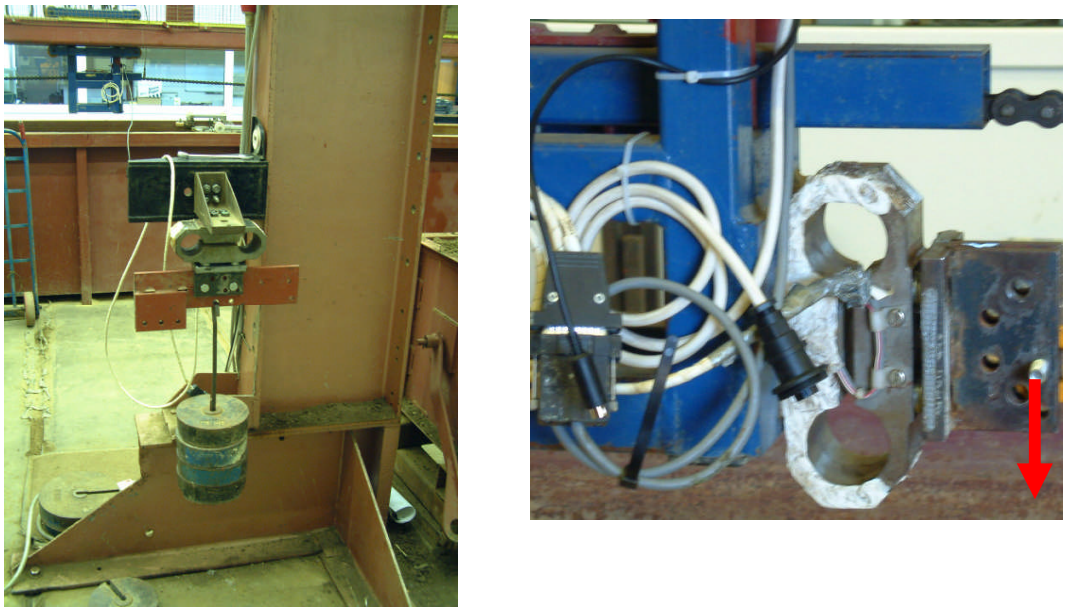

Figure II-1 EORT callibration

To measure the draught force (Fx) the EORT was bolted to a special bracket horizontally to the ground (Figure II-1). The distance (*l*) from the centre of the EORT to the applying load point was 160 mm and 110 mm for the draught force and vertical force respectively. The load to the EORT was applied at 98.1 N intervals up to the capacity of 392.4 N. A data acquisition system (Fylde Electronic Laboratory Ltd, UK) was scanning and the software DASYLab version 8 was recording the output strain of the mounted strain gauges on the EORT. The dynamometer was calibrated for the

draught (Fx) and vertical (Fz) force and the moment (My). The cross sensitivity of the forces were measured simultaneously.

The plotted calibration graph (Figure II-2) shows that applied load and measured output of the EORT were highly correlated. The linearity equations for draught force, vertical force and the moment expressed by the following equations:

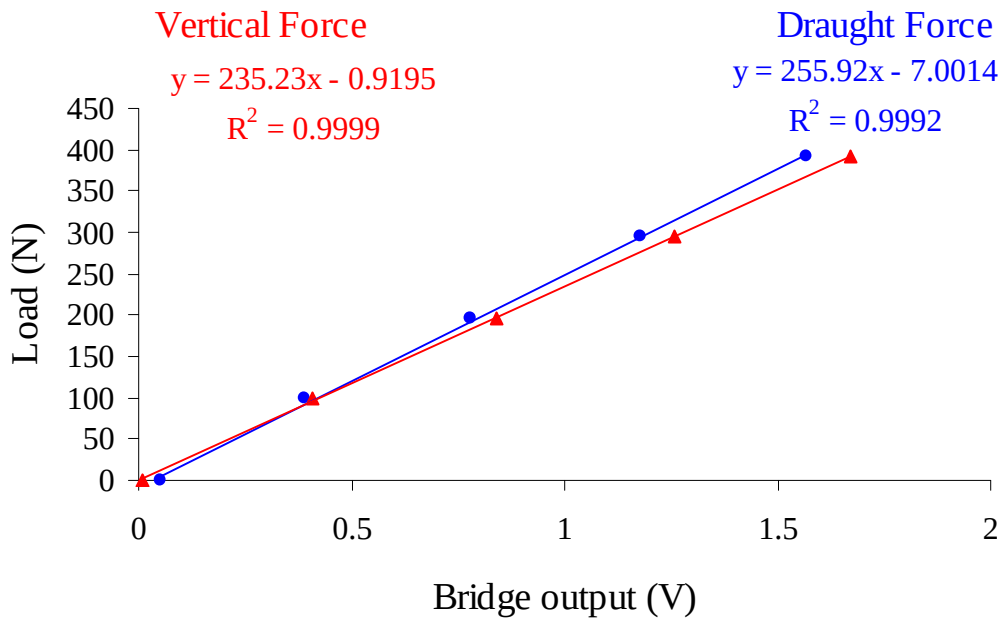

Figure II-2 Calibration graph for draught and vertical force

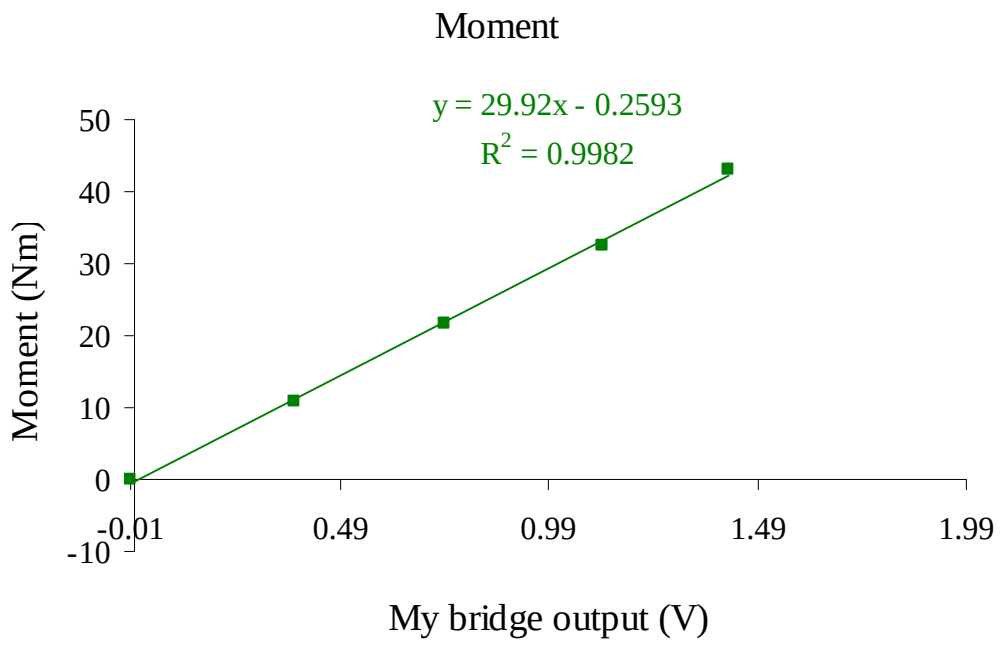

Figure II-3 Calibration graph for moment

DRAUGHT *Fx bridge output (V)*	**VERTICAL** *Fz bridge output (V)*	**MOMENT** *My bridge output (V)*	*Weight (kg)*	*Load (N)*	l=0.11m *(Nm)*
0.05	0.01	-0.01	0	0	0
0.39	-0.41	0.38	10	98.1	10.791
0.78	-0.84	0.74	20	196.2	21.582
1.18	-1.26	1.12	30	294.3	32.373
1.57	-1.67	1.42	40	392.4	43.164

These three equations are used in DASYLab software to read the measure strain output from the EORT in Newton's (N). The coefficient of determination (R^2) was ≥ 0.99 for draught and vertical force and moment. The statistical significantly (p) value was less than $p<0.05$. A noise problem was encountered at the earlier stage of calibration. A filter used in DASYLab to solve that problem. The cross sensitivity between channels was less than 2%. The cross sensitivity for the draught force channel was 1.51% and for the vertical force channel was 1.11%.

As it can be seen from Figures II-2 and II-3 the EORT's output is linear with coefficients of determination of ≥ 0.99. Also hysterisis was not occurred during the calibration. The cross sensitivity was small < 2% and according to Godwin (1975) meets our requirements for measuring force systems in tillage studies.

II.2 Torque cell calibration

WEIGHT (kg)	LOAD (N)	SENSOR OUTPUT V REP1	REP2	REP3	REP4	MEAN
0	0	0.01	0.010004	0.01	0.01	0.010001
0.5	4.905	-0.19826	-0.1903	-0.1906	-0.19032	-0.19237
1	9.81	-0.39991	-0.39997	-0.4	-0.39995	-0.39996
1.5	14.715	-0.60039	-0.60281	-0.6	-0.60012	-0.60083
2	19.62	-0.82653	-0.80335	-0.80466	-0.80603	-0.81014
2.5	24.525	-1.00472	-1.00811	-1.01195	-1.01	-1.0087

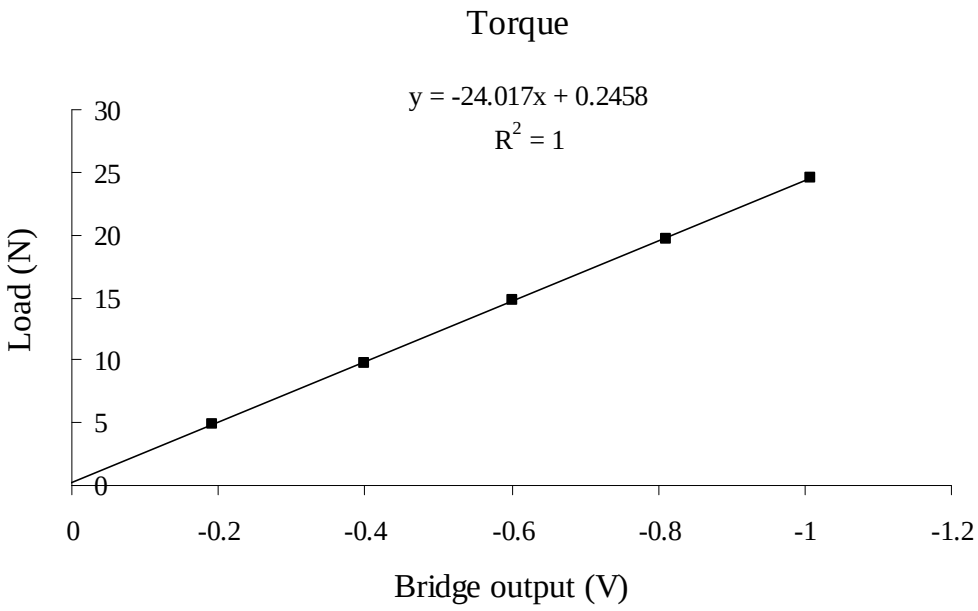

Figure II-4 Torque cell calibration

Appendix III Engineering drawings

Drawings of the prototype disc-hoe for commercial use. Provided by Garford Farm Machinery, UK.

Front view

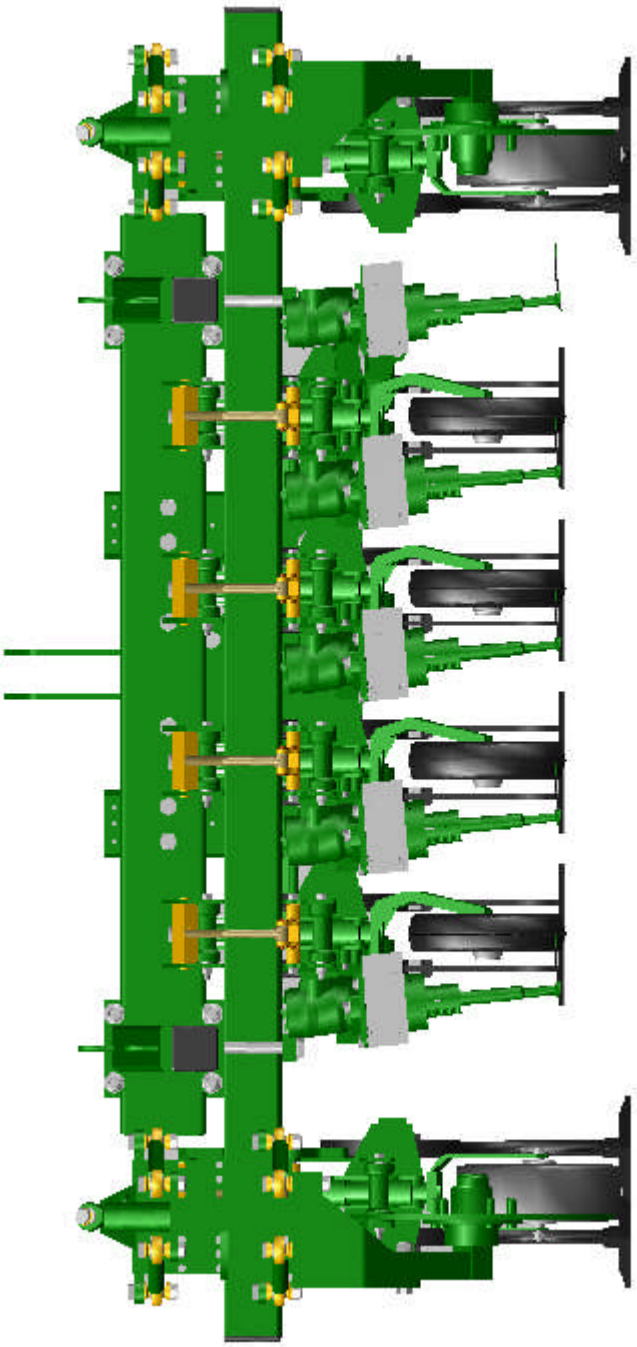

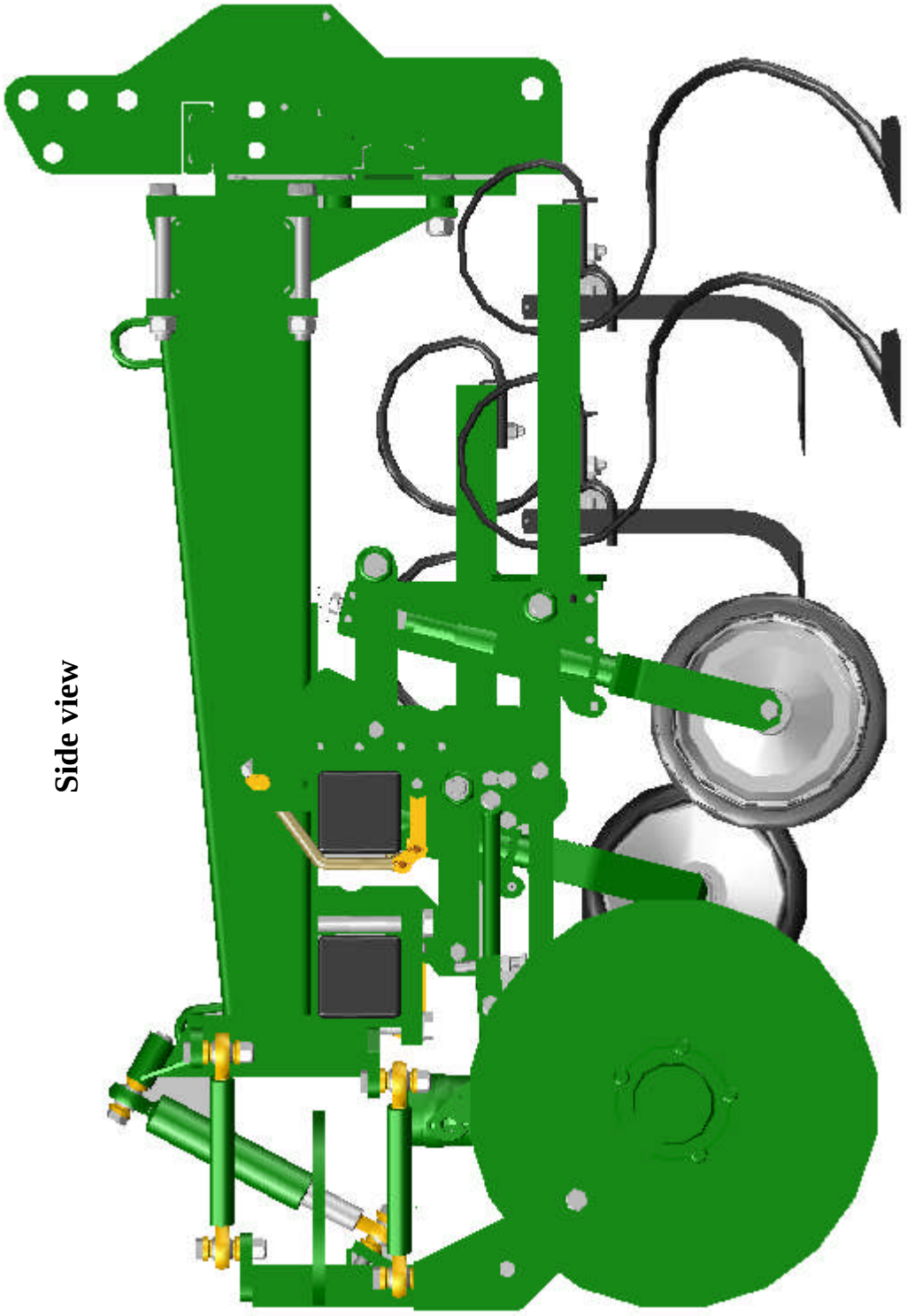

Side view

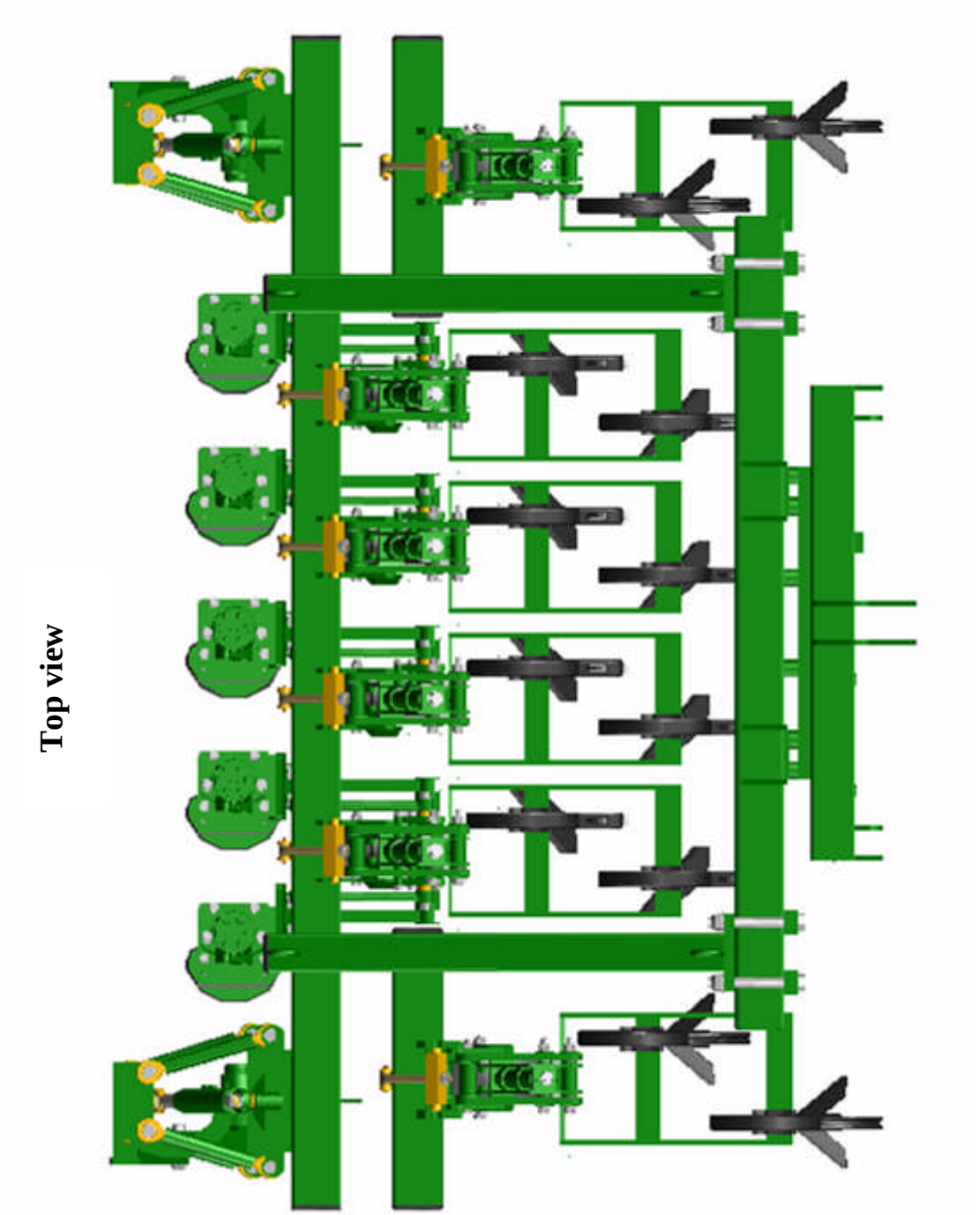

Top view

One unit front view

One unit side view

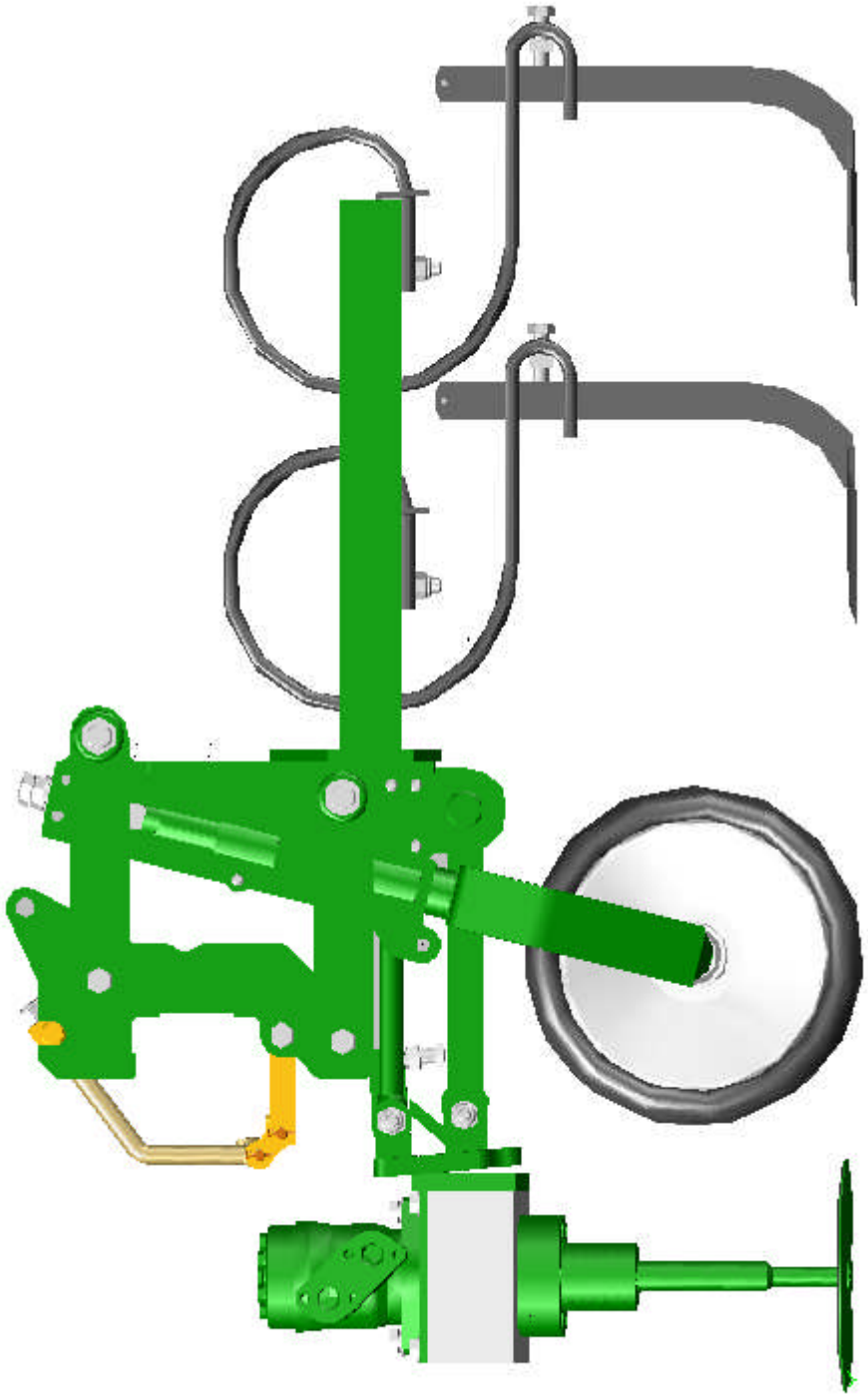

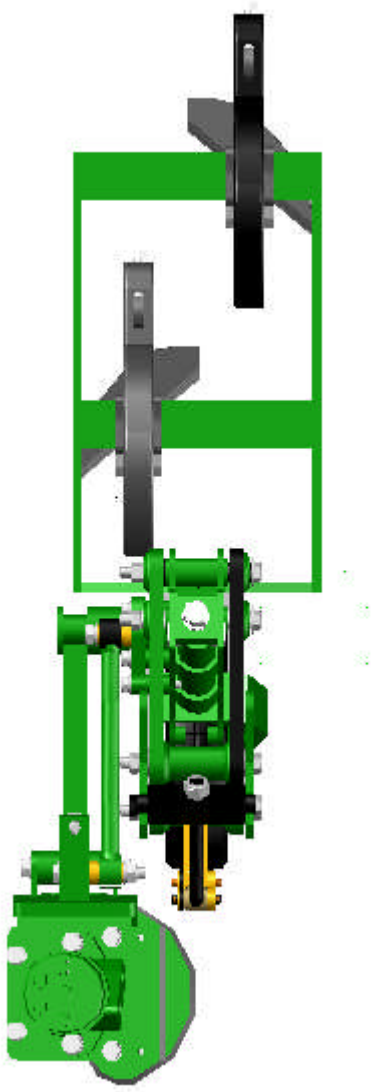

One unit top view

Appendix IV Controlled laboratory experiments results

IV.1 Analysis of variance on the mean values

IV.1.1 Max values draught force

	Solid No Rotation		Solid Rotation		Cut-Out		
Inclination (deg)	***Flat***	***Convex***	***Flat***	***Convex***	***Flat***	***Convex***	***Bowtie***
0	59.49	85.76	245.4	191	449.7	346.5	268.7
5	72.71	59.07	100.1	101.3	168.7	221.3	138.3
10	43.59	71.86	115.7	106.2	132.3	94.5	176.8
15	62.71	68.11	120.1	113.2	113.9	97.9	68.8
Speed (m/s)	***Flat***	***Convex***	***Flat***	***Convex***	***Flat***	***Convex***	***Bowtie***
0.5	192.4	92.4	231.1	229.2			
1	290.4	145.1	370.2	295.6			
1.5	300.1	229.5	376	284.5			
2	330.9	224.3	435.3	348.8			
Depth (mm)	***Flat***	***Convex***	***Flat***	***Convex***	***Flat***	***Convex***	***Bowtie***
10	215.9	86.5	310.9	196	319.2	349.1	188.7
15	234.5	109.4	406.3	294.2	346.1	346.7	254.7
20	262.3	201.2	411.1	185.1	364.5	442.1	215.7
25	379.5	238.2	402.8	265.2	474.5	384.1	318.4

IV.1.2 Mean values draught force

	Solid No Rotation		Solid Rotation		Cut-Out		
Inclination (deg)	***Flat***	***Convex***	***Flat***	***Convex***	***Flat***	***Convex***	***Bowtie***
0	21.86	38.13	98.01	76.6	172.36	152.83	121.22
5	30.95	24.2	31.57	26.81	45.52	47.48	35.96
10	18.85	21.32	35.69	24.52	40.99	26.26	34.96
15	24.02	17.99	28.37	28.7	30.83	16.45	12.18
Speed (m/s)	***Flat***	***Convex***	***Flat***	***Convex***	***Flat***	***Convex***	***Bowtie***
0.5	114.56	32.45	96	102.6			
1	62.26	50.47	133.8	98.6			
1.5	133.24	85.84	138.8	117.7			
2	142.76	119.21	150.1	139.6			
Depth (mm)	***Flat***	***Convex***	***Flat***	***Convex***	***Flat***	***Convex***	***Bowtie***
10	132.8	27.6	109.6	59.3	135.4	185.6	52.8
15	147.6	40.2	158.7	117.7	152.6	174.2	90
20	92.3	95.3	155.7	78.1	143.5	214.6	60.8
25	224.1	119.5	199.5	113.4	264.3	219.6	132.4

IV.1.3 Min values draught force

	Solid No Rotation		Solid Rotation		Cut-Out		
Inclination (deg)	***Flat***	***Convex***	***Flat***	***Convex***	***Flat***	***Convex***	***Bowtie***
0	-9.602	-2.742	-5.75	-8.05	14.17	-25.27	3.79
5	-1.026	-7.382	-45.05	-21.71	-13.2	-25.18	-21.62
10	-12.531	-3.998	-15.74	-40.35	-16.58	-30.62	-40.93
15	-0.237	-2.904	-17.57	-26.75	-28.10	-30.11	-30.89
Speed (m/s)	***Flat***	***Convex***	***Flat***	***Convex***	***Flat***	***Convex***	***Bowtie***
0.5	29.02	6.76	-26.45	-0.63			
1	-6.01	-46.1	-33.11	-28.16			
1.5	4.88	5.07	-2.84	2.35			
2	-47.83	0.46	-31.22	-12.49			
Depth (mm)	***Flat***	***Convex***	***Flat***	***Convex***	***Flat***	***Convex***	***Bowtie***
10	30.83	-2.68	-26.97	0.08	5.38	-10.06	-17.53
15	66.69	-4.3	0.78	24.08	12.97	8.33	-38.25
20	19.48	-4.36	22.36	1.73	0.33	-8.87	-16.78
25	43.06	36.72	15.28	-13.32	36.82	29.05	22.1

IV.1.4 Max values vertical force

	Solid No Rotation		Solid Rotation		Cut-Out		
Inclination (deg)	***Flat***	***Convex***	***Flat***	***Convex***	***Flat***	***Convex***	***Bowtie***
0	44.7	71.61	500	211.2	486.8	413.7	314.6
5	54.79	44.96	120.7	119.2	161.8	201.6	148.1
10	57.59	73.47	132.6	108.5	136.4	158.4	127.4
15	45.56	38.24	147.1	106.6	115.4	97.6	84.3
Speed (m/s)	***Flat***	***Convex***	***Flat***	***Convex***	***Flat***	***Convex***	***Bowtie***
0.5	219.8	122.8	440.5	244.2			
1	276.3	122.9	637.6	337.8			
1.5	437.1	191.7	633.3	300.3			
2	478.9	232.2	761.7	374.9			
Depth (mm)	***Flat***	***Convex***	***Flat***	***Convex***	***Flat***	***Convex***	***Bowtie***
10	328.8	128.2	484.1	186.5	425.5	350.7	211.3
15	248.3	93.9	493.5	241.9	481.8	355.6	313.7
20	417.2	209.8	618.5	186.3	465.9	465.5	217.2
25	376.5	220	529.2	247	498	387.3	289.3

IV.1.5 Mean values vertical force

	Solid No Rotation		Solid Rotation		Cut-Out		
Inclination (deg)	***Flat***	***Convex***	***Flat***	***Convex***	***Flat***	***Convex***	***Bowtie***
0	-1.081	8.567	184.34	98.34	245.62	167.74	172.64
5	5.711	-0.262	19.74	18.21	33.88	41.91	23.63
10	15.108	10.626	20.7	4.07	26.47	24.62	26.58
15	-0.679	-2.502	10.94	8.31	24.43	13.34	10.09
Speed (m/s)	***Flat***	***Convex***	***Flat***	***Convex***	***Flat***	***Convex***	***Bowtie***
0.5	73.89	10.84	192.4	105.7			
1	24.18	26.04	227.4	103.8			
1.5	193.14	47.13	202	120.6			
2	180.3	89.31	233.1	126.6			
Depth (mm)	***Flat***	***Convex***	***Flat***	***Convex***	***Flat***	***Convex***	***Bowtie***
10	182.34	11.88	161.7	60.9	204.9	180.3	89.1
15	105.75	23.47	205.7	106	230.6	178.8	123.6
20	109.26	65.66	200.3	79.6	207.8	209.1	98.8
25	137.05	93.67	270.4	116.2	290.3	208.5	134.2

IV.1.6 Min values vertical force

	Solid No Rotation		Solid Rotation		Cut-Out		
Inclination (deg)	***Flat***	***Convex***	***Flat***	***Convex***	***Flat***	***Convex***	***Bowtie***
0	-32.91	-43.5	-29.01	-15.43	32.5	-35.39	29.5
5	-41.48	-36.75	-67.83	-45.36	-44.99	-43.26	-40.3
10	-25.84	-41.87	-71.49	-86.84	-52.4	-54.96	-78.95
15	-38.84	-38.24	-101.36	-68.07	-64.81	-47.64	-44.93
Speed (m/s)	***Flat***	***Convex***	***Flat***	***Convex***	***Flat***	***Convex***	***Bowtie***
0.5	-95.8	-37.34	-8.63	-6.18			
1	-120.2	-62.44	-30.49	-70.52			
1.5	-68.02	-90.44	-47.9	-67.02			
2	-101.99	-49.58	-75.95	-99.11			
Depth (mm)	***Flat***	***Convex***	***Flat***	***Convex***	***Flat***	***Convex***	***Bowtie***
10	-82.29	-34.35	-50.62	-22.61	4.607	-20.146	-0.042
15	-95.25	-33.24	-36.63	-10.78	-3.673	5.827	-0.107
20	-37.77	-50.66	-9.75	-9.42	-15.3	12.767	-10.41
25	-29.52	0.84	11.37	-12.78	22.375	16.067	-2.86

IV.1.7 Max values torque

	Solid No Rotation		Solid Rotation		Cut-Out		
Inclination (deg)	***Flat***	***Convex***	***Flat***	***Convex***	***Flat***	***Convex***	***Bowtie***
0			19	24	26	34	27
5			15	15	23	29	22
10			22	17	23	15	27
15			16	19	18	15	14
Speed (m/s)	***Flat***	***Convex***	***Flat***	***Convex***	***Flat***	***Convex***	***Bowtie***
0.5			20	23			
1			27	30			
1.5			28	36			
2			34	30			
Depth (mm)	***Flat***	***Convex***	***Flat***	***Convex***	***Flat***	***Convex***	***Bowtie***
10			22	23	20	34	28
15			24	25	23	32	27
20			21	22	24	34	23
25			26	28	29	33	28

IV.1.8 Mean values torque

	Solid No Rotation		Solid Rotation		Cut-Out		
Inclination (deg)	***Flat***	***Convex***	***Flat***	***Convex***	***Flat***	***Convex***	***Bowtie***
0			8.299	11.408	12.258	18.258	11.731
5			4.584	4.488	6.286	8.332	5.767
10			5.662	3.709	6.976	4.661	5.819
15			2.927	3.546	5.185	3.876	2.364
Speed (m/s)	***Flat***	***Convex***	***Flat***	***Convex***	***Flat***	***Convex***	***Bowtie***
0.5			9.81	13.22			
1			12.35	14.62			
1.5			10.9	12.45			
2			13.98	10.98			
Depth (mm)	***Flat***	***Convex***	***Flat***	***Convex***	***Flat***	***Convex***	***Bowtie***
10			10.26	9.1	9.53	20.15	9.14
15			11.79	11.9	11.01	19.5	11.53
20			12.8	10.97	11.72	19.81	9.44
25			13.55	12.58	15.83	20.73	13.69

IV.1.9 Min values torque

	Solid No Rotation		Solid Rotation		Cut-Out		
Inclination (deg)	***Flat***	***Convex***	***Flat***	***Convex***	***Flat***	***Convex***	***Bowtie***
0			0	-3	0	-2	-1
5			-5	-3	-5	-3	-4
10			-9	-4	-4	-8	-6
15			-5	-6	-9	-6	-9
Speed (m/s)	***Flat***	***Convex***	***Flat***	***Convex***	***Flat***	***Convex***	***Bowtie***
0.5			0	3			
1			0	2			
1.5			-5	-8			
2			-11	-9			
Depth (mm)	***Flat***	***Convex***	***Flat***	***Convex***	***Flat***	***Convex***	***Bowtie***
10			-1	-1	-1	0	-5
15			2	-1	0	-1	-2
20			0	2	1	2	-1
25			-1	-2	-3	5	0

IV.2 Analysis of variance on the mean-max values

IV.2.1 Max values draught force

	Solid No Rotation		Solid Rotation		Cut-Out		
Inclination (deg)	***Flat***	***Convex***	***Flat***	***Convex***	***Flat***	***Convex***	***Bowtie***
0	59.48	85.02	245.4	191	449.6	343.3	268.7
5	72.7	58.78	100.1	101.3	168.7	221.3	138.3
10	43.59	71.85	115.7	104.6	132.3	94.5	175.2
15	62.7	68.11	120.1	113.2	113.9	97.9	68.8
Speed (m/s)	***Flat***	***Convex***	***Flat***	***Convex***	***Flat***	***Convex***	***Bowtie***
0.5	191.9	92.4	231.1	229.2			
1	290.4	145.1	370.2	295.6			
1.5	300.1	229.5	376	284.5			
2	330.9	224.2	435.3	348.8			
Depth (mm)	***Flat***	***Convex***	***Flat***	***Convex***	***Flat***	***Convex***	***Bowtie***
10	215.9	86.5	310.9	196	319.2	349.1	188.7
15	231.3	109.4	406.2	294.2	346.1	346.7	250.5
20	262.3	197.2	411.1	185.1	364.5	442.1	215.7
25	378.9	238.2	402.8	265.2	474.4	384.1	318.4

IV.2.2 Mean values draught force

	Solid No Rotation		Solid Rotation		Cut-Out		
Inclination (deg)	***Flat***	***Convex***	***Flat***	***Convex***	***Flat***	***Convex***	***Bowtie***
0	47.5	70.92	216	139.3	304.3	290.3	225
5	59.32	45.98	79.6	72.2	99	116.6	105.8
10	35.92	53.73	91.6	63.4	104.3	82.6	101.1
15	50.15	38.68	72.8	78.6	93.9	65.7	50.7
Speed (m/s)	***Flat***	***Convex***	***Flat***	***Convex***	***Flat***	***Convex***	***Bowtie***
0.5	161.1	61.1	207.6	180.9			
1	169.1	114.6	308.7	200.2			
1.5	206.8	164.4	310.7	219.2			
2	239.2	191.3	332.4	259.5			
Depth (mm)	***Flat***	***Convex***	***Flat***	***Convex***	***Flat***	***Convex***	***Bowtie***
10	183.7	60.8	227.9	128.1	268.5	298.9	128.6
15	198.5	78.3	298.2	215.1	271.9	275.1	201
20	137.3	157.6	293.8	152.6	274.5	351.6	146.5
25	289.2	188	325.5	191.1	394.5	310.2	276.1

IV.2.3 Min values draught force

	Solid No Rotation		Solid Rotation		Cut-Out		
Inclination (deg)	***Flat***	***Convex***	***Flat***	***Convex***	***Flat***	***Convex***	***Bowtie***
0	37.8	23.67	177.54	96.99	237.5	233.9	192.7
5	39.5	29.04	56.7	34.04	74.4	69.9	63.1
10	28.28	41.01	58.23	38.94	64.1	67.9	63.2
15	30.49	25.13	42.78	49.1	67.8	44.4	31.8
Speed (m/s)	***Flat***	***Convex***	***Flat***	***Convex***	***Flat***	***Convex***	***Bowtie***
0.5	106.1	39.95	185.3	155			
1	103.51	71.22	257.7	158.4			
1.5	99.43	101.93	259.7	168.2			
2	123.89	139.38	272.9	194			
Depth (mm)	***Flat***	***Convex***	***Flat***	***Convex***	***Flat***	***Convex***	***Bowtie***
10	149.9	40.8	163.3	78.5	162	254.8	91.5
15	175.6	62.1	232.3	122.2	161.1	246.6	133.7
20	73.3	125.7	207.9	112.6	216	232.4	75.7
25	175.1	157.1	252.2	106.7	310	217.3	220.8

IV.2.4 Max values vertical force

	Solid No Rotation		Solid Rotation		Cut-Out		
Inclination (deg)	***Flat***	***Convex***	***Flat***	***Convex***	***Flat***	***Convex***	***Bowtie***
0	44.7	71.15	500	211.2	481.6	413.7	314.6
5	54.79	44.96	120.7	119.2	161.8	201.6	148.1
10	57.59	73.46	132.6	108.5	136.4	158.4	127.4
15	45.56	38.23	147.1	106.6	115.4	97.6	84.3
Speed (m/s)	***Flat***	***Convex***	***Flat***	***Convex***	***Flat***	***Convex***	***Bowtie***
0.5	219.8	122.8	439.9	241.4			
1	276.6	122.9	637.6	337.8			
1.5	437.1	191.7	633.3	300.3			
2	478.9	223.2	758.6	374.9			
Depth (mm)	***Flat***	***Convex***	***Flat***	***Convex***	***Flat***	***Convex***	***Bowtie***
10	328.7	128.2	482.4	185.6	448.8	350.7	211.3
15	246.2	93.9	493.2	241.8	479	355.6	313.6
20	414.8	208.3	610.7	185	464.3	465.5	217.2
25	372.9	220	523.4	247	498	384.3	289.3

IV.2.5 Mean values vertical force

	Solid No Rotation		Solid Rotation		Cut-Out		
Inclination (deg)	***Flat***	***Convex***	***Flat***	***Convex***	***Flat***	***Convex***	***Bowtie***
0	31.66	56.77	406.5	172.9	418.3	316.3	273.3
5	45.48	33.49	93.6	83.7	109.7	128.2	90.3
10	39.76	48.58	108.8	61.3	101.8	110.8	99.4
15	31.08	27.74	69.9	67.7	94	71.5	63.5
Speed (m/s)	***Flat***	***Convex***	***Flat***	***Convex***	***Flat***	***Convex***	***Bowtie***
0.5	131	53.6	396.3	189.3			
1	142.4	109.2	558.7	226.6			
1.5	309.7	141.4	525.2	260.1			
2	352.1	196.4	582.7	303.8			
Depth (mm)	***Flat***	***Convex***	***Flat***	***Convex***	***Flat***	***Convex***	***Bowtie***
10	245.3	63.6	376.1	135.4	377.4	285.1	177.2
15	172.1	68.8	425.9	200.7	393.5	298	240.1
20	153.2	149	426.5	162.6	361.9	369.7	180.6
25	206.9	171.9	452.6	210.4	436.7	316.2	230.9

IV.2.6 Min values vertical force

	Solid No Rotation		Solid Rotation		Cut-Out		
Inclination (deg)	***Flat***	***Convex***	***Flat***	***Convex***	***Flat***	***Convex***	***Bowtie***
0	20.7	40.64	305.23	137.93	340.8	264.1	233.2
5	35.35	21.94	67.23	39.57	77.2	88.4	56.6
10	19.61	29.79	82.07	28.17	89	86.5	61.8
15	19.96	14.78	34.56	48.77	70.8	49.5	39.2
Speed (m/s)	***Flat***	***Convex***	***Flat***	***Convex***	***Flat***	***Convex***	***Bowtie***
0.5	39.41	16.09	340.9	151.5			
1	58.66	74.97	496.7	184.2			
1.5	98.46	104.68	457	201.7			
2	169.25	146.99	508.1	229.3			
Depth (mm)	***Flat***	***Convex***	***Flat***	***Convex***	***Flat***	***Convex***	***Bowtie***
10	128.47	34.18	295.7	87.4	229.9	190.7	151.6
15	38.21	47.75	350.8	128.2	281.5	260.7	161.6
20	48.58	96.7	310.1	136.8	289	287.8	118.9
25	109.06	132.56	308.5	140.6	363.8	260.8	175.9

IV.2.7 Max values torque

	Solid No Rotation		Solid Rotation		Cut-Out		
Inclination (deg)	***Flat***	***Convex***	***Flat***	***Convex***	***Flat***	***Convex***	***Bowtie***
0			19	24	26	34	27
5			15	15	23	29	22
10			22	17	23	15	27
15			16	19	18	15	14
Speed (m/s)	***Flat***	***Convex***	***Flat***	***Convex***	***Flat***	***Convex***	***Bowtie***
0.5			20	23			
1			27	30			
1.5			28	27			
2			34	30			
Depth (mm)	***Flat***	***Convex***	***Flat***	***Convex***	***Flat***	***Convex***	***Bowtie***
10			22	23	20	34	22
15			24	25	23	31	27
20			21	22	24	34	23
25			26	28	29	33	28

IV.2.8 Mean values torque

	Solid No Rotation		Solid Rotation		Cut-Out		
Inclination (deg)	***Flat***	***Convex***	***Flat***	***Convex***	***Flat***	***Convex***	***Bowtie***
0			16.33	20.33	21.11	28.67	22.78
5			12.67	12.33	15	18.89	15.22
10			15.89	9.89	12.67	12.44	17.22
15			9.89	12.56	14.56	11.33	9.67
Speed (m/s)	***Flat***	***Convex***	***Flat***	***Convex***	***Flat***	***Convex***	***Bowtie***
0.5			16.78	20			
1			23.67	24.89			
1.5			25.56	24.67			
2			29.44	27.11			
Depth (mm)	***Flat***	***Convex***	***Flat***	***Convex***	***Flat***	***Convex***	***Bowtie***
10			18.33	17.33	17.33	28.22	17.33
15			20.89	20.89	19.11	28.11	22.11
20			20.33	19	19.89	31.22	17.22
25			22.67	23	23.67	28.56	24.11

IV.2.9 Min values torque

	Solid No Rotation		Solid Rotation		Cut-Out		
Inclination (deg)	***Flat***	***Convex***	***Flat***	***Convex***	***Flat***	***Convex***	***Bowtie***
0			14	15	19	22	20
5			10	6	10	15	11
10			12	6	11	10	10
15			6	10	11	8	6
Speed (m/s)	***Flat***	***Convex***	***Flat***	***Convex***	***Flat***	***Convex***	***Bowtie***
0.5			15	16			
1			22	21			
1.5			20	22			
2			26	22			
Depth (mm)	***Flat***	***Convex***	***Flat***	***Convex***	***Flat***	***Convex***	***Bowtie***
10			15	11	14	25	12
15			18	17	14	23	16
20			20	15	15	28	12
25			19	19	20	26	18

Appendix V Statistical analysis reports

The data were analysed with GenStat v.8.1 and two analysis of variance (ANOVA) were performed one for the mean values and the second for the mean-max values as for all transducer channels, for each of the inclination angle, depth and speed effect experiment. Below there are two example reports from the mean and mean-max analysis of non-rotating solid discs and rotating cut-out discs.

V.1 The effect of depth on non-rotating solid discs Mean analysis

Analysis of variance

Variate: Draught

Source of variation	d.f.	s.s.	m.s.	v.r.	F pr.
Replica stratum	2	2944.	1472.	0.76	
Replica.*Units* stratum					
Disc	1	29851.	29851.	15.38	0.002
Depth	3	29709.	9903.	5.10	0.014
Disc.Depth	3	7955.	2652.	1.37	0.294
Residual	14	27169.	1941.		
Total	23	97627.			

Tables of means

Variate: Draught

Variate: DRAUGHT

Grand mean 109.93

DEPTH	10.	15.	20.	25.
	80.24	93.91	93.77	171.81

DISCCONVEXPLAIN

70.67	149.19

DEPTH	DISC	CONVEX	PLAIN
10.		27.63	132.85
15.		40.23	147.59
20.		95.28	92.26
25.		119.54	224.07

Standard errors of means

Table	Disc	Depth	Disc Depth
rep.	12	6	3
d.f.	14	14	14
e.s.e.	12.72	17.98	25.43

Standard errors of differences of means

Table	Disc	Depth	Disc Depth
rep.	12	6	3
d.f.	14	14	14
s.e.d.	17.98	25.43	35.97

Least significant differences of means (5% level)

Table	Disc	Depth	Disc Depth
rep.	12	6	3
d.f.	14	14	14
l.s.d.	38.57	54.55	77.15

Stratum standard errors and coefficients of variation

Variate: Draught

Stratum	d.f.	s.e.	cv%
Replica	2	13.56	12.7
Replica.*Units*	14	44.05	41.3

V.2 The effect of depth on cut-out rotating discs Mean-Max analysis

Analysis of variance

Variate: DRAUGHT

Source of variation	d.f.	s.s.	m.s.	v.r.	F pr.
REPLICA stratum	2	2918.	1459.	1.11	
REPLICA.*Units* stratum					
DISC	2	111062.	55531.	42.33	<.001
DEPTH	3	46951.	15650.	11.93	<.001
DISC.DEPTH	6	35849.	5975.	4.55	0.004
Residual	22	28864.	1312.		
Total	35	225645.			

Tables of means

Variate: DRAUGHT

Grand mean 266.4

DEPTH	10.	15.	20.	25.
	232.0	249.4	257.4	326.9

DISC	bowtie	convex	plain
	188.0	309.0	302.4

DEPTH	DISC	bowtie	convex	plain
10.		128.6	298.9	268.5
15.		201.0	275.2	271.9
20.		146.2	351.6	274.5
25.		276.1	310.2	394.5

Standard errors of means

Table	DISC	DEPTH	DISC DEPTH
rep.	12	9	3
d.f.	22	22	22
e.s.e.	10.46	12.07	20.91

Standard errors of differences of means

Table	DISC	DEPTH	DISC DEPTH
rep.	12	9	3
d.f.	22	22	22
s.e.d.	14.79	17.08	29.57

Least significant differences of means (5% level)

Table	DISC	DEPTH	DISC DEPTH
rep.	12	9	3
d.f.	22	22	22
l.s.d.	30.67	35.41	61.33

Stratum standard errors and coefficients of variation

Variate: DRAUGHT

Stratum	d.f.	s.e.	cv%
REPLICA	2	11.03	4.1
REPLICA.*Units*	22	36.22	13.6

Appendix VI Prediction model integration

VI.1 Draught and vertical force integration

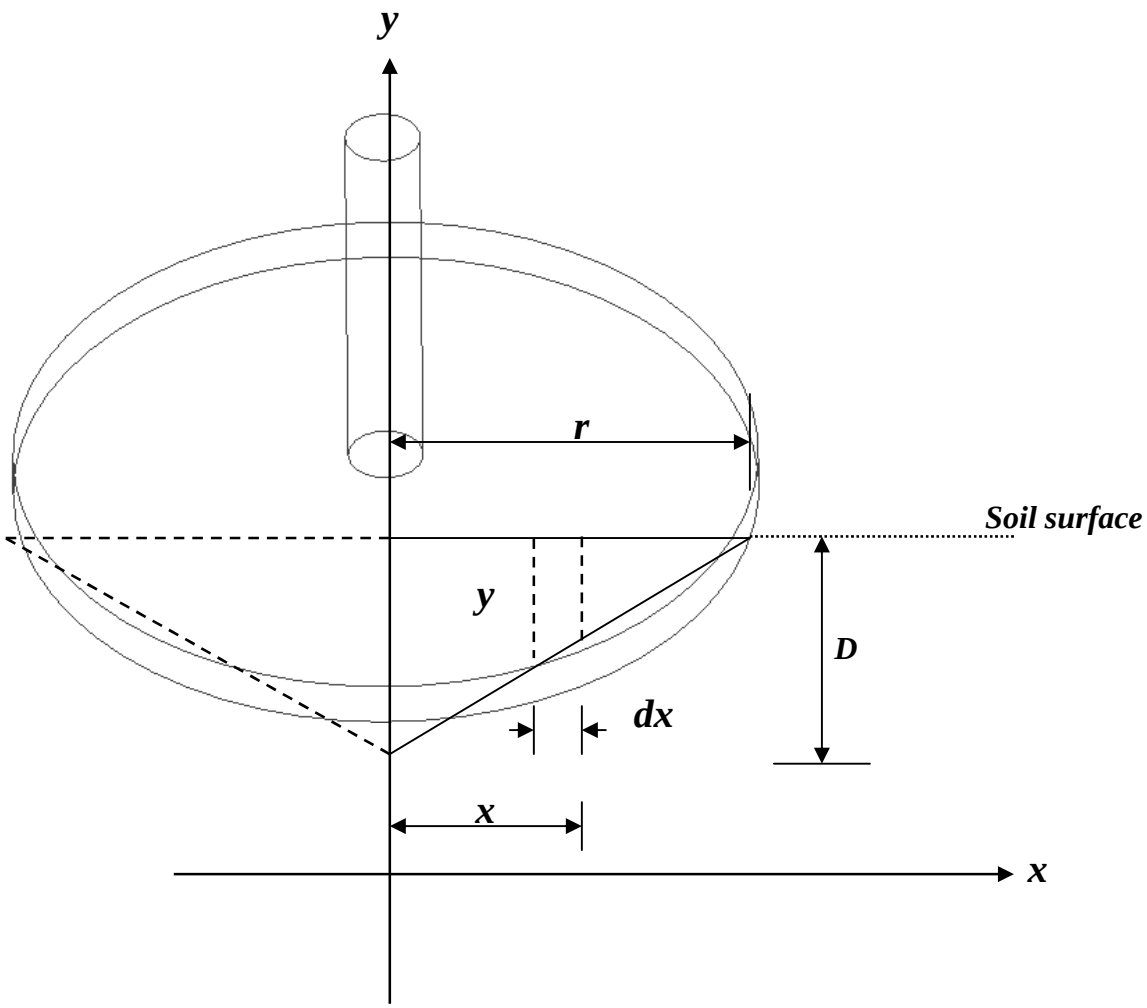

Figure VI-1 Width-depth relationship for inclined disc

$$y = \frac{D \cdot (r - x)}{r} \quad \text{.....(1)}$$

$$\delta P = \left(\gamma \cdot y^2 \cdot N_\gamma + c \cdot y \cdot N_c + q \cdot y \cdot N_q + \frac{\gamma \cdot v^2 \cdot N_\alpha \cdot y}{g} \right) \cdot \delta x \quad \text{.....(2)}$$

Equation (2) will be integrated by replacing the width-depth linear relationship as given in equation (1)

P_γ

$$P_\gamma = 2 \cdot \gamma \int_0^r \left(\frac{D \cdot (r - x)}{r} \right)^2 \cdot dx$$

$$P_\gamma = 2 \cdot \gamma \int_0^r \left(\frac{D \cdot r - D \cdot x}{r} \right)^2 \cdot dx$$

$$P_\gamma = 2 \cdot \gamma \int_0^r \frac{\left(D^2 \cdot r^2 + D^2 \cdot x^2 - 2 \cdot D \cdot r \cdot D \cdot x \right) \cdot dx}{r^2}$$

$$P_\gamma = \frac{2 \cdot \gamma}{r^2} \cdot \left[D^2 \cdot r^2 x + \frac{D^2 \cdot x^3}{3} - \frac{2 \cdot D^2 \cdot r \cdot x^2}{2} \right]_0^r$$

$$P_\gamma = \frac{2 \cdot \gamma}{r^2} \cdot \left[D^2 \cdot r^2 + \frac{D^2 \cdot r^3}{3} - D^2 \cdot r^3 \right]$$

$$P_\gamma = \frac{2 \cdot \gamma}{r^2} \cdot \frac{D^2 \cdot r^3}{3}$$

$$P_\gamma = 2 \cdot \gamma \cdot \frac{D^2 \cdot r}{3} \quad \text{.....(3)}$$

P_c

$$P_c = 2\int_0^r c \cdot \frac{D \cdot (r - x)}{r} \cdot dx$$

$$P_c = \frac{2 \cdot c}{r} \int_0^r D \cdot r - D \cdot x \cdot dx$$

$$P_c = \frac{2 \cdot c}{r} \cdot \left[D \cdot r^2 - \frac{D \cdot r^2}{2} \right]_0^r$$

$$P_c = \frac{2 \cdot c}{r} \cdot \left[D \cdot r^2 - \frac{D \cdot r^2}{2} \right]$$

$$P_c = \frac{2 \cdot c}{r} \cdot \frac{D \cdot r^2}{2}$$

$$P_c = c \cdot D \cdot r \text{ ……..(4)}$$

P_q

$$P_q = 2\int_0^r q \cdot \frac{D \cdot (r - x)}{r} \cdot dx$$

$$P_q = \frac{2 \cdot q}{r} \int_0^r D \cdot r - D \cdot x \cdot dx$$

$$P_q = \frac{2 \cdot q}{r} \cdot \left[D \cdot r^2 - \frac{D \cdot r^2}{2} \right]_0^r$$

$$P_q = \frac{2 \cdot q}{r} \cdot \left[D \cdot r^2 - \frac{D \cdot r^2}{2} \right]$$

$$P_q = \frac{2 \cdot q}{r} \cdot \frac{D \cdot r^2}{2}$$

$P_q = q \cdot D \cdot r$ ……..(5)

P_α

$$P_\alpha = 2\int_0^r \frac{\gamma \cdot v^2}{g} \cdot \frac{D \cdot (r - x)}{r} \cdot dx$$

$$P_\alpha = \frac{2 \cdot \gamma \cdot v^2}{r \cdot g} \int_0^r D \cdot r - D \cdot x \cdot dx$$

$$P_\alpha = \frac{2 \cdot \gamma \cdot v^2}{r \cdot g} \left[D \cdot r \cdot x - \frac{D \cdot x^2}{2} \right]_0^r$$

$$P_\alpha = \frac{2 \cdot \gamma \cdot v^2}{r \cdot g} \cdot \left[D \cdot r^2 - \frac{D \cdot r^2}{2} \right]$$

$$P_\alpha = \frac{2 \cdot \gamma \cdot v^2}{r \cdot g} \cdot \frac{D \cdot r^2}{2}$$

$$P_\alpha = \frac{\gamma \cdot v^2}{g} \cdot D \cdot r \quad \text{.....(6)}$$

The force (H) can be calculated by replacing equations (3) to (6) into equation (2), that includes also the dimensional soil resistance coefficients: N_γ; N_c; N_q; and N_α

So the draught force (H) can be calculated by:

$$H = \left[\left(2 \cdot \gamma \cdot \frac{D^2 \cdot r}{3} \cdot N_\gamma \right) + \left(c \cdot D \cdot r \cdot N_c \right) + \left(q \cdot D \cdot r \cdot N_q \right) - \right.$$

$$\left. + \left(\frac{\gamma \cdot v^2 \cdot N_\alpha}{g} \cdot D \cdot r \right) \right] \cdot \sin(\alpha + \delta) \qquad (7)$$

The vertical force (V) can be calculated by:

$$V = \left[\left(2 \cdot \gamma \cdot \frac{D^2 \cdot r}{3} \cdot N_\gamma \right) + \left(c \cdot D \cdot r \cdot N_c \right) + \left(q \cdot D \cdot r \cdot N_q \right) - \right.$$

$$\left. + \left(\frac{\gamma \cdot v^2 \cdot N_\alpha}{g} \cdot D \cdot r \right) \right] \cdot \cos(\alpha + \delta) \qquad (8)$$

VI.2 Torque addition

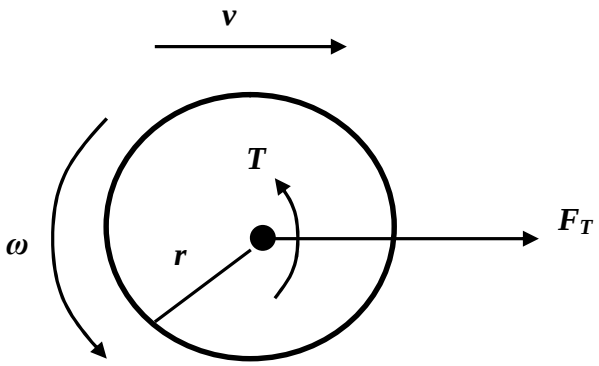

In time, *t*, the disc moves forward by *vt* and the disc revolves through an angle ωt

In energy terms:

$$T \cdot \omega \cdot t = F_T \cdot v \cdot t \tag{1}$$

Hence:

$$F_T = \frac{\omega \cdot T}{v} \tag{2}$$

or

$$F_T = \frac{2 \cdot \pi}{d} \cdot T \tag{3}$$

The time, *t*, between plants is $\frac{d}{v}$ in, *s*, hence the disc revolves over in this time. So if *R*, in, *rev* s^{-1}:

$$R = \frac{1}{d/v} \tag{4}$$

So the rotational speed of the disc, *R*, in s^{-1}, is given by:

$$R = \frac{v}{d} \tag{5}$$

or

$$\omega = \frac{2 \cdot \pi \cdot v}{d} \quad \text{in, } rad\ s^{-1} \quad (= 2 \cdot \pi \cdot r) \tag{6}$$

Hence:

$$\frac{\omega}{v} = \frac{2 \cdot \pi}{d} \tag{7}$$

If F_D is the draught force, then

$$T = \mu \cdot F_D \cdot r \tag{8}$$

So that:

$$F_T = \frac{2 \cdot \pi}{d} \cdot \mu \cdot r \cdot F_D \tag{9}$$

Appendix VII Computer vision guidance

The information on the computer vision guidance in this Thesis was extracted from the paper:
Tillett N.D., Hague T., Grundy A.C. & Dedousis A.P. (2007) Mechanical within-row weed control for transplanted crops using computer vision. *Biosytems Engineering* (in press).

VII.1 Computer vision guidance software

The position of the plants and their phase relative to the rotating disc was detected using computer vision. Ratios of red, green and blue channels from colour images of the crop scene were taken to reduce the effects of shadows. In the resulting mono-chrome images plant material appears bright against a dark soil background. An algorithm based on two dimensional wavelets has been developed to locate individual crop plants. These wavelets defined by equation (1) provided a spatially localised means of extracting a periodic planting pattern based on individual plants and their near neighbours (Figure VII-1).

$$z = (2 - x^2 - y^2)\, e^{\frac{-(x^2+y^2)}{2}} \qquad (1)$$

Where x and y are axis perpendicular and parallel to the crop rows respectively and z is the wavelet function.

Initial placement of the Mexican hat wavelets was based on predicted plant position from a Kalman filter tracking algorithm (Bar-Shalom and Fortmann, 1988). Distortion caused by perspective was taken into account. An adaptive step size hill climbing technique was used to position the Mexican hat over individual plants which were tracked by the Kalman filter as they proceeded down subsequent images (Figure VII-2).

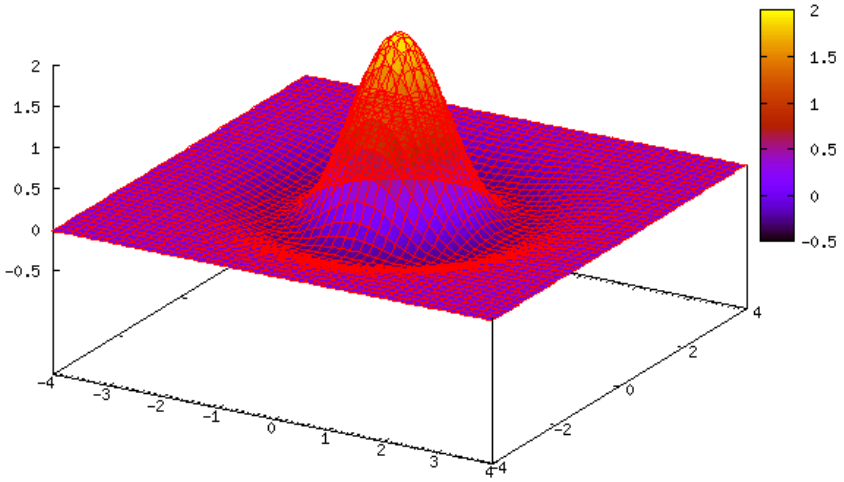

Figure VII-1 Visualisation of the two dimensional Mexican hat wavelet defined by Equation 1 (Tillett *et al.*, 2007)

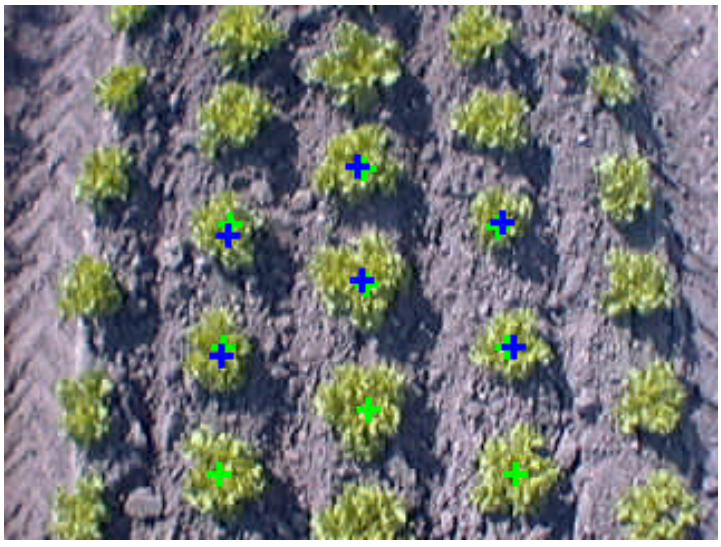

Figure VII-2 Sample lettuce image superimposed with green crosses indicating Kalman filter predictions and blue crosses indicating refined positions based on wavelet application.

Any error in phase between tracked plant position and disc cut out was corrected via a proportional valve controlling a hydraulic motor that drove the cultivating disc. The controlling equation is given in Equation 2. Figure VII-3 illustrates the process diagrammatically and shows that the controller output (U) undergoes a non linear transformation in the conversion to solenoid valve current (I) to compensate for valve characteristics. For convenience angles are measured in revolutions i.e. they take the value 0 to 1.

$$U = V_t / D + (\theta_c - D_V / D) K_1 + (\dot{\theta}_c - V_t / D) K_2 \qquad (2)$$

Where:

V_t = Tractor forward speed (m/s)

D = nominal spacing between plants within the row (m)

D_V = distance to next plant within the row measured by the vision system (m)

θ_c = cultivator angle (revolutions)

$\dot{\theta}_c$ = angular velocity of the cultivator (revolutions/s)

K_1 = proportional to phase error gain

K_2 = proportional to speed error gain

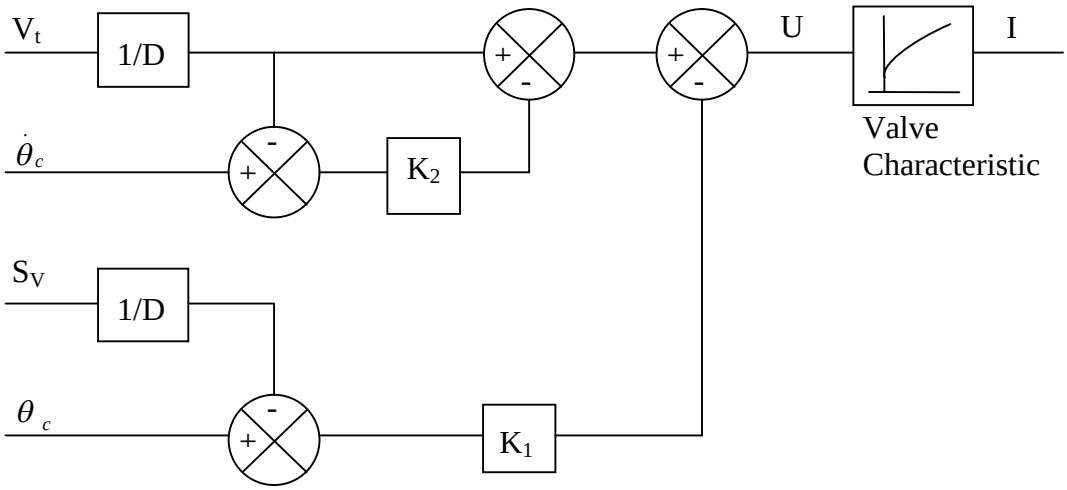

Figure VII-3 Schematic of phase lock loop control system for synchronising disc rotation with approaching plants

VII.2 Computer vision guidance hardware

The computing system was based on a single board PC with a 1.7GHz Pentium M processor. This board received images of the crop scene from a 320 by 240 pixel colour camera via an IEEE1394 (Firewire) serial interface. Inputs from encoders and proximity detectors, and outputs to proportional hydraulic flow control valves were made via a custom built interface board. This board communicated with the main PC board via a RS232 serial interface and included a 80C517 microprocessor that performed low level control algorithms and managed the inputs and outputs. The main PC board and custom built interface board along with their power supply were mounted within a metal enclosure attached to the implement (Figure VII-4). An interface with the user was provided by a commercially available console mounted in the tractor cab. This console incorporated another single board PC packaged with a screen and push button interface. The console was networked with the main PC via IEEE802.3a (Ethernet) and displayed live video from the camera superimposed with graphical guidance information. The push buttons allowed the user to switch between different pre entered configurations and to make fine adjustments in bias. The step size for lateral movement perpendicular to the crop rows is 10mm and the step size in phase shift along the row is 3°.

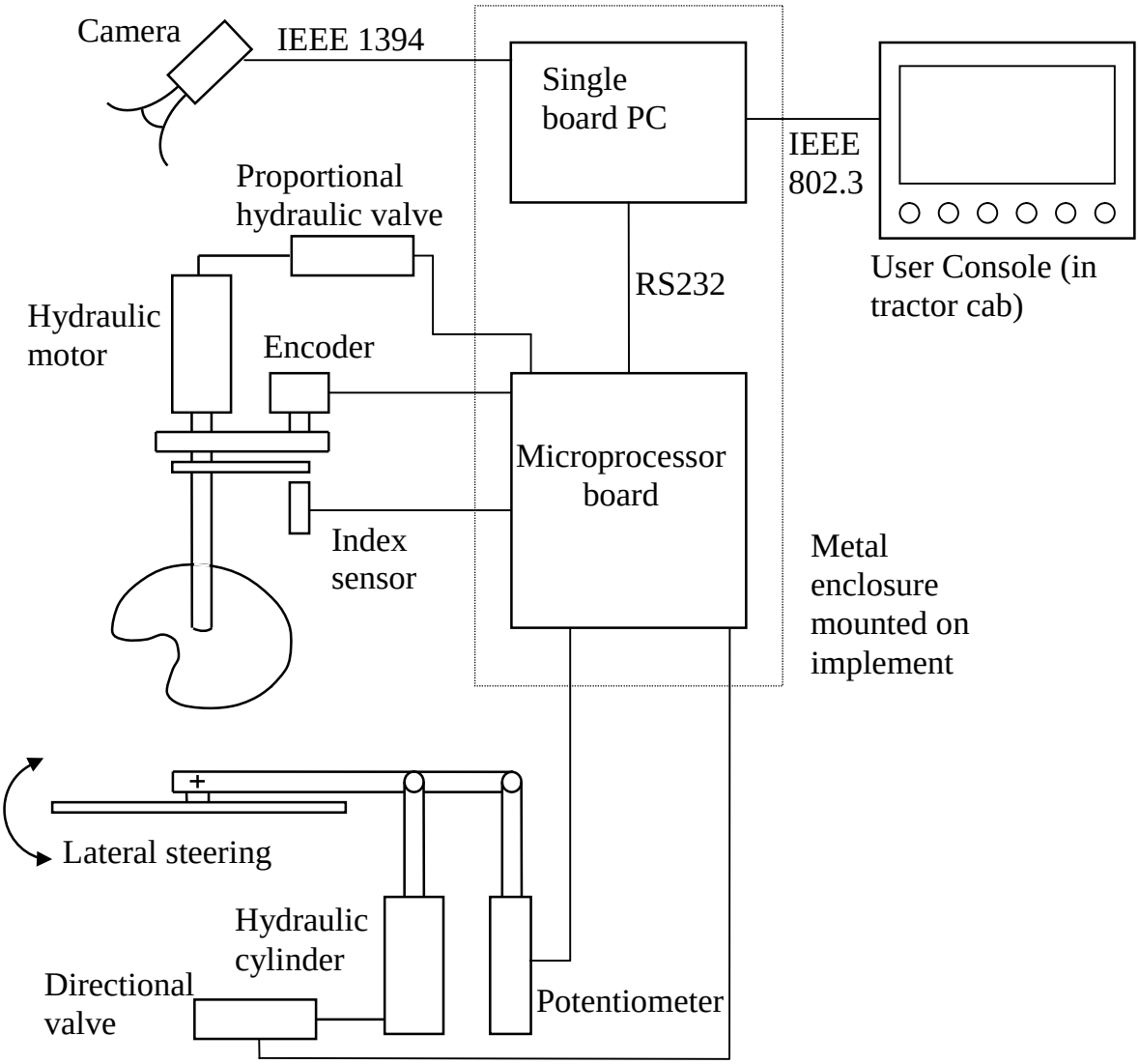

Figure VII-4 Schematic of experimental computing and control system showing a single rotary disc cultivator module.

Appendix VIII Disc design

The appropriate radius of the non-tilled circle is considered to be equal to 40 mm in practice. The disc centre should move as close as possible to the crop row and this is taken as a distance of 50 mm so that the disc can hoe between the plant non-tilled circles without having an excessively large radius. This radius will then be equal to about 90 mm in practice. It is then only necessary to modify the disc design parameters to accommodate the plant spacing. Tables VIII-1 and VIII-2 show the appropriate disc parameters for plant spacing from 150 mm to 500 mm.

Table VIII-1

Plant spacing (mm)	150	200	250	300	350	400	450	500
Disc design	A	A	B	C	D	D	D	E
Plant spacing appropriate for disc design (mm)	≥ 150	≥ 200	≥ 250	≥ 300	≥ 300	≥ 300	≥ 300	≥ 500

Table VIII-2

A	Design in Figure 3-19
B	Design in Figure 3-13 (b)
C	Design in Figure 3-13 (a)
D	Design in Figure 7-5
E	Design in Figure 7-6